

New sealing system as a surgical technique to avoid the iatrogenic Preterm Premature Rupture of fetal Membranes (iPPROM)

Germán Febas Bosomba

<http://hdl.handle.net/10803/671901>

ADVERTIMENT. L'accés als continguts d'aquesta tesi doctoral i la seva utilització ha de respectar els drets de la persona autora. Pot ser utilitzada per a consulta o estudi personal, així com en activitats o materials d'investigació i docència en els termes establerts a l'art. 32 del Text Refós de la Llei de Propietat Intel·lectual (RDL 1/1996). Per altres utilitzacions es requereix l'autorització prèvia i expressa de la persona autora. En qualsevol cas, en la utilització dels seus continguts caldrà indicar de forma clara el nom i cognoms de la persona autora i el títol de la tesi doctoral. No s'autoritza la seva reproducció o altres formes d'explotació efectuades amb finalitats de lucre ni la seva comunicació pública des d'un lloc aliè al servei TDX. Tampoc s'autoritza la presentació del seu contingut en una finestra o marc aliè a TDX (framing). Aquesta reserva de drets afecta tant als continguts de la tesi com als seus resums i índexs.

ADVERTENCIA. El acceso a los contenidos de esta tesis doctoral y su utilización debe respetar los derechos de la persona autora. Puede ser utilizada para consulta o estudio personal, así como en actividades o materiales de investigación y docencia en los términos establecidos en el art. 32 del Texto Refundido de la Ley de Propiedad Intelectual (RDL 1/1996). Para otros usos se requiere la autorización previa y expresa de la persona autora. En cualquier caso, en la utilización de sus contenidos se deberá indicar de forma clara el nombre y apellidos de la persona autora y el título de la tesis doctoral. No se autoriza su reproducción u otras formas de explotación efectuadas con fines lucrativos ni su comunicación pública desde un sitio ajeno al servicio TDR. Tampoco se autoriza la presentación de su contenido en una ventana o marco ajeno a TDR (framing). Esta reserva de derechos afecta tanto al contenido de la tesis como a sus resúmenes e índices.

WARNING. The access to the contents of this doctoral thesis and its use must respect the rights of the author. It can be used for reference or private study, as well as research and learning activities or materials in the terms established by the 32nd article of the Spanish Consolidated Copyright Act (RDL 1/1996). Express and previous authorization of the author is required for any other uses. In any case, when using its content, full name of the author and title of the thesis must be clearly indicated. Reproduction or other forms of for profit use or public communication from outside TDX service is not allowed. Presentation of its content in a window or frame external to TDX (framing) is not authorized either. These rights affect both the content of the thesis and its abstracts and indexes.

DOCTORAL THESIS

Title	New sealing system as a surgical technique to avoid the iatrogenic Preterm Premature Rupture of fetal Membranes (iPPRM)
Presented by	Germán Febas Bosomba
Centre	IQS School of Engineering
Department	Bioengineering
Directed by	Dr. Salvador Borrós Gómez

A sa meua gent i a qui ho vulgui llegir

“No ens atrevim a moltes coses perquè son difícils, però son difícils perquè no ens atrevim a fer-les.” (Mestre Séneca)

Acknowledgments

Com no només és una tradició, sinó que més bé és una mostra d'afecte i gratitud a totes aquelles persones que m'han acompanyat durant els anys en que he fet el que realment m'agradava, a continuació escriuré una petita part de tot allò que em ve de gust remarcar. Quedant a la memòria col·lectiva, o al menys a la que ens atorga el paper, així com ho sento. Demano disculpes per avançat si m'oblido d'algú o escric en les següents línies alguna cosa indeguda. Serà l'espontaneïtat amb que vull fer aquest agraïments la única culpable de tal ofensa, si es donés el cas. Perquè *il messaggero non è importante*.

Com ja sabeu tots/es, diuen que els agraïments és la part de la tesis que més es llegeix. Per tant intentaré estar a l'alçada d'aquesta realitat, fent que qui se senti al·ludit al menys li dibuixi un somriure (ni que sigui lleu) al seu rostre i es pugui traslladar (ni que sigui per segons) en aquell passat no tan llunyà.

És de vital importància esmentar que aquest últims anys han estat un dels més feliços de la meua vida. No tan sols pel fet de dedicar temps i esforç al que m'agrada, que és la recerca aplicada, donant forma a un dispositiu mèdic a partir d'un conjunt d'idees i convertir-les amb cosa tangible, sinó també a poder compartir històries, emocions i vivències amb totes aquells membres que han format part del laboratori de Biomaterials, i per extensió a tots/es aquells/es que constitueixen "la casa" que em va acollir.

Inevitablement he de començar per donar les gràcies a una persona que, després d'obrir-me les portes del seu despatx i d'escoltar alguna que altra proposta en recerca més o menys esbojarrada però factible, va confiar en mi: el Salvador. Va començar oferint-me un raconet al lab on fer "les meves cosetes" mentre es donava forma al que al final va ser el projecte que acompanya aquesta tesi. No oblidaré mai la confiança que va depositar en mi, ni les escridassades constructives, ni alguna cançó acompanyada d'una espècie de ball, dient coses com "Uuh, ara ve l'estrella!", "Uuh, el super Germán!". Jajaja!! Entre altres moltes coses, admiro la capacitat de fer que no ens perdem i ens dispersem, de la manera que té d'orientar-nos i de fer-nos veure el bosc però sense perdre de vista el arbres. Només puc que donar mil gràcies al nostre "papa" que ens ha aguantat a cadascun de nosaltres durant tot el doctorat. De fet, sorprenentment, encara no sé com no ha tingut un atac de cor per culpa nostra. Si pot aguantar alumnes de grau, de màster, doctorands i postdocs ho pot aguantar tot. Gràcies de tot cor, Salvador. I ja aviso que no et lliuraràs de mi tan fàcilment perquè tinc més idees i projectes per fer-los tangibles, i de segur que t'agradaran.

Dono les gràcies com és obvi a tots aquells doctorands i ja doctors que m'han acompanyat i amb qui hem viscut moment inoblidables. Històries irrepetibles com la moneda de cinc

cèntims del l'Alberto i la pantalla del super Mac nou del Joan (que *pesao* amb els Macs, Deu meu! Pobre enganyat). Per ells va ser traumàtic però per nosaltres era pura xispa i diversió. Vam viure com el Robert i l'Alberto s'anaven tornant calbs amb el doctorat. Un dels dos caminava per la corda fluixa perdent i recuperant "privilegis" (Te quiero, Tito!) i l'altre encara no ho ha acabat d'assumir-ho però canta amb la seva gran veu cançons com la dels miserables i no sé quina més. Impossible no unir-s'hi. La sandwichera va ser com una mena centre neuràlgic en el que la Laura, la Balmorio, l'AnnaMas-mucho-más, i tots els demès, ens posàvem les botes amb sandvitxos de diferent naturalesa. Nocillos, xoriço, pernil dolç Duroc... Crec que aquella època, a l'anàlisi mèdic anual de l'IQS em van trobar un xic de colesterol. D'ençà, ja no me atrevit a fer-me mai més un anàlisi. Que cal dir de los jueves con Peri i dels "firazos"? Vaya líder, el Peri! Allò era un moment per desetressar-nos sanament compartint històries de dintre i fora del lab, *machacando* junt amb el Mario a qui ens volgués reptar al futbolin, realitzant danses socials i algun que altre brindis. La Nunu, el Polete, la Cris, no només no fallaven tampoc, sinó que eren peces bàsiques amb l'alegria i destresa que els caracteritza. Que cal dir del Brugada, que apart de ser un màquina al lab amb lo nano ens va deixar gravats al cor un "ja no tinc por, por, por..." que encandilava les nenes i a tots nosaltres. Del Miguel Àngel, què n'hauríem fet sense ell al lab, resolent-nos dubtes des de química bàsica fins informàtica i arts de la guerra. De la Marina i la Núria que hagués estat de nosaltres i del lab sense el seu puny de ferro, intentant controlar lo incontrolable. Si és que es fan estimar, de veritat. Tot i que algun que altre paquet m'he emportat sense saber ni d'on em venien els tirs. A la Mariana i la seva cèlebre frase de "hay un calbo que me pregunta cosas". A la Carla Font i a l'Àlex per voler formar part del projecte com a màsters i ajudar-me a posar a punt l'equip d'*electrospinning*, fent-me més o menys cas. Reconesc que no és la tècnica més emocionant de fer servir però ho va fer força bé. Al Yagüe per ensenyar-me a utilitzar el super iCVD i per acompanyar-me fins casi les 22h de la nit, fins que la polimerització estés feta, a canvi d'alguna hamburguesa en sortir del lab. A tots els/les *young* i no tan *young members* com la Coral, la Glòria, l'Olmo, el Toni, la Patri, Roberta, Benja, Martí, Carles, les dos Martes, etc. Als/les de bioquímica per fer pinya de tant en tant. Al Chema i al David, per aguantar-nos bastant sovint demanant coses complicades al magatzem. Al Cristian que quan el trucava tard ja sabia que era jo. Falta taaanta gent que me fa mal no poder incloure a tothom. Espero que em dispenseu. Gràcies a tots, de veritat. Impossible escriure el agraïments sense donar les gràcies a la Fundació CELLEX, al Pere Mir i Puig (un dels més important mecenes de Catalunya. Que en pau descansi) i a l'Enric Banda, per confiar en nosaltres pel projecte. També al Dr. Gratacós, a l'Elisenda, al Sergio i a la Talita per treballar braç a braç per desenvolupar el sistema de segellat des de zero. Des

del dia que me van convidar a presenciar una cirurgia fetal i a toquetejar una membrana amniòtica humana, vaig ser conscient del gran repte i de la importància real d'incorporar un pegat en aquest tipus de teixit, sabent que és un teixit fet perquè res s'hi pugui adherir. Llargues hores hem treballat junt a la Talita fent els assajos *ex vivo*, sempre intentant tenir-ho tot preparat per quan ella o l'Elisenda m'avisaven de que tindríem una membrana que complia els criteris. Estar a primera línia, junt amb elles i algun membre més de l'*staff* mèdic als assajos *in vivo* en ovelles és una de les experiències més enriquidores que he tingut mai. Sempre procurant ser el més crític possible amb els resultats obtinguts. Dir-lis que moltíssimes gràcies i que cada cop estem més a prop del sistema de segellat definitiu.

I per acabar a tots els membres d'Aortyx, especialment al Jordi Martorell i la Noemí per confiar en mi i fitxar-me sabent que havia d'acabar d'escriure una tesis, i encara defensar-la. Hi ha hagut algun moment que no era fàcil treballar i acabar d'escriure la tesis al mateix temps. Tenir una participació al meu cap d'aquest nivell i poder separar cada cosa crec que m'ha ajudat a enfocar millor la distribució del treball futur. Pau, Carlos, Carlota, Àlex, Juan, Paquito, Maite...és un orgull compartit aquests moments amb vosaltres. Noé, sento no fer-te una dedicatòria especial per tu. Jajaja!

Com ja he dit, segurament em deixo d'incloure a algunes persones. Ah! No oblidó als meus pares i la meva família, que per fi crec ja saben exactament que estic fent. I sinó, espero que estiguin atents el dia de la defensa, que llegeixin aquesta tesis, o que m'ho demanin els cops que faci falta. Us estimo. A les meves ex per aguantar-me, a la família Rabionfílica per aquelles *science beer afternoons* i per tot el que em viscut i viurem, i a tots els meus *roomies* que han passat pel pis del carrer Provença.

Gràcies, sincerament a tothom. De veritat.

This project has been funded by Fundació privada CELLEX, in collaboration with Hospital Sant Joan de Déu, Hospital Clínic de Barcelona, Fetal Medicine Research Center, and BCNatal.

Fundació Privada
CELLEX

CLÍNIC
BARCELONA
Hospital Universitari

Sant Joan
de Déu
HOSPITAL MATERNINFANTIL
UNIVERSITAT DE BARCELONA

B
C
NATAL

fetal iD
FETAL MEDICINE
RESEARCH CENTER

Abstract

New sealing system as a surgical technique to avoid the iatrogenic Preterm Premature Rupture of fetal Membranes (iPPROM).

This thesis is focused on the creation of a sealing system that blocks the orifices of the chorioamniotic membrane produced by minimally invasive surgical instruments during fetal operations.

Currently, with the improvement of imaging techniques for fetal diagnosis used to monitor pregnancy, the detection of fetal anomalies has increased. In this scenario, it is essential to develop surgical procedures to directly access the fetus in a safer manner.

Over the past few years, the use of fetoscopy has provided less invasive surgical procedures. Fetoscopy is a technique in which, by inserting a trocar through the abdominal cavity, we are able to introduce the necessary instruments to perform the corresponding fetal surgery. Even so, the access to the fetus from a single point limits the possibilities of the technique, as opposed to having access from several points, since it would allow the fetus to be approached from several axes.

One of the problems associated with fetal surgeries is the remaining presence of the orifice in the chorioamniotic membrane once the trocar is removed. The permanence of the orifice, especially in the first hours after surgery, can cause different pathologies: oligohydramnios, chorioamnionitis, pulmonary hypoplasia of the fetus, etc., and also the rupture of the chorioamniotic membrane, which could result in fetal death. This rupture of the membrane is called iatrogenic preterm premature rupture of membranes (iPPROM) and is one of the most common complications during pregnancy.

The aim of this work is to create a patch that allows the sealing of these orifices and significantly reduces the leakage of amniotic liquid and the risk of chorioamniotic membrane rupture during the first days after fetoscopy.

The development of the sealing system has been divided into three parts, which experiments, advances and results have been obtained in a semi-parallel process until a final medical device was obtained: on the one hand, the development of an adhesive with bioadhesive properties in a wet environment, which is activated when it comes into contact with the amniotic fluid itself; on the other hand, the substrate where the adhesive will be placed and which acts as a patch; and finally, an insertion system that allows the placement of this patch as quickly and safely as possible by the medical team involved in the surgery.

Resum

Nou sistema de segellat com a tècnica quirúrgica per evitar el Trencament Prematur iatrogènic a Preterme de les Membranes fetals (iPPROM).

Aquesta tesi es centra en la creació d'un sistema de segellat que permet taponar els forats de la membrana corioamniòtica produïts per l'instrumental quirúrgic de mínima invasió en operacions fetals.

Actualment, amb la millora de les tècniques d'imatge per al diagnòstic fetal que s'utilitzen per fer el seguiment de l'embaràs, ha augmentat la detecció d'anomalies fetals i, per tant, també la necessitat de dur a terme intervencions quirúrgiques amb les que accedir directament al fetus de forma segura.

Ja des de fa alguns anys, per a realitzar cirurgies de la manera menys invasiva possible s'utilitza la fetoscòpia. Tècnica en la que mitjançant la inserció d'un trocar a través de la cavitat abdominal som capaços d'introduir les eines necessàries per dur a terme la cirurgia fetal corresponent. Tot i així, l'accés al fetus des d'un sol punt limita les possibilitats de la tècnica, en contraposició de si es tingués accés des de diversos punts, ja que permetria abordar al fetus des de diversos eixos.

Un dels problemes associats a les cirurgies fetals és la presència romanent de l'orifici a la membrana corioamniòtica un cop s'extreu el trocar i finalitza l'operació, ja que per si sola és incapaç de regenerar-se. La permanència de l'orifici, sobretot en les primeres hores, pot causar diferents patologies. Des d'oligohidramnios, corioamnionitis, hipoplàsia pulmonar del fetus, ..., fins trencament de la membrana corioamniòtica, que pot cursar amb la mort del fetus. Aquest trencament de la membrana rep el nom de Ruptura Prematura de les Membranes a Preterme per causes iatrogèniques (iPPROM) i és una de les complicacions més comuns durant l'embaràs.

L'objectiu d'aquest treball és crear un pegat que permeti el segellat d'aquests orificis i que es redueixi de manera significativa el risc de pèrdua de líquid amniòtic i el trencament de la membrana corioamniòtica durant els primers dies després de la fetoscòpia.

El desenvolupament del sistema de segellat s'ha dividit en tres parts, en que els experiments, avenços i resultats s'han obtingut de forma semi-paral·lela fins a obtenir un prototip final de dispositiu mèdic: d'una banda, desenvolupar un adhesiu amb propietats bioadhesives en medi humit i que s'activa en entrar en contacte amb el propi líquid amniòtic; d'altra banda, el substrat on estarà disposat l'adhesiu, i que junts actuen com un pegat; i finalment un sistema d'inserció que permeti la col·locació d'aquest pegat de la forma més ràpida i segura possible per part de l'equip mèdic partícip en la cirurgia.

Resumen

Nuevo sistema de sellado como técnica quirúrgica para evitar la Rotura Prematura iatrogénica a Pretérmino de las Membranas fetales (iPPROM).

Esta tesis se centra en la creación de un sistema de sellado que permite taponar los orificios de la membrana corioamniótica producidos por el instrumental quirúrgico de mínima invasión en operaciones fetales.

Actualmente, con la mejora de las técnicas de imagen para el diagnóstico fetal que se utilizan para hacer el seguimiento del embarazo, ha aumentado la detección de anomalías fetales y, por lo tanto, también la necesidad de llevar a cabo intervenciones quirúrgicas con las que acceder directamente al feto de forma segura.

Ya desde hace algunos años, para realizar cirugías de la manera menos invasiva posible se utiliza la fetoscopia: técnica en la que mediante la inserción de un trócar a través de la cavidad abdominal somos capaces de introducir las herramientas necesarias para llevar a cabo la cirugía fetal correspondiente. Aun así, el acceso al feto desde un solo punto limita las posibilidades de la técnica, en contraposición de si se tuviera acceso desde varios puntos, ya que permitiría abordar al feto desde varios ejes.

Uno de los problemas asociados a las cirugías fetales es la presencia remanente del orificio en la membrana corioamniótica una vez se extrae el trócar y finaliza la operación, ya que por sí sola es incapaz de regenerarse. La permanencia del orificio, sobre todo en las primeras horas, puede causar diferentes patologías. Desde oligohidramnios, corioamnionitis, hipoplasia pulmonar del feto, ..., hasta rotura de la membrana corioamniótica, que cursa con la muerte del feto, si éste aún no es viable. Esta rotura de la membrana recibe el nombre de Rotura Prematura de las Membranas a Pretérmino por causas iatrogénicas (iPPROM) y es una de las complicaciones más comunes durante el embarazo.

El objetivo de este trabajo es crear un parche que permita el sellado de estos orificios y que se reduzca de forma significativa la pérdida de líquido amniótico y el riesgo de rotura de la membrana corioamniótica durante los primeros días tras la fetoscopia.

El desarrollo del sistema de sellado se ha dividido en tres partes, cuyos experimentos, avances y resultados se han obtenido de forma semiparalela hasta obtener un prototipo final de dispositivo médico. Por un lado, el desarrollo de un adhesivo con propiedades bioadhesivas en medio húmedo y que se activa al entrar en contacto con el líquido amniótico; por otro lado, el sustrato donde se depositará el adhesivo, y que juntos actúan como un parche; y finalmente un sistema de introducción que permita la colocación de este parche de la forma más rápida y segura posible por parte del equipo médico participante en la cirugía.

Table of contents

Acknowledgments.....	VII
Abstract.....	XIII
Resum.....	XIV
Resumen.....	XV
Table of contents.....	XVII
Index of Figures.....	XIX
Index of Tables.....	XXII
List of Abbreviations.....	XXIII
Chapter I. Motivations and Aims.....	1
1.1. Motivations and aims.....	3
1.2. Content of this Dissertation.....	10
Chapter II. Design and Election of the Patch.....	13
2.1. Introduction.....	15
2.2. Material and Methods.....	23
2.2.1. Selection and use of the material for the patch.....	23
2.2.2. Design of the patch.....	24
2.2.3. Incorporation of a micropattern in the patch surface.....	25
2.2.4. Production of the patches with flat and hemi-lens design.....	27
2.2.5. Integration of an electrospun layer of Polycarbonate-urethane.....	28
2.3. Results and Discussion.....	32
2.3.1. Selection and use of the material for the patch.....	32
2.3.2. Design of the patch.....	33
2.3.3. Incorporation of a micropattern on the patch surface.....	36
2.3.4. Production of the patches with flat and hemi-lens design.....	38
2.3.5. Integration of an electrospun layer of polycarbonate-urethane (PCU).....	42
2.4. Concluding remarks.....	52
Chapter III. Insertion system.....	55
3.1. Introduction.....	57
3.2. Materials and Methods.....	62
3.3. Results and Discussion.....	63
3.4. Concluding remarks.....	67
Chapter IV. Bioadhesives with activation on wet environment.....	69
4.1. Introduction.....	71
4.1.1. Bioadhesive thin film by Chemical Vapor Deposition.....	80
4.1.2. Bioadhesive inspired on marine mussel glue.....	85
4.1.3. Bioadhesive inspired in the formation of hydrogels with cellulose derivates.....	87
4.2. Materials and Methods.....	91
4.2.1. Bioadhesive thin film by Chemical Vapor Deposition.....	91
4.2.2. Bioadhesive inspired on marine mussel glue: dopaminated Hyaluronic Acid.....	96
4.2.3. Bioadhesive inspired in the formation of hydrogels with cellulose derivates.....	101
4.3. Results and Discussion.....	104
4.3.1. Bioadhesive thin film by Chemical Vapor Deposition.....	104
4.3.2. Bioadhesive inspired on marine mussel glue: dopaminated Hyaluronic Acid (DHA).....	116

4.3.3.	Bioadhesive inspired in the formation of hydrogels with cellulose derivates	129
4.4.	Concluding Remarks.....	143
Chapter V.	Latest advances and next steps	145
5.1.	Introduction	146
5.2.	Materials and Methods.....	148
5.2.1.	Incorporation of a microarpoons corona	148
5.2.2.	Validation assays for the patch	149
5.3.	Results and Discussion.....	150
5.3.1.	Incorporation of a microarpoons crown.	150
5.3.2.	Validation assays for the patch	154
5.4.	Next steps	160
5.4.1.	Internal hexagonal mesh for the patch	160
5.5.	Concluding Remarks.....	162
Conclusions.....		164
References.....		166
Annex.....		179

Index of Figures

Figure I-1. Pictures with the different classes of surgeries:.....	4
Figure I-2. Images with the movement between the chorion and-amnios.....	5
Figure I-3. Images with the layers of the chorio-amniotic membranes.....	7
Figure II-1. Examples of PU implants and medical devices.	18
Figure II-2. Picture in time lapse of the fibers produced in electrospinning process.....	19
Figure II-3. Scheme of our electrospinning equipment.....	20
Figure II-4. SEM images of the surface modification.....	21
Figure II-5 Examples of the firsts designs of the lens/semi-lens patch.	24
Figure II-6. 3D design of the micropattern with convex hemi-spheres.....	25
Figure II-7 Schematic diagram of contact angles of a drop obtained with DSA.	27
Figure II-8. Scheme of the customized plasma reactor.....	26
Figure II-9. Mold design with Solid Works software with semi-lens shape.....	28
Figure II-10. Electrospinning equipment used. Fluidnatek® LE-10 from Bioinicia.	29
Figure II-11. Results obtained with strain-stress assay of the silicone samples.....	32
Figure II-12. Design and approximated measures of the flat disc/ hemi-lens patches.....	33
Figure II-13. Stainless steel mold with the five depth patterns.....	36
Figure II-14. Images obtained with optical microscopy (5x) of stainless-steel molds.....	37
Figure II-15. Modelized image of the two pieces of the mold.	39
Figure II-16. Image showing parts that make up the mold to produce hemi-lenses.....	40
Figure II-17. Images with the real stainless-steel molds to produce the patches.....	41
Figure II-18. Scheme of the traction system with the anchor thread integrated.....	42
Figure II-19. Images of the electrospun PCU films for the macroscopic evaluation.....	45
Figure II-20. Some examples of the conditions applied to the electrospinning.....	47
Figure II-21. Results of strain-stress assay with samples of electrospun PCU.....	48
Figure II-22. Results obtained of strain-stress assay.....	49
Figure II-23. Images of the real patches with the PCU layer incorporated.....	51
Figure III-1. Models of different medical devices that actually exist.....	60
Figure III-2. Various designs created with Solid Works 2018 modeling software.....	63
Figure III-3. Final design of the two disassembled parts of the insertion system.....	64
Figure III-4. Images of the complete process of placing the patch.....	65
Figure IV-1. Scheme of the four types of failure.....	72
Figure IV-2. Graphic when the deposition grade and functional group.....	82
Figure IV-3. Schematic picture of a standard iCVD reactor.....	83

Figure IV-4. Library of the functional polymers	84
Figure IV-5. Possible interactions and reactions of the catechol groups.....	86
Figure IV-6. Cellulose molecular structure.....	89
Figure IV-7. Scheme of the horizontal plasma reactor	92
Figure IV-8. Scheme of the customized iCVD reactor.....	93
Figure IV-9. Synthesis of dopaminated hyaluronic acid.	97
Figure IV-10. Scheme of the equipment to make the multiaxial <i>ex vivo</i> test.....	99
Figure IV-11. Scheme of the equipment used to realize the adhesion phantom test.....	100
Figure IV-12. Sauter dynamometer installed at the test bank	102
Figure IV-13. Comparative graph with the ATR results of PAA thin film	106
Figure IV-14. Images of thin films of PAA and PAA/EGDA	107
Figure IV-15. Microscope images that show the solubilization.....	108
Figure IV-16. Comparative graph of ATR	109
Figure IV-17. Graph of ATR to compare the intensity of the band	110
Figure IV-18. Images obtained by optical microscopy of the PAITC thin film.....	112
Figure IV-19. Process of deposition of the PAITC thin film and reaction	113
Figure IV-20. SEM images of PAITC surface where adhering <i>E. coli</i> bacteria	113
Figure IV-21. Macroscopic view of the disc with biofilm of <i>P. aeruginosa</i>	114
Figure IV-22. Images of culture of human normal dermal fibroblastes (HNDF)	115
Figure IV-23. 1H-NMR spectra of one of the first dopaminated hyaluronic acid (DHA)	118
Figure IV-24. Images where the DHA film is separated from the silicone disc.....	119
Figure IV-25. Optical microscopy images of the silicone surface with the micropattern	120
Figure IV-26. Images of the silicone and silicone/PCU electrospun discs	121
Figure IV-27. Image of the adhesion test.....	122
Figure IV-28. Results obtained with the multiaxial test.....	124
Figure IV-29. Results obtained in toxicity tests of pyknotic index (A) and LDH.....	125
Figure IV-30. Images of peritoneal rabbit surgery	127
Figure IV-31. Images of pregnant rabbit surgery	128
Figure IV-32. Results obtained with the multiaxial test.....	130
Figure IV-33. Images of the pregnant rabbit surgery.....	132
Figure IV-34. Results obtained in the solubility test.....	133
Figure IV-35. Graphs with the results obtained from the pyknotic nuc. and LDH test.....	134
Figure IV-36. Image of implantation process in pregnant sheep	135
Figure IV-37. Comparative graph of the remaining total HPMC	137
Figure IV-38. Comparative graph of the remaining total cellulose.....	139

Figure IV-39. Picture of the first patch tested at 96 h. 140

Figure V-1. Some strategies that exist in nature and that serve as examples for bio-inspired engineering. 147

Figure V-2. Three possible designs with three repeating subunits of the microarpoons 151

Figure V-3. Microarpoons tape 152

Figure V-4. Real image of the crown of microarpoons 153

Figure V-5. Real image of the microarpoons tape..... 153

Figure V-6. Image of the silicone patch with micropattern and microarpoons crown..... 154

Figure V-7. Images with the folded patch inside the cannula of the introducer..... 155

Figure V-8. Two examples of the microarpoons integrity 156

Figure V-9. Images of the implantation of the patches 157

Figure V-10. Patches recovered after evaluation surgery at 7 days 158

Figure V-11. Design of the internal hexagonal mesh 160

Index of Tables

Table I-1. Table with some different strategies used since the actuality.	6
Table II-1. Table with some products used in biomedical research.....	17
Table II-2. Parameters affecting the electrospinning process.	20
Table II-3. Product details of NuSil MED-4950.	23
Table II-4. Table with the results obtained with different sizes of the flat patch	34
Table II-5. Table with the physical properties of solvents used to prepare the PCU solution.	43
Table II-6. Results of the macroscopic analysis of the electrospun PCU films.	44
Table II-7. Table with the range of limits for the polymer solution and process variables.	46
Table II-8. Criteria used to classify the obtained films based on a microscope analysis.	46
Table III-1 Resume of plastics commonly used in medical devices applications. ⁷¹	59
Table IV-1. Table of some marketed products presents in the biomedical market.	75
Table IV-2. Table with the composition of some bioadhesives and strategies used in research to get new bioadhesives.	79
Table IV-3. Comparative table for some CVD techniques.....	81
Table IV-4. Results of the <i>ex vivo</i> assay with phantom test.	126
Table IV-5. Results obtained in the phantom test.....	131
Table IV-6. Summary table of the results obtained in the <i>in vivo</i> assay with sheep.....	136
Table IV-7. Summary table with the tension forces supported by the patches	142
Table V-1. Summary table with the implantation times in sheep.....	158

List of Abbreviations

AA	Allylamine
AITC	Allyl isothiocyanate
ATR	Attenuated Total Refraction
AFM	Atomic Force Microscope
CVD	Chemical Vapor Deposition
CA	Citric acid
DHA	Dopaminated hyaluronic acid
DCM	Dichlormethane
DMA	Dynamometric Mechanical Assay
DMF	N, N-dimethylformamide
DMSO	Dimethyl Sulfoxide
DSA	Drop Shape Analyzer
DC	Duty Cycle
EGDA	Ethylenglicol diacrylate
GMA	Glycidyl methacrylate
HA	Hyaluronic acid
HAM	Human amniotic membranes
HPMC	Hydroxypropyl methyl cellulose
HEC	Hydroxyethyl cellulose
HNDF	Human normal dermal fibroblasts
iPPROM	Iatrogenic preterm premature rupture of membranes
iCVD	Initiated Chemical Vapor Deposition
LDH	Lactic acid dehydrogenase
MMDA/GFP	Mammary gland derived from metastatic adenocarcinoma with GFP
MIS	Minimally Invasive Surgery
PBS	Phosphate-buffered saline
PDMS	Poly(dimethylsiloxane)
PU	Polyurethane
PCU	Polycarbonate-urethane
PSA	Pressure Sensitive Adhesives
PPECVD	Pulse-Plasma Enhanced Chemical Vapor Deposition
PECVD	Plasma Enhanced Chemical Vapor Deposition
PFM	Pentafluorophenyl methacrylate

SEM	Scanning Electron Microscopy
SBF	Simulated Body Fluid
THF	Tetrahydrofuran
TCBP	1,1-Thiocarbonyldi-2 (1H)-pyridone
TGA	Thermogravimetric analysis

Chapter I. Motivations and Aims

This thesis has generated the following patent: Patch for sealing an amniotic membrane and device for placing said patch on an amniotic membrane.

EP19382512 (2019)

Motivations and Aims

The present chapter summarizes the state of the art about the rupture of the amniotic sac after the realization of minimally invasive techniques on fetal surgeries. Feature a brief introduction about the anatomical, physiological and histological view of the membranes that form the fetal sac. Also summarizes the strategies applied by different research groups until the current date to seal the remaining hole on the membranes. This thesis focuses in the development of a sealing system to avoid the iatrogenic preterm premature rupture of membranes (iPPROM). As well as shows the conditions and criteria that should satisfy this sealing patch to carry out *in vitro*, *ex vivo* and *in vivo* assays, to finally facilitate compliance with the current regulatory framework of medical devices.

1.1. Motivations and aims

Historically, traditional surgical interventions are carried out by open surgery (Figure I-1 A). Through a cut in the skin and tissues, the surgeon has access to the structures and the exposed lesion, so that he can work completely on it with a direct vision of it.

The minimally invasive surgery (MIS) is a technique (Figure I-1B) that has led to a breakthrough in the world of surgery. MIS consist of the introduction of one or several trocars through different layers and tissues to access the affected area in a non-traumatic way. Through these trocars, apart from a camera with which to see inside of the affected area, all the surgical instruments are introduced to perform the surgery. The MIS presents a series of advantages in front of the open surgery: less operative trauma, lower incidence of wound complications, fewer complications due to adhesions, shorter hospital stay, minor convalescence, and lower postoperative immunosuppression. But also present some drawbacks: technically more demanding, learning curve, fatigue and stress of the surgeon, dependent on technology, limited applicability, and restriction of the handling and extraction of the specimen¹.

With the appearance of new advances in the development of biomaterials and techniques, surgeons increasingly perform MIS. MIS such as arthroscopy, splenectomy, colectomy, vascular, cardiac, ear, nose, and throat surgery, ..., have been updated over the years. A special type of MIS is laparoscopic surgery used in gynecology and obstetrics. This surgery is really special because it involves making a small incision in the abdomen of a pregnant woman to introduce a trocar through which the surgical material necessary to perform surgery

on the fetus is introduced. Understanding that there really is great complexity in any type of surgery that can be done. In addition to opening an ethical and moral discussion or debate that each country or region must legislate to identify and mark the limits that such surgeries must have.

It is estimated that approximately 5% of women in the developed world will ever undergo an invasive procedure during their pregnancy. Currently, with the improvement of imaging techniques for fetal diagnosis used to monitor pregnancy, fetal anomalies have been detected and, therefore, the need to carry out surgical interventions with which to access the fetus directly. Already, for the last few years, fetoscopy or fetal surgery (Figure I-1 C) is used to perform these surgeries in the least invasive manner possible. By inserting a trocar of 10-12 F (3.3-4 mm in diameter) we are able to introduce the necessary surgical instruments for the corresponding surgery. Even so, the access to the fetus from a single port limits the possibilities of the technique, as opposed to if it had access from several ports.

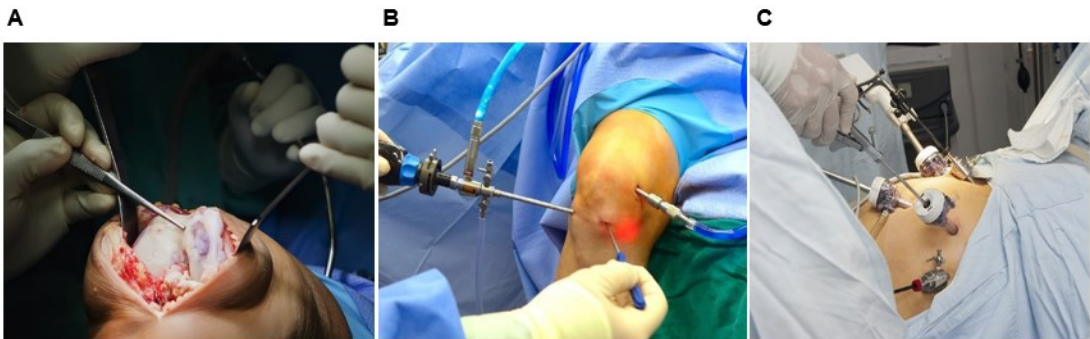


Figure I-1. Pictures with the different classes of surgeries: Traditional open surgery (A); Minimally invasive surgery (B); and fetal surgery (C).

There are some fetal diseases such as twin to twin transfusion syndrome², sever congenital diaphragmatic hernia³, or the detachment of amniotic bands that are operable through a single entry point. On the other hand, other diseases such as spina bifida syndrome o myelomeningocelle demand a greater number of ports in order to perform the surgery optimally, making the process more difficult and increasing the risks associated with the greater number of incisions and orifices made to the patient^{4,5}.

This risk in fetoscopies is defined by the remaining presence of the orifice in the chorio-amniotic membrane once the trocar is extracted. The possible post-surgical complications range from oligohydramnios, corioamnionitis, pulmonary hypoplasia, ... to even the death of the fetus if it is not viable. *In vitro* and *in vivo* studies do not show significantly cell proliferation nether self-heal capacity of the membrane. Although naturally, the membranes slide one over

the other until the amniotic fluid is blocked (Figure I-2). The permanence of this orifice can cause a subsequent rupture of the chorio-amniotic membrane when the amniotic liquid soaks between both membranes^{6,7}.

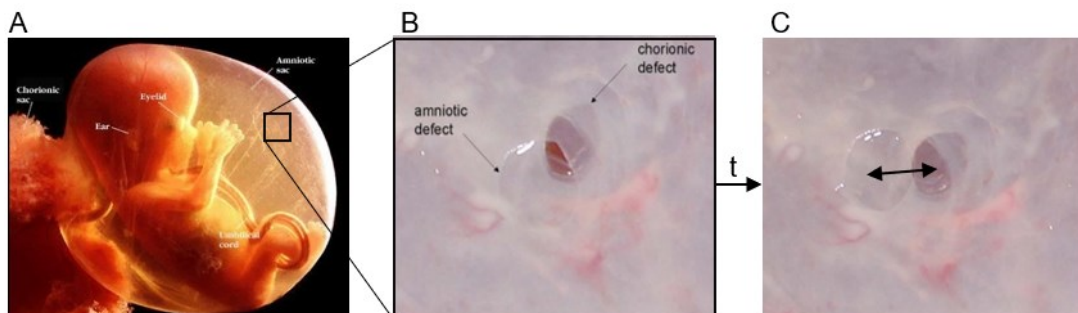


Figure I-2. Images with the movement between the chorion and-amnios. Picture of a fetus with an amniotic sac(A). (B) and (C) show the natural movement of the amnios and corion after remove the trocar⁷.

The breakdown of the membranes is called iatrogenic preterm premature rupture of membranes (iPPROM) and is one of the most common complications during pregnancy if a minimally invasive surgery is performed.

Reported data show an incidence of iPPROM of 1% after an amniocentesis to make a genetic analysis^{8,9}, up to 10% after laser coagulation for twin-twin transfusion syndrome¹⁰, >30% after fetoscopic cord ligation¹¹, and >62% after fetoscopic tracheal clipping¹².

The risk of rupture also depends on the number and diameter of the trocars, the time of the surgery, and the state of gestation. For example, the risk is 6-10% in surgeries with a single trocar, up to 47% with two trocars, and finally increase to 62% with multiple trocars.

In recent years, to avoid iPPROM, attempts have been made to seal the chorioamniotic membranes using different strategies and techniques (Table I-1). One of the most commonly used strategies has been the direct application of a plug to seal the orifices produced by the trocar. These plugs are composed of different biomaterials such as collagen (Colgen, TissueFoil E, TissueFleece, ...), Matrigel®, gelatin sponges (Gelfoam®), decellularized amniotic membrane, polyesterurethane (Degrapol®), etc. And, in order for these plugs to be retained by obturating the orifice, it is necessary to add stitches or different adhesives (Dermabond, Histoacryl, fibrin-tissucol glue, dopaminated polyethylene glycol, etc.). Although these approaches to resolving iPPROM have yielded positive results, none have shown a clear improvement in the integrity of the chorioamniotic membrane. Therefore, having evaluated the strategies used so far and understood the reasons why the iPPROM problem has not been solved, it is necessary to develop a new sealing system.

Table I-1. Table with some different strategies used since the actuality.

Study	Plugging material /Adhesive
Papadopulos et al. (1998) ¹³	Collagen (Colgen)
Deprest et al. (1999) ¹⁴	Collagen (Colgen)
Quintero et al. (1999) ¹⁵	Amniopatch (platelets and cryoprecipitate)
Luks et al. (1999) ¹⁶	Gelatin sponge (Gelfoam)
	+ myometrial suture
Gratacós et al. (2000) ¹⁷	Collagen (Colgen)
	+ myometrial suture
Gratacós et al. (2000) ¹⁷	Matrigel + myometrial suture
Devlieger et al. (2003) ¹⁸	Porcine small intestine (bioSIS) contains transforming growth factor-b and basic fibroblast factor
Ochsenbein-Kölble (2003) ¹⁹	Fibron microbeads with human amnion epithelial and mesenchimal cells
Papadopulos et al. (2006) ²⁰	Collagen (TissueFoil E®) + fibrin sealant + myometrial suture
Papadopulos et al. (2006) ²⁰	Tissue banked human amnion membrane + fibrin sealant + myometrial suture
Papadopulos et al. (2006) ²⁰ , Mallik et al. (2007) ²¹	Collagen foil (TissueFleece®) + fibrin sealant + myometrial suture
Mallik et al. (2007) ²¹	Decellularized human amnion + fibrin sealant + myometrial suture
Ochsenbein-Kölble et al. (2007) ²²	Decellularized rabbit amnion + myometrial suture
Ochsenbein-Kölble et al. (2007) ²²	Polyetherurethane (Degrapol®)
Bilic et al. (2010) ²³	DermaBond Histoacryl Tissucol Duo S fibrin glue photopolymerized PEG (pPEG) catechol-functionalized PEG (cPEG) SprayGel
Haller et al. (2011) ²⁴	cPEG
Haller et al. (2012) ²⁵	cPEG + fibrin
Perrini et al. (2015) ²⁶	Catechol-modified Tetronic (cT) cPEG
Pensabene et al. (2015) ²⁷	Ultrathin, self-adherent, Poly-L-lactic acid (PLLA) patch
Devaud et al. (2018) ²⁸	Nitinol mesh covered by an electrospun polyether (Degrapol®) membrane +Hystoacril®/Tisseel®/mussel glue

Before proposing our own solution to avoid the iPPROM we must understand the causes of this rupture and also understand the physiological, anatomical, and histological aspects of the different parts of the fetal sac.

As already mentioned, in a physiologically normal pregnancy it is an imperative requirement that the fetal membrane retains its physical integrity until the water breaks and birth. The fetal membrane has the function of containing the fetus surrounded by amniotic fluid in a kind of

sac. This membrane must support the increased pressure of the amniotic fluid, the size of the fetus itself as it grows, and the deformations caused by fetal movements.

Although the fetal membrane acts as one, it is really composed of two membranes joined together: the chorion and the amnion.

The chorion is the outermost layer, has a thickness of about 0.15 mm, is vascularized and contains three sublayers: the cytotrophoblast that is firmly adhered to the maternal decidua; The Reticular Layer and the Basal Membrane are rich in extracellular matrix formed by collagen of various types, laminin, fibronectin and proteoglycans^{29,30}.

The amnion is 20 % thinner than the chorion, it is not vascularized and contains five sublayers: The Spongy, the Fibroblastic, the Compact layers and the Basement membrane are responsible for the strength and resistance of the amnion against mechanical forces. They are rich in collagens, fibronectin, laminin, nidogen and proteoglycans. The epithelial sublayer is the innermost one, so it is in contact with the amniotic fluid, and is formed by a mono-stratified epithelium. Reason why once an injury occurs in the amnion does not self-heal^{29,30,31}. In fact, the pig is the only research animal model that can regenerate its fetal membrane(ref).

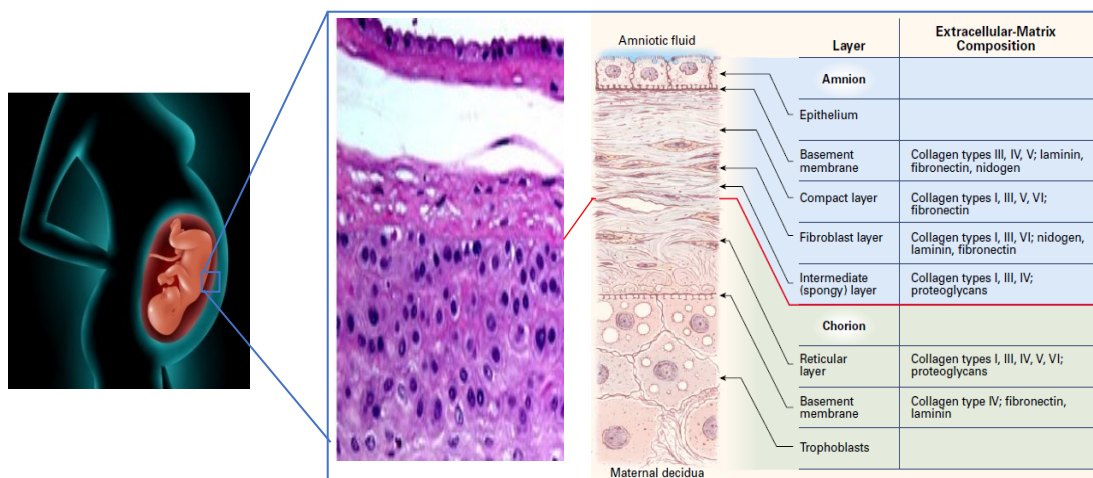


Figure I-3. Images with the layers of the chorio-amniotic membranes. H & E staining of the full thickness of human fetal membranes showing the constituent layers³² and schematic representation of the structure of the fetal membranes at term and the extra-cellular composition of the layers.

Once we have understood the structure of the different membranes, and especially that of the amnion, we are able to propose a solution for this unsolved problem.

Therefore, a sealing system is proposed consisting of a patch with adhesive properties, which will be introduced into the fetal cavity through the same trocar once the surgery on the fetus is completed. Ideally, the patch should remain adhered to the amnion until delivery, without causing any toxicological reaction to the mother or the fetus.

Although exist a natural movement of amnion sliding over the chorion during the first few minutes after the extraction of the trocar, sometimes this time is not enough to prevent the leakage of amniotic fluid. In fact, the effectiveness of this movement is key to avoiding the iPPROM, so the new patch should allow this movement.

Following our medical-scientific criteria, it would be acceptable to obtain a patch that remained adhered to the amnion for at least three days, allowing the chorioamniotic membranes to slide over each other avoiding the introduction of amniotic fluid between them and their subsequent separation and rupture.

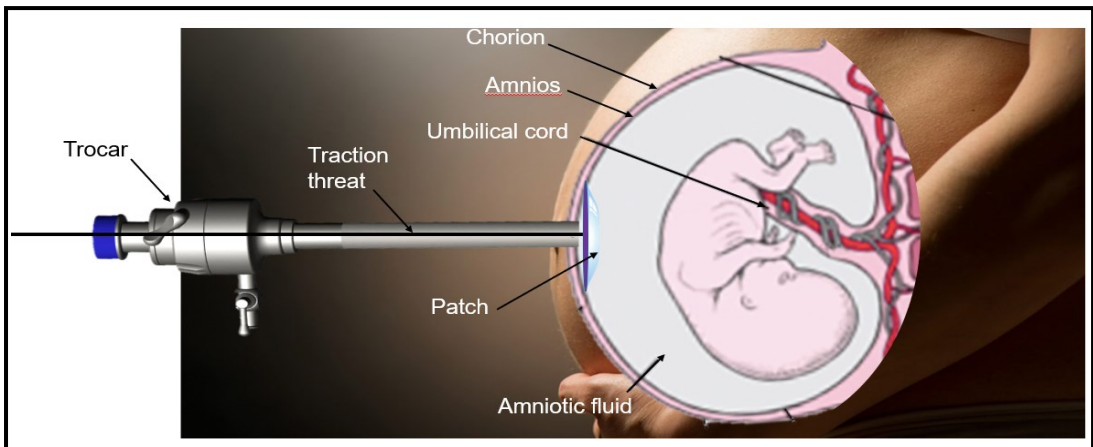


Figure I- 4. Image with the general scheme of the proposal. Placing a patch on the inner layer (amnion) with the same trocar that it uses during the fetal surgery.

Therefore, we have established a series of firsts criteria that the sealing system must accomplish:

- Non biodegradable and biocompatible patch. The patch will be removed with the placenta during at time of birth.
- A patch with disc and/or semi-lent design with small size, around a diameter of 3 mm to enter in a cannula on a folded form.
- A patch with elastomeric properties and adaptability to tension movements of the amniotic membrane.
- Biocompatible adhesive. It should not affect the integrity of the amnios either the composition of the amniotic liquid. The adhesion must less that the amniotic liquid stays in contact with the cells of monolayer of the amnios. They need oxygen and nutrients exchange.
- The adhesive must be a thin and flexible nonactivated layer when is folded. And it must be activated when enter in contact in a wet environment as is the amniotic liquid.

- The adhesive must have a quick activation (<2 mins).
- The adhesive must have a low solubility in amniotic liquid.
- The adhesive must avoid the orifice obstruction and allows the natural movement of the chorio-amniotic membranes.
- The integration of the patch and the adhesive, that is the biopatch, must remain attached to the amniotic membrane more than three days.
- The biopatch must avoid the leakage of the amniotic liquid, and the consequent detachment and break of the chorio-amniotic membranes.
- An insertion system that allows the patch unfolding across the last trocar used in the fetal surgery.
- Insertion system with optimum handling.
- A sterilizable insertion system.
- An insertion system with different lengths and diameters.
- All the parts and compounds of the sealing system must to accomplish the medical regulatory for medical devices.
- The manufacture of the different parts must be simple and fast, and with the lowest possible costs.

According to the information presented and the previously stated criteria, the final aim of the thesis are to develop a medical device that allows seal the remained orifice after fetal surgery with minimally invasive techniques. To achieve this, a patch must first be manufactured that allows the optimal deposition of a bioadhesive, and that acting together prevents the leakage of amniotic fluid and the rupture of the amniotic membrane. In addition to developing an insertion system that allows this patch to be inserted and positioned optimally on the inner side of the amnion quickly and safely.

1.2. Content of this Dissertation

Due to the non-existence in the international market of a solution to avoid iPPROM, there is an excellent opportunity to develop a sealing system that can meet a need in the sector of fetal surgeries, and that can also be a starting point for the development of other medical devices and associated technologies.

This doctoral thesis shows the steps followed to develop this sealing system, and is divided into 4 main parts or chapters:

In the Chapter II shows the design and election of the patch. The data that has been considered to choose a material with desired viscoelastic properties and that works as an optimum substrate to apply a thin adhesive layer on the top. In what way and for what reason has this surface been modified. Also explains the reason of the measures and design.

In the next part, the Chapter III shows the process to develop a device to introduce the patch without the adhesive developed yet. This process shows the evolution of the first introducer or insertion system models until the final prototype. Also shows the steps to allow assemble the final sealing system and the user manual to apply the patch quickly and safely.

In the third part, corresponding to Chapter IV, the evolution that the development of the adhesive has followed in its different phases and types is reflected. From the first idea and attempt to create a thin film with adhesive properties to the subsequent development of an adhesive based on rehydration with the amniotic fluid itself to achieve sufficient adhesive properties for the patch to adhere to the amniotic membrane and cover the hole created by the surgeon. It reflects the paradigm shift from an initial adhesion strategy to a final one, which is explained by obtaining results and discovering new factors that we were initially unaware of.

Finally, Chapter V shows the latest results obtained in *in vivo* assays on pregnant sheep. The latest update of the patch involves the incorporation of microarpoons on its surface that serve as a physical and complementary attachment to the adhesive on the amnion. Also shown are some of the latest ideas for improving the sealing system. The integration of new components would improve both the adhesion and new functions of the patch.

Chapter II. Design and Election of the Patch

Design and Election of the Patch

This chapter explains the developing process of the patch, that is, only the substrate where the adhesive is deposited. From its first designs and forms to the final designs in the form of disc and semi-lens. It shows the measures and materials chosen, as well as the different production methodology of these patches. It also includes the various surface modifications that have been applied to increase the contact surface for the deposition of the adhesive layer. Finally, it includes a section explaining the integration of a polymeric layer produced with the electrospinning technique.

2.1. Introduction

The choice and composition of the patch materials are of utmost importance. It is necessary that the materials fulfill their function and that they can be modified to create the shape we want to obtain. One factor to take into account is that the materials used must already comply with the regulatory standards for implantable materials. This will significantly accelerate the development and subsequent acceptance by regulatory agencies, if the sealing system fulfills its function.

The selection of material and the design of the patch or support for the adhesive is given by the compliance with the requirements that the patch must meet, as stated in Chapter I. Of course, the patch must be biocompatible. The material of the patch should not alter the physiological composition of the amniotic liquid or cause toxicological effects on the fetus or on the fetal membranes. Must be a non biodegradable patch because the patch must maintain its physical integrity and the composition must remain unaltered until the moment of childbirth. This is the moment when the patch will be removed together with the placenta. The material of the patch must have elastomeric properties since it must adapt to tension movements of the amniotic membrane and supports the different forces without breaking. The patch must block the leakage of the amniotic liquid through the created orifice. The designs of the patch must allow the distribution of forces on a homogeneous way, and must have a small size, around a diameter of 15-20 mm to enter in a trocar on a folded form.

Regarding the selection of the materials, the current regulations and the classification of the medical devices have been considered. We should know that on May 26th of 2020 the new Medical Device Regulation MDR (EU) 2017/745 will be applied, which will replace the current Directive of Medical Devices MDD 93/42/EEC and the Active implantable Medical Devices

Directive AIMDD 90/385/EEC. Even so, according to the current MDD 93/42 / EEC, our patch is part of the category of invasive and implantable medical device. We must keep in mind that according to rules 7 and 8, that classify implantable medical devices in the short (<30 days) and in the long term (> 30 days) successively, our medical device belongs to class III. For this reason, and in order to avoid the increase of the economic and temporary costs destined to the fulfillment of the current regulation, materials already certified for use in implantology have been chosen. Thing that considerably shortens the path to future validations.

In the international market currently a great variety of products manufactured from non-biodegradable polymers exists (Table II-1), that after fulfilling the requirements of the regulatory organism are suitable for their use in biomedical applications^{33,34}. Even though these polymers have a big interest for us, in order to find a material for the development of our patch, since the initial phase and after evaluating several options, elastomeric silicone has been chosen. For the first tests poly(dimethylsiloxane) PDMS has been used. PDMS, which is a member of a group of polymeric organosilicone compounds that are widely known as silicones, is an elastomeric polymer with interesting properties as nontoxicity, biocompatibility, blood compatibility, elasticity, transparency, and durability^{33,35}. PDMS can be used for a variety of research applications, including microfluidic devices³⁶ as lab-on-a-chip³⁷ and organ-on-a-chip³⁸, surface to control the cell adhesion in cell cultures³⁹, etc. The mechanical properties of elastomers are great interest due to their resistance to tensile force and their elasticity. This implies that the final designs manufactured with silicones retain the initial shape after applying forces of crushing, stretching, folding, twisting, provided that its Young's modulus stay within their elastic region. As we have commented, the use of PDMS is of great interest for the first laboratory tests, but it cannot be used in implantology since it does not comply with the current regulations for such use. A member of the family of silicones that does comply with the regulations for use in implantology is medical grade silicone. Having practically similar properties to PDMS, medical grade silicone has the advantage that new tests should not be carried out to comply with current regulations, since the manufacturer has already obtained the certification of medical use for said material.

Chapter II- Design and Election of the Patch

Table II-1. Table with some products used in biomedical research.

Chemical name	Chemical Structure	Key Property	Applications	Trade name (manufacturer)
Poly(ethylene) (PE)	$\left(\begin{array}{c} \text{H}_2 \\ \\ \text{C} - \text{C} \\ \\ \text{H}_2 \end{array} \right)_n$	Strength and lubricity	Orthopedic implants and catheters	
Poly(propylene) (PP)	$\left(\begin{array}{c} \text{CH}_3 \\ \\ \text{CH} - \text{C} \\ \\ \text{H}_2 \end{array} \right)_n$	Chemical inertness and rigidity	Drug delivery, meshes and sutures	Actisite® (Procter & Gamble)
Poly(tetrafluorethylene) (PTFE)	$\left(\begin{array}{c} \text{F}_2 \\ \\ \text{C} - \text{C} \\ \\ \text{F}_2 \end{array} \right)_n$	Chemical and biological inertness and lubricity	Hollow fibers for enzyme immobilization, vascular graft, guided tissue regeneration and barrier membrane in the prevention of tissue adhesions	Teflon® (DuPont), Gore-Tex® (W.L. Gore & Associates)
Poly(methylmetacrylate) (PMMA)	$\left[\begin{array}{c} \text{CH}_3 \\ \\ \text{C} - \text{C} \\ \\ \text{H}_2 \quad \text{CO}_2\text{CH}_3 \end{array} \right]_n$	Hard material, excellent optical transparency	Bone cement, ocular lens	Palacos® and Osteopal® (Merck)
Ethylene-co-vinylacetate (EVA)	$\left[\begin{array}{c} \text{H}_2 - \text{C} - \text{C} \\ \quad \\ \text{H}_2 \quad \text{H}_2 \end{array} \right]_x \left[\begin{array}{c} \text{H}_3 \\ \\ \text{C} - \text{C} \\ \\ \text{H} \quad \text{OH} \end{array} \right]_y$	Elasticity, film forming properties	Implantable drug delivery devices	Elvax® (DuPont), Ocuser® (Alza), Implanon® (NV Organon)
Poly(dimethylsiloxane) (PDMS)	$\left[\begin{array}{c} \text{CH}_3 \\ \\ \text{Si} - \text{O} \\ \\ \text{CH}_3 \end{array} \right]_n$	Ease of processing, biological inertness, oxygen permeability and excellent optical transparency	Implantable drug delivery devices, device coatings, gas exchange membranes, ocular lens, orbital implants	Silastic® and Sylgard® (Dow Chemicals), NuSil® (Avantor)
Poly(ether-urethanes) (PU)	$\left[\text{Aromatic} - \text{N} - \overset{\text{O}}{\parallel} \text{C} - \text{O} - (\text{Polyther}) \right]_n$	Blood compatibility and rubber-like elasticity	Vascular grafts, heart valves, blood contacting devices, coatings	Tecoflex® and Tecothane® (Thermedeis), BioSpan® (Polymer Technology Group, Inc)
Poly(ethylene terphthalate) (PET)	$\left[\begin{array}{c} \text{O} \\ \parallel \\ \text{C} - \text{C} \\ \quad \\ \text{C}_6\text{H}_4 \quad \text{O} \\ \quad \\ \text{O} - \text{C} - \text{O} - (\text{CH}_2)_2 - \text{O} \end{array} \right]_n$	Fiber forming properties and slow <i>in vivo</i> degradation	Knitted Dacron vascular grafts, coatings on degradable sutures, meshes in abdominal surgery	Dacron® (DuPont)
Poly(sulphone) (PS)	$\left[\text{Aromatic Ether} - \overset{\text{O}}{\parallel} \text{S} - \overset{\text{O}}{\parallel} \right]_n$	Chemical inertness, creep resistant	Hollow fibers and membranes for immobilization of biomolecules in extra-corporeal devices	Radel® and Udel® (Solvay)
Poly(ethyleneoxide) (PEO, PEG)	$\left(\begin{array}{c} \text{H}_2 \\ \\ \text{C} - \text{C} - \text{O} \\ \quad \\ \text{H}_2 \quad \text{H}_2 \end{array} \right)_n$	Negligible protein adsorption and hydrogel forming characteristics	Passivation of devices toward protein adsorption and cell encapsulation	
Poly(ethyleneoxide-co-propyleneoxide) (PEO-PPG)	$\left(\begin{array}{c} \text{H}_2 \\ \\ \text{C} - \text{C} - \text{O} \\ \quad \\ \text{H}_2 \quad \text{H}_2 \end{array} \right)_x \left(\begin{array}{c} \text{CH}_3 \\ \\ \text{C} - \text{C} - \text{O} \\ \quad \\ \text{H} \quad \text{H}_2 \end{array} \right)_y$	Ampiphilicity and gel forming properties	Emulsifier	Pluronic® (BASF)
Poly(vinylalcohol) (PVA)	$\left(\begin{array}{c} \text{H}_2 \\ \\ \text{C} - \text{C} \\ \quad \\ \text{CH} \quad \text{OH} \end{array} \right)_n$	Surfactant and gel-forming properties	Emulsifier in drug encapsulation processes and matrix for sustained drug delivery	

Another polymeric biomaterial of interest is polyurethane (PU). PU is a another elastomeric compound with excellent mechanical properties and stability, and it is commonly used for medical application and the developing of medical devices as catheters, artificial heart valves⁴⁰, breast implants⁴¹, aortic grafts, dialysis membranes, intra-aortic balloon pumps and others common short-term implants and bioadhesives.^{42,43} The physico-mechanical properties of PU depend mainly on the proportion of its three components: a diisocyanate, an oligomeric macromonomer and a chain extender, which in turn form repeated blocks with soft and hard segments.

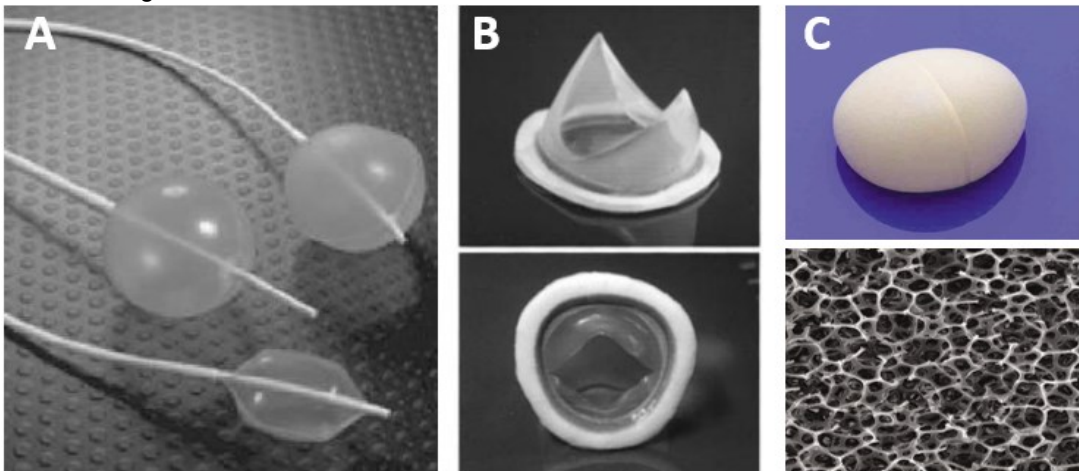


Figure II-1. Examples of PU implants and medical devices. Low pressure balloons(A)⁴²; heart valve with special design for the mitral position (B)⁴⁰; PU foam-covered silicone gel-filled breast implant and SEM view of the open-cell PU foam (C).

For the commented reasons and due to its excellent biocompatibility, the integration of a microfibers or microsp sponge of PU on the surface of the silicone patch could be interesting. This incorporation would allow obtaining a suitable substrate on which to deposit the bioadhesives that will be developed in Chapter III. While the silicone substrate would be manufactured by additive injection techniques, to obtain a layer of PU microfibers it is necessary to use another manufacturing technique such as electrospinning.

The electrospinning technique allows the creation of polymeric matrices or films from the deposition of micro and nanofibers, and a porosity which depends on the space between fibers (Figure II-2 C). In contrast to the classical methods of manufacturing PU parts by additive manufacturing in molds, we can modify the mechanical properties of a PU film by manufacturing it in the form of fibers, which together form a mesh with a large increase in surface area per unit volume. Electrospun nanofiber mats are used in a wide variety of science applications as scaffolds for cell cultures, drug delivery, wound dressing materials, air filters, sensors, etc.⁴⁴

The electrospinning equipment also allows the electro spraying technique, with which micro and nano beads can be obtained from different polymeric solutions. Depending of the final result that we want to obtain, it uses one technique or another (Figure II-2).

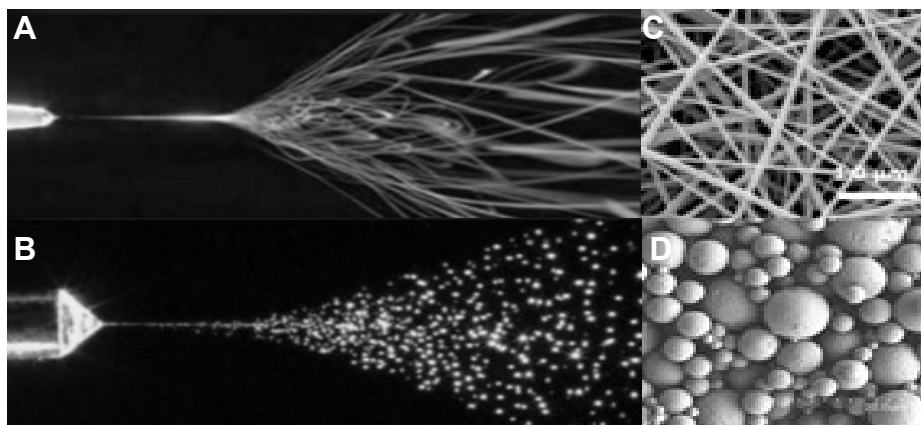


Figure II-2. Picture in time lapse of the fibers produced in electrospinning process during the deposition (A) and the microdroplets produced in the electro spraying process (B). SEM images of electrospun fibers (C) and electro sprayed microbeads (D). Images adapted of Bioinicia website.

Currently, the electrospinning technique has become a very attractive process thanks to the ability to transform a wide range of nanofiber materials at low cost and with relative simplicity.⁴⁵ Electrospun nanofibers of synthetic polymers (such as Polyurethane (PU)^{44,46}, Poly(L-lactide) (PLLA)⁴⁷, Poly(ϵ -caprolactone) (PCL)⁴⁸ or Polystyrene (PS))⁴⁹, natural polymers (proteins such as collagen^{50–52}, fibrinogen⁵³ and silk⁵⁴), and even polysaccharides (such as chitosan⁵⁵ and ⁵⁶) have been reported, and they are increasingly used as extracellular matrix cell research and in tissue regeneration therapies.⁵⁷

To understand better the electrospinning technique, we must consider some briefs and basics concepts that explain the morphology of the fibers that are intended to form. The electrospinning equipment (Figure II-3) is formed by a syringe filled with a polymer solution, whose flow can be modified by means of a syringe pump. This polymer solution is injected through a needle to which a high voltage is applied. When leaving, and due to surface tension, conductivity and surface charge density, the Taylor cone is formed, and the solution is transformed into microfibers/ microdroplets that are directed to a collector because that is in contact with a ground. Therefore, due to the potential difference between the needle and the collector they are deposited on said collector. The distance between the needle and the collector is critical since the solvent present in the polymer solution needs to be evaporated so that dry fibers/ drops are deposited on the collector. Depending on the orientation of the polymer fibers we want to get, it can be used from a flat collector, to a rotatory collector, or other customized collectors.^{45,58}

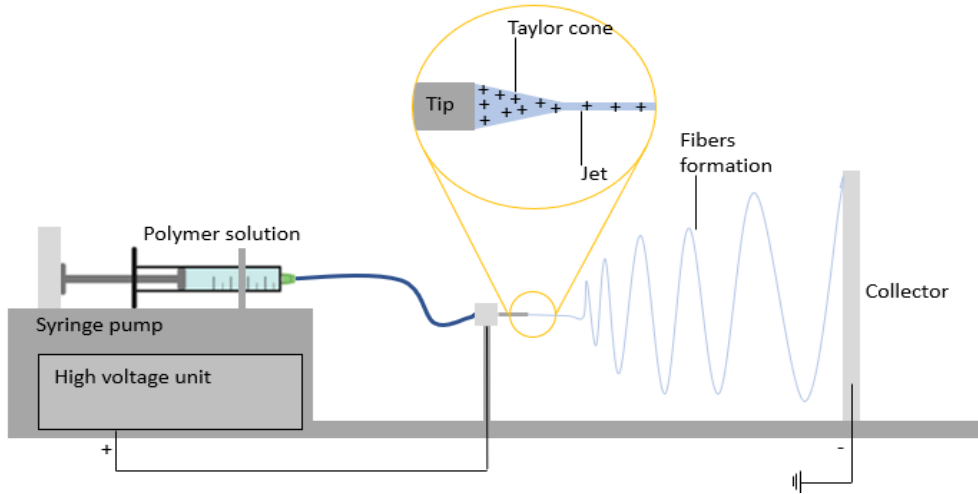


Figure II-3. Scheme of our electrospinning equipment.

The morphology of the fibers changes if its changes the solution parameters (polymer concentration, molecular weight, viscosity, solvents used, surface tensions and conductivity/surface charge density), the process parameters (applied voltage, feed/flow rate, types of collectors, distance between the tip and the collector, tip diameter), and finally, the ambient parameters (humidity, temperatures, etc.)(Table II-2).^{57,59}

Table II-2. Parameters affecting the electrospinning process.

Solution parameters	Process parameters	Environmental properties
Concentration.	Electrostatic Potential	Temperature
Viscosity	Electric Field Strength	Humidity
Surface Tension	Electrostatic Field Shape	Local Atmosphere Flow
Conductivity	Working distance	Atmospheric composition
Dielectric constant	Feed Rate	Pressure
Solvent volatility	Orifice Diameter	

Therefore, one of our hypotheses is that the silicone layer has, on the one hand, a mechanical support function for its viscoelastic properties, and on the other, an impermeable effect on the amniotic fluid as a physical barrier. While the electrospun layer of PU has the function, once integrated into the silicone, to be a mat in which the adhesive can interact with a larger contact surface.

Once a time the substrate is obtained, it is necessary to establish a strategy to deposit the adhesives on the surface of the patch. If it wants to covalently attach an adhesive to the surface of the patch, it must be taken into account that silicone and PU are not a reactive compounds. Due to this lack of reactivity, it is necessary to apply some technique on these materials to achieve a reactive surface.

Cured silicone has hydrophobic properties due to the presence of methyl groups exposed in its most superficial part. This means that its surface repels water and, therefore, prevents possible interactions between its surface and some type of adhesive that we would deposit later. For this reason, the surface properties must be modified. One strategy to get this is to create radicals in the surface to make covalent bonds between the adhesive and the silicone surface. In our lab we are experts in the surface modification of wide variety of biomaterials, for this reason the functionalization of the silicone surface by plasma techniques⁶⁰ has been selected.

Exist plasma treatments with oxygen, argon, hydrogen, ..., and each gas produce a unique effect in the surfaces. For example, plasma surface etching is realized with argon gas or a mixture with oxygen, and usually is used on metallic surfaces to create non-oxidizable micro- and nano-rough surfaces⁶¹ and remove impurities⁶² (Figure II-4).

In our case we use a plasma surface activation with oxygen on silicone and PU. This treatment attaches the surface layer of the both biomaterials forming oxygen radicals that impact with the molecules on the surface creating different families of radicals, perfects to bind to lateral reactive chains of the selected adhesives.

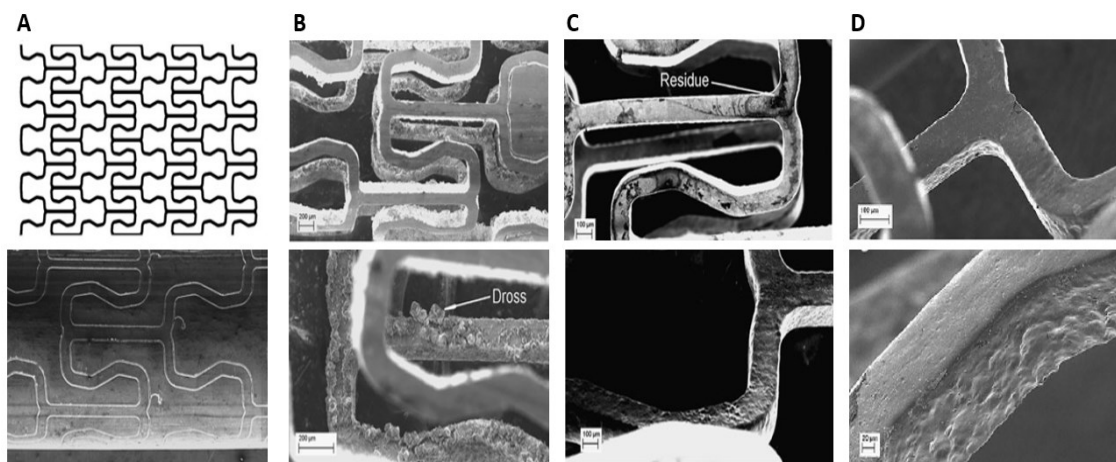


Figure II-4. SEM images of the surface modification of absorbable magnesium stent by etching. A 2-D CAD model of the unfurled stent geometry and SEM image of a tube in which the stent pattern was machined; Machined stent remaining without the inner sections and dross that formed on the inner surface of the stent (B); Stent surface after chemical etching with a mixture of 90% Ar and 10% O₂, when can observe some residues (dark areas) (C); and the aspect of a finish stent after oxygen plasma cleaning process(D).⁶²

Therefore, this chapter aims to show the process to develop a biocompatible patch that can be used to seal the orifice in the chorioamniotic membrane, and act as a substrate for the adhesives that will be developed in Chapters IV and V. The mechanical properties of the materials that will form the patch will be evaluated. Several surface modification techniques will also be used to increase the interaction between the patch and the future adhesives.

2.2. Material and Methods

2.2.1. Selection and use of the material for the patch

Among the different possibilities to choose the material with which the patch was made, silicone was chosen. Silicone has been selected because has a great form memory, and this is a very interesting property because allows been fold and unfold several times without affect their viscoelastic properties.

In the firsts approaches Sylgard® 184 silicone elastomer (Dow Corning) was used since it is a PDMS which commonly is used for the development of microfluidic devices. In view of the final implantable product it was decided to replace it by a medical grade silicone. MED-4950 (NuSil™) is part of the Liquid Silicone Rubber (LSR) that cure with platinum and is also widely used in mold injection. MED-4950 was selected for its interesting final viscoelastic properties, conditions of curing, price, and to facilitate compliance with current regulations Table II-3). Even that NuSil MED-4950 shall not be considered for use in human implantation for a period of greater than 29 days, exist the top compatible model MED-4850 which is implantable above these 30 days.

Table II-3. Product details of NuSil MED-4950.

PROPERTY	AVERAGE RESULT
Durometer	50 Type A
Tensile	6.9 MPa
Elongation	400 %
Tear	42.86 kN/m
Appearance	Translucent
Cure	5 minutes / 150 °C
Cure Rate Scorch	1.4 minutes
Cure Rate T90	2.35 minutes
Cure System	Platinum
Extrusion Rate	95 g/minute
Mix Ratio	1:1
Specific Gravity	1.14
Stress @ Strain	2.76 MPa / 200 %
Work Time	>72 hours
Comment	Injection Molding Elastomer

As a general preparation, to obtain de cured silicone, MED-4950 is prepared with a mix ratio of 1:1 of both components, mixed in the DAC-150 SpeedMixer™ during minimum 10 cycles of 60 seconds to 3000 rpm until the major part of the bubbles are removed, and opening the tap to avoid to increase the temperature. Deposit or inject the degassed mix of silicone in a

selected mold and cure the silicone in a 130 °C oven for 20 mins according the data obtained in a lab and depending of the mold. And then let it sit at room temperature overnight so that the silicone chains stabilize. To characterize the properties of medical grade silicone it has used the strain-stress assay of four films with a thickness of 0.2, 0.4, 0.5 and 0.6 mm with DMA Q800 (TA Instruments) and Universal V4.5A software. The sizes of the samples have been of 0.5 mm x 2 mm with three repetitions for every size of sample, the speed was 4000 $\mu\text{m}/\text{min}$ during 10 000 μm .

2.2.2. Design of the patch

Together with the medical team, to decide the design of the patch, the possibility of developing it in two different designs was considered. Both designs should allow folding inside the cannula and unfolding once it is inside the fetal cavity, always maintaining the original shape. These designs and next to the selected material should have a memory effect.

To facilitate the tests, study the behavior, and evaluate the use of different adhesives in the patch we decided to work with a flat disc-shaped design. The sizes of this patch have been selected according to the diameter of the hole in the chorio-amniotic membrane and the capacity of the patch to fold into de canula and unfold it without loss the final form.

The second design is based on the lens or semi-lens form. This form is similar of a contact lens, but with the addition that an outer ring is incorporated as a support surface for the adhesive (The methodology for the bioadhesive deposition can be seen in chapter IV). Several designs were presented (Figure II-5) and their folding and unfolding capacity was evaluated.

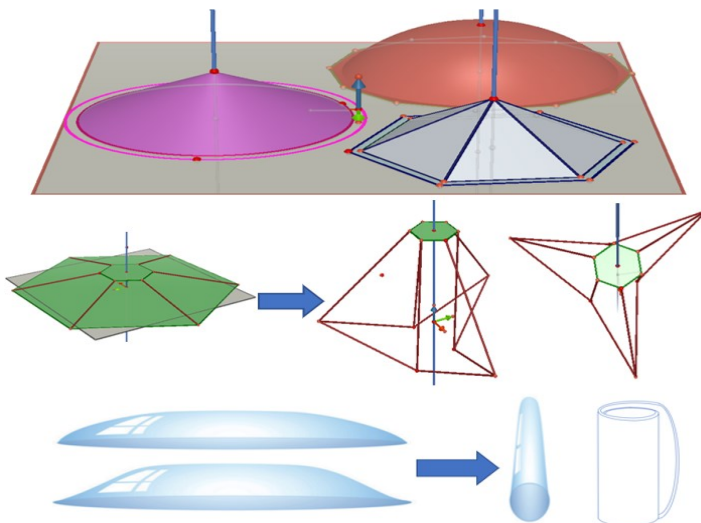


Figure II-5 Examples of the firsts designs of the lens/semi-lens patch.

After several meetings with the medical team, the simple semi-lens was selected since the initial hypothesis is based on the fact that the dome helps to support the intrauterine pressures exerted by the amniotic fluid on the patch, and at the same time it avoids the deformation and collapse of the patch at the moment of exerting mechanical traction to keep it attached to the amnion while the adhesive present in the outer ring is activated.

The selection of the flat disc measurements has been realized evaluating several factors qualitatively in a table: the ability of the patch to be able to roll up, the ability to be inserted into an 8 F and 10 F cannula, the ability to be deployed, and even which point retains the original shape. To obtain the flat disc samples, films of medical silicone with 0.28 mm, 0.37 mm, 0.5 mm and 0.66 mm thick have been used, and the films have been cut with a metal hole punch of 10.37 mm, 15.1 mm and 20 mm diameter.

The sizes of the semi-lens patches will be selected according with the similar factors considered for the flat disc.

2.2.3. Incorporation of a micropattern in the patch surface

Due to a smooth silicone offers a limited contact surface resulting in a deficient interaction with the adhesive, the increase of the surface with the incorporation of micropattern is considered. To increase this contact surface on the adhesive side of the flat and semi-lens patch a micropattern with concave hemi-spheres have been added.

Initially, a stainless-steel mold with a convex hemi-sphere matrix with depths of 0.02, 0.05, 0.1, 0.15 and 0.2 mm was designed (Figure II-6). The objective is to evaluate the capacity of the mold to obtain an entire structure with the designed pattern in the surface of the silicone. Optical microscopic techniques with Leica DM2500M are used to evaluate the structure of the pattern, identify the possible aberrations on the surface, and guarantee the reproducibility in the production of the selected pattern on the silicone.

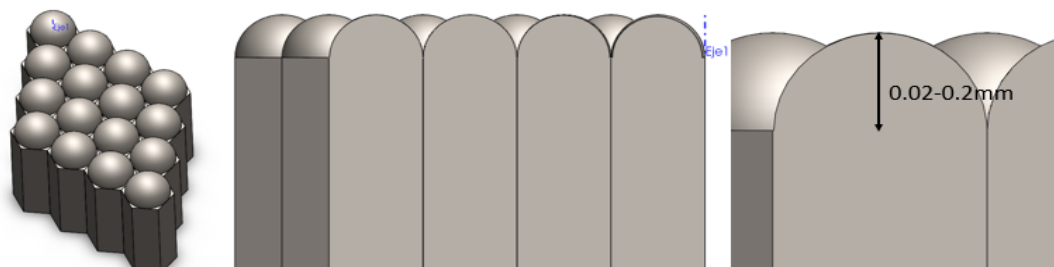


Figure II-6. 3D design of the micropattern with convex hemi-spheres made with SolidWorks software

Furthermore, the wettability of the silicone surface obtained using the different molds has also been evaluated, choosing the one with the lowest values in the analysis of contact angle (Figure II-8) to create a final mold with higher size.

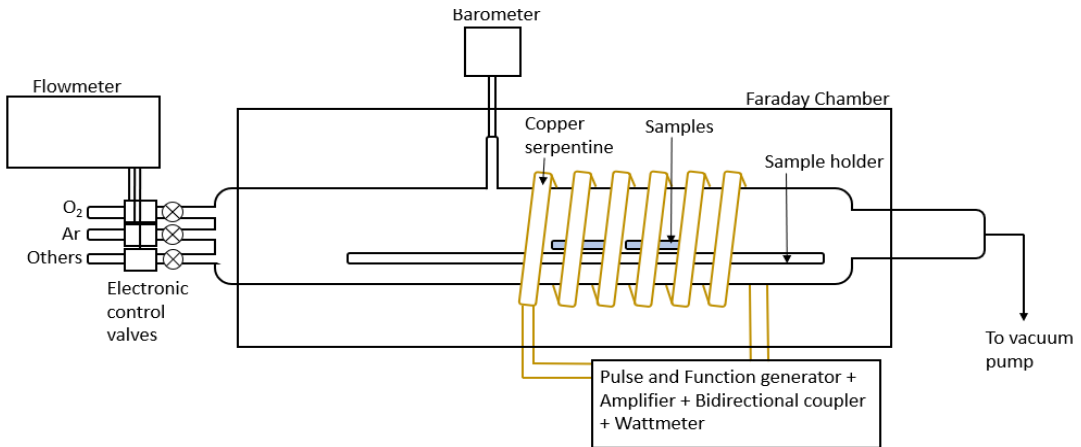


Figure II-7. Scheme of the customized plasma reactor. The gas enters thanks to the gas control of the flowmeter to the glass vacuum chamber. Once the time the working press gas is the optimal, the generator is switch on with the voltage selected and the plasma process begins. This allows the creation of active radicals on the samples surface.

The data have been obtained with a Drop Shape Analyzer (DSA)100S (Krüss) by sessile drop method before and after oxygen plasma activation. The sessile drop method is the standard arrangement for optical measurement of the static contact angle. This method is used to determine the surface free energy of a solid. According to Young's equation ($\sigma_s = \sigma_{sl} + \sigma_l \cdot \cos\Theta$), there is a relationship between the contact angle Θ , the surface tension of the liquid σ_l , the interfacial tension σ_{sl} between liquid and solid and the surface free energy σ_s of the solid. In our case this method shows the wettability changes of the five silicone patch surfaces produced with the five stainless steel molds with and without plasma activation. The surface hydrophobicity rises as the value of the contact angle with the drop, in our case of miliQ water, increases. While hydrophilicity rises as the contact angle of the same drop decreases.

Activations of the silicone surfaces have been made by a plasma reactor of its own manufacture (Figure II-7). This plasma reactor allows to work from 2.2×10^{-2} mbar of minimum pressure and to apply voltages between 10 and 210 W with different duty cycles. After some tests, the optimized conditions of the surface activation are oxygen flow of 9 mL/min with an oxygen final work pressure of 1.5×10^{-1} mbar, power of RF generator of 60 W, continuous plasma or duty cycle ($DC = (t_{on}/t_{on} + t_{off})$) of 1/1, during 2 mins.

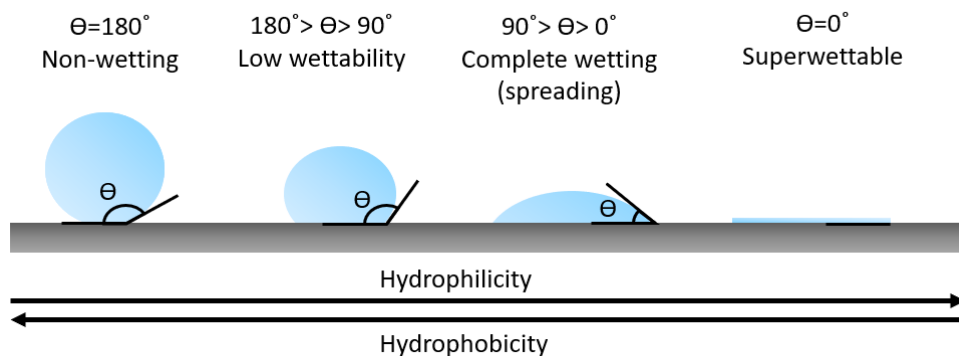


Figure II-8 Schematic diagram of contact angles of a drop obtained with DSA.

2.2.4. Production of the patches with flat and hemi-lens design

To obtain the flat design, the mixed, degassed, and uncured silicone (as shown in the previous point) is deposited gently on the texturized stainless-steel mold with a spatula. Immediately the leftover silicone is removed with a paint applicator until a thickness of 0.5 mm is reached. Then, cure the silicone in a 130 °C oven for 20 mins. Finally let stand for 24 hours at room temperature and it use a metallic punch with a 16.7 mm diameter to obtain de disc shape patch.

To obtain the semi-lens design, it needs two molds created in the first step with a Solid Works software (Dassault Systems) according with the selected dimensions (Figure II-9). The bottom mold has the convex shape with six channels to remove the leftover silicone, and it is made by stainless steel (Microrrelleus SA, Sabadell). The top mold has the concave design and is printed with the HP Multi Jet Fusion 4200 3D printer (Barel SA, Molins de Rei). This top mold is made with PA12, a polyamide and not in stainless steel by practical and economic reasons, and it is the way to test various thicknesses on quick way. The final intention is to also produce the top mold in stainless steel.

To produce the semi-lens patch, the silicone is mixed as described in flat design. Approximately 250 µl of mixed silicone is injected into the two pieces of the mold. The pieces of the mold are pressed firmly and gently with a holding clamp and are introduced in a 120 °C oven during 30 mins. Then, both molds are carefully separated, and finally the left cured silicone is removed with a round metal puncher.

Finally, in order to have an anchor point in the patch and to be able to exert tensile forces towards the amnion until the adhesive is activated, a suture thread used in ophthalmology is incorporated inside it just after depositing the uncured silicone. Currently this thread is made of braided multifilament silk (Laboratorio Aragó, Barcelona). This type of thread has some interesting characteristics as it has a high tensile strength and a high flexibility. Threads of other materials have also been used such as Nylon, Norefil, polypropylene, Supramid, Supolene, etc.

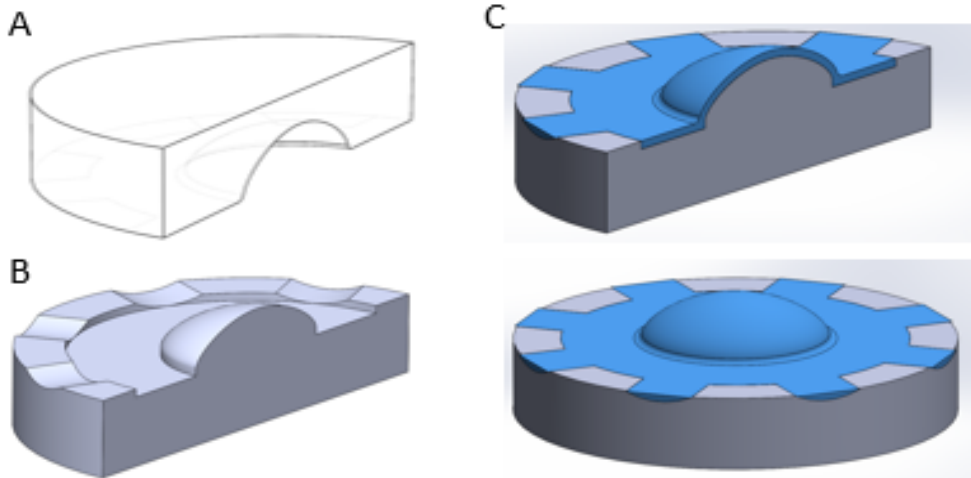


Figure II-9. Mold design with Solid Works software with semi-lens shape. Top mold design (A); Bottom mold design (B); Bottom mold design with the semi-lens patch (C).

2.2.5. Integration of an electrospun layer of Polycarbonate-urethane.

Once the patches have been obtained with the flat and semi-lens design, and a texturing in the form of a hemisphere pattern has been applied to the surface in order to increase its contact surface, it is decided to create another type of surface for the same patches. It is intended to create other types of surface by replacing the hemisphere pattern with a mesh-shaped surface layer using the electrospinning technique of a thermoplastic to further increase the contact surface with the adhesive. In this way, patches with two different types of surface are obtained that can later be compared by quantifying the interaction between adhesive and substrate. Interaction that influences the final adhesion of the patch to the amniotic membrane.

To produce the thermoplastic electrospun layer, Fluidnatek® LE-10 of Bioinicia has been used (Figure II-10). This electrospinning equipment allows to deposit a polymeric nano and microfilaments in layer form, applying and modifying different parameters:

- Voltage between 0-30 KV.
- Distance between the tip and the collector from 1 to 29cm.
- Use of different collectors as planes, customized and rotatory drum (200 - 2000 rpm).
- Tips with two diameters (0.88 or 1.7 mm).
- Use one or two polymeric solutions with a coaxial tip.
- Feed rate of the polymeric solution from 0.07 µl/h to 21 500 mL/h.
- Camera to check the Taylor cone.
- Check but not control the environmental conditions into the chamber.



Figure II-10. Electrospinning equipment used. Fluidnatek® LE-10 from Bioinicia.

Final polymeric formulation used

The 10% w/v polycarbonate-urethane (PCU) polymer (Bionate® II PCU, DSM) solution to be used for electrospinning is prepared by heating the PCU Bionate® II PCU from DSM pellets to approximately 80°C in a glass bottle with ISO screw for 30 min, with continuous agitation. The temperature is then lowered to 60 °C, N, N-dimethylformamide (DMF for analysis, PanReac AppliChem) and tetrahydrofuran (THF anhydrous, ≥99.9%, Sigma-Aldrich) are added in 3:2 ratio, and the bottle is quickly closed. It is left stirring at the same temperature for 48h.

Final established condition of electrospinning technique

The final conditions established so that the PCU fibers are homogeneous, have a diameter of 1.22 µm and the film has a thickness of 0.025 mm are: polymeric solution flow of 2 mL/h with a nozzle of 1.7 mm inside diameter with the collector 100 x 100 mm custom stainless steel plane, 18 cm tip-collector distance and 13 kV of voltage. The voltage may vary depending on the stability of the Taylor cone. Once the electrospun PCU film is obtained, it is carefully separated from the collector, let it stabilize at room temperature overnight and put it in a weak vacuum chamber so that the solvents evaporate.

Production of the patch of silicone and integrated PCU electrospun layer

Once the PCU electrospun film is ready, a layer of medical grade silicone with a thickness of 0.5 mm is deposited in a smooth stainless steel mold, and carefully the electrospun PCU film is placed on the silicone with the face of the collector down. Press lightly with a flat weight and place it on the oven at 120 °C for 20 mins.

The semi-lens shaped patch is produced in a similar way, but first it is necessary to cut the PCU layer in a ring shape and place it in the convex mold. Then fill the mold with silicone, close it as a sandwich with a clamping pliers and place it on the oven at 60 °C for 2 hours. Once the silicone has cured, the mold pieces are carefully separated and the half-lens is removed, which must be trimmed.

Methodology to evaluate the conditions to get a homogeneous electrospun PCU

There are a group of variables that intervene in the formation of a homogeneous electrospun film from each polymer solution. Therefore, it is necessary to identify possible study variables and establish the limits associated with each of them. It is imperative to know to what degree each of them influences. These variables can be divided between the variables that we can control, such as those of each polymer solution and those of the electrospinning process, and the environmental variables that we practically cannot control.

a. Variables of the polymer solution.

- The concentration of the polymer, its molecular weight and the solvents used influence the electrospinning process. To prepare the polymer solutions, medical grade PCU (Bionate® II PCU, DSM) was used with a molecular weight of 1.1×10^5 g/mol, and at concentrations between 5 % and 15 % w/v, and ratios of DMF:THF 2:3 and 3:2.
- The viscosity of the prepared solutions was evaluated with the AR 2000 rheometer from TA Instruments, with a flow test applying the following conditions: Branch of effort (stress) of 0.1 – 200 Pa for 60 seconds, at a temperature of 20 °C and using a head in 40 mm conical.
- The surface tension was quantified with the Drop Shape Analyzer (DSA) 100 from Krüss GmbH, by the pendant drop technique at room temperature.
- Conductivity was assessed with the CRISON EC-Meter Basic 30+ conductivity meter with a 50 70 HACH probe.

b. Variables of the electrospun process.

In the electrospinning process, independent and dependent variables have been considered.

- The distance between the nozzle and the collector.
- The feed rate or flow rate.
- The diameter of the nozzle.
- The applied voltage, which depends on the previous variables.
- The volume deposited that depends on the thickness of the electrospun layer that we want, and therefore, on the duration of the experiment.

c. Environmental variables.

Environmental variables such as temperature and humidity can influence the morphology of the fibers and the electrospinning process. Although it is true that the moment to electrospun could have been chosen within a range of temperatures and humidity, in our case the environmental variables were only recorded to identify if they could influence on the result. The EasyLog EL-USB-2-LCD thermohygrometer was used for the recording.

The morphology of the fibers (diameter, % porosity, homogeneity, aberrations, alignment, etc.) was analyzed by SEM (JEOL JSM-6460). To analyze these images the Image J free software was used.

To characterize the mechanical properties of the PCU electrospun films and silicone + PCU a strain-stress assay has made, with a DMA Q800 (TA Instruments). A strain-stress assay is established with 12 mm x 3 mm specimens and 500 μm thick. Silicone specimens are compared with electrospun PCU specimens and silicone specimens with an integrated electrospun CPU layer. Assay conditions: 4 000 $\mu\text{m}/\text{min}$ with a total elongation of 10 000 μm .

2.3. Results and Discussion

2.3.1. Selection and use of the material for the patch

In order to develop a patch that would adapt to the movements of the membranes, that could preserve the initially designed shape, and that would prevent the passage of amniotic fluid through the orifice created by the trocar, an implantable elastomeric material was selected. Starting the tests using a substrate made of a material that met the regulations for use in implantology was crucial as it would pave the way in the event of developing a patch that finally met the objectives set. Although PDMS was mainly used to do the first tests, it was quickly replaced by medical grade silicone, since PDMS did not comply with the regulations for short or long-term implantology.

Once the medical grade silicone was selected, we wanted to find out what thickness would be the most suitable for the patch, since it had to be rigid enough to be able to unfold outside the cannula and not deform by the pressure of the amniotic fluid, but not so much as to avoid membrane movements. That is, it had to accompany, at least in part, its natural movement without creating points of tension in it. To obtain some type of data in reference to the properties of medical silicone, a strain-stress test was carried out in DMA to characterize it. The data obtained (Figure II-11) showed the characteristic curves of the elastomeric materials, where even at 80 % stretching there is no plastic deformation or breakage of the samples. These data confirm the properties of the medical grade silicone we are looking for. The Young's modulus of this medical grade silicone is between 1.16 MPa and 1.84 MPa, and

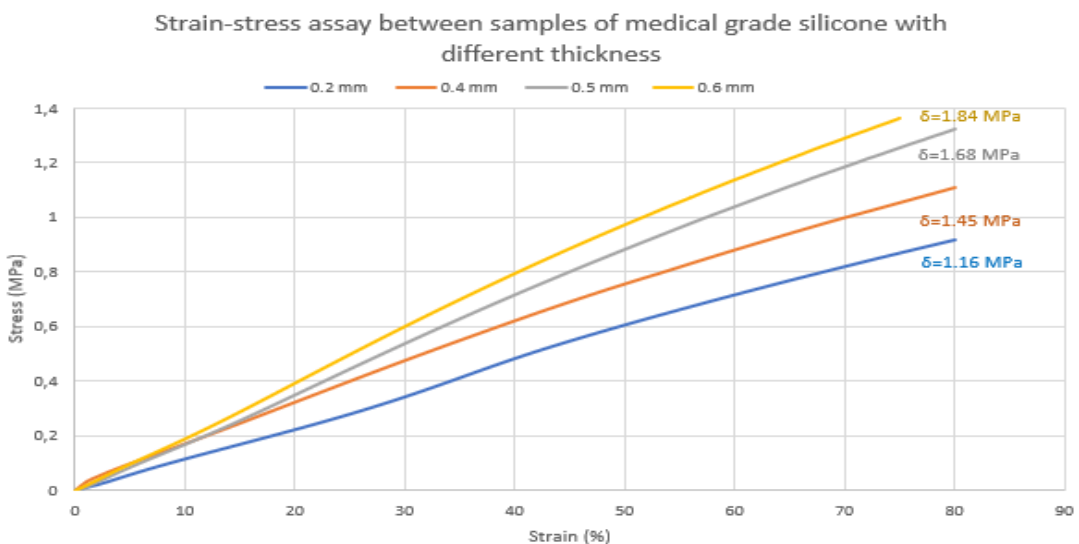


Figure II-11. Results obtained with strain-stress assay of the silicone samples of 0.2, 0.4, 0.5 and 0.6 mm thick.

the stress forces at 50% strain are between 0.6 MPa and 1 MPa. These values were considered acceptable for the purpose of our patch.

After analyzing the sensations of rolling and stretching the different thicknesses of silicone films by hand, it was concluded that an acceptable thickness of the NuSil™ medical grade silicone substrate could be about 0.5 mm.

Considering the results obtained in this first strain-stress assay and that the design and shape would influence the mechanical properties of the patch, it was decided to use this reference thickness to design the shape and sizes of the different patches.

2.3.2. Design of the patch

Considering that the remaining hole in the chorio-amniotic membrane is about 3-5 mm of diameter after the removal of a trocar, and that the patch must fit rolled and folded inside a 10 F standard canula (3.33 mm diameter), the initial decision was made that the dimensions of the patch should have a thickness between 0.25 and 0.6 mm, and a diameter between 15 and 25 mm.

Therefore, a design is established in the flat disc shape and one in the form of a half-lens, whose measurements can later be modified (Figure II-12). The flat disc design will be used mainly to carry out the tests in a more agile and dynamic way since to test the different adhesives, their deposition is significantly easier, and the half-lens design will be reserved as a promising design. With the half-lens design, hypothetically, the tensile forces of the membrane and the pressure of the amniotic fluid are better distributed thanks to the existence of the empty dome. In addition, this free space, in future designs, would allow us to incorporate

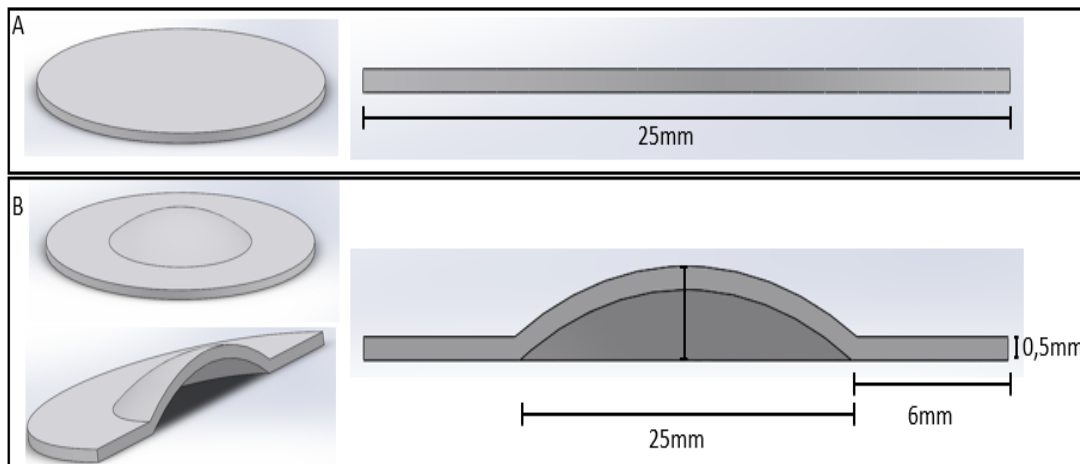


Figure II-12. Design and approximated measures of the flat disc (A) and hemi-lens (B) patches before the selection of the measures.

some type of miniaturized sensor in order to monitor the status of the fetus during the rest of the pregnancy.

A qualitative test, represented in a table of values and colors (Table II-4), was carried out in order to narrow down the measures to be chosen for the flat disc. The ability of the flat disc to roll, fold, unfold according to the diameter of the cannula (8 F and 10 F), and to deform when pulled against a PDMS film with a 4 mm diameter hole was evaluated on a scale of 1 to 3. Being 1 (red) = bad, 2 (orange) = insufficient, and 3 (green) = optimal. In this way, visually, the best scoring measurements can be chosen.

Table II-4. Table with the results obtained with different sizes of the flat patch according with the rolling, folding, deployment and deformation parameters, for 8 F and 10 F canula. Qualitative score: 1=bad, 2=insufficient, 3=optimal.

Canula size	Diameter disc (mm)	Thickness	Rolling	Folding	Deployment	Deformation
8 F	10.4	0.28	3	3	3	1
		0.37	3	3	3	2
		0.51	2	3	3	3
		0.66	1	3	3	3
	15.1	0.28	3	3	3	1
		0.37	3	2	2	2
		0.51	3	1	1	2
		0.66	2	1	3	3
	20.2	0.28	3	1	1	1
		0.37	3	1	1	2
		0.51	3	1	1	2
		0.66	3	1	1	3
10 F	10.4	0.28	3	3	3	1
		0.37	3	3	3	2
		0.51	2	3	3	3
		0.66	1	1	1	3
	15.1	0.28	3	3	3	1
		0.37	3	3	3	2
		0.51	3	3	3	3
		0.66	2	1	1	3
	20.2	0.28	3	2	3	1
		0.37	3	2	3	2
		0.51	3	1	1	3
		0.66	3	1	1	3
10 F	16.7	0.34	3	3	3	2
		0.51	3	3	3	3
		0.61	2	1	1	3
	17.1	0.44	3	3	3	3

Analyzing the table, we can observe that the patches with thicknesses of 0.28 and 0.37 mm have difficulty in maintaining their shape when they are unfolded and are pulled against the inner face of the perforated PDMS film. They deform and penetrate through the hole, regardless of their diameter. So, initially, the choice of these thicknesses would not be recommended to produce the patch. In contrast, discs with a thickness of 0.5 and 0.66 mm maintain their shape and are rollable, except for those with a diameter of 10.4 mm which cannot be rolled.

Discs with a diameter of 20.2 mm cannot be inserted in the 8 F or 10 F cannula, due to their size. The only patches whose measurements meet the criteria for rollability, folding into cannula, unfolding and shape maintenance for a 10 F cannula are patches with a diameter between 15 and 17 mm. The data indicate that patches with diameters slightly larger than 10.37 mm could also be used. Thus, patches with a diameter between 12 and 17 mm could be used for a 10 F cannula. For an 8 F cannula there are no conditions that present optimal results, so this diameter is not advisable for our sealing system.

Taking into account several factors, such as that the patch must have a maximum diameter and thickness determined to be able to fold into a trocar of 10 F, the patch must be fully deployed and perfectly cover the entrance hole of the trocar without deforming, and also taking into account the results obtained in the strain-stress assay, it concludes that the flat patch should have an approximated measures about 16.7 mm in diameter and about 0.5 mm \pm 0.05 mm thick. In this way it can be folded and deployed optimally without being forced at any time.

In our assays, a cannula with a maximum diameter of 10 F were used because this is the largest diameter that fits in a 12 F trocar. Although 12 F trocars are usually the most commonly used in fetal surgeries, the new sealing system would allow the use of larger caliber trocars, and therefore the diameter of the introducer cannula could also be increased. If the effectiveness of this sealing system is demonstrated, further tests should be carried out by filling in this table. This qualitative assessment will allow new limits to be set as patch and cannula sizes are modified. The same would occur if it were decided, for example, to change material of the patch for one with less deformation, or if we were to incorporate a mesh or internal skeleton in the patch that would give us greater rigidity. We could use thinner patches that would maintain their shape when unfolded, in a cannula of less than 10 F diameter.

2.3.3. Incorporation of a micropattern on the patch surface

After some initial tests with some commercial adhesives on smooth silicone films, it was concluded that it was necessary to increase the contact surface in some way. It was intended to modify the flat surface of the silicone for a rough or shaped one. It was then proposed to incorporate a micropattern on the face of the adhesive. This pattern, therefore, would have the function of increasing the contact surface on the patch, making the adhesive better able to adhere to the medical silicone. To create this increased surface area, a pattern in the form of convex hemispheres was selected. Linear geometry micropatterns with microchannels in the patch were tested, but when incorporating low viscosity adhesive, they circulated through these channels and did not deposit homogeneously, even falling out of the patch. In addition, the hemisphere pattern is one of the most similar patterns to the hexagonal compaction patterns observed in nature. A clear example is the honeycomb. And in this direction the design is justified because it would be the theoretical and simplest way to add the most amount of adhesive per unit area.

A test was established to measure the contact angle of this pattern and to select the one that showed the best wettability results at a lower manufacturing cost. The ultimate goal was to produce an entire stainless steel sheet with the selected pattern and thus manufacture more patches in less time.

Five medical silicone films were obtained with a textured stainless steel mold with a repeating pattern in the form of convex hemispheres of 0.1 mm in diameter and depths between 0.02 mm and 0.2 mm (Figure II-13). Images were taken with an optical microscope to evaluate the homogeneity of the pattern present on their surface. In addition, to determine if the depth of the pattern influences the wettability, the angle formed by a drop of miliQ water with respect to the surface where it is deposited was measured.

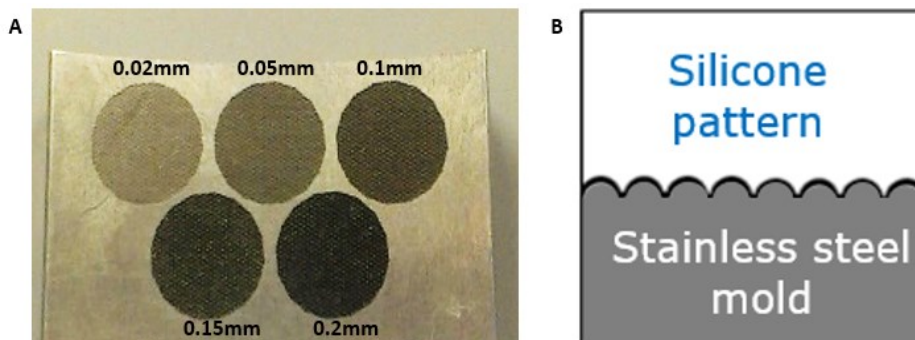


Figure II-13. Stainless steel mold with the five depth patterns (A), and a scheme that represents the silicone over the mold with the texturized micropattern.

The photographs obtained by optical microcopy of the silicone samples (Figure II-14 middle) showed homogeneity in the 0.1, 0.15 and 0.2 mm pattern, while in the 0.2 and 0.5 mm pattern irregularities were observed on its surface. These irregularities are caused by air trapped in the lowest part of the mold, which corresponds to the area where three hemispheres converge. This phenomenon can also be observed in the other patterns, but in a more homogeneous way. In addition, an increase in the depth of the hemispheres could be observed as the pattern was deeper.

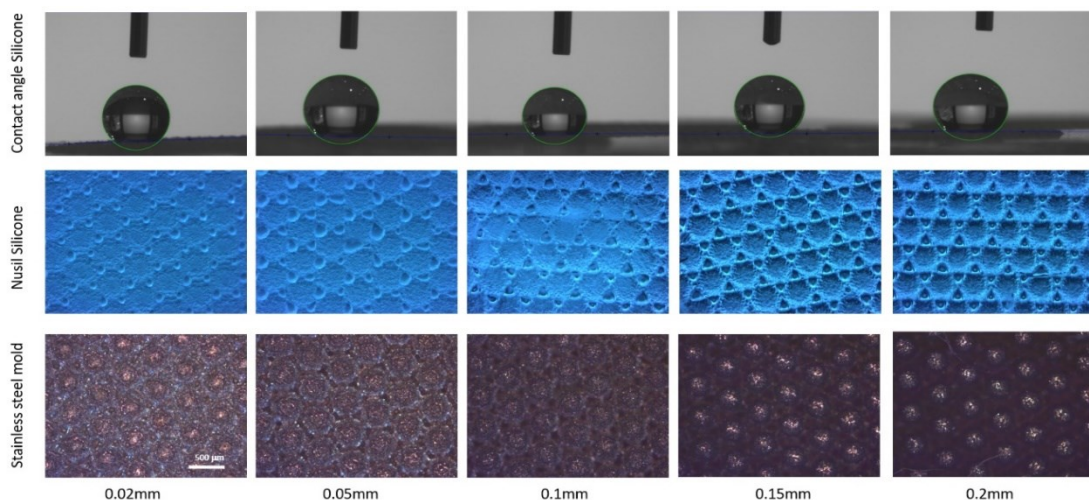


Figure II-14. Images obtained with optical microscopy (5x) of stainless-steel molds with convex hemispheres micropattern (down), the medical silicone surface with concave hemispheres micropattern (middle), and images of water drops with DSA of the five samples of silicone with the depth micropatterns.

In order to choose one of the patterns for the surface of the patches by studying their wettability, contact angle measurements were performed on the medical silicone samples. The images obtained with the DSA showed that in all patterns the hydrophobicity was very high (Figure II-14 top). Although a high hydrophobicity was already assumed in the samples due to the nature of the material, some reduction of the contact angle was expected due to the different depths. This was not the case, so it was concluded that the depth of this type of pattern does not influence its wettability. Subsequently, it was decided to evaluate the wettability of the samples with the same depths as those previously used but with the difference that the surfaces would be treated with oxygen plasma. With the same conditions applied to the samples in the plasma reactor, the contact angle with a drop of mQ water was measured again. The results showed that all samples were super wettable from the moment the drop was deposited. Thus, it was again observed that there was no appreciable difference in surface behavior among the five samples. We concluded from these two tests that neither

the depth of the pattern nor the plasma treatment was sufficient to indicate the depth to be chosen. So then, based more on the microscopy images obtained from the samples and knowing that the cost of the mold increased significantly as the depth of the texturing increased, we chose the pattern that, with a shallower depth, showed a regular and homogeneous surface. This requirement was found in the micropattern (Figure II-14 middle) obtained with the mold textured with convex hemispheres of 0.1 mm depth.

2.3.4. Production of the patches with flat and hemi-lens design.

Once the definitive designs of the flat and semi-silent disc-shaped patch were chosen, its measurements were established, and the concave hemisphere micropattern on its surface was selected, the designs and plans of the molds to be manufactured were created with the 3D modeling software Solid Works. These molds will be manufactured in different materials such as polycarbonate, polyamide and/or stainless steel. Ideally in a final phase all molds should be made of a durable metallic material that will remain unchanged after a large number of uses. By injecting liquid silicone into the molds, the two types of patches will be obtained, once the silicone has cured in the oven.

To produce the flat disc shaped patches first and in large numbers, a 100 x 100 mm stainless steel plate with the incorporated micropattern of 0.1 mm deep hemispheres was fabricated (Figure II-17 up mold). On this flat mold a layer of silicone was deposited whose thickness of 0.5 ± 0.05 mm was adjusted with a paint applicator. Due to its high viscosity this must be done with great care so as not to trap air bubbles. The mold with the silicone was placed in an oven at 120 °C for 30 min to cure the silicone and cross-link its chains. The silicone film was then unmolded from the stainless steel mold after 10 minutes. Finally, 16.7 mm diameter discs were cut with a metal hole punch.

In order to produce the semi-lens shaped patches it was necessary to manufacture the molds individually. First, we had to find the design that would allow us to optimally fill the mold with the uncured silicone and to demold it once the silicone was cured. Several molds were designed with different sizes that allowed us to manufacture the semi-lens shapes patches, without adding any micropatterns yet. Each mold is made up of two pieces that are sandwiched together. The lower piece gives rise to the inner part of the semi lens while the upper piece gives rise to the outer part of the semi lens (Figure II 16 A and B). At this point, we were simply interested in evaluating each of the patches obtained and improving the

technique to manufacture them. First the molds were printed in ULTEM™ 9085 with a fusion 3D printer (FDM Fortus 400) (Figure II-15 B). ULTEM™ is an amorphous thermoplastic polyetherimide (PEI) resin which has high strength and stiffness, and has a heat deflection temperature (HDT) of 153°C. This temperature is above the cure temperature of the silicone so the mold parts will not be affected. FDM 3D printers deposit a thermoplastic material through a extruder head that forms a filaments weft that hardens as it cools. The closer together the thermoplastic filaments that form the weft are, the better the quality of the printed piece will be. Even if the distance between the filaments was reduced as much as possible, the first molds left the silicone with a rough appearance. The spaces in the weft were manually filled with plastic putty, sanded and polished to have a smooth finish on the surface of the semi lens shape patch (Figure II 15 B).

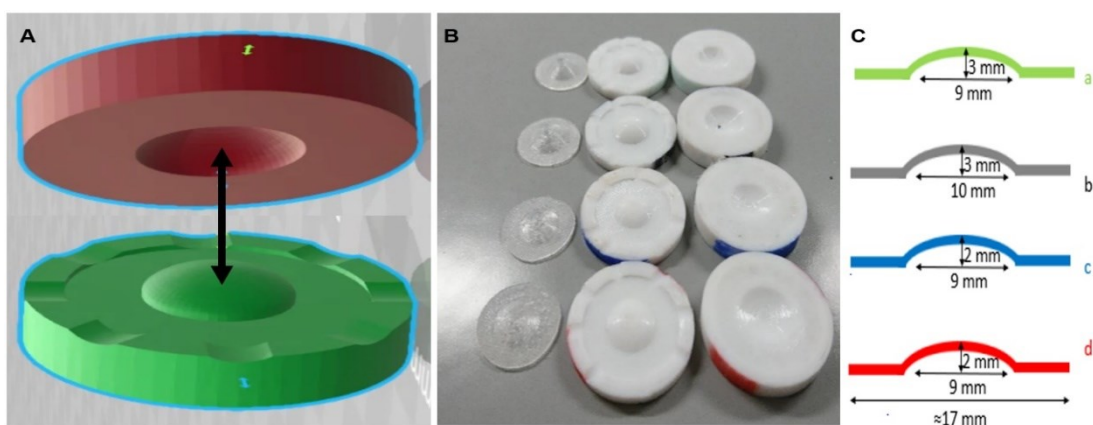


Figure II-15. Modelized image of the two pieces of the mold. The upper piece of the mold (red) and the lower piece (green) are closed in the form of a sandwich. The cavities on the outside of the lower part allow the excess silicone to escape (A). First molds of ULTEM™ resin and silicone patch obtained for each mold (B) with different sizes (C).

Together with the medical team, once the first semi-lens shaped patches were obtained (Figure II-15 B), the diameter, thickness, elasticity, sensations to touch, ..., were evaluated. Finally, it was decided to apply some changes in the measurements and design with the Solid Works software (Annex 1). Next, a stainless steel lower mold was made with the texturing in the form of convex hemispheres located in the part of the ring (Figure II-16 B). This part corresponds to the area of the silicone substrate where the adhesive would be deposited. While the surface of the convex dome would be smooth and there would be no adhesive, being free to react to intrauterine pressure variations. Several upper mold pieces were fabricated (Figure II-16 A) with small variations in the measurements to adjust the thickness of the semi-lens to 0.5 mm. These upper mold parts were fabricated in PA12 polyamide with the HP Multijet Fusion 4200 powder 3D printer. These types of 3D printers, which printing

parts by means of photopolymerized powder, have the advantage to not create any weft, obtaining pieces with soft and smooth surfaces.

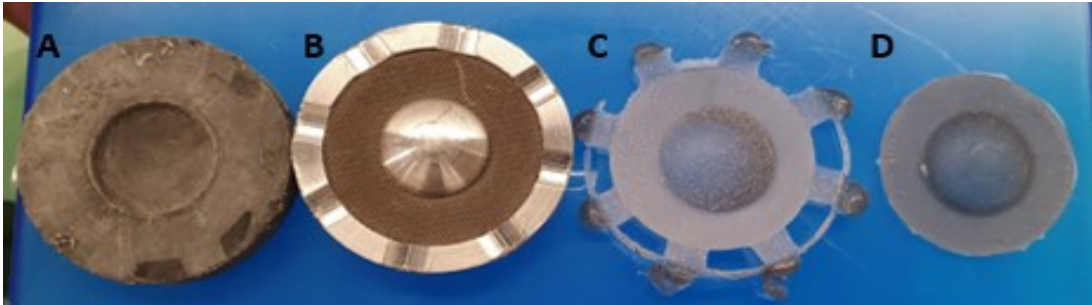


Figure II-16. Image showing parts that make up the mold to produce the silicone hemi-lenses. The mixed and degassed silicone is inserted between the two pieces of the mold forming a sandwich. The upper piece is printed in PA (A) and the lower is made of stainless steel with the micropattern textured in the ring surrounding the central convexity (B). Once the silicone is cured (C) it is removed from the mold and the leftover silicone that has come out of the channels of the lower mold is cut to form the final hemi-lens (D).

Applying the latter modifications, we finally have two models of medical grade silicone patches, one with a flat disc design and the other with a semi-lentil design (Figure II-17), each with its advantages and disadvantages. The flat disc design allows for easier and faster manufacturing, allows for more standardized testing, allows for more adhesive to be added more evenly, and allows for better rolling and folding on the cannula. But having an area of the amnion where an injury has occurred and covering it completely by a patch with adhesive could cause the amnion cells to have some unwanted reaction by blocking the supply of nutrients and gas exchange. In addition, adhesive could penetrate through the hole and hinder the natural movement of the chorion over the amnion. In the half-lentil design, if the adhesive has a high bonding strength with a smaller amount deposited in the ring, it would leave the area near the orifice free of adhesive for nutrient and gas exchange. In addition, the empty dome could act as a absorber for the pressure of the amniotic fluid near the orifice, dissipating the forces exerted. On the other hand, the half-lentil design makes it difficult to roll and fold into the cannula. In addition, the patch could become detached because it has less surface area in contact with the amnion and could protrude if the fetus accidentally tears it off because it is not completely flat to the wall.

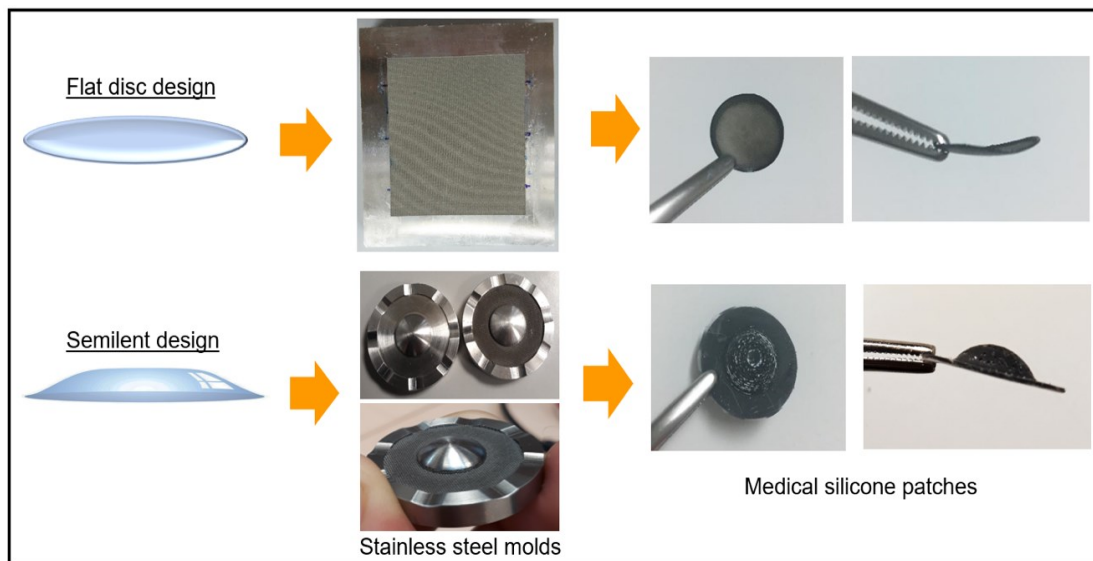


Figure II-17. Images with the real stainless-steel molds to produce the patches with flat (top row) and semi-lens shape (bottom row). The patches are carbon black stained for better look.

Finally, in order to attach any of the patches, it is necessary to add an anchor point. For this reason, it was thought to integrate some kind of structure inside the silicone and thus be able to pull the patch against the amniotic membrane thanks to the use of a fastening/traction thread. With this objective in mind, we thought of integrating a thread inside the silicone, so that the thread crosses the entire patch through the center. Thus, the traction thread has an attachment point right in the center of the patch to be pulled through (Figure II-18). The integration of the anchor thread allows the tensile thread to have a point of resistance in the middle of the patch. It was observed that when too much tensile force was exerted, the tensile thread broke the patch without an anchor thread in the middle of the patch. This did not occur with the integrated anchor thread. Suture threads of different materials such as Nylon, polypropylene, Norefil, etc. were used. The best results were obtained with a braided silk thread, probably because the silicone before to be cured can penetrate between the silk fibers, thus integrating the thread better. It was also thought of incorporating another more sophisticated anchoring system with extra functions, which is described in Chapter V.

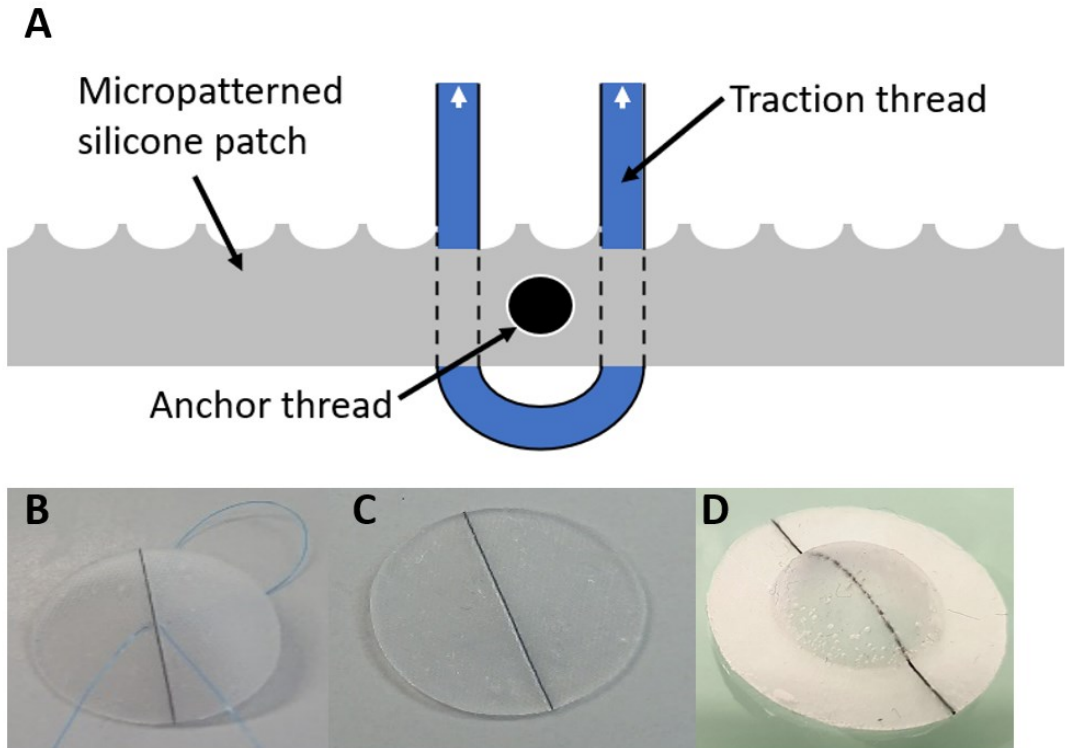


Figure II-18. Scheme of the traction system with the anchor thread integrated (A) and the real view of the flat disc with the traction and anchor thread (B). Flat disc (C) and semi-lens design (D) with the anchor thread integrated inside the cured silicone.

2.3.5. Integration of an electrospun layer of polycarbonate-urethane (PCU)

The incorporation of any type of adhesive on a biomaterial such as medical grade silicone has always been difficult due to the low availability of reactive groups on its surface. It is precisely this lack of reactive groups that causes a low interaction with the tissues, motivating the industry to produce implants with this type of materials.

To improve the interaction between the patch surface and any future adhesives, it is proposed to incorporate an integrated electrospun layer of another medical grade biomaterial, such as polycarbonate-urethane (PCU), Bionate® from DSM. The incorporation of carbonate groups to the PU makes PCU widely used in implantology due to its higher load resistance and durability. With the incorporation of this electrospun layer, the contact surface should be substantially increased, improving the capacity for interactions between the adhesive and the substrate. The incorporation of this layer, depending on its mechanical properties, could even make it possible to reduce the thickness of the patch and thus be able to use smaller diameter trocars.

The first step to obtain a homogeneous electrospun layer is to identify the conditions under which the PCU must be electrospun. Regarding the polymeric solution to be used and the conditions to be applied to the electrospinning equipment.

It is essential to find the formulation of the PCU polymeric solution that will stabilize the polymeric jet and homogeneously deposit the fibers on the collector. Factors such as concentration and solvent types are critical, due to their direct influence on viscosity, conductivity, and surface tension.

Influences of the variables on the polymeric solution and selection of the final formulation.

Solvent properties such as boiling point, vapor pressure, dielectric constant and surface tension can be key to the final solution formulation. From the literature, it is clear that a mixture of DMF and THF gives optimal results, both in dissolution of PU granules and evaporation during electrospinning^{44,46}. The addition of carbonate groups to PU as a soft segment, produces an increase in flexibility, toughness, resistance to oxidation and hydrolysis. Due to the presence of these carbonates to the PU chain, a new formulation study is required in terms of solvent concentration and composition.⁶³⁻⁶⁶ For this reason, it is necessary to search for the optimum ratio of DMF and THF, since even though they have different physical properties, they can complement each other (Table II-5).

Table II-5. Table with the physical properties of solvents used to prepare the PCU solution.

	Boiling point (°C)	Vapor pressure (Pa) to 20 °C	Dielectric constant	Superficial tension (mN/m)
DMF	153	351	36.7	37.1
THF	66	17 253	7.6	26.4

The literature consulted showed the formation of films with homogeneous fibers from a 10% w/v PU polymer solution with a mixture of DMF and THF in a 3:2 ratio, and with similar electrospinning conditions.^{44,46,67} In addition, 5% and 10% PCU formulations with DMF:THF (3:2 and 2:3) were added to obtain data about films and electrospun fibers. From the results obtained in a previous experimental design to familiarize ourselves with the use of the electrospinning equipment and to tune it, it was decided to use the following electrospinning conditions as a starting point:

- Feed rate → 1.5 mL/h.
- Voltage → 14.3-19.9 kV.
- Small needle diameter 0.88 mm.
- Time of deposition → 60 mins.
- Gap or distance between nozzle and collector → 16 cm.

Among those PCU polymer solutions that were able to deposit fibers on the collector, only the 10 % concentrations with DMF:THF ratios of 2:3 and 2:3 resulted in homogeneous films. The PCU fiber films obtained with the 5 % concentrations were wet, and those with the 15 % concentrations formed droplets or the needle was constantly clogged because the PCU concentration was too high. (Table II-6 and Figure II-19 A). The differences between the physical properties of the two solvents can be observed in the two 5% PCU films. The film with the 3:2 ratio of DMF:THF (M1) is much wetter than the 2:3 (M2). This can be explained by the fact that THF has a higher vapor pressure than DMF, and this effect can be observed at the macroscopic level when the polymer concentration is lower. Such an effect cannot be observed in 10% PCU films, or at least not until the fibers are analyzed with SEM.

Table II-6. Results of the macroscopic analysis of the electrospun PCU films.

Sample	[PCU] (% w/v)	DMF:THF ratio	Macroscopic results
M1	5	3:2	Wet film
M2	5	2:3	Partially wet film
M3	10	3:2	Homogeneous PCU film
M4	10	2:3	Homogeneous PCU film
M5	15	3:2	Unstable jet. Droplets
M6	15	2:3	Tip obturation

The homogeneity and morphology of the fibers of all the films obtained were evaluated by SEM images (Figure II-19B). The films in which fibers with more defined edges are observed belong to the PCU solutions with a 10% concentration, both with the 3:2 (M3) and 2:3 (M4) ratio of DMF:THF. It can be observed that in M4 the fibers have a larger diameter and a more homogeneous shape than in M3. Affirming that at the same concentration of PCU the formulation with a higher amount of THF produces a larger diameter fibers.

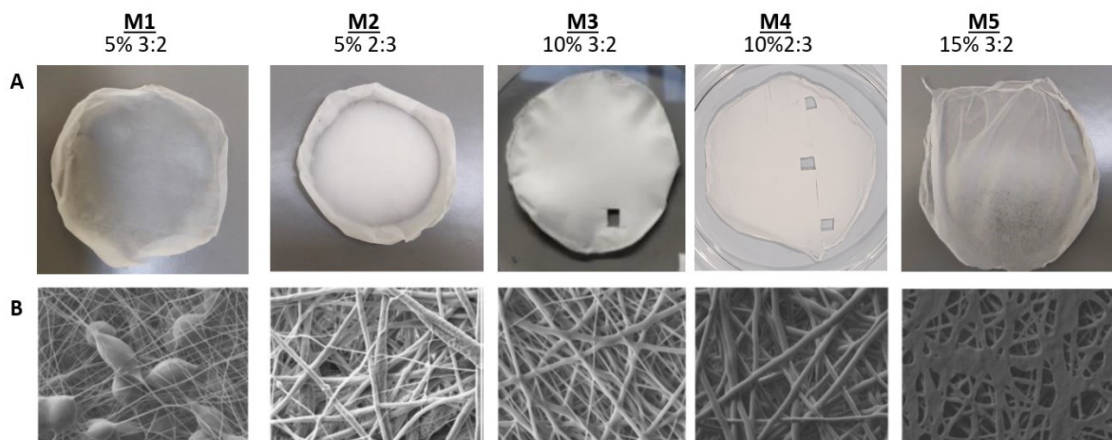


Figure II-19. Images of the electrospun PCU films for the macroscopic evaluation (A) and SEM images (Mx:3500x and V:10kV) of the formed microfibers for the microscopic evaluation (B) of each formulation.

In the films created with the 5% PCU solution (M1 and M2) it can be observed that with a higher proportion of DMF the fibers are smaller in diameter, although beads appear throughout the fiber network. These beads have been widely reported and usually appear when the polymer concentrations are too low, the surface tension is too high and the loading density is low^{68,69}. In M2 regular fibers of smaller diameter and thicker fibers with irregularities can be seen. These irregularities are called spindle-like beads and usually appear when the fibers start to stretch but do not have enough time to do so and arrive partially wet. As the solvent evaporates, these irregular shapes appear in the fibers^{68,69}.

Fibers analysis of the film produced with the 15 % PCU solution (M5) shows an overlapping of the fibers without defined edges, since the formation of droplets during the electrospinning process is reflected at both macro and micro levels. When an unstable jet is formed and sometimes with difficulty to be directed towards the collector, it is necessary to increase the voltage producing droplets. This usually occurs when polymer concentrations are too high, giving high viscosity values to the solution and making it difficult to pass through the needle. At this point it was concluded that the concentration values of 5 % and 15 % were too extreme to be able to identify the PCU concentration limits above which we can homogeneously electrospun. It is also not possible to know which factors influence the electrospinning process and how they do it, since it was not possible to obtain homogeneous films at 5 % and 15 %. These results previous to the setting up of the method show that both the PCU concentration and the solvent ratio (DMF and THF) affect the fiber morphology and the electrospinning process itself.

Production of electrospun PCU fibers with desired morphology

It is important to identify how the formulation and electrospinning process variables influence in order to find the final electrospinning conditions that interest us. First, the limits of the variables that allowed homogeneous electrospinning and the formation of regular and defined fibers were sought. If electrospinning is carried out within the limits, it is possible to identify how each variable intervenes. And once these limits were established (Table II-7), an experimental design was carried out. The influence of the different variables, the limits and the final conditions were obtained thanks to a final master thesis done in our research group by Alejandro Martín Valladares, with the title "Development of bioactive patches through the electrospinning technique".

Table II-7. Table with the range of limits for the polymer solution and process variables.

	Variables	Range
PCU formulation	Concentration (%)	7-13
	DMF:THF	3:2-2:3
	Viscosity (Pa·s)	0.4-2.4
	Surface tension (mN/m)	29.6-31.6
Electrospinning conditions	Feed rate (mL/h)	0.5-3.5
	Needle internal diameter (mm)	0.88-1.70
	Distance tip to collector (cm)	18-24
	Deposited volumen (ml)	0.5-2.0

Several films were electrospun within the range of limits found for the PCU polymer solution. The morphology of the fibers was analyzed by SEM (Figure II-20). Fiber diameters and porosity percentages were classified into three categories: low, medium and high (Table II-8). Porosity and fiber diameter values can be better interpreted by qualifying them in the following way.

Table II-8. Criteria used to classify the obtained films based on a microscope analysis.

Fiber diameter (FD)		Porosity percentage (%pore)	
Low FD	<1 μm	Low %pore	<50 %
Medium FD	1.0-1.5 μm	Medium %pore	50-70 %
High FD	>1,5 μm	High %pore	>70 %

After several discussions it was concluded that it was desirable to have a film with fibers of medium/low diameter and a pore percentage with a medium/high value. With this choice, we would theoretically have less influence on the change of mechanical properties of the silicone, and the adhesives could have better penetrability within the fiber matrix. Thus, in order to

obtain an electrospun PCU film with a medium/low FD and a medium/high %pore, the following conditions were established:

- PCU concentration: 10 %w/v.
- DMF and THF ratio: 3:2.
- Tip collector distance: 18 cm.
- Feed rate: 2 mL/h.
- Tip diameter: 1.7 mm.
- Voltage: 12.8 kV aprox.

Fibers diameter (mcm)	Low→ 0.88	Medium→ 1.22	Medium→ 1.28	Medium→ 1.39	High→ 1.69
%pore	Medium→ 58%	High→ 72%	Medium→ 60%	Low→ 41%	Medium→ 50%
[PCU] %w/v	8	10	10	12	12
DFM:THF ratio	2:3	3:2	2:3	3:2	2:3
Viscosity (Pa·s)	0.67	0.8	1.51	1.8	1.94
Surface tension (mN/m)	29.63	31.4	29.63	31.49	29.7
Tip collector distance (cm)	24	18	20	20	18
Feed rate (ml/h)	0.5	2	1.5	2.5	1
Tip diameter (mm)	0.88	1.7	0.88	1.7	0.88
Voltage (kV)	14,4	12.8	15.6	17.3	19.1
Temperature (°C)	23,5	24.5	22.5	23	23
Relative humidity (%)	41	45	43.5	40	42.5

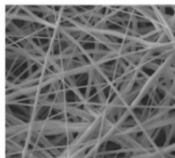
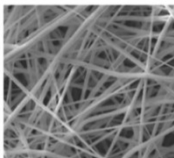
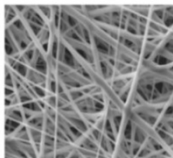
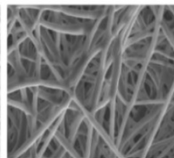
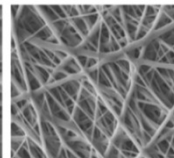






Figure II-20. Some examples of the conditions applied to the electrospinning technique to obtain fibers with different FD and %pore.

Analysis of the mechanical properties of electrospun PCU films

Applying the previously selected conditions, which allowed to create a homogeneous film of low/medium diameter fibers and medium/high pore %, it was necessary to evaluate the influence of the thickness of the PCU film in order to integrate it into the silicone patch.

Four films of electrospun PCU were prepared with theoretical thicknesses of 25, 50, 75 and 100 µm. These four films were characterized by a stress-strain test with the DMA, with an elongation ramp at 4 000 µm/min and a total elongation of 1 000 µm. Microscopic analysis prior to the stress-strain test of the four films resulted in four films of 26, 51, 75 and 109 µm thickness, with a fiber diameters of 1.2-1.4 µm and a pore percentage of 54-59 %. In our opinion, acceptable values within a small range of variability where it is believed that they should not influence the final result of the test.

The results obtained (Figure II-21) showed that there was a direct relationship between the thickness and the force required to deform the films. It was observed that with 80% stretching of the samples, for every 25 μm increase in PCU film thickness the tensile strength increased by approximately 0.5 MPa. The 26 and 51 μm thick samples did not undergo plastic deformation making them serious candidates to be integrated into the silicone patch. In contrast, plastic deformation was observed in the samples with a thickness of 75 and 109 μm due to the fact that, after the test, the 75 μm sample permanently increased its length by 25 μm and the 109 μm sample increased by 650 μm . This deformation is not clearly seen in the curves of the graph, although it is slightly seen in the 75 μm specimen with a stretch of approximately 15 %. These data make us totally rule out the 109 μm thickness for use. The 75 μm thickness cannot be completely ruled out due to the fact that the patch would hardly stretch more than 20 % bidirectionally, so theoretically no plastic deformation should be observed and it would not affect the patch.

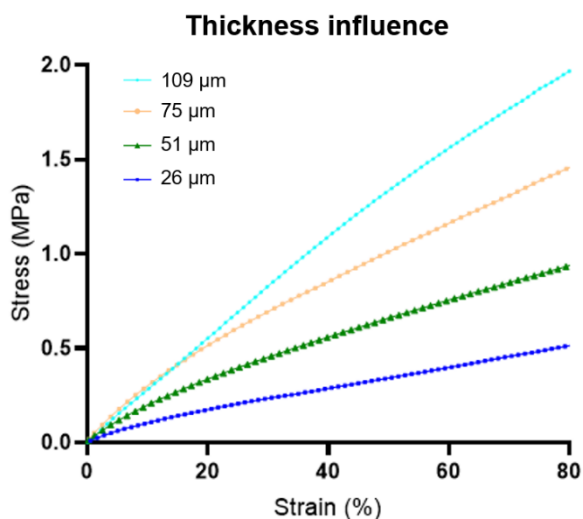


Figure II-21. Results of strain-stress assay with samples of electrospun PCU with a thickness of 26, 51, 75 and 109 μm .

To identify how the electrospun PCU films influenced the mechanical properties of the silicone, 26, 51 and 75 μm PCU films were integrated into a 500 μm thick silicone film, and another stress-strain test was performed. It is important to remember that the thickness of the selected silicone patch is 500 $\mu\text{m} \pm 50 \mu\text{m}$ so some variability may be seen in the results. The DMA results (Figure II-22 left) indicated that the silicone sample had, as expected, a behavior typical of viscoelastic materials. Viscoelastic materials such as silicone typically exhibit curves in which there is a steep initial slope that gradually reduces and stabilizes. Samples with the PCU incorporated seem to tend to lose this viscoelastic effect slightly. Tests with two different

materials integrated are sometimes difficult to interpret due to the fact that the curve usually shows the behavior of the predominant material. For this reason, it was decided to use a strain of 80 %. Such a large strain allows a better comparison of the differences between the different samples. Even so, the silicone sample did not differ practically from the results of silicone with PCU of 26 and 51 μm thickness. Although there is a small difference of about 0.1 MPa between the latter and the silicone. A difference of more than 0.5 MPa was observed in the silicone sample with a PCU of 75 μm thickness, with respect to all the others.

Therefore, it was concluded that it could be interesting to incorporate an electrospun PCU film between 26 and 51 μm with fibers between 1.2-1.4 μm in diameter and a porosity of 54-59 % to the 500 μm silicone film, due to the final stretch at 80 % being very similar to silicone alone.

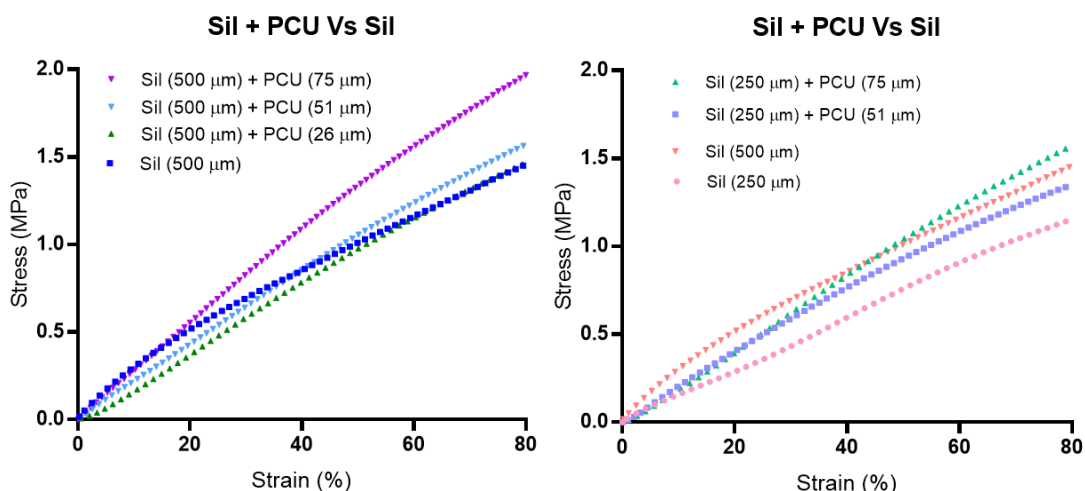


Figure II-22. Results obtained of strain-stress assay of sample of silicone with 500 μm thickness Vs silicone/PCU (A) and silicone 250 μm thickness Vs silicones/PCU (B).

Subsequently, in order to find out if it was possible to reduce the total thickness of the patch by incorporating the PCU film while maintaining mechanical properties similar to the 500 μm silicone, the thickness of the silicone was reduced to 250 μm . The 51 and 75 μm films were integrated (the production method could see in the next section) and another stress-strain test was performed.

The results obtained (Figure II-22 right) showed very similar curves. As a reference we have the two curves for the 250 μm and 500 μm medical silicone samples. The curves corresponding to the silicone samples with PCU, although they did not show such a typical viscoelastic behavior as the 500 μm silicone, showed a small stress difference at 80 % of about 0.2 MP. The bending of the 250 μm silicone sample with 51 μm thick PCU has a

behavior that follows a similar trend to the 500 μm silicone, even with a somewhat lower value of strength at 80% stretch and throughout the test. This result led us to conclude that it was perfectly possible to use a 250 μm silicone patch incorporating a 51 μm thick PCU film. In the pending of verifying its behavior in real conditions by performing the tests with adhesives, it could be a serious option to be taken into account. Since it is thinner and has mechanical properties similar to those of the 500 μm silicone patch, it would allow it to be rolled up and inserted more easily into a cannula, it would be possible to increase the diameter of the patch, and it would even allow the use of smaller diameter cannulas. This would mean reducing the size of the hole in the chorioamniotic membrane, decreasing leakage and reducing the risk of rupture.

Patch production with plane and hemilens shape with electrospun PCU film

Once the thickness of the electrospun PCU film with a given fiber diameter and pore size has been selected, it is very important to integrate this film into the silicone so that the two layers cannot separate and act as one. The first strategy was to electrospun directly on the uncured silicone film and then cure the silicone in the oven, but the silicone, being poorly conductive, destabilized the polymer jet and the film was not homogeneous. Finally, it was decided to electrospun the PCU film with the desired characteristics (fiber diameter, pore percentage, film thickness) and incorporate it into an uncured silicone film, and press it lightly. In this way, the liquid silicone penetrates between the fibers in the first micrometers of the PCU layer. It is during the oven curing process that the silicone cross-links its chains trapping the fibers inside (Figure II-23 B), preventing the separation of the electrospun PCU layer after being subjected to tensile and stretching forces.

In the manufacture of the flat disc-shaped patches, the integration of the electrospun PCU film is relatively simple due to the fact that the size of the PCU film can be easily adjusted on the silicone film in the mold. While for the semi-silicone patches, the option that gave the best results was to cut the PCU film into a ring shape to fit the individual stainless steel molds. In both designs it is possible to choose to incorporate the hemisphere micropattern used in the silicone patches on the surface of the PCU layer, although this should not be necessary due to the purpose of incorporating the PCU fibers is to increase the contact surface on the surface of the patch. And with the incorporation of the PCU electrospun layer we have already achieved this purpose (Figure II-23 A).

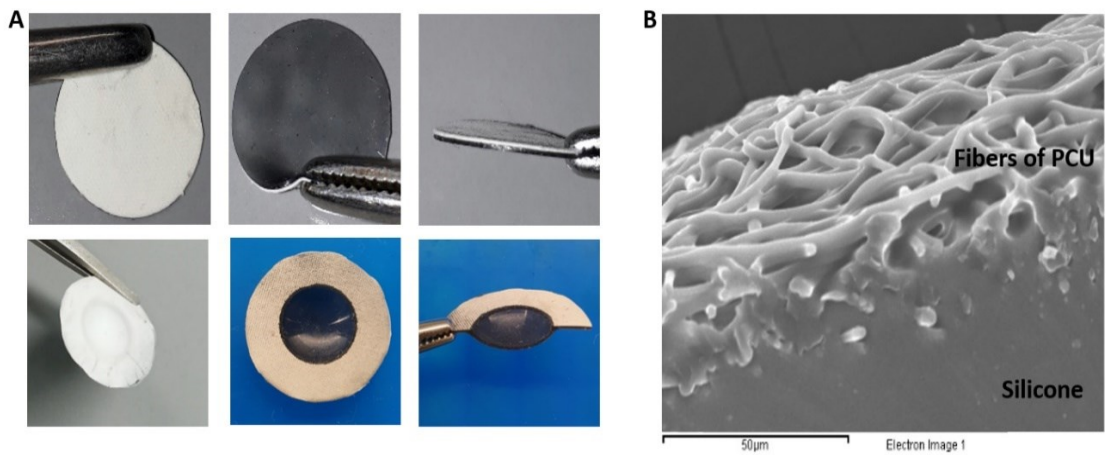


Figure II-23. Images of the real patches with the PCU layer incorporated on flat (A upper) and hemi-lens (A lower) shape. And SEM image with sagittal section of the patch, where it can see the integration of the cured silicone onto the PCU fibers (B).

2.4. Concluding remarks

It has been possible to manufacture patches with two different designs and with certain mechanical properties that allow their folding and unfolding while preserving their initial shape unaltered. The surface of these patches has been temporarily modified by oxygen plasma activation, and permanently by the incorporation of a micropattern in the form of concave hemispheres and by the integration of a layer of electrospun PCU. The integration of this PCU film can reduce the thickness of the patch. With the physical modification of the patches, the contact surface is increased, which improves the physicochemical interaction with the adhesives that will be developed in chapter IV. The results obtained during the development of the different families of adhesives will determine the choice of one or another surface.

The first patch has a simple design in a flat disc shape, with the objective of having its entire surface in contact with the inner face of the amniotic membrane having the adhesive as an interface. This type of design implies a larger surface area on which a greater amount of adhesive is deposited and, therefore, should increase the adhesion capacity of the patch. A flat design also implies that the patch can be easily rolled inside the cannula, so that we can use a patch of the largest possible diameter, provided that it fits into the cannula that we will use as part of the introducer (Chapter III). In addition, most of the *in vitro* and *ex vivo* tests to evaluate adhesion, that will be seen in Chapter IV, will be performed with the flat disc design due to its versatility. This design, in conclusion, promotes progress in the development of the patch, the adhesive and the introducer.

The second patch has a semi-lentil design, where the adhesive is deposited only on the outer ring, thus leaving the dome area free to better absorb the pressure of the amniotic fluid and leave the hole free of adhesive. While it is true that there is a reduction of the adhesive surface compared to the flat disc design, with an optimal adhesion this surface could be enough. This strategy would avoid adhesive penetration between the chorion and amnion, preserving unaltered its natural movement and reducing the number of amnion cells that are in contact with the adhesive. Moreover, in the future, this dome, having a "free" space, may play a key role in adding sensors and other technologies that allow monitoring of intrauterine conditions and the evolution of the fetus.

Once the different patch designs and materials have been selected and evaluated, as well as the manufacture of the first prototypes in with flat disc and semi-lentils shape, it is time to design an introducer to be able to use them. The development of an introducer and insertion strategy will determine the most promising patch design to be used.

Chapter III. Insertion system

Insertion System

This chapter shows the development of a manual introducer or insertion system that allows the deployment and fixation of the patch inside the fetal sac through the same trocar used in minimally invasive surgery. It shows the creation of several designs and the corresponding plans, the materials and the methodology used to create the first prototypes, the modifications performed and the final insertion system that will be used.

3.1. Introduction

In order for the surgeon to be able to fix the patch on the inner side of the amnion in a simple, effective and safe manner, the need arises to develop an introducer or insertion system. This introducer, first of all, must have the function of keeping the patch folded and protected inside until the moment of its use. In addition, it must be introduced through the same trocar used during surgery. And finally, it must allow the patch to be unfolded, fixed to the inner side of the amnion and cover the hole caused by the trocar itself. This should be done using materials certified for medical use and by means of a mechanical and manual system that is as simple as possible, in order to facilitate the regulatory process. According to the regulation (EU) 2017/745 on medical devices, unlike the developed patch that would belong to class III because it is a long-term implantable device, an introducer of this type would be part of the already existing group of laparoscopy accessories in gynecology and would belong to class I.⁷⁰ Having a less restrictive regulation allows us to greatly expand the range of materials we can use (Table II-1) and simplify the steps we have to take to obtain certification, unlike the patch which is a long-term implantable device and which, moreover, includes an adhesive. However, there is one thing to keep in mind. And that is that, if the insertion system (adhesive + introducer) is presented as a single and indivisible one, it would become a class 3 medical device, since the final classification is given by that component of the highest class. Independent of the class that the other parts would have if presented separately.

Considering the regulatory aspect, one must inevitably focus on existing products that comply with the regulations for use in medical devices. In the biomedical field, there are now an uncountable number of surgical devices and systems that make minimally invasive surgeries more and more common and easier to perform. Manufacturers such as Boston Scientific Corporation, Cook Medical Inc, Ethicon Endo-Surgery Inc, Hologic, Fujifilm Holdings Corporation, HOYA Corporation, Intuitive Surgical Inc, Medtronic, among others, have a wide range of medical devices and dominate a large part of the world market. These companies

already have extensive experience in manufacturing medical devices in which each piece is made of a specific material according to the device's own characteristics.

In a general way, in the selection of a plastic material to be used to manufacture a part for the medical device (also extrapolated to metals, glass and ceramics) a series of criteria are followed. In this way, their suitability is evaluated according to their physical and mechanical, thermal, electrical, chemical, sterilization resistance, biocompatibility, joining and welding properties. These plastics can be divided into commodity plastics, engineering thermoplastics, high-temperature engineering thermoplastics, and other polymers (Table III-1)⁷¹.

With regard to physical and mechanical properties, it is important to know the dimensions and weight of each piece, as well as the stress and impact it must support during use. This includes density, transparency, color, water absorption, lubrication, tensile strength, tensile elongation, flexural modulus for stiffness, etc.

Thermal considerations are important during the manufacturing process, during processing and during use, as well as environmental temperature and humidity. Melting point and softening point, processing temperatures, heat deflection, glass transition, thermal conductivity, etc. are included.

The sterilization capability is very important because the material has to support the different sterilization techniques, such as steam, dry heat, ethylene oxide, gamma-radiation, e-beam, ..., and maintain its properties unaltered.

The electrical criteria have been more related to electronic medical devices, although some materials need to dissipate accumulated static charges, and others need to be electrically isolated. These include conductivity, dielectric strength, volume or surface resistivity, and comparative tracking index.

With regard to chemical resistance, some parts may need to be resistant to odors, grease, processing aids, disinfectants, lye, and other hospital chemicals.

With the increase in MIS and the use of implants, many materials must be biocompatible, nontoxic, and nonirritating. They must be in contact with body tissues and fluids, and must not alter them.

Long-term durability is related to thermal properties since during the time a medical device is packaged and protected inside its packaging it can be subjected to variable conditions of temperature and humidity. Therefore, it is necessary to use materials that are more resistant to changes in environmental conditions over time.

Table III-1 Resume of plastics commonly used in medical devices applications.⁷¹

	Commodity Plastics	Engineering Thermoplastics	High-Temperatures Engineering Thermoplastics and other Polymers
% usage in medical device applications	70% of all plastics	20% of all plastics	10% of all plastics
Types of plastics	<ul style="list-style-type: none"> • Polyethylenes (PE, HDPE, LDPE) • Polypropylene (PP) • Polystyrenes (PS, ABS, SAN, MABS, SBC) • Polyvinyl chloride (PVC) 	<ul style="list-style-type: none"> • Polyamides (PA, Nylons) • Polyesters (PBT, PET) • Polycarbonates (PC) • Polyurethanes (PU) • Acrylics • Acetals 	<ul style="list-style-type: none"> • Polyimides • Polyetherimides (PEI) • Polysulfones • Polyether ether ketone (PEEK) • Polyphenylene sulfide (PPS) • Fluoropolymers (PTFE, FEP, PFA, ECTFE/ETFE, PVF/PVF2) • Liquid crystalline polymers • Biopolymers (PLLA, PLA, PLGA, PCL, PHB) • Elastomers (silicones, TPU, TPC, TPA, TPS, TPO) • Thermosets and adhesives (epoxies, phenolics, alkyds, vinyl esters)
Medical device applications	<ul style="list-style-type: none"> • Tubing • Films, packaging • Connectors • Labware • IV bags • Catheters • Face masks • Drug-delivery components • Housings • Luers • Connectors • Membranes • Sutures • Syringes 	<ul style="list-style-type: none"> • Surgical instruments • Balloons • Blood set components • Blood bowls • Blood oxygenators • Syringes • Moving parts and components • Luers • Catheters 	<ul style="list-style-type: none"> • Surgical instruments • Surgical trays • Syringes • Implants • Dental implants • Bone implants • Moving parts and components • High precision parts • Electronic components • Luers • Bioresorbable sutures

The step prior to the manufacturing of a mold to produce many units of the same part is the prototyping phase. The purpose of this phase is to produce a small number of parts to be evaluated. While in the past prototypes were made by hand, nowadays 3D printers are used for this purpose. Having the great advantage that by using a computer program you can create

multiple designs with different measures, versions and sizes. And finally the parts or prototypes can be printed in a few minutes.

There are several types of printers that, due to their technological base, produce parts of different materials. Depending on the printing technology, 3D printers can be divided into: Stereolithography (SLA) whose material is usually a photocurable resin; Fused Deposition Modelling (FDM) which melts a polymer (PLA, ABS, PET, PC, etc.) and extrudes it through a small head until it cools; Selective Laser Sintering (SLS) which by means of a laser melts powder (ceramic, glass, nylon, polystyrene, etc.) to shape the parts; and finally Multi Jet Fusion (MJF) that through the injection of a special ink on a layer of powder (Polyamide and polypropylene) melts the material with the desired design.

Thus, 3D printing technology gives us the opportunity to create a wide variety of parts and prototypes easily and quickly, in order to evaluate their mechanism and functionality. So the choice of material is not very important at this point. However, it would be of vital importance at the time of manufacturing the final prototype, which would lead to the scaling of pieces by means of additive manufacturing with molds.

The proposed insertion system is inspired by the design and mechanism that can be found in syringes, laboratory micropipettes, and other instruments commonly used in laparoscopic surgery (Figure III-1). This means that the end user, i.e. the surgeon, is familiar with this type of instrumentation and can learn how it works more easily and intuitively, without the need for lengthy training beforehand.



Figure III-1. Models of different medical devices that actually exist in the market. ENSEAL™G2 Articulating tissue sealer of Ethicon (A); Pipetman micropipette of Gilson™ (B); Type CW aspiration anesthetic syringe of Hu-Friedy (C); and Performer™ Introducer (Cook® Medical).

Therefore, the aim is to create a prototype of an introducer that will allow the patch to be implanted inside the fetal sac. Designs will be made, the parts will be manufactured and the handling and shape will be discussed with the medical team. An optimal method will be looked

for so that the introducer can store the patch inside and keep it protected from external agents. The introducer must be able to be introduced through the trocar or trocars used in surgery. Once introduced through the trocar, it must allow the patch to be deployed inside the fetal cavity by means of a attachment system. Finally, it must be able to be used and removed without losing amniotic fluid during the process. Above all, the insertion system must be effective, safe, fast and easy to use.

3.2. Materials and Methods

Solid Works 2018 CAD (computer-aided design modeling) software has been used to make the drawings and designs of the insert system. With the advantage that modifications can be made quickly and easily, and that the file system is fully compatible for the production of parts and molds.

To produce the first prototypes, some parts have been reused from medical devices already on the market, and others have been designed and manufactured with 3D printing. The cannula and inner sliding rod, made of polypropylene, have been obtained from an existing introducer model already on the market that is used in aortic and peripheral interventions (Figure III-1 D). The thumb pusher and the clamping system were designed according to handling comfort criteria and were manufactured in PA12 polyamide using the HP Multi Jet Fusion 4200 industrial 3D printer (Barel S.A).

Once the final design of the introducer has been established and definitively decided, a manufacturer producing parts by injection and extrusion of plastics certified for medical use will be sourced to replace the components and parts of the prototype that are now reused and/or produced by 3D printing.

The materials used to produce the introducer allow it to be sterilized by steam autoclaving with a standard program, and also with ethylene oxide (EtO), among other methods.

The evaluation of the mechanism and parts is performed by simulating in the laboratory the process of patch attachment. A 0.1 - 0.2 mm thick silicone film placed in a 30 mL glass vial, and tensioned with a customized stopper, is used as a model. This film has a hole in the center of about 3 mm in diameter, to simulate the diameter that would be formed in the fetal membranes. A 12 F trocar is introduced through this hole, through which we introduce the insertion system manufactured with the patch inside. In order to improve the introducer or insertion system we basically evaluate the handling and stability, as well as the individual parts that form it, and if there are any design problems. At this point the opinion of the medical team is of great importance due to the fact that they are the end users, and they help to design a system that is already familiar to them.

3.3. Results and Discussion

Initially, two types of design for the introducer were considered: one inspired by the way laboratory micropipettes are operated and the other inspired by commonly used syringes (Figure III-1 B and C). Both designs would have in common that the mechanism for pushing and deploying the patch would be the same, but the way to pick up and handle the introducer would be slightly different, from the point of view of the grip and the position of the arm when performing the technique.

The introducer must protect the patch on the inside in a rolled-up form so that it can later be unfolded and the patch can be fixed to the amnion by means of a thread or traction device. Therefore, the introducer or insertion system consists of a cannula attached to a manual clamping piece adapted to the ergonomics of the hand, and of an internal dipstick with a longitudinal hole attached to a pressing piece for the thumb at the base of which there is a hole. Through this hole is arranged the thread through which, once the patch is unfolded and the insertion system is removed, allows the patch to be fastened and fixed on the amnion.

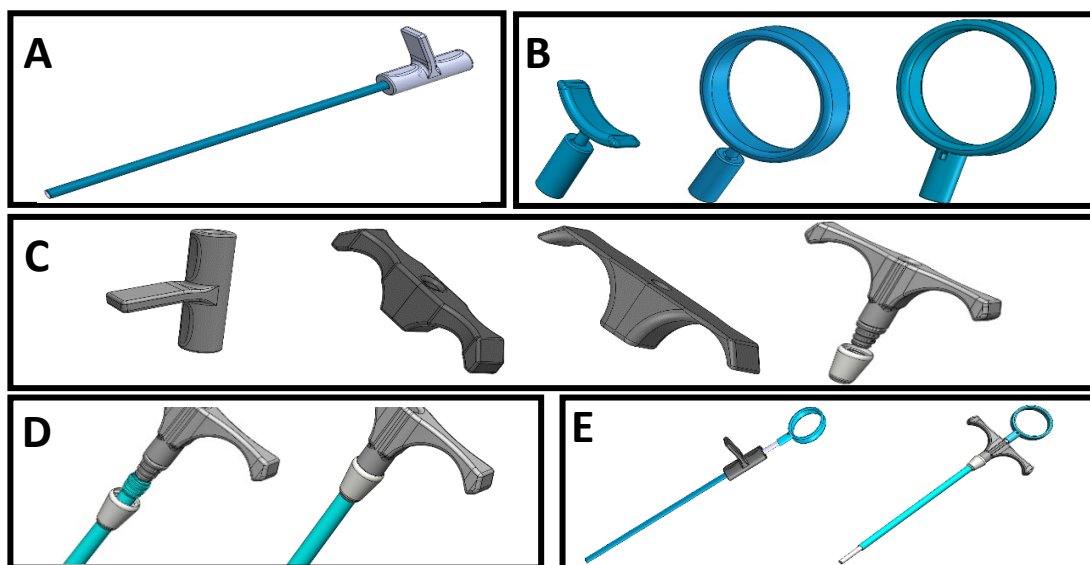


Figure III-2. Various designs created with Solid Works 2018 modeling software of the micropipette-inspired manual cannula (A); thumb pushers (B); different designs of the manual clamping system inspired by micropipette and syringe (C); fixation mechanism of the cannula to the manual clamping system (D); and the two final designs complete with cannula and pusher (E).

For this purpose, some sketches were drawn and several clamping and pressing pieces were designed (Figure III-2). Prototypes were fabricated and handling tests were performed. Initially it was thought that the micropipette-based design (Figure III-2 A and E left) would be the most suitable due to the fact that it would allow the arm to be more relaxed and less arched when

introduced through the trocar during surgery. However, after evaluating the handling with the medical team, we opted for the syringe design (Figure III 2 E right) due to the fact that surgeons and other healthcare personnel are much more familiar with this type of handling. After the results obtained and thanks to the suggestions made by the collaborating physicians, the required modifications were applied to arrive at a final prototype of the insertion system (Figure III-3) (Annex 1).

The final design of the insertion system consists of a cannula where in its proximal part there is a support to place the index and the medium finger. Inside it there is a longitudinally dipstick with a ring-shaped support on the proximal part. In this way we obtain a mobile mechanism similar to a commonly used syringe (Figure III-3 A and B).

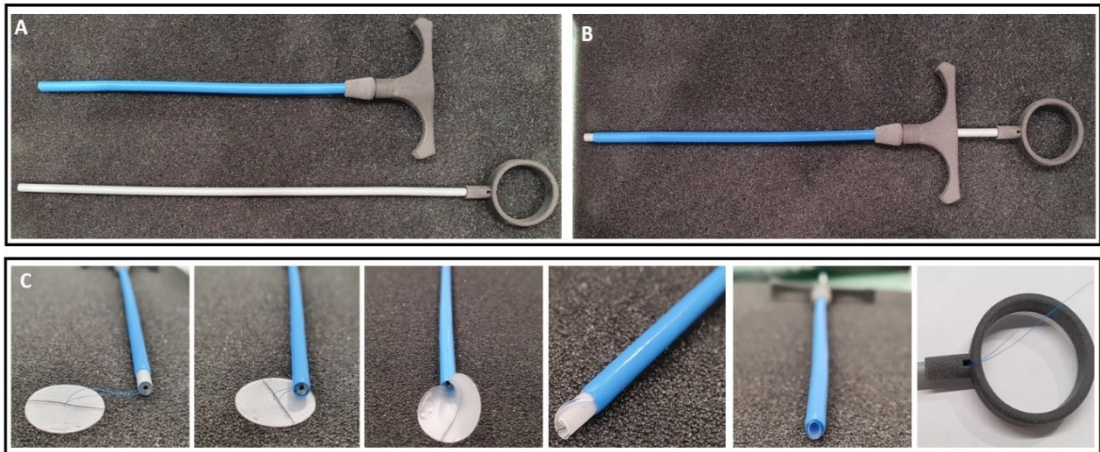


Figure III-3. Final design of the two disassembled parts of the insertion system prototype (A), and the ensembled insertions system that is used in the *ex vivo* and *in vivo* assays, with the modifications proposed by the collaborating doctors (B); process of placing the rolled patch inside the cannula. The entry of the clamping/pulling wire through the pierced rod can be observed, with the consequent exit through the hole of the thumb pusher (C).

At the distal part of the interior of the cannula there is the rolled patch (Figure III-3 C). The anchoring wire integrated to the silicone, which acts as a fixing point, allows the glue to be held with a subsection wire with which we will make the traction. The two caps of this fastening wire go through the dipstick through the existing hole until they come out through the base of the pusher ring. In this way, once the adhesive is deployed inside and the optimal activation time of the adhesive has passed, the insertion system and the trocar used during surgery can be removed simultaneously. Next, the adhesive is fixed by pulling with the double thread of subsection the indicated time without deformation. Once the adhesive is fixed to the amnion we remove the traction wire stretching one of the two caps of the wire, which is smoothed thanks to the anchor wire integrated to the adhesive until it is completely extended (Figure III-4). Finally, ultrasound would verify that the patch is correctly attached and would proceed to suture the incision point of the muscle layers and the skin.

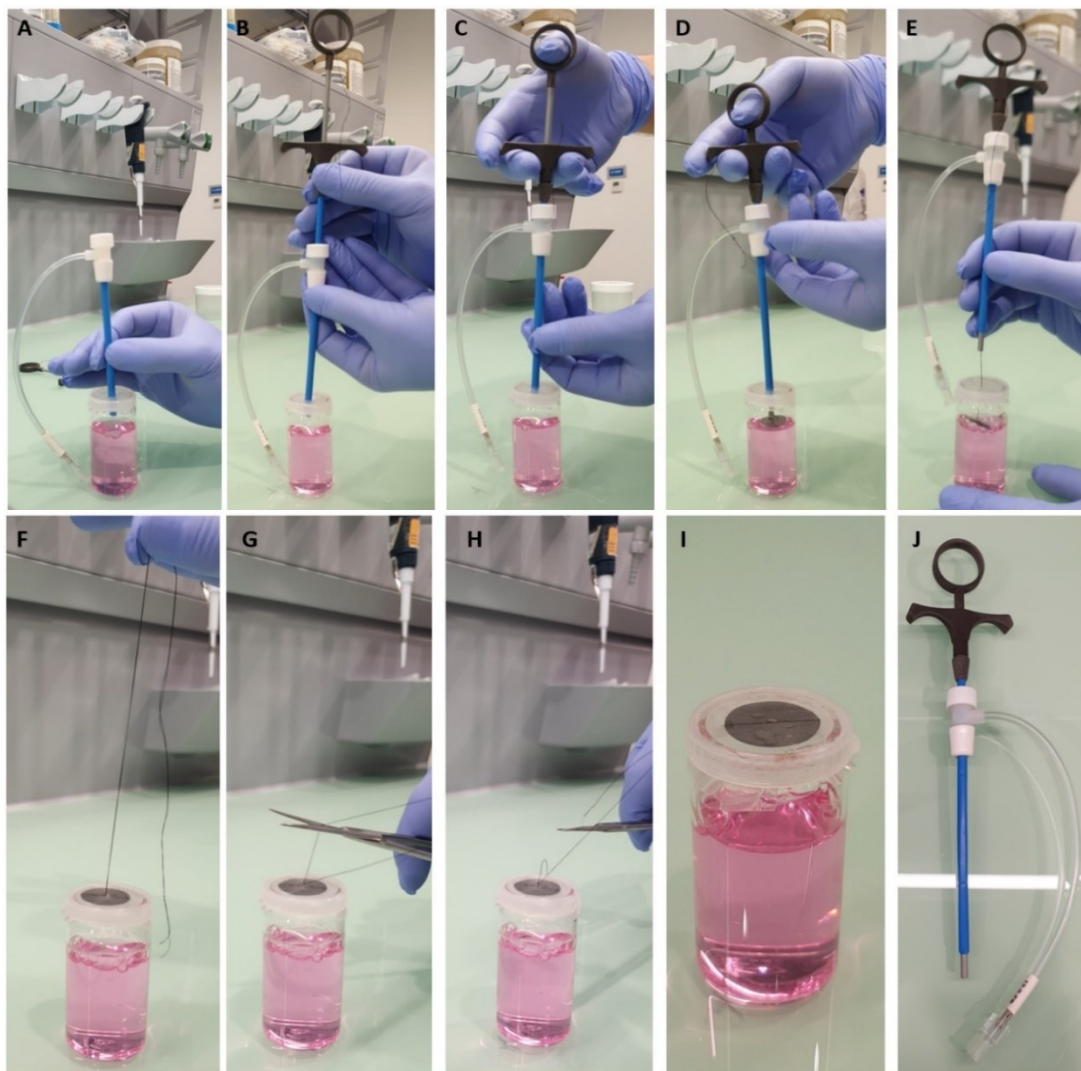


Figure III-4. Images of the complete process of placing the patch on a silicone membrane with the final prototype introducer. First step: introduction of the introducer, with the patch rolled inside, through the trocar until the introducer cannula emerges from the distal end of the trocar cannula (A and B); Second step: hold the introducer like a syringe and press the pusher with your thumb until the patch comes out of the cannula (C and D); Third step: with the patch already deployed, remove the trocar along together with the introducer (J) until leaving only the double thread and gently pull to keep the patch attached to the membrane (E and F); Final step: cut one of the ends of the traction thread and pull the other so that the thread slides and only the patch is stuck to the membrane (G-I).

It should be said that in order to finish pointing the insertion system, not only was it developed and tested in the laboratory, but it was also tested, modified and pointed during some of the *ex vivo* phantom and *in vivo* assays that will be carried out in Chapter IV. It is precisely during these assays, together with the medical team, that decisions regarding design and measurements are evaluated and taken. The introducer must be comfortable, easy to use, simple, intuitive, but above all it must be effective.

In future versions, outside of this thesis, the material of the dipstick will be modified to be more rigid, and the pieces currently produced by 3D printing will be produced by additive manufacturing by injection molding. Moreover, reserving modifications in the design of the manual clasper and the pusher, we can customize the introducer so that it can be used in a robotic surgical system, such as the Da Vinci (Intuitive Surgical).

3.4. Concluding remarks

A prototype introducer has been manufactured with a mechanism validated by medical personnel that, when introduced through a trocar used in minimally invasive surgery, allows the protection, release, unfolding and attachment of the patch to the amniotic membrane. It should also allow the quick activation of the adhesives developed in chapter IV. The introducer can be manufactured with different diameters and lengths according to market needs, and easily modified due to the 3D modeling software that allows changes to be made simply and quickly. In addition, the software incorporates a tool with which to create the mold planes. This is a very useful tool when, in the future, we want to manufacture larger scale introducers with materials that comply with the regulations for medical devices of this type.

Both the final prototype of the individual introducer and the entire sealing system (introducer + patch) allow sterilization with ethylene oxide, and can certainly be sterilized with other methods that, although considered, have not been used.

Thus, then, we have an introducer system that will be used in some *ex vivo* tests and in the *in vivo* tests in the following chapters to evaluate the adhesion of the patch to the amniotic membrane.

Chapter IV. Bioadhesives with activation on wet environment

This thesis has generated the following article: T. Micheletti, E. Eixarch, S. Berdun, G. Febas, E. Mazza, S. Borrós, E. Gratacos, Ex-vivo mechanical sealing properties and toxicity of a bioadhesive patch as sealing system for fetal membrane iatrogenic defects, Sci. Rep. 10 (2020) 1–10. <https://doi.org/10.1038/s41598-020-75242-y>.

Bioadhesives with activation on wet environment

This chapter discusses the different strategies followed to create a layer with adhesive properties on the designed patches. It includes the development of the bioadhesives and the tests that have been carried out to evaluate their stability on the patch, as well as their adhesion capacity on human amniotic membranes (HAM). The creation of thin polymeric films with potential adhesive properties produced by Chemical Vapor Deposition techniques, an adhesive inspired by the glue of marine mussels, and finally an adhesive based on cellulose derivatives will be discussed. As well as the paradigm shift in terms of the strategies followed in the development of the adhesive

4.1. Introduction

There are an abundance of adhesives on the market with the fundamental function of joining two materials of the same or different natures and preventing them from separating. An adhesive is defined as a substance that acts as an interface between the surfaces of these two materials, called substrates, and prevents them from separating by means of physical and chemical forces (adhesion) between the adhesive and the substrate, and the internal force of the adhesive (cohesion).

The evaluation of the adhesion can be done by means of an adhesive bond breakage assay, with which we will find four possible cases (Figure IV-1):

- Separation by adhesion appears when separation occurs at the substrate-adhesive interface.
- Separation by cohesion occurs when adhesive bonding occurs.
- Intermittent separation, which would be a mixture of the two previous ones.
- Separation by substrate breakage occurs when the substrate breaks before the adhesive bond or interface does.

When an adhesive is designed, it is intended that the separation never occurs at the substrate-adhesive interface, but that the breakage is intended to be cohesive.

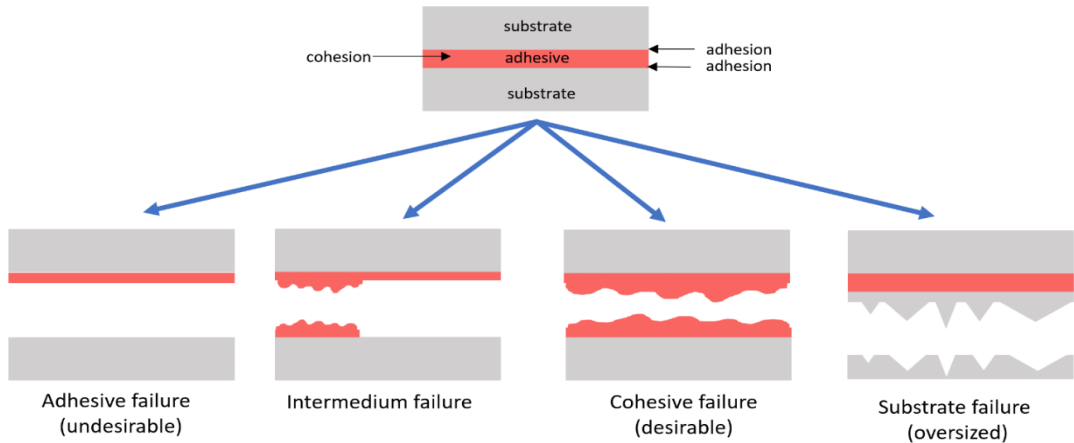


Figure IV-1. Scheme of the four types of failure that exist when two pieces joined by an adhesive are separated.

One of the most commonly used classifications is based on the formation mechanism of the adhesive joint, which can be divided into two main groups: pre-polymerized adhesives, in other words, those in which the polymer already exists before being applied to the substrate; and reactive adhesives, those in which the adhesive in liquid, viscous, gel, . . . , state is formed by monomers or oligomer chains that polymerize or crosslink during the polymerization process when they are placed between the two substrates to be bonded⁷².

-Pre-polymerized adhesives:

a) In liquid phase:

- i. Aqueous solutions such as cements, glues or starch.
- ii. Organic solutions such as natural rubber
- iii. Emulsions or liquid solutions such as PVC-based adhesives.

b) In solid phase:

- i. Piece-sensitive adhesives such as contact adhesives or adhesive tapes.
- ii. Hot melt adhesives.

-Reactive adhesives:

- a) That cure by polyaddition. Addition by opening a double bond of a monomer containing it, such as cyanoacrylates, anaerobics or acrylics.
- b) Curing by polycondensation. Condensation of single molecules in the reaction of difunctional monomers with reactive end groups, like epoxies or silicones.

When developing an adhesive, it is important to identify the adhesive bond formation process. That is, adhesives must be substances with very specific properties before and after the assembly of the two substrates. Before assembly the adhesive must be able to completely wet the entire surface of the materials to be bonded or sealed, including penetrating into all microcavities. And after assembly, the adhesive must hold the substrates together, in addition to serving as a physical-chemical barrier to prevent the ingress or leakage of liquids, gases or contaminants.

To explain the phenomenon of adhesion, there is no single theory, but it is necessary to know the different models. These explain the physical and chemical phenomena that occur at the substrate-adhesive interface. The physical phenomena can be explained by the mechanical adhesion model, the diffusion theory and the electrical theory. Chemical phenomena are explained by the thermodynamic adsorption or surface wetting theory.⁷²⁻⁷⁴

Most of these principles and concepts of adhesive development can also be applied to the field of surgical adhesives, but not always. Surgical adhesives are defined as biocompatible and biodegradable substances that polymerize or crosslink two surfaces where at least one of them is of biological origin (cells, tissue, organ, etc.). There is a great variety of them, both of biological and synthetic origin. The substrates of biological origin and the wet environment of the body are two factors that make it very difficult both to develop a bioadhesive and to evaluate this adhesion. There is a big difference in the development of an adhesive for external use (e.g. skin) and one for internal use (e.g. bone, blood vessels, lung, gut, etc.), where each tissue has its own characteristics. They have different stiffness, flexibility, elasticity and roughness. They have different surrounding fluids (blood, urine, amniotic fluid, mucus, saliva, etc.) and a certain cellular growth. A unique regeneration and vascularization, etc. At the laboratory level, it is often difficult to create a model whose results can be transferred to *in vivo* studies, due to the lack of a standardized methodology. The use of human samples is limited, and simulating organs and tissues, as well as their environment, is not an easy task. This difficulty also lies in the fact that the use of internal adhesives is relatively new. Perhaps not so much in open surgeries but in minimally invasive surgeries and in increasingly complex reconstructive procedures. Currently, the great advances in minimally invasive complex reconstructive surgery are linked to advances in the field of bioadhesives and biomaterials, where research itself is fed back.⁷⁵

Surgical adhesives have traditionally been used initially as wound dressings, skin adhesives and dental fixings. Until now, the major players in adhesive development were biomedical companies, traditional adhesive companies or medical device developers such as Baxter,

BBraun, BD Global, Ethicon, etc. It is in the last two decades that the interest of the pharmaceutical industry in adhesives has grown. Mainly due to their great potential for controlled release of drugs at sites of action (e.g. in the cornea or oral cavity) or at sites of absorption (e.g. in the small intestine or nasal cavity). Adhesives can also be used as therapeutic agents due to the fact that they can coat and protect damaged tissues (gastric ulcers or oral mucosal lesions) or be used as lubricants (oral cavity, eyes, and vagina). Also of interest are skin adhesives, tissue sealants, dental adhesives and bone cements. Due to all these uses and increasing research efforts in the biomedical and pharmacological sector, more and more adhesives for medical use are appearing on the market (Table IV-I).^{43,74-77}

Adhesives for medical use can be classified in different ways according to several criteria. According to their molecular origin they can be of biological origin (gelatin, chitosan, collagen, fibrinogen, etc.) or of synthetic origin (cyanoacrylates, methacrylates, polystyrenes, polyvinylalcohol, etc.). Depending on the type of tissue where it is to be used, they can be classified into adhesives for hard tissues (dental cements, bone cements, etc.) or adhesives for soft tissues (pressure sensitive adhesives (PSA) for skin wounds, 2-octyl cyanoacrylate for joining blood vessels, fibrin and albumin-based organ sealants, etc.). Depending on whether it binds to cells and cell surfaces (cytoadhesives) or whether it binds to mucous membranes (mucoadhesives) such as the inside of the mouth, nose or intestine. Depending on whether the use is external on skin or internal on organs and tissues. Depending on the desired effect on the tissue, they can be hemostatic agents, tissue sealants, hydrocolloids, cements, fixatives, or binding agents. An authoritative criterion is therefore necessary to clarify the classification of bioadhesives that have been developed and are in the process of development. In addition, a systematic standard for new emerging formulations is urgently needed, such as a well-accepted manual on evaluation protocols for each medical application linked to a condition or disease. For example, the same test will not be used to evaluate a bioadhesive for bone application as one developed to prevent seroma.^{75,76,78,79}

Table IV-1. Table of some marketed products presents in the biomedical market.

Trade names	Manufacturer	Composition	Crosslinker	Use
Band-Aid®	Johnson & Johnson	PVC, polyethylene or polyurethane		Skin injuries
BioGlue®⁸⁰	CryoLife	Purified bovine serum albumin (BSA)	Glutaraldehyde	Vascular surgery
Coseal®	Baxter Healthcare	Two modified PEG dilute hydrogel chloride	Sodium phosphate/sodium carbonate solution	Surgical sealant. Hemostatic agent
Crosseal	Omxix Biopharmaceuticals	Human-derived proteins as tranexanemic acid		
Dermabond®⁸⁰	Ethicon	2-octyl cyanoacrylate		
Duraseal®⁸¹	Confluent Surgical Inc.	Hydrogel of PEG ester solution	Trilysine amines solution	Neurologic surgeries (sutures)
FloSeal	Baxter Healthcare	Bovine-derived Gelatingranules + bovine thrombin solution		hemostatic
Glubran®⁸²	GEM	Ethyl-2-cyanoacrylate, butyl acrylate and methacryloxysulpholane		
Glubran® 2	GEM	n-butyl-2-cyanacrylate and methacryloxysulphane		Laparoscopic and traditional surgery and digestive endoscopy. Embolizing agent
Glubran® Tiss 2	GEM			Cutaneous use
Hystoacryl®	B.Brown	n-butyl 2-cyanoacrylate		Closure of clean surgical wounds with minimal tension. Sclerotherapy of esophageal varices and gastric fundus.
Preveleak®	Baxter Healthcare	BSA	Polyaldehyde	Blood vessels and tissues around the heart
SurgiFlo®	Ethicon	Gelatin matrix	Thrombin	
Tisseel	Baxter Healthcare	Human Fibrinogen/Bovine aprotinin	Human thrombin/calcium Chloride dihydrate	Hemostatic, mesh fixation, gastrointestinal anastomoses, neurosurgery
Tissucol®	Baxter Healthcare	Human fibrinogen, Factor XIII, human fibronectine, human plasminogen,	Bovine aprotinine, human thrombine	Local Hemostasis
Tridyne™ VS	BD Global	Polyethilenglycol + Human serum albumine		Extravascular leakage

Thus, the strategy to follow in the development of an adhesive for medical use, although not entirely clear, in our opinion is defined by:

- The type of tissue where we want to use the bioadhesive and its environment.
- How and when the adhesive should cure.
- How long it should remain acting.
- If we want to release some type of drug in the area.
- If we want tissue regeneration.
- Whether it should have flexible or elastic properties.
- If we want to use or not a support substrate together with the adhesive.
- If the adhesive will be of biological (bioadhesive) or synthetic origin.

Although we follow different strategies in the development of an adhesive, it must meet certain common criteria, in which bonding performance is the most important property. At the macro level, the total bond strength of an adhesive is defined as the maximum force required to separate two sections of adherent tissue joined by it, assuming that this force is equal to or greater than the original bond strength of the target tissues. At the micro level, and as mentioned above the total bonding performance of a bioadhesive is equal to the sum of the adhesive and cohesive forces.^{74,83,84}

Due to the fact that the quantity of functional groups in a formulation tends to be constant, the increase in adhesive strength is generally to the detriment of cohesive strength, and vice versa. Thus, to achieve ideal bonding performance, it is necessary to establish a balance between adhesive and cohesive strengths.⁸⁵ Two indispensable aspects during the gelation of an adhesive are its penetration into the surface of the tissue and its mechanical interlocking. A higher crosslinker density leads to a higher cohesive strength. While a good penetration ability can give better adhesion due to higher wetting and adsorption of the tissue surface, more uniform distribution and more mechanical interlocking. Thus, the degree of penetration of the adhesives and their crosslink densities are important factors affecting the overall bonding performance.^{74,86} As mentioned above, there must be a balance between adhesion and cohesion. Very high levels of cohesion can lead to a stiff and hardened bonding interface and cause tissue irritation. While the level of adhesive strength should be designed according to the selected tissue and applications. Adhesive and cohesive interactions typically include mechanical interlocking, intermolecular bonding, electrostatic bonding, chain entanglement and cross-linking formation. Adhesion generally involves molecular attractions while cohesion is practically due to mechanical interlocking.^{76,87,88}

Bonding performance is totally related to the effectiveness of the adhesive per se. That along with safety, usability, cost and approval, adds to the set of five categories proposed by Spontnitz and Bruke as criteria to be followed for the development of an ideal bioadhesive. As mentioned above, the biomaterial or adhesive must fulfill its function, it must be effective. Although the effectiveness of an adhesive system, which is quantitative, is in many cases determined by the surgeon's skills and the decisions taken at the time, especially with regard to sealants and hemostatics. There are no generic instructions for their use, due to the fact that it will depend on the complications, the type of intervention, the amount of fluids in the area, etc. For example, a plastic surgeon who must control a small but important exudate will need a greater amount of slow-acting material than a cardiovascular surgeon performing a reconstruction of a portion of the aorta. This is to say that a great effort must still be made to establish standards for the efficacy of hemostatic, sealing and bioadhesive agents. Some are not widely used because of the added difficulty of having to make different decisions depending on how the surgery evolves.^{77,89}

Safety is the second and most important category. Even if an adhesive is effective, it cannot be used in an intervention if it is not safe. Safety is defined by the toxicity (cytotoxicity, histotoxicity, organ toxicity and systemic toxicity) of the molecules that form the adhesive in the deposited area and the secondary products, by-products or metabolites resulting from the biodegradation of this adhesive in the same area or in the periphery, which can have a toxic effect and accumulate in distant tissues and organs through the bloodstream. In addition, it must avoid the risk of infection, be non-carcinogenic, and not cause immunological reactions, both in the short and long term.^{77,89}

The third category pertains to usability or ease of use. It is usually the operating room nurse who is in responsible for preparing the material. Therefore, easy and intuitive reconstitution or preparation of the bioadhesive is key to success. It is even better if this step can be eliminated or minimized, due to the fact that it is the surgeon who must apply the material to the site. Product efficacy or polymerization time is crucial, as is the ability to apply the material in a wide variety of procedures through applicators designed for linear, spray, endoscopic, laparoscopic or robotic techniques. While it would be ideal to have bioadhesives, sealants or hemostatics that can be used in multiple processes and interventions, the wide variety of these inevitably leads to establishing a specific use in a specific situation.^{77,89}

The fourth is the cost that the adhesive must have, both to produce it and to sell it. How cost-effective is its use. If its use shortens the duration of the procedure or the length of post-surgical hospitalization, there can be significant savings in the final medical cost. It is therefore very important that the price of the bioadhesive, sealant or hemostatic be below this cost.

Although many surgeons believe that the cost of such material should be below \$100 per application. Many times this cost-benefit analysis is not taken into account, so it should gain importance in the near future.⁹⁰

Finally, approval and regulatory approval are also crucial, due to the fact that the capacity to obtain a product certified by regulatory agencies such as the FDA or EMA is not a trivial problem. During development, the use of certain materials must be considered with an eye on the ability to save cost and time in the arduous regulatory process, where developing a new adhesion system or a new polymer or biomaterial will always be risky. An example is the fibrin sealant hemostatic that was approved in Europe in 1972 but not in the United States until 1998. It required 25 years of additional effort on the part of manufacturers and physicians to receive final approval. So a strategy focused on a small modification of an already accepted polymer never assures a quick and easy approval, although certainly with more speed and less effort than a new material that has never been used before and has no data.^{89,90}

In recent years, a wide variety of adhesives have been developed for medical use, each one targeted to a specific application and tissue, and with a curing strategy characteristic to the type of activation intended (Table IV-2). There are bioadhesives that polymerize by applying ultraviolet light, such as methacrylated gelatin.⁹¹ Bioadhesives that polymerize when they come into contact with environmental humidity, such as cyanoacrylates.²³ Bicomponent bioadhesives that are instantly activated when mixed with an oxidant as polymers bound to catechol groups.^{23,92} Bioadhesives in hydrogel form that adhere to mucous membranes by capturing water, such as carbomers or celluloses^{86,93}. There is a wide variety to choose from, each with its strengths and weaknesses. For this reason, it is of vital importance to establish a strategy for the bioadhesive developed to fulfill its function.

The strategy adopted for the development of our adhesive is partially defined because it must act in such a wet environment as the inside of the fetal sac, which is filled with amniotic fluid. It must be able to be introduced together with the patch inside the cannula without adhering to itself or to its internal walls, which would prevent it from being unfolded. It must also join two totally different substrates such as a biological surface (like the internal cellular monolayer of the amnion) and a silicone patch without detaching. At least it must remain adhered until the chorion and amnion are sealed by their natural overlapping movement, without loss of amniotic fluid.

Table IV-2. Table with the composition of some bioadhesives and strategies used in research to get new bioadhesives.

Bioadhesive	Composition	Crosslinker	Use
ASA/AG ⁹⁴	Sodium Alginate (SA)/Gelatin	Amino gelatin (AG)	Soft tissue adhesive
CAD-C ⁹⁵	Collagen (type I)	Citric Acid Derivative (CAD) with three active ester groups	Bonding reagent for soft tissue
GelMa ⁹¹	Methacrylated Gelatin	UV light	Lung leakage prevention
DCTA ⁹⁶	Gelatin	FeCl ₃ and genipin	Seroma prevention
	Gelatin		
PEG/DEX ⁹⁷	PEG amine + linear dextran aldehyde polymers + L-DOPA		
Gel/Alg/C ⁹⁸	Gelatin + alginate	Carbodiimide	
Dex-U-AD ⁹⁹	Gelatin + Dextrane	UV light	
CPT ¹⁰⁰	Chitosan + PEG	H ₂ O ₂	Wound closure and hemostasis
CS-PEG ¹⁰¹	Chondroitin sulfate (CS)	PEG-(NH ₂) ₆	Wound healing and regenerative medicine
PACA/PLLA ¹⁰²	Allyl 2-cyanoacrilate (PACA)+ Poly (L-lactic acid) (PLLA)	Poly (L-lactic acid)	Dermal wound healing
CHI-C ¹⁰³	Chitosan conjugated with catechol groups	Thiolates pluronic F-127 (Plu-SH)	Hemostasis
PEG4-D ¹⁰⁴	4armed PEG-NHS end-capped with dopamine	NaIO ₄	Tissue repair and drug delivery
cPEG4 ^{24,25,105}	4armed PEG-amine + 3,4-duhydroxydrocinnamic acid (DOHA) incorporation	NaIO ₄	Bioadhesive in extrahepatic islet transplantation
iCMBA ¹⁰⁶	Injectable Citrate-bases mussel-inspired bioadhesive iCMBA): Citric acid + PEG + dopamine	NaIO ₄	Suture replacement, tissue grafts, hemostatic wound dressing, waterproof sealants.
HA-CA ¹⁰⁷	dopaminated Hialuronic acid (HA)	NaIO ₄	Minimal invasive cell therapy
HA-ME	Methacrylated hyaluronic acid + irgacure 2959	UV light	
PAA-Dopa ¹⁰⁸	Dopaminated Poly(acrylic acid) (PAA)	ZnCl ₂	Biomedical adhesion and tissue
PE-dop ¹⁰⁹	Copolymer of 3,4-dihydroxystyrene-styrene	Fe ³⁺ , IO ₄ ⁻ , Cr ₂ O ₇ ²⁻	Underwater adhesion
DMA/UV-PVA ¹¹⁰	Dopamine methacrylamide (DMA) + photocurable poly (vinyl alcohol) (PVA)	Uv light and Darocur 1173	Bioadhesive hydrogel

Having made a brief review of the adhesives for medical use that have been developed and are currently being developed, and of the points and criteria to be taken into account for the development of the bioadhesive, the following points explain the three different strategies followed to obtain a patch that adheres to the amnion. It should be taken into account that each of the choices of these three strategies has been given by the results obtained and the discussions produced after the experiments carried out with the adhesives together with the proposed viscoelastic substrate (Chapter II), applying the conclusions and knowledge acquired during the process.

4.1.1. Bioadhesive thin film by Chemical Vapor Deposition.

One of the basic criteria proposed was that the adhesive layer should be sufficiently thin, flexible and elastic so that once the patch was rolled onto the cannula it would not separate from the silicone substrate, and that it would allow the patch to unfold correctly without altering its initial shape. In addition, in the choice of the strategy it was taken into account that the adhesive deposition process should be fast, relatively low cost and easily scalable. In this direction, the deposition of a thin adherent polymeric layer by Chemical Vapor Deposition (CVD) techniques was proposed.¹¹¹ These techniques have the basic and general foundation of forming a solid film on a substrate through a reaction of gas phase compounds (monomers or reactants). They are currently used in different industrial and biomedical applications such as the manufacture of coatings, powders, fibers and uniform components.¹¹²

In our case, monomers of interest are used as reactants to create an adhesive polymeric thin film on the patch surface. CVD techniques include Plasma Enhanced Chemical Vapor Deposition (PECVD), Pulse-Plasma Enhanced Chemical Vapor Deposition (PPECVD), initiated Chemical Vapor Deposition (iCVD), initiated Plasma Enhanced Chemical Vapor Deposition (iPECVD), oxidative Chemical Vapor Deposition (oCVD), grafting, and other variants. All of them have in common that it is necessary to use volatile reactants that will react inside a vacuum chamber. PECVD and PPECVD use the continuous and pulsed plasma state, respectively, as the energy source to form the polymers.¹¹³ iCVD uses a gas-phase initiator such as tetrabutylperoxide (TBPO) to create free radicals and facilitate the polymerization of the monomers. Whereas oCVD uses oxidizing species such as $\text{Fe}^{\text{III}}\text{Cl}_3$ or $\text{Fe}^{\text{III}}\text{p-toluenesulfonate}$ ($\text{Fe}^{\text{III}}\text{tosylate}$) for this purpose.^{114–116}

There are numerous research works realized and published in the last 20 years by the reference researchers in the field of CVD deposition techniques such as Gleason et al, Choy et al, and Yasuda et al, who, although working in the same field, surprisingly do not share the

same terminology for the same techniques.^{114,117,118} However, in recent years, reviews have also been published that attempt to integrate, update and standardize this terminology.^{119,120} Being fully aware of the advantages and disadvantages (Table IV-3)¹¹⁹, as well as their deposition ratio and retention of functional groups¹¹⁵ (Figure IV-2) PPCVD and iCVD techniques have been chosen for the creation of our thin film with bioadhesive properties. These techniques are commonly used in our research group, which gives us a certain advantage. This choice will allow us to compare, identify and select the most suitable technique for the polymerization of the different monomers or precursors to be used.

Table IV-3. Comparative table for some CVD techniques.

CVD techniques	Advantages	Drawbacks
CVD	<ul style="list-style-type: none"> • Avoids the line-of-sight. • High deposition rate. • Production of thick coating layers. • Co-deposition of material at the same time. 	<ul style="list-style-type: none"> • Requirement of high temperature. • Possibility of toxicity of precursors. • Mostly inorganic materials have been used.
PECVD ¹¹³	<ul style="list-style-type: none"> • Avoids the line-of-sight issue to certain extent. • High deposition rate. • Medium-low temperature. • Both organic and inorganic materials as precursors. • Unique chemical properties of the deposited films. • Thermal and chemical stability. • Wide range of monomer usable. • Resistances. • No limitations on substrates: complicated geometries and composition. 	<ul style="list-style-type: none"> • Random radical recombination occurs. • Instability against humidity and aging. • Time consuming specially for super-lattice structures. • Existence of toxic, explosive gases in the plasma stream. • High cost of equipment.
PPECVD	<ul style="list-style-type: none"> • More chemically-regular products. • More linear products. • Low temperature. 	<ul style="list-style-type: none"> • Difficult to find the right parameters • Existence of compressive and residual stresses in the films.
iCVD	<ul style="list-style-type: none"> • High stable polymerization process. • High number of unaltered functional groups. • Regular copolymerization. • Possibility to make an unaltered gradient of different polymer in the same sample. • Less energy. • Us of crosslinkers. 	<ul style="list-style-type: none"> • Slow process. • Low deposition rate. • Difficult to clean the chamber. • Use of strong oxidants as peroxides. • It is necessary to activate the substrate previously.

Plasma deposition techniques allow the functionalization of surfaces of various types. That is, the modification of the physical and chemical properties of the exposed surface of any part that is introduced into the reactor, through the addition of thin films of nanometer thickness. Thus obtaining a surface covered with the reactive groups of interest.^{121–126}

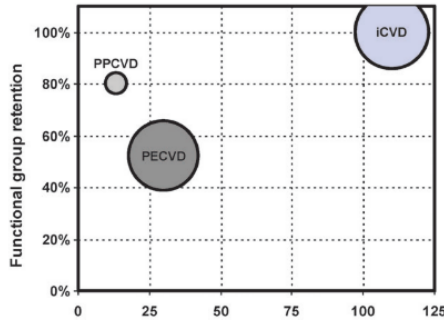


Figure IV-2. Graphic when the deposition grade and functional group retention of PECVD, PPECVD and iCVD can be observed.¹¹⁵

Pulsed Plasma Enhanced Chemical Vapor Deposition (PPECVD)

As briefly discussed above, CVD techniques are generally based on the creation of a thin polymeric film on a surface from the monomers in the gas phase. Specifically, the PECVD and PPECVD techniques do so by using plasma in a vacuum chamber. The basis of the technique is that the plasma creates ions and radicals in the monomers that are introduced in such a way that they react with each other and bind to the substrate forming a layer that grows the longer the process progresses. The deposition rate of PPECVD and PECVD is typically higher than non-plasma methods. Control is easier due to the fact that the plasma-activated precursor is more reactive, and a selective voltage can be applied to control the concentration of ionized precursors inside the chamber.^{113,119} While PECVD energy is delivered continuously to the monomer, leading to multiple fragmentation pathways and the creation of new molecules, in PPECVD this energy is applied in short bursts, allowing molecules exposed to the electric field to return to a ground state between each pulse. Förch et al. characterize the pulsed plasma deposition mechanism in terms of plasma on-time or t_{on} , off-time or t_{off} , and input power or P_{peak} . Plasma modulation is defined by the Duty Cycle (DC), which is the ratio of t_{on} to the total pulse duration ($t_{on}+t_{off}$),

$$DC = \frac{t_{on}}{(t_{on} + t_{off})}$$

while the equivalent power, or P_{eq} , experienced by the substrate material during the pulse duration is expressed as the product of DC and P_{peak} .¹²⁷

$$P_{eq} = DC * P_{peak}$$

Thus, the thickness of the polymeric layer, its flexibility and the nature of the reactive groups available are defined by the type of monomer used, the polymerization time, the P_{eq} applied, the internal vacuum pressure of the reactor, the on/off cycles of the plasma or DC, and by the volatility and the input flow of the monomer or monomer mixture.

Induced Chemical Vapor Deposition (iCVD)

The iCVD technique (Figure IV-3) is another versatile method for forming polymer films by radical polymerization, in which polymers are formed by growing their chain. A thermal initiator is introduced simultaneously with one or more vapor-phase monomers into the vacuum chamber. The filaments, which are suspended a few centimeters from the sample, are heated and when the thermal initiator flows through them, selective decomposition of the initiator takes place. The resulting fragments react with the monomers adsorbed on the surface of the cooled substrate and polymerization occurs. iCVD is compatible with vinyl monomers, acrylates, methacrylates and styrenes. The functional groups of the monomers, such as epoxies, amines or carboxylic acids, remain intact, converting the deposited polymer layer into a reactive polymer layer, even at high deposition rates. The conservation of these functional groups is key to making thin films that respond to changes in humidity, temperature or pH.

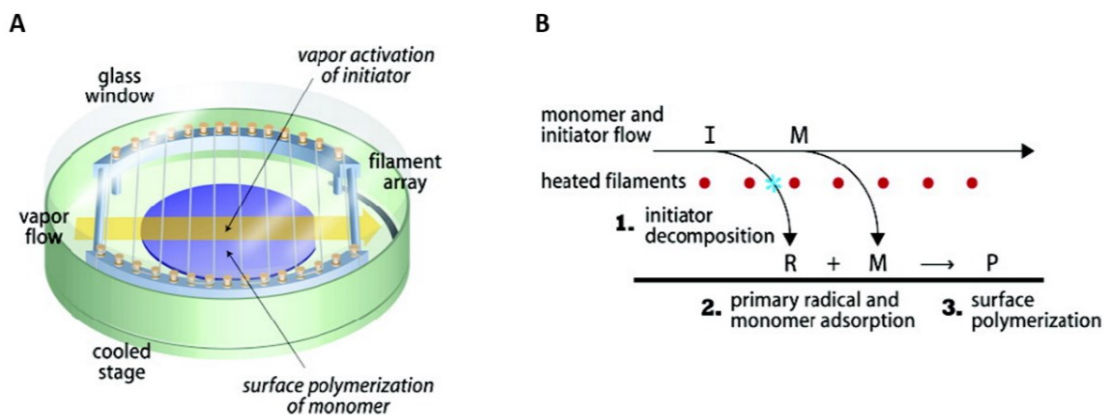


Figure IV-3. Schematic picture of a standard iCVD reactor (A) and a scheme of the polymerization process that occurs into the vacuum chamber.¹¹⁶

Monomers Library

There is a wide library of monomers (Figure IV-4) that can be used to create films by CVD techniques which, as mentioned above, are based on the creation of radicals that react with each other to produce a growth of the polymer chain. This occurs in a wide variety of vinyl monomers, especially acrylates and methacrylates. Many of these monomers are commercially available, which has led to the rapid development of biocompatible, functional and biofunctional surfaces.^{115,128}

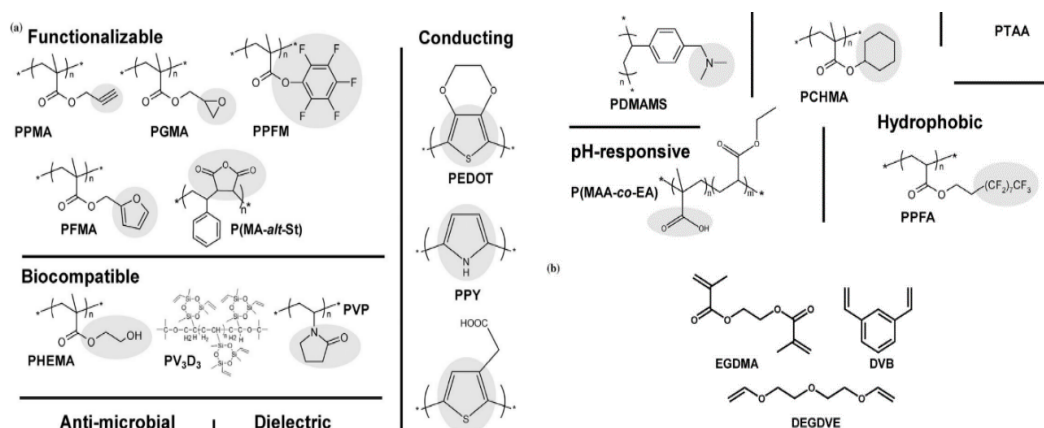


Figure IV-4. Library of the functional polymers formed by PPECVD and iCVD techniques.¹¹⁵

The library of functional polymers is formed by the polymerization of different monomers, and each family has characteristic properties. Existing polymers with bio-compatible properties are poly(2-hydroxyethyl methacrylate) (PHEMA) and poly(trivinyltrimethylcyclotrisiloxane) (PV₃D₃), polymers with anti-microbial properties are poly(dimethylaminomethyl styrene) (PDMAMS) and poly(dimethylaminoethyl methacrylate) (PDMAEM), polymers with hydrophobic properties are poly(perfluorodecyl acrylate) (PPFA), polymers with conductivity properties are poly(3,4-ethylenedioxythiophene) (PEDOT), poly(pyrrole) (PPY) and poly(3-thiopheneacetic acid) (PTAA), monomers used as crosslinkers are ethylene glycol diacrylate (EGDA), ethylene glycol methacrylate (EGDMA) and divinylbenzene (DVB), and of course exist a list of monomers with functionalized groups. In other words, they have a reactive group and the polymerization of these monomers allows binding and blocking molecules on their surface by additive or substitutive reactions. These polymers are, among others, poly(glycidyl methacrylate) (PGMA), poly(pentafluorophenyl methacrylate) (PFM), poly(propargyl methacrylate) (PPMA), poly(furfuryl methacrylate) (PFMA), poly(acrylic acid), poly(allylamine) (PAA), etc.^{111,115}

From the existing library of monomers, we have great interest in those that can exert an adhesion function thanks to their functional groups. GMA has an epoxy group that can covalently bind to amino groups of membrane proteins.¹²³ PFM is also highly reactive to amino groups.¹²⁹ AITC is not part of the library of monomers commonly used to create thin films but it has been found convenient to use it to create the first PAITC thin films. AITC has an isothiocyanate group which should also react rapidly with the amino groups of the membrane. Allylamine, on the other hand, has an amino group to which a reactive molecule can be attached and could also be useful to make an in vitro model of the amniotic membrane by simulating its surface with amino groups.¹²³ And finally, EGDA has the function of crosslinking the polymeric chains in case it is necessary to stabilize them when forming the thin film, due to the fact that the substrate used is viscoelastic, so the thin film should also be elastic.^{111,130}

Therefore, theoretically and for our final objective, the deposition of a thin film based on the functional and reactive monomers GMA, PFM and AITC, and using PPCVD and iCVD techniques would allow us to deposit a thin polymeric layer that would only have adhesive properties when enter in contact with the amniotic fluid and with the amino groups of the lysines of the proteins present in the cell membrane of the cells that form the cubic monolayer of the amnion.

4.1.2. Bioadhesive inspired on marine mussel glue.

Mussel adhesion is a natural process which involves the secretion of a type of protein glue that hardens into a solid and turns into a water-resistant adhesive.^{131,132} These types of mussel foot proteins (Mfps) are known to cure rapidly to form adhesive plates with high interfacial bond strength, durability and toughness. 3,4-Dihydroxyphenylalanine (Dopa), which is modified from tyrosine through post-translational hydroxylation, is one of the basic building blocks of Mfps. The catechol group of Dopa has the ability to form various types of chemical interactions and crosslinks rapidly. It is believed that the presence of these catechol groups fulfills the functions of interphase binding and solidification of adhesive proteins. The catechol group is capable of reacting in various ways, allowing it to bind to organic and inorganic surfaces, through the formation of reversible non-covalent and irreversible covalent bonds (Figure IV-5). This variety of interactions proposed by several authors provides the opportunity for the development of bioadhesives based on the utilization of some of these reactions.¹³³⁻¹³⁵

A good strategy to follow in the development of an adhesive based on the reactivity of Dopa groups is to add these groups to polymeric chains of biological or synthetic origin. In this direction, researchers around the world are adding these catechol groups to polyethylene glycol chains (cPEG)^{23,136}, to chitosan chains⁹², to tetronic acid (cT) and even extracting mussel proteins to create a mussel adhesive protein solution (MAPS)¹³⁷. Researchers are also working on the deposition of poly(Dopamine) (PDA) on surfaces to render them reactive.^{138,139}

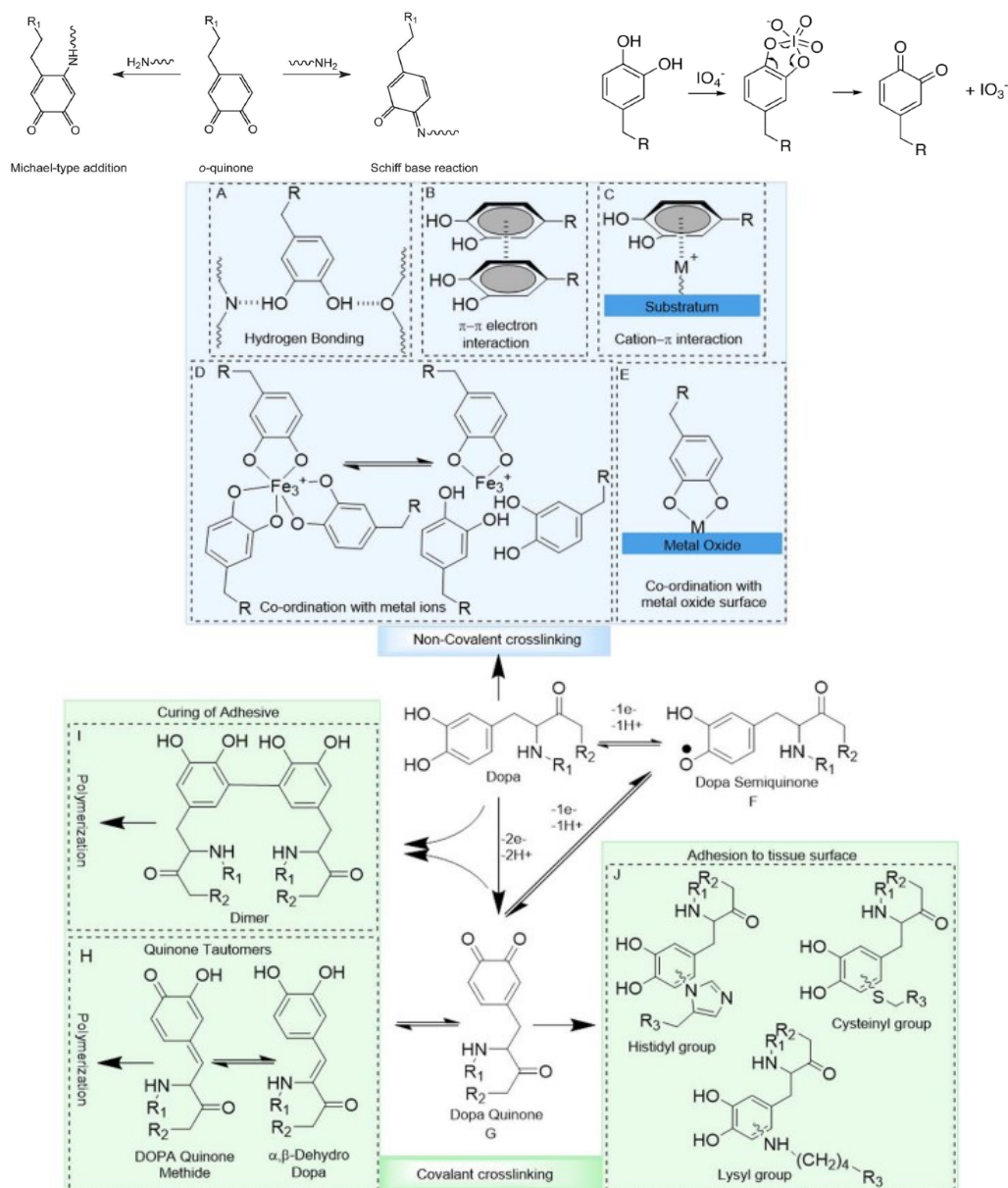


Figure IV-5. Possible interactions and reactions of the catechol groups of dopa.¹³³

Thus, there is an excellent opportunity to develop a bioadhesive of this type from natural polymers such as collagen, hyaluronic acid or gelatin, due to the fact that theoretically they would be more similar in nature to the amniotic membrane. In addition to having a hydrogel behavior, which gives a greater affinity on tissues and an increase in molecular interactions in an aqueous medium, such as the inside of the fetal sac, filled with amniotic fluid.

4.1.3. Bioadhesive inspired in the formation of hydrogels with cellulose derivates.

Soft tissue wounds can be due to traumatic injuries or wounds caused by surgery. Traditionally, the way to close these wounds has been by sutures, but these sutures are not the ideal method due to the fact that, in addition to being an invasive method, the material from which the suture thread is made does not actively participate in the healing, scarring and regeneration process of the affected tissue. Compared to traditional sutures, soft tissue adhesives have effective homeostasis, require less equipment and less time, and avoid the appearance of secondary wounds caused by the removal of non-absorbable sutures.

As mentioned above, commercial adhesives for soft tissue application include cyanoacrylates, gelatin, and fibrin glue, which, although they offer certain advantages, do not solve the problems and demands of surgeons. An ideal adhesive for soft tissues should have a high-water content, be safe, easy to apply, degradable and have the desired adhesion for each type of tissue. Cyanoacrylate can cause toxicity and inflammation. Fibrin is extracted from plasma, so it has a very high cost and can transmit disease. And the cross-linking stability of gelatin is very low. All this has led many researchers to look at hydrogels as potential bioadhesives. Both in cell migration, growth and organization during regeneration, as well as in their adhesive and sealing properties.⁹⁴

Hydrogels are polymers that have a high-water content due to their water absorbing properties. Their polymer chains once cross-linked become insoluble, forming a large water-trapping network. The resulting hydrogel can consist of 1-2 % polymer and 98-99 % water by volume. In addition, they can be dehydrated and then swollen in water to regain their hydrated form. Although in recent years they have been used more for drug encapsulation applications and as extracellular matrix-like scaffolds, recently there has been growing interest in their use as bioadhesives. Their high hydration capacity allows them to maintain the native physiological microenvironment, to present good properties against bacterial infections in the wound, and to mimic certain properties of the extracellular matrix serving as a substrate for wound regeneration or healing.¹⁴⁰

Hydrogels can be of synthetic origin, natural origin, and a mixture of both. Synthetics have the advantage of greater reproducibility, adaptable mechanical properties and control of the scaffold architecture, macroscopic characteristics and cross-linking of the polymer chains. In contrast, to form the hydrogel, most synthetic polymers require hard processing conditions such as the use of organic solvents or high temperatures, which are not suitable for cells or the tissues they form. During the last decades, some synthetic polymers have emerged as potential candidates due to their solubility in water. These polymers usually contain hydrophilic groups and can be nonionic, cationic, anionic, or amphoteric. Depending on the molecular forces, synthetic polymers can be classified into thermoplastics and elastomers. Examples are PEG, PVA, polyacrylamide, polypropylene and poly(N-isopropyl acrylamide) (PNIOAAm). A common problem associated with these synthetic hydrogels is the lack of biological recognition for cell attachment, migration and proliferation.^{141,142} On the other hand, hydrogels of natural origin usually consist of proteins and polysaccharides. Commercial molecular matrices are formed from animal and plant tissues. They include proteins such as collagen from bovine skin, fibrinogen from blood products and silk proteins from silkworm cocoon. Polysaccharides such as hyaluronic acid are obtained from rooster combs and chitosan is obtained from the partial deacetylation of chitin isolated from crustacean shells. Given concerns about the possibility of infectious agents being transferred into animal tissue materials, alternative sources such as plant tissues are often selected and even produced by biosynthesis. Plant-derived polymers that have been studied include alginate, cellulose, and starch-based polymers.

Cellulose (Figure IV-6 A) is the most abundant, reusable and biodegradable polymer of natural origin used in different applications. Similar to other polysaccharides, cellulose has long been used in medical applications due to its lack of toxicity (monomeric residues are part of the metabolites that can be found in the body), its biodegradability, its insolubility in water and other organic compounds, its hydrophilicity and swelling, its stability to temperature and pH variations, and its chirality, as well as its lack of taste and odor.¹⁴³⁻¹⁴⁵

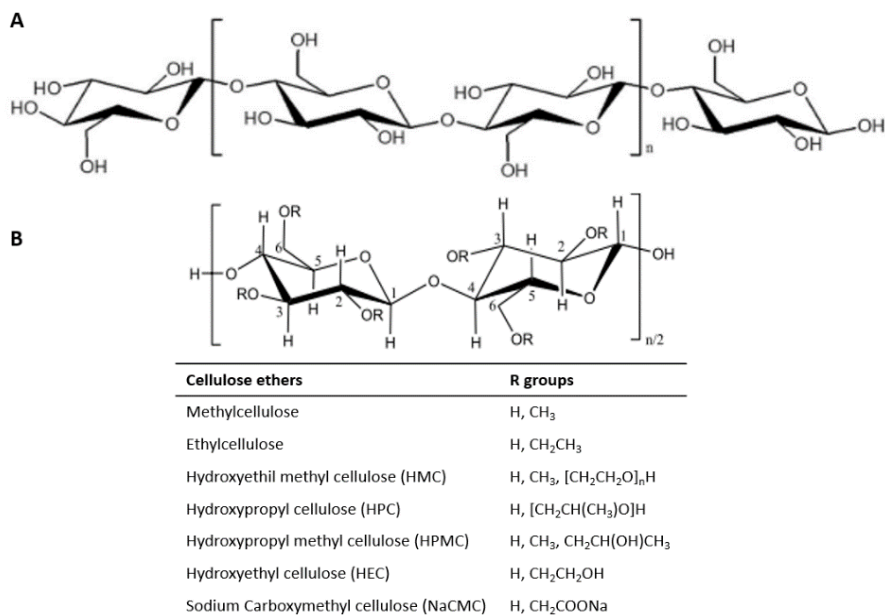


Figure IV-6. Cellulose molecular structure (A) and chemical structures of ether derivatives (B).¹⁴⁷

Functionalization and modification of celluloses is usually carried out through their hydroxyl groups, which has partial or full reactivity by using various reagents to produce derivatives such as cellulose esters and cellulose ethers with useful properties. Pure cellulose is insoluble in both cold and hot water due to its strong intramolecular hydrogen bonding, so these derivatives acquire some solubilization in water.^{141,146} The group of cellulose ethers (Figure IV-6 B) are of great interest and differ from each other by type of substituent, level of substitution, molecular weight (viscosity), and particle size. The average number of hydroxyl etherified groups in each glucose unit determines the degree of substitution, which can modify the properties to obtain a desired solubility and viscosity. The most common types of cellulose ethers are hydroxypropyl methyl cellulose (HPMC) or hypromellose, hydroxypropyl cellulose (HPC), hydroxyethyl cellulose (HEC) and sodium carboxymethyl cellulose (NaCMC).¹⁴⁷

In this direction, although traditionally celluloses are used more for drug encapsulation and release, the choice of cellulose is justified because some of its derivatives such as HPMC are soluble in water at low temperatures, but as the temperature increases it becomes less soluble, so theoretically we can control its solubility at body temperature. In addition to their high swelling capacity, their quick formation of hydrogen bridges with hydroxyl groups on the surface of tissues, and the ability to vary their viscosity, make them molecules of great interest to form a hydrogel with bioadhesive capabilities.

Therefore, the objectives of this chapter are to find a strategy that allows the patch surface to have wet adhesive properties on the amniotic membrane. The adhesive must be able to be deposited on the patch surface in such a way that it can be folded and unfolded without the adhesive separating or breaking. The adhesive must be deactivated when the patch is folded in the introducer and activated when it unfolds and enters in contact with the amniotic fluid. And *in vitro*, *in vitro*, *ex vivo* and *in vivo* tests must be created and set up to evaluate the efficacy of each of the adhesives to be developed, first without the introducer and then using the introducer developed in Chapter III.

4.2. Materials and Methods

The tests and trials to evaluate the adhesion of adhesives will be carried out taking into account the existing tests for the evaluation of adhesives but adapted to the tissue, the type of adhesive and the substrate chosen. It should be noted that the way of evaluating adhesives has been evolving and improving as the thesis progressed, so that at the end of the project a sequential methodology has been established that was not available at the beginning of the project. The characterization and evaluation of adhesion has been carried out according to the nature of the adhesive, so that sometimes the same tests are not performed. This can also be explained by the lack of a methodology and *ex vivo* tests with human amniotic membrane (HAM) at the beginning of the project. In addition to the first stages of development of an adhesive surface, an attempt was made to obtain a model of an artificial membrane that would behave physically and chemically as close as possible to the human amniotic membrane. This attempt was abandoned due to the availability of HAM from time to time. *Ex vivo* models with HAM were developed in parallel to the different adhesion strategies. Therefore, it is sometimes not possible to compare the results of the same test between different adhesives. Having HAM gave us the advantage of directly testing the patches with adhesive on the target tissue. For ethical and legal reasons, HAM tests could not be performed in our laboratory due to the fact that it is not accredited to work with human samples. So the *ex vivo* tests with HAM were performed in the laboratories of the Hospital de la Maternidad de Barcelona, together with members of the team of doctors collaborating in the project. Therefore, in our laboratory the adhesive development techniques were used, the different formulations were prepared, characterization techniques were used and the patches and the insertion system were fine-tuned. The *ex vivo* tests, as mentioned above, were performed at the Hospital de la Maternidad, the *in vivo* tests on rabbits at the Hospital de Sant Joan de Deu, and the *in vivo* tests on sheep at the Hospital de Bellvitge.

4.2.1. Bioadhesive thin film by Chemical Vapor Deposition

Deposition of the polymeric thin films

The functional monomers used to create the polymeric thin films are glycidyl methacrylate (GMA), allylamine (AA), ethylene glycol diacrylate (EGDA), hydroxyethyl methacrylate (HEMA) and allylthiocyanate (AITC). Terbutyl peroxide (TBPO) was used as reaction initiator in iCVD technique.

The thin films produced by PPECVD and iCVD techniques were deposited on medical grade silicone (NuSil 9340), and on silicon wafers as a deposition pattern.

Prior to initiating the polymerizations with both PPECVD and iCVD, the surface of the silicone samples was activated according to our standardized oxygen plasma activation process. (2.2.3)

A horizontal tubular borosilicate reactor, customized by our research group, has been used to create the different thin films by PPECVD (Figure IV-7).

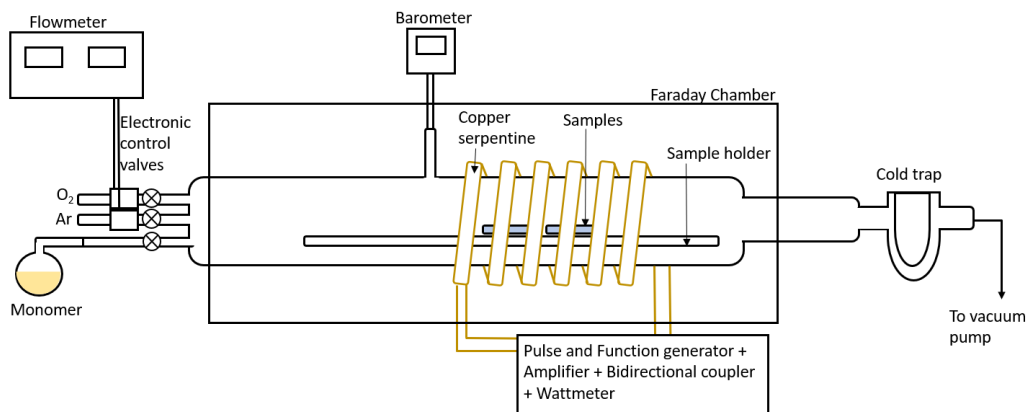


Figure IV-7. Scheme of the horizontal plasma reactor used to make the polymeric thin films by PPECVD techniques.

The conditions established for the deposition of the respective polymer thin films are as follows:

- a. AA thin film: Power= 15 W; t_{on} = 10 ms; t_{off} = 20 ms; $P_{O_{sist}}$ = 4.6×10^{-2} mbar; P_{wAlil} = 4×10^{-1} mbar; Temperature AA= RT; Time= 10 mins.
- b. AA/EGDA thin film: Power= 15 W; t_{on} = 10 ms; t_{off} = 20 ms; $P_{O_{sist}}$ = 4.5×10^{-2} mbar; P_{wAlil} = 5×10^{-1} mbar; P_{wEGDA} = 2.6×10^{-2} mbar; Temperature GMA= 75 °C; Temperature EGDA= RT; Time= 10 mins.
- c. AITC thin film: Power= 30 W; t_{on} = 10 ms; t_{off} = 20 ms; $P_{O_{sist}}$ = 3.7×10^{-2} mbar; P_{wAITC} = 7×10^{-2} mbar; Temperature AITC= 40 °C; Time= 3 mins.

To create the thin films by iCVD we have also used a customized reactor in which a 632.8 nm Helium-Neon laser (Thorlabs HNLS008R), a sensor (Thorlabs S120C) and the ThorlabsPowerMeter 1.0.2 software allow us to measure and calculate the thickness of the film during the polymer deposition process and stop the polymerization process when the film has the desired thickness (Figure IV-8).

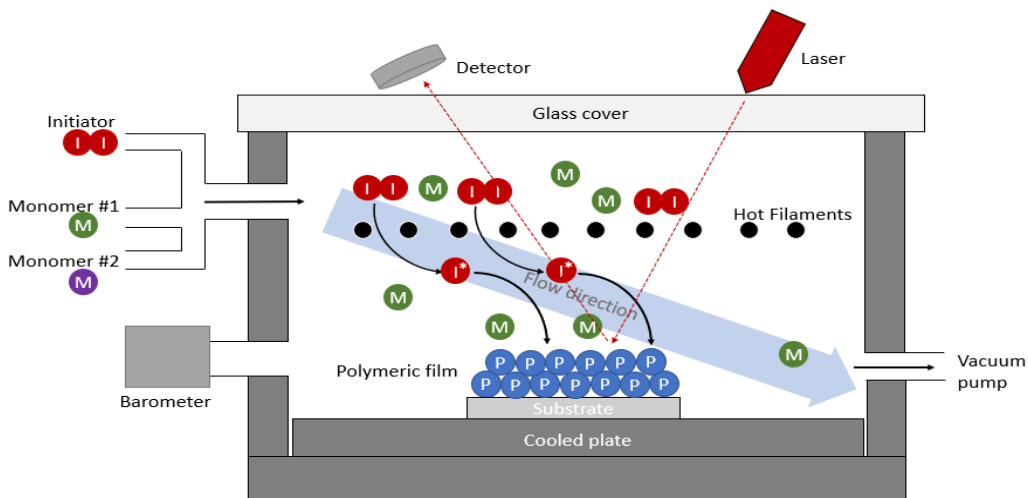


Figure IV-8. Scheme of the customized iCVD reactor to make the polymeric thin films and the position of the laser to measure the thickness.

The calculations to obtain the flow rates of the monomers, for all the depositions, start from a basal vacuum pressure of the system of $2-4 \times 10^{-2}$ mbar. Thus, the conditions established for obtaining the polymeric thin films on the medical silicone substrate by iCVD are as follows:

- a. GMA thin film: TBPO= 1.7 sccm; GMA= 1.5 sccm; $P_w = 8 \times 10^{-1}$ mbar. Plate $T^\circ = 15-24$ °C; TBPO $T^\circ = RT$; GMA $T^\circ = 70$ °C; tubes $T^\circ = 110$ °C; Filament $T^\circ = 300$ °C; Time 2.5 hours to obtain a 700 nm film.
- b. HEMA/EGDA/GMA thin film: TBPO= 1.7 sccm; HEMA= 0.26 sccm; EGDA= 0.13 sccm; GMA= 0.23 sccm; $P_w = 8 \times 10^{-1}$ mbar. Plate $T^\circ = 15-24$ °C; TBPO $T^\circ = RT$; HEMA $T^\circ = 80$ °C; EGDA $T^\circ = 60$ °C; GMA $T^\circ = 70$ °C; tubes $T^\circ = 110$ °C; Filament $T^\circ = 300$ °C; Time 1h to obtain a 200 nm film.
- c. HEMA/EGDA/PFM thin film: TBPO= 1.59 sccm; HEMA= 1.56 sccm; EGDA= 0.34 sccm; PFM= 3.22 sccm; $P_w = 8 \times 10^{-1}$ mbar. Plate $T^\circ = 15-24$ °C; TBPO $T^\circ = RT$; HEMA $T^\circ = 80$ °C; EGDA $T^\circ = 60$ °C; GMA $T^\circ = 70$ °C; tubes $T^\circ = 110$ °C; Filament $T^\circ = 300$ °C; Time 1h to obtain a 200 nm film.

Modification of the functional groups of silicone already polymerized with functional groups.

The modification of the allylamine thin film on the silicone substrate is done by adding a volume of X mL of 1,1-Thiocarbonyldi-2 (1H)-pyridone 95% (TCBP) (Alfa Aesar) at 200 mg/mL in DCM for x minutes. In this way theoretically an isothiocyanate group is obtained from allylamine.

Evaluation and characterization of different polymer thin films.

The way of evaluation has been improved as results were obtained, and the deposition strategy was modified. There is still no sequential order of tests to evaluate the suitability of the patch as a bioadhesive surface. On the one hand there is a physical and chemical evaluation and characterization of the film, and on the other hand adhesion tests using *ex vivo* human amniotic membrane (HAM) models.

The stability of the deposited polymer layer is evaluated by a simple visual cracking test on silicone without micropattern, in which the silicone is slightly stretched and observed for cracking with a microscope (Leica DM2500M). A solubility test is also performed by adding a drop of milliQ water or whatever solvent we are going to use to perform some reaction on the functionalized surface.

The presence of isothiocyanate groups on the silicone surface is evaluated by with a FTIR-ATR spectrometry (Nicolet iS10, Thermo Scientific).

The thickness of the most promising films is characterized by atomic force microscopy (AFM XE70, Park Systems).

The adhesion capacity is evaluated in 4 ways:

1. Adhesion of fluorescent proteins on the functional groups of the thin film.

Fluorescein-labeled albumin 6 mg/mL (Sigma-Aldrich) in 10X PBS is used to evaluate protein adhesion. Medical silicone discs with a hexagonal patterned copper grid (SPI Supplies) are used as a mask to exclusively polymerize the part not covered by the grid. Adhesion evaluation is qualitative, by comparison between the polymerized and unpolymerized areas with a Nikon Eclipse TE 2000-U fluorescence microscope.

2. Bacterial adhesion on thin film functional groups.

a) Bacterial biofilm adhesion.

Pseudomonas aeruginosa culture and biofilm formation on silicone discs with polymeric thin film in a half disc. Seeding of 100 000 cells/well in a 6-well plate with a volume of 5 mL TSB culture medium for 48 hours at 37 °C. Removal of the medium with care not to wash away the biofilm and staining with crystal violet. Evaluation of the edge of the film by optical microscopy for the presence of violet biofilm.

b) Adhesion of isolated bacteria.

Culture of *Escherichia coli* on silicone discs with polymeric thin film with hexagonal pattern. Seeding of 100 000 *E. coli* cells/well in a 48-well plate with a volume of 0.5 mL LB medium, at 37 °C under gentle agitation for 24 hours. Visualization of bacterial distribution with SEM.

3. Cell adhesion on the functional groups of the thin film.

Two types of cells are seeded in a 96-well plate with silicone on the bottom of the well. Human Normal Dermal Fibroblasts (HNDF) and Mammary gland derived from metastatic adenocarcinoma with GFP (MDA/GFP). 0.1 mL per well with 10 000 cells/well, 24 hours at 37 °C and 5 % CO₂. The silicone is half polymerized and half unpolymerized so that cell adhesion will be evaluated qualitatively by observing the deposition of cells on the transition line of the thin polymeric film with the silicone.

4. *Ex vivo* adhesion test

By means of *ex vivo* tests with human amniotic membrane, adhesion is evaluated with a manual lateral traction test and subsequent lifting 5 and 10 minutes after contact between the silicone thin film and the HAM. Saline and 10X PBS are added to maintain tissue wetting and to favor the interaction between the thin film and the amnion.

4.2.2. Bioadhesive inspired on marine mussel glue: dopaminated Hyaluronic Acid

The second family of bioadhesives developed and tested is dopaminated hyaluronic acid (DHA). This DHA has been obtained by modifying and adjusting a synthesis previously performed in our research group¹⁴⁸, based on the results obtained by Zhang et al¹⁴⁹. The objective is to establish a DHA formulation in which the application of an oxidizing agent causes a partial oxidation of the catechol groups to quinone groups, which are reactive to amino and hydroxyl groups. Therefore, this preliminary oxidation is intended to form a flexible dehydrated film that upon contact with the amniotic fluid finishes reacting with the amniotic membrane molecules.

Synthesis of dopaminated hyaluronic acid (DHA)

The hyaluronic acid used is of high molecular weight ($mw= 1 \times 10^6$) and pharmaceutical grade (F002104, from Bioibérica). The synthesis of DHA is divided into the oxidation phase of the hyaluronic acid chain (Figure IV-9 a) , and the incorporation phase of the dopa groups into the oxidized hyaluronic acid chain (Figure IV-9 b):

-Phase 1. Oxidation of HA.

Dissolve the HA in cold miliQ water at 10 mg/mL in a reaction balloon. The volume corresponding to 5% of a 0.5 M aqueous solution of sodium periodate is added dropwise. In the absence of light it is shaken during 2 h. Then a volume equivalent to 1% of the total volume of the initial HA solution of 1,2-propanediol is added to inactivate any unreacted sodium periodate and stirred for 1 h at room temperature. The solution is purified by exhaustive dialysis with miliQ water under gentle agitation, using a volume at least 20 times the volume to be dialyzed. The dry product is obtained by lyophilization.

The following amounts are attached as an example:

- 1) 1 g HA + 100 mL miliQ water (10 mg/mL) under stirring until complete dissolution.
- 2) 5 mL of 0.5 M NaIO₄ is added dropwise and allowed to react for 2 h in the dark.
- 3) To inactivate the unreacted NaIO₄ 1 mL 1,2 propanediol is added and stirred for 1 h at room temperature.
- 4) Dialysis is performed in miliQ water every 4 hours. Three changes of miliQ water.
- 5) It is lyophilized to obtain the dry product.

-Phase 2. Dopamination of the oxidized HA chain.

Once the freeze-dried ox-HA is obtained, the dopamination of the hyaluronic acid is performed. For this purpose, the desired grams of ox-HA are dissolved in 0.1 M sodium borate buffer at pH 8, containing 0.1 M NaCl until a concentration of 10 mg/mL is reached. The amount of dopamine hydrochloride is added to achieve a 1:3 reaction molar ratio of aldehyde groups of ox-HA to amines of dopamine groups. The mixture is stirred until complete dissolution for 1 h at room temperature.

Then the necessary amount of sodium cyanoborohydride (NaBH_3CN) is added as needed to achieve a reaction molar ratio of 1:6 of aldehyde groups of HA-ox to moles of sodium cyanoborohydride. The reaction is incubated under hood at 45 °C and in nitrogen atmosphere for 24 h. The solution is purified by exhaustive dialysis with milliQ water with a minimum of three changes every 4 hours, with a volume 20 times greater than that of the mixture to be dialyzed. Finally, it is lyophilized.

The following amounts are attached as an example:

- 1) 1 g oxidized HA + 3.15 g dopamine hydrochloride (molar ratio 1:5 aldehyde diamine) + 100 mL 0.1 M sodium borate and 0.1 M NaCl at pH 8. Shake until dissolution.
- 2) Add 2.09 g NaBH_3CN (molar ratio 1:6 aldehyde to NaBH_3CN). It is shaken and incubated at 45 °C for 24 h in N_2 atmosphere.
- 3) Dialysis is performed in MilliQ water 3 times every 4 hours.
- 4) Lyophilized to obtain the dry product.

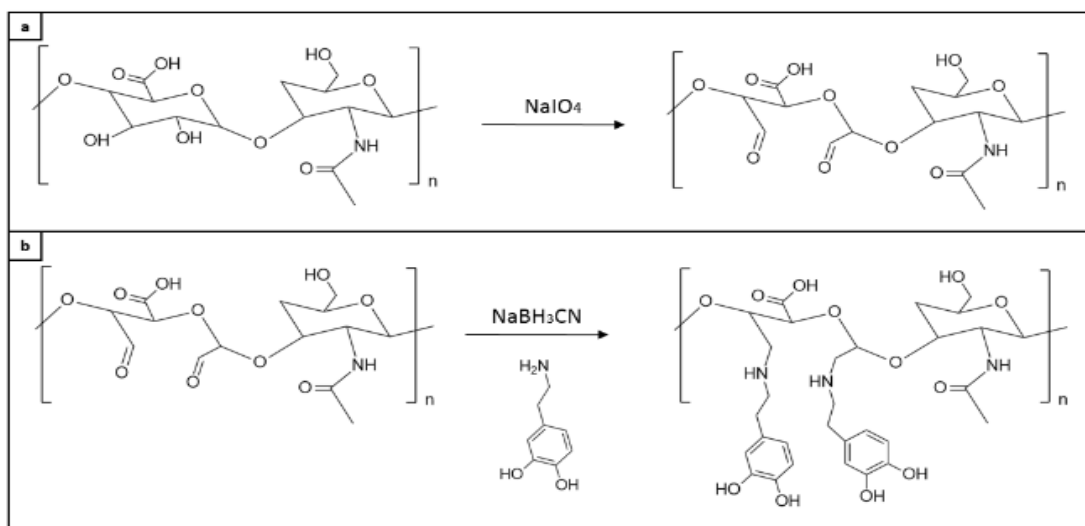


Figure IV-9. Synthesis of dopamine hyaluronic acid. Oxidation of HA (a) and incorporation of dopamine groups (b).¹⁴⁸

Synthesis evaluation.

The evaluation of the synthesis is performed by means of $^1\text{H-NMR}$ (400 MR spectrometer) and Mestrenova 9.0 software (Mestrelab Research), which calculates the degree of substitution (SD) or the percentage of dopa groups that have been substituted to the lateral chains of the hyaluronic acid.

Evaluation of the oxidation/adhesion reaction.

Different formulations of different concentrations of DHA with oxidizing agents such as Fe_3Cl_2 and NaIO_4 are provided. The volumes are deposited on a glass surface and different ratios of oxidants are mixed until a hydrogel or coagulate is formed. It should be remembered that these oxidants have to make a first partial conversion from catechol to quinone because if they do it completely, all the chains will react with each other and there will be no reactive groups available to react with the amino and hydroxyl groups of the amnios.

The ability to form a hydrogel or clot is evaluated, and the selected formulations are deposited on silicone disc activated with oxygen plasma. It is dehydrated in an oven at $40\text{ }^\circ\text{C}$ for 3 hours. It is left to rest at room temperature over night and then its flexibility is evaluated after being rolled. Finally, the adhesion to the amnios is evaluated with an adhesion test by uprising with a fragment of HAM.

HAM adhesion evaluation.

1. Multiaxial test.

The multiaxial test (Figure IV-10) consists of a low height stainless steel cylinder where we fix a piece of HAM at the top. We fix the HAM with a metallic ring with a load-bearing ring so that it is well sealed. The membrane is connected to a tank with a solution of PBS with fluorescein, and is blown up by a peristaltic pump at a speed of 2 mL/min. The cylinder has a manometer that registers the pressure changes in the system, so that when the pressure inside the chamber increases, the HAM is inflated until leakage and/or amnion rupture occurs, even exceeding the intrauterine pressures. In this way, by making a hole in the HAM and attaching the patch on the inside, we can record the pressure changes in the membrane, establishing the pressure at which the first leak appears and the pressure at which the membrane is ruptured, if the leak allows the rupture pressure to be reached. Before placing the patch in contact with the HAM, it is left to rehydrate with PBS for 1 minute and then a strong pressure force of approximately 1-2 N is applied for another 1 minute before placing it in the chamber and beginning to inflate it with the fluid. The evaluation of each sample with the multiaxial is stopped when the system pressure stops increasing. All the data of pressures and images

are recorded by a computer offering us images at the time of braking/leakage and creating pressure graphs.

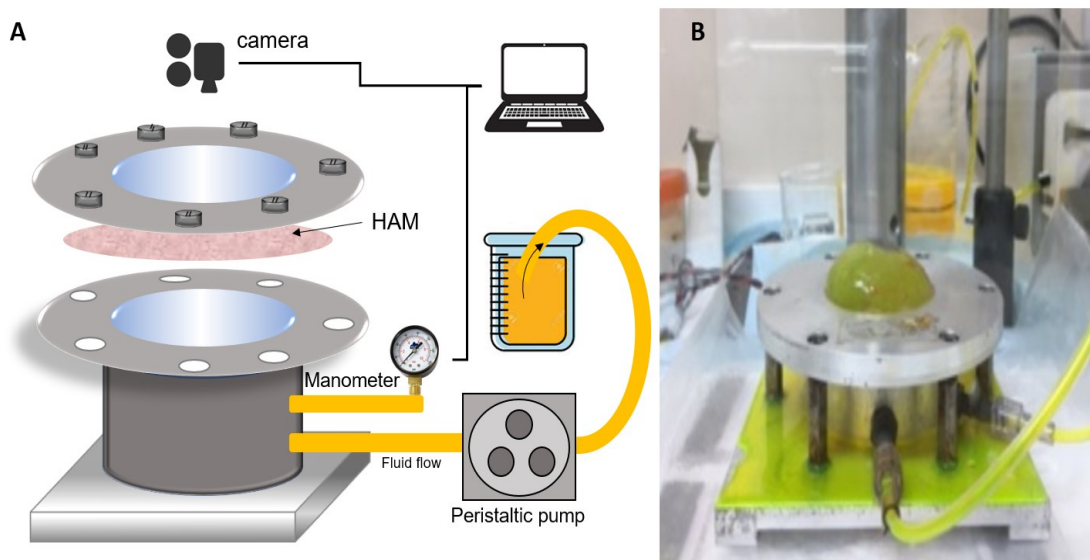


Figure IV-10. Scheme of the equipment to make the multi-axial *ex vivo* test (A) and the real image of the system (B).

2. Phantom test.

The patches that pass the multi-axial test are evaluated with another *ex vivo* test: the phantom adhesion test. (Figure IV-11). This type of phantom is made of silicone and simulates the layers of the skin and abdomen muscle of pregnant women up to the chorioamniotic membrane, so that by attaching the HAM to the lower part of the phantom we can simulate in a more realistic way all the human tissues that we find. The cylinder, about 20 cm high, is filled with PBS and the phantom acts as a stopper by fixing it at the bottom. The pressure is regulated by varying the height of a full PBS cylinder to stabilize the pressure inside the cylinder to about 30 mmHg. Different from the multi-axial test, in the phantom test we can introduce the adhesive with the developed insertion system, which at the same time is introduced through the inside of the trocar, reproducing the same steps that we would perform during the fixation of the adhesive to the fetal surgery.

Finally, the patches that give acceptable values in the phantom adhesion test are used in an assay with pregnant rabbit.

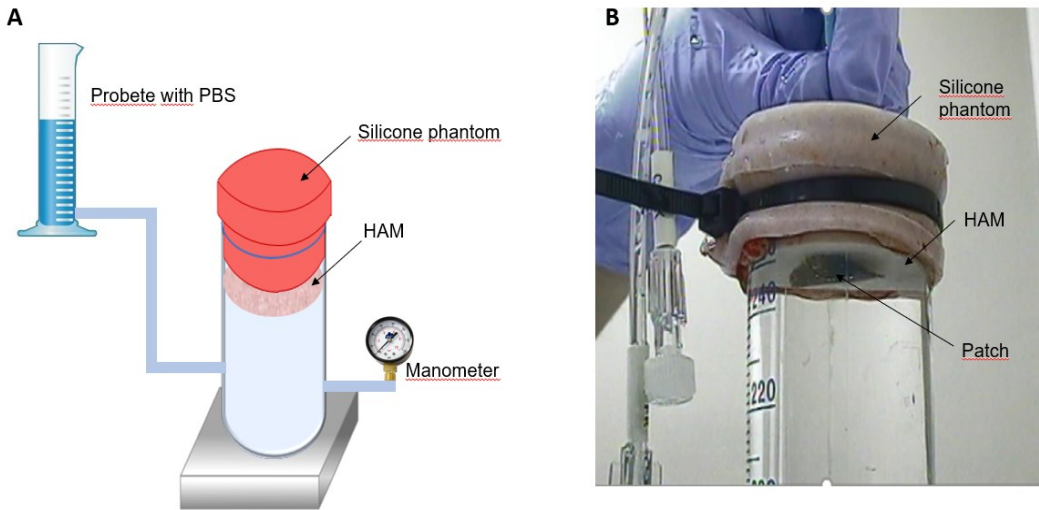


Figure IV-11. Scheme of the equipment used to realize the adhesion phantom test (A) and real image of a test with a silicone patch with DHA (B).

3. *In vivo* test with rabbits

The *in vivo* assay in pregnant rabbits is performed by making an incision in the abdomen to open it completely and remove the fetal sac with the fetuses inside. Once outside, a hole is made with a 10 F trocar and the patch is inserted with a 7 F introducer or introduction system adapted to the small size of the animal rabbit model. The patches have been adapted with a final diameter of 10 mm and a volume of adhesive proportional to the corresponding surface. Small sutures are made next to each patch to mark the position, and the fetal sac is reinserted. Finally, the tissue layers are closed and sutured. After 7 days the fetal sac is removed again, and the position of the patches to the chorioamniotic membrane and the presence of adhesive are evaluated by direct visualization.

4.2.3. Bioadhesive inspired in the formation of hydrogels with cellulose derivates.

Formulations.

The third type of adhesives are based on the formation of hydrogels from cellulose derivatives. After extensive pre-testing, the most promising formulations have been selected. The relevant volumes and concentrations were deposited on medical silicone discs with the micropattern and on medical silicone discs with the integrated electrospun PCU layer. All depositions have been made after activation in an oxygen plasma reactor (as discussed in section 2.2.3).

These formulations are:

- a. 0.3 mL HPMC to 10 mg/mL (H7509 de Sigma-Aldrich) with a viscosity of 2600-5600 mPa·s to 2 wt % in H₂O (20 °C) and a un mw of 86 kDa, for use in research.
- b. 0.3 mL HPMC to 10 mg/mL (Metolose® 90SH of ShinEtsu) with a viscosity of 15000 mPa·s al 2 wt % (20 °C), pharma grade.
- c. 0.3 mL HPMC to 10 mg/mL (Metolose® 90SH of ShinEtsu) with a viscosity of 100000 mPa·s at 2 wt % (20 °C), pharma grade.
- d. 0.3 mL HPMC 100000 M 10 mg/mL + HEC (250 HHX of Natrosol™ de Ashland™) 10 mg/mL, with different ratios.
- e. 0.3 mL HPMC 100000 M 10 mg/mL + AC 0.5%.
- f. 0.3 mL HPMC 100000 M + HEC HHX + AC 0.5%.

Sample preparation.

After activation of the silicone discs with oxygen plasma (see Chapter X), volumes of the selected formulations are deposited with a micropipette. The oxygen plasma treatment increases the hydrophilicity of the silicone disc and the adhesive formulations are spread homogeneously on its surface.

For the HPMC and HPMC/HEC samples without citric acid, once the formulation is deposited on the discs, they are dehydrated in an oven for 4 hours at 55 °C. The samples with citric acid are also dehydrated in the oven but with a first phase of 5 hours at 40 °C and a second phase of 10 hours at 80 °C. Afterwards, both are left to rest at room temperature.

Solubility evaluation of cellulose derivates adhesives.

The evaluation of the solubility is made by thermogravimetric analysis (TGA) (TGA 2 of Mettler Toledo) of the samples before and after immersion in mQ water and Simulated Body Fluid (SBF) at 37 °C under gentle agitation for a maximum of 168 h. The conditions of the analysis by TGA consist of a temperature ramp from 30 °C to 900 °C, with a temperature increase of 10 °K/min with nitrogen atmosphere. Three samples of 4.3 mm diameter are obtained from

each disc and the average is calculated to obtain the percentage of weight loss compared to the untreated samples.

Evaluation of adhesion in HAM.

1. *Ex vivo* tests.

The *ex vivo* adhesion and sealing tests are performed using the multiaxial test and the phantom test, in the same way as described in section 4.2.2. In addition, following the *in vivo* results with sheep, described below, an adhesion test based on the use of a dynamometer was set up to test the formulations with pharmacological grade HPMC. Adhesion tests are performed with a manual dynamometer (Sauter FH200) placed on a test bench (Sauter TVP-L). To perform the test, a disc with the adhesive to be tested is glued to the base with double-sided tape. A 20 mm diameter flat circular metal head is used. The first tests were performed with the bare head (data not shown), while the final tests are performed by adding a 0.6 mm thick polystyrene sponge attached to the head, which serves as an interface between the steel head and the chorioamniotic membrane, to reduce the hardness and make it look more like the real thing. Thus, the test is performed by adding 0.2 mL of PBS (10x) to the patch adhesive. After 60 seconds of hydration we pull the movable part of the upper head to make a force of 1.5 N on the disc with adhesive for 120 seconds. Then the dynamometer is set to zero and we make an opposite force, recording the maximum force produced in separating the patch from the head with the HAM. Finally, the formulations with the highest force values are selected.

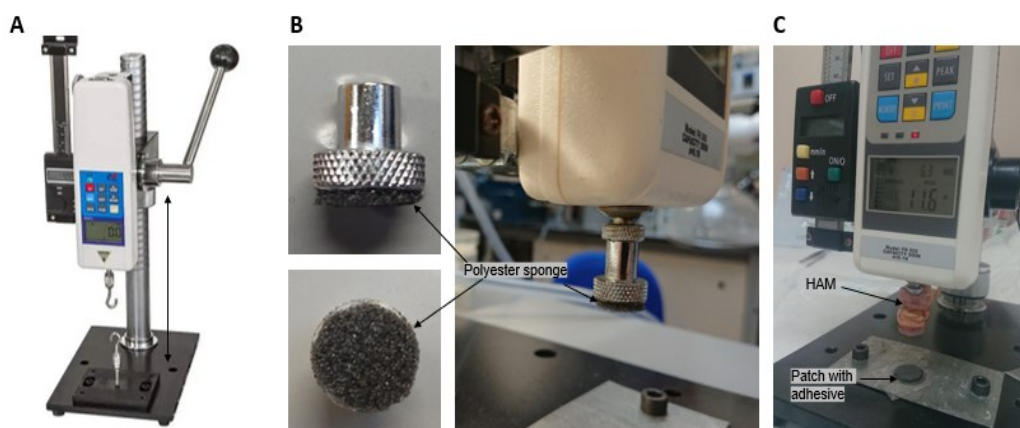


Figure IV-12. Sauter dynamometer installed at the test bank (A); round plane metal head customized with the polystyrene sponge (B); and customized head with the HAM and the patch (C).

2. *In vivo* test.

The *in vivo* tests have been carried out first in a pregnant rabbit animal model and finally in a pregnant sheep.

In the *in vivo* rabbit assay, a 25-day-old pregnant rabbit is used. A large incision is made in the abdomen through which the fetal sac is brought out. Two 14 mm diameter silicone patches with 203 μL of dehydrated HPMC (10 mg/mL) are implanted using an 8 F introducer, adapted to the small size of the animal model. The technique of insertion and fixation of the patches in the amnion during the procedure and just before closing the incisions is evaluated. The position of the patches 4 days after surgery is also evaluated by visualization of the patches adhered to the amnion. Finally, the amount of adhesive to each of the patches is evaluated by thermogravimetric analysis (TGA), with the same conditions described in section "Solubility evaluation of cellulose derivatives adhesives". The analysis of a patch submerged in 10 mL of SBF at 37 °C and gentle agitation during the same days as the implantation in the rabbit has been incorporated.

In the *in vivo* pregnant sheep trial, 16 patches were implanted in 4 sheep. Each approached uterine horn is perforated 4 times using the Seldinger technique of catheter insertion. Each orifice is sealed with a 17 mm diameter patch where 300 μL of HPMC (10 mg/mL) has been previously deposited and dehydrated using the 10 F introducer developed in Chapter III, which is introduced through a 12 F trocar. Once the patch is deployed inside, it is left to hydrate for 60 seconds and then it is pulled by means of the double traction thread against the amnion for 120 seconds. After this time, one of the strands of thread is dropped and the other is stretched. This causes the traction thread to slide off the patch fixation thread (see chapter III). The use of fetoscopy allows visualization of the attached patches during the entire surgery. The adhesion to the amnion is evaluated by monitoring the first 5 minutes of attachment and just before introducing the entire new fetal sac into the uterine cavity. After 7 days the fetoscope is reintroduced to quantify the number of patches adhered to the amniotic membrane. The state of the orifices made in the chorioamniotic membrane, the loss of amniotic fluid, and the appearance of lesions and the state of the fetus are evaluated. The amount of HPMC remaining in the patches is also quantified by TGA. Finally, the sheep are euthanized in accordance with current regulations.

4.3. Results and Discussion

The results obtained in each family of adhesives and adhesion systems that we have developed, give rise to conclusions that explain the reason why we have been modifying the strategy to obtain optimal adhesion of the patch on the amnion. We could say that during the process of developing an adhesive that meets all the requirements set, a paradigm shift has been made that has caused us to change our way of perceiving the reactivity of a tissue such as the amniotic membrane, which has the unique property that nothing can stick.

4.3.1. Bioadhesive thin film by Chemical Vapor Deposition

Poly glycidyl methacrylate (PGMA) thin film

The first strategy focused on the deposition of a polymeric thin film with reactive groups that would establish a covalent bond with the amino and hydroxyl groups of some amino acids such as lysines, arginines, serines, ..., of the membrane proteins of the monolayer of cells that form the surface of the amnion. The first approach was to deposit a thin film of poly glycidyl methacrylate (PGMA) on the silicone. GMA contains an acrylate group, by which the GMA or PGMA polymer is formed by a radical reaction, and an epoxy group. These epoxy groups in resins, during the curing process, usually react easily with amino groups and hydroxyl groups¹⁵⁰ Thus, using the iCVD technique, films with a thickness of 200 nm and 700 nm were deposited, and an adhesion test was performed on human amniotic membrane (HAM). The membrane was wetted with saline and the patches were deposited on top for 5 and 10 min, and lightly pressed. The evaluation was intended to qualitatively identify the resistance caused by the patch on the amniotic membrane. In case of adhesion, when the patch is pulled laterally the membrane should follow the movement of the patch. It was observed that the patches did not adhere to the amnion in either time interval. In addition, water repulsion was observed on the surface of the GMA patches, indicating that the surface was hydrophobic.

This first approach gave way to the idea of decreasing this hydrophobicity to bring the thin film as close as possible to the amnion. Therefore, hydroxyethyl methacrylate (HEMA) was added to the PGMA thin film. The HEMA was cross-linked with ethylene glycol diacrylate (EGDA) so that it would not have an exaggerated swelling effect when in contact with water. Without a crosslinker the PHEMA chains would have little cohesion, and the thin film would easily break under shear stress. Thus, a deposition of several thin films was made, where the layer closest to the silicone was formed by PHEMA and EGDA, and the most external one by PGMA. The first thin film had a thickness of 100 nm of PHEMA / EGDA and 100 nm of PGMA,

with a total thickness of 200 nm. The second had 175 nm of HEMA / EGDA AND 220 nm of GMA, with a total thickness of 395 nm. The third had 350 nm of PHEMA / EGDA and 50 nm of PGMA. And the fourth 800 nm of PHEMA / EGDA and 75 nm of PGMA.

The adhesion ability of the four patches were again evaluated with the lateral pull test in HAM at 5 and 10 minutes, resulting in insufficient adhesion. It should be remembered that one of the requirements to be met is that the developed adhesive should react at a maximum time of about 5 minutes.

The results concluded that, being true that epoxy groups react with amines and hydroxyls, the reaction of our PGMA + PHEMA / EGDA thin film with the amnion either does not occur or occurs at an insufficient rate to be of interest as a bioadhesive surface within the minimum required time.

PPFM thin film

Next, we wanted to deposit another thin film preserving the HEMA/EGDA layer. This layer gave us the capacity of swelling and above all the ability of the reactive groups to be closer to the amnion proteins. In order to have a higher reactivity, GMA was replaced by PFM. PFM also forms a polymer with a methacrylic group and has the advantage that the five-fluorine ring is very reactive. Therefore an iCVD deposition of a first HEMA/EGDA layer of 220 nm and a PFM layer of 150 nm is deposited.

The adhesion results with HAM showed a lack of adhesion to the HAM at 5 and 10 min, since it did not show resistance to lateral movement. Although the hydrophilicity of the film increased (contact angle of 31°), the substitution of GMA by PFM did not give optimal adhesion results either. This could be explained by the fact that the amount of amino groups is not enough to fix such a bond and/or that the reaction is slower than initially thought.¹⁵¹

PAA thin film to isothiocyanate

After these results it was decided to test another reagent group such as isothiocyanates, which also react with amino groups. This decision was made because isothiocyanate groups are commonly used in research to label and immobilize proteins. Molecules such as fluorescein isothiocyanate (FITC) are widely known and used precisely because the isothiocyanate group attached to fluorescein reacts with the primary amine of lysines, labeling proteins and emitting fluorescence. Thus, as a first approach it was decided to make a thin film with isothiocyanate groups but with the previous step of depositing an allylamine polymer (PAA) and then converting its amino groups into isothiocyanates by reacting with 1,1-Thiocarbonyldi-2 (1H)-pyridone (TCBP).¹⁵² In this way, theoretically, we obtained a thin polymeric film full of isothiocyanate groups, which we know for sure react with amine groups of proteins. To achieve this, two types of polymeric film were created, one of PAA alone and the other of PAA with EGDA as a crosslinker. In both types the PPECVD technique was used, which, unlike iCVD, is faster and allows an oxygen plasma activation to be performed just a few seconds before starting the polymerization in the same reactor.

In contrast to the previous depositions with GMA and PFM monomers, we wanted to incorporate some characterization techniques to know if we really have a PAA film. The presence of amino groups on the surface was evaluated using the attenuated total reflection (ATR) technique of two PAA thin films polymerized for 5 and 10 minutes. The results obtained (Figure IV-13) showed that at 3250 cm^{-1} there was a band corresponding to NH_2 , with an

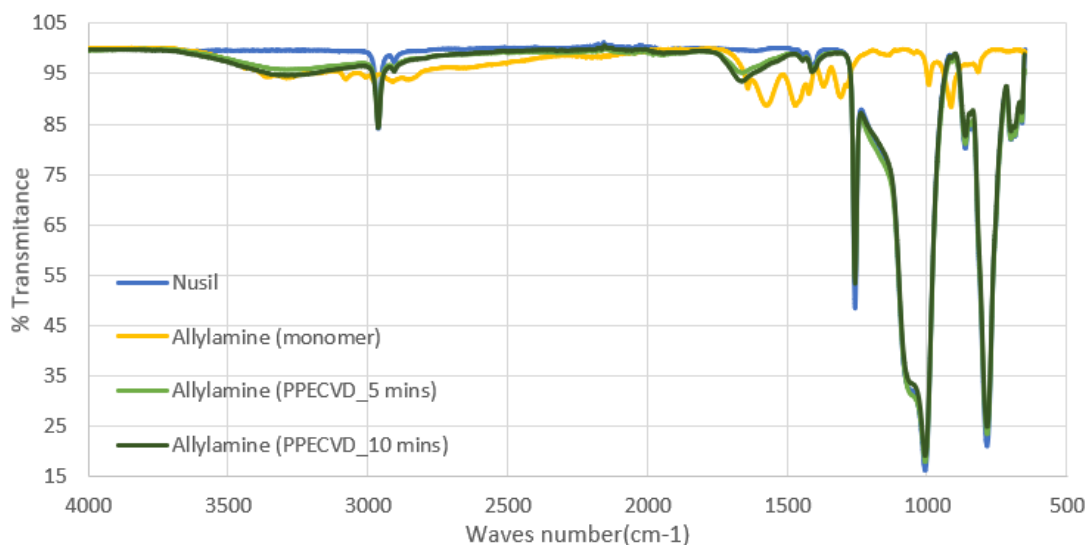


Figure IV-13. Comparative graph with the ATR results of PAA thin film at 5 and 10 mins.

increase of the signal in the PAA thin film at 10 min compared to 5 min of polymerization. This indicates a higher presence of these amino groups on the surface as the PPECVD deposition lasts longer.

Furthermore, we wanted to know if this film was enough flexible and resistant to follow the subsequent reaction with TCBP, where toluene and dichloromethane (DCM) are used. Toluene and DCM, like many other solvents, have a swelling effect on the silicone producing an increase in volume and associated deformation¹⁵³. It was found that the toluene deformed the silicone excessively. Therefore, the reaction was tested only with DCM. In order to know if the thin film would resist the DCM treatment, the elasticity of these films was evaluated microscopically (Figure IV-14). By stretching slightly at the ends and leaving the disc in repose, we could see if cracking appeared. The images obtained with optical microscopy showed an initial cracking in the PAA thin films before stretching the samples. This cracking has two morphologies, one in which the cracking is seen in the form of large plaques or macrocracking (black arrows), and the other in the form of microcracking (white arrows). The crushing into large plates or macrocracks before performing the stretching test is explained by the fact that during the polymeric deposition process the silicone receives a negative pressure to establish the vacuum. The vacuum in the reactor causes the silicone to expand slightly, so that once the deposition of the PAA thin film is complete, the reactor chamber returns to atmospheric pressure. It is precisely at this moment that the silicone is contorted and the thin film, if not too elastic, undergoes macrocracking. This effect is not observed in the PAA thin film with EGDA since the crosslinker prevents this macrocracking in reinforcing the polymeric chains. After stretching the samples and reanalyzing the films, a series of microcracks can be seen in both types of thin films, which are slightly superior to the PAA samples.

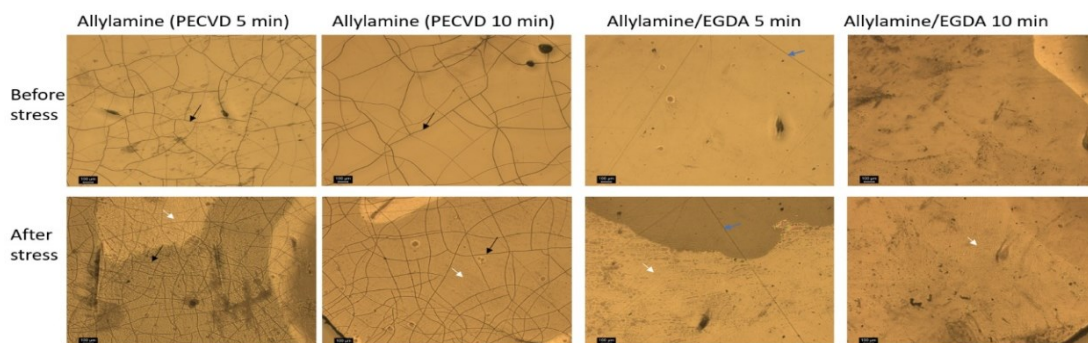


Figure IV-14. Images of thin films of PAA and PAA/EGDA deposited over medical grade silicone. The images show the difference of cracking level before and after stress process. Black arrows show macrocracking of the thin film, white arrows show microcracking, and blue arrows show the marks and irregularities that exist usually in the silicone, due to the molding process.

This microscopic evaluation discarded the use of thin film with only PAA but not yet PAA/EGDA thin film. To demonstrate that these microcracks were due to an excessive stretching force that we had manually caused, we applied a drop of 50 μl of milliQ water and DCM on top of the PAA/EGDA thin film, and we evaluated the integrity of the surface microscopically. The images (Figure IV-15) showed that the PAA/EGDA film is dissolved with milliQ water, but not with DCM. Moreover, with DCM the microcracking did not appear. The integrity of the PAA/EGDA film was subsequently demonstrated by submerging the PAA/EGDA samples for 10 minutes in various solvents such as milliQ water, methanol, DMSO and DMC, and performing ATR analysis. The results (annex) showed the presence of amino groups at the surface in the samples submerged in DCM at 3250 cm^{-1} , but not in the samples submerged in milliQ water, methanol or DMSO, demonstrating that the PAA layer was highly soluble in several solvents but not in DCM.

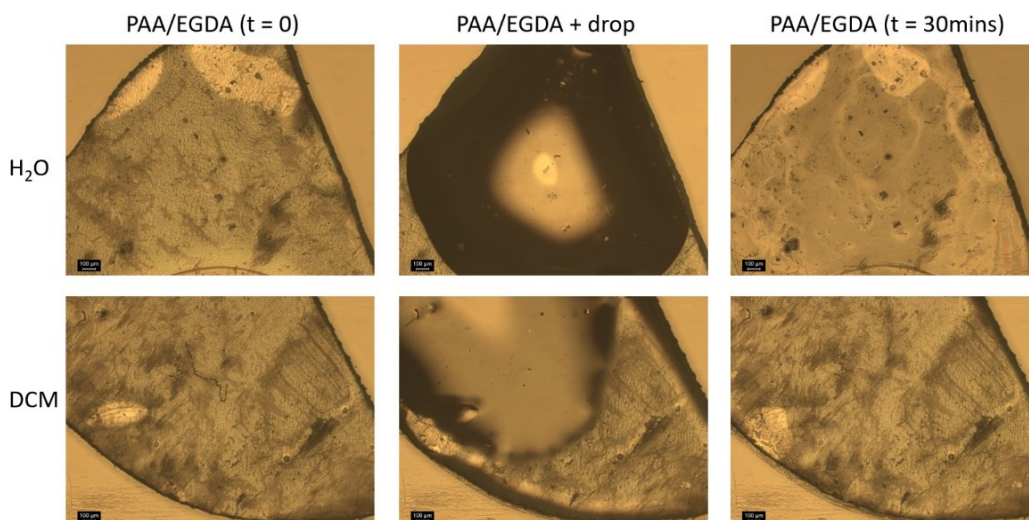


Figure IV-15. Microscope images that show the solubilization and disappearance of the polymeric thin film with a drop of water but not with DCM drop.

Knowing these results, we knew that we could convert the surface amines to isothiocyanates without degrading the thin film. Thus, after several unsuccessful attempts to convert the amines to isothiocyanates it was finally established that the best way to produce the isothiocyanate conversion reaction was to submerge the silicone discs with PAA/EGDA in a solution of TCBP (20 mg/mL) with DCM for 48 hours under gentle agitation. Once the reaction was finished, the appearance of isothiocyanate groups was evaluated with ATR, which reduced the intensity of the band at 3250 cm^{-1} to the detriment of a band at 2100 cm^{-1} . The data obtained by ATR (Figure IV-16) show a low band at 2100 cm^{-1} indicating a low presence of isothiocyanate groups.

A manual lateral traction adhesion test was then performed to evaluate the adhesion sensations with the HAM. A slight resistance to lateral movement was observed, but not very much because the patch remained adhered to the HAM. This can be explained by the low presence of isothiocyanate groups due to the low conversion of amines by the reaction with TCBP

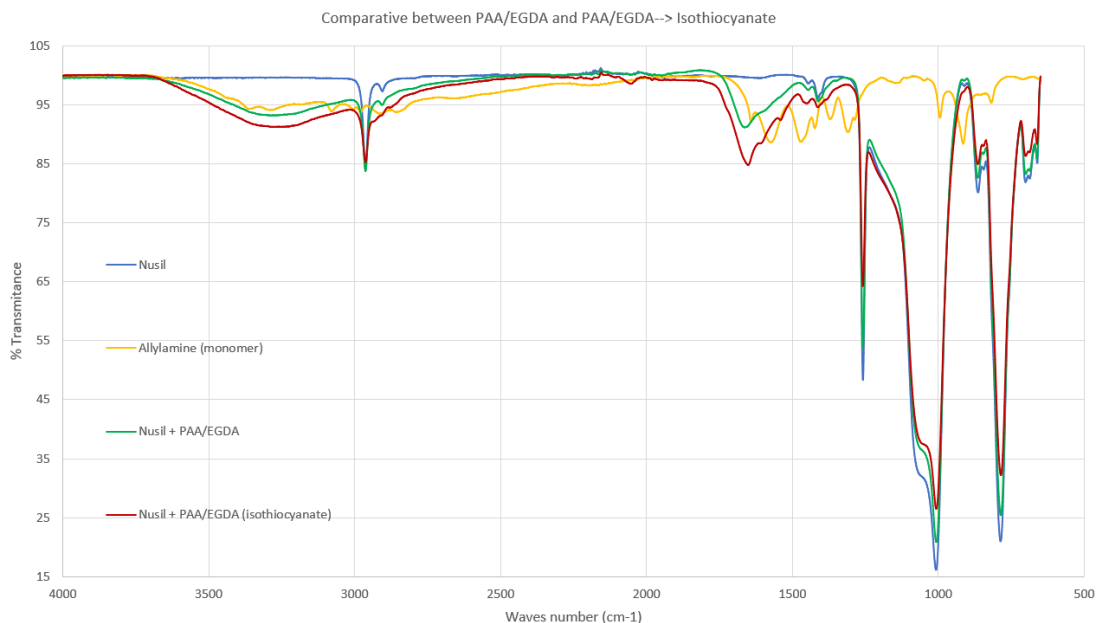


Figure IV-16. Comparative graph of ATR to evaluate the conversion of the NH_2 groups (3250 cm^{-1}) of PAA/EGDA thin film to isothiocyanate (2100 cm^{-1}).

Poly allyl isothiocyanate (PAITC) thin films

After spending a lot of time depositing a homogeneous layer of PAA, followed by a reaction to convert primary amines to isothiocyanates, and not having optimal results neither in conversion nor in adhesion capacity, it was decided to look for an alternative. After searching for possible molecules with isothiocyanate groups, allyl isothiocyanate (AITC) was found to be an interesting candidate. Although AITC is not part of the known library of monomers for creating thin films by CVD techniques, its allyl group makes it theoretically capable of forming a polymeric thin film. AITC is a compost derived from cruciferous plants and is present in mustard, horseradish, and wasabi. Antibacterial, antifungal and anticarcinogenic activity has recently been described in its monomeric form. Activity that it would not have in its polymeric form unless it is degraded in monomers over time. According to its vapor pressure value (0.49 kPa at $20 \text{ }^\circ\text{C}$) similar to GMA (0.42 kPa at $25 \text{ }^\circ\text{C}$) it is a good candidate for thin film deposition by PPECVD and iCVD.

Thus, after adjusting the polymerization conditions of both PPECVD and iCVD, a band corresponding to the isothiocyanates around 2100 cm^{-1} appeared in the corresponding graphs obtained by ATR (Figure IV-17). The results show a higher intensity in the thin film obtained by iCVD, probably because this technique preserves better the integrity of the reactive groups of the monomer. On the other hand, with PPECVD a less intense signal is obtained, but with a higher presence of amino groups (3250 cm^{-1}).

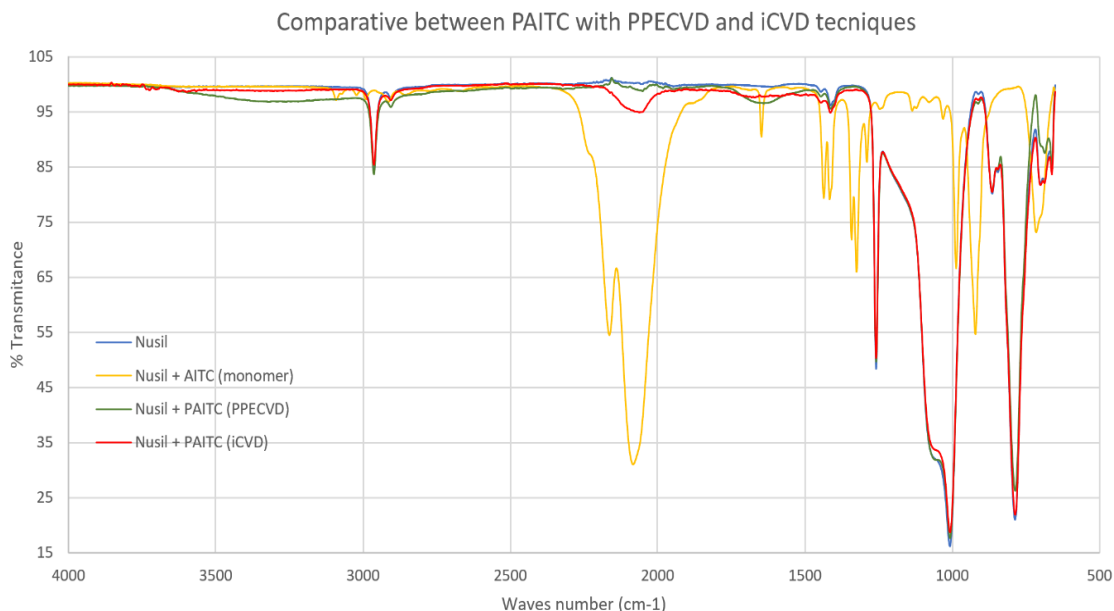


Figure IV-17. Graph of ATR to compare the intensity of the band corresponding to isothiocyanates groups (2100 cm^{-1}) of PAITC thin films obtained by PPECVD (green line) and iCVD (red line).

At this point, it should be noted that due to technical problems with the iCVD equipment it was not possible to make more samples. Nevertheless, the number of samples obtained and characterized was sufficient to be able to perform the adhesion test in HAM with the PAITC patches obtained with the two techniques. The results obtained at 5 and 10 minutes showed a certain resistance to lateral movement but not in elevation. This adhesion was not enough, which made us reconsider the strategy to follow in the development of the adhesive.

Before taking any decision, we wanted to understand why the PAITC thin film did not have enough adhesive properties. We did not know if it was because the reaction speed of these isothiocyanate groups was not fast enough or if we could not adhere proteins to our thin film. So, we did some experiments to determine the cause.

The PPECVD technique was used to make the new samples because it is the fastest technique and, moreover, it allows the deposition on the medical silicone discs without having to change the reactor to activate its surface with oxygen plasma. Some copper grids with a hexagonal pattern were added on top of the silicone to act as a mask. In this way a thin PAITC film in the form of a hexagonal pattern was obtained. Polymer is only deposited in those areas where the grid does not cover the surface. In the area covered by the grid there remained the unmodified silicone. The structure was evaluated under optical microscopy both on the silicon wafers serving as a deposition pattern and on the silicones functionalized with PAITC thin film.

The images obtained of the silicones with PAITC did not show cracking, unlike the other thin films tested previously. However, a wrinkled structure of the polymeric layer was observed (Figure IV-18, D and F). The presence of wrinkles in polymeric films is well described in the literature since it is due to the movements that the substrate suffers during the pressure changes in the reactor. In our case, the medical silicon disc is contracted when it is made the vacuum in the reactor and recovers its initial shape at the end of the polymerization and returns to the atmospheric pressure. As already commented, this effect was the one that produced the cracking of some thin films tested previously but it seems that in the PAITC deposition it does not happen, and these wrinkles appear. It is described that geometries can be created depending on the direction from which the subtraction is tensioned and the applied force^{154–158}. But what is not yet described is the directionality of these wrinkles that we observed in some sectors of the samples. Straight line wrinkles appear (Figure IV-18, E and F, black arrows) due to the imperfections present in the silicon. That is to say, the straight lines that appear in the silicone (Figure IV-18 E, white arrows) are due to scratches in the mold that is used to manufacture the silicone films and where they are cured, to later obtain the discs. Thus, according to these results, and taking into account that it would be necessary to do some experiments to control the polymeric deposition according to a geometry etched on the silicone and to verify that this is always completed, it would be possible to make polymeric patterns without the need to apply stresses on the substrate to cause different shapes in the wrinkles. It would only be necessary to etch or print the geometry on the substrate so that the deposited polymer would acquire the geometry of the engraving. It would represent a great advantage especially in rigid substrates where it is not possible to apply tensile forces. This could be of great interest in the fields of materials engineering, microfluidics, organ-on-a-chip, lab-on-a-chip, etc.

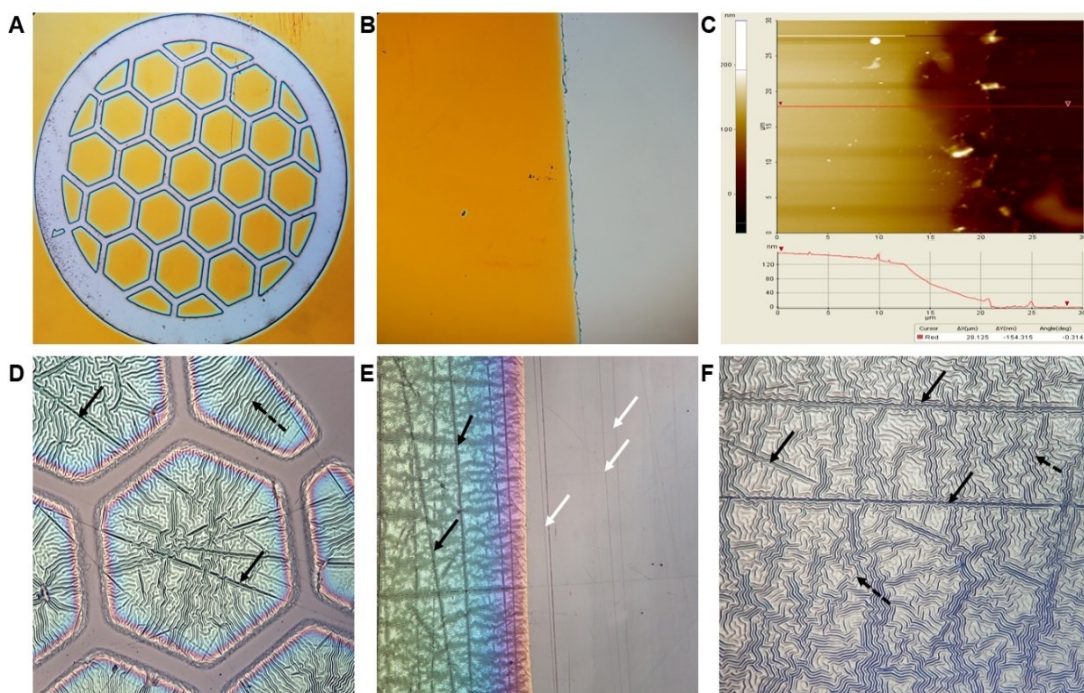


Figure IV-18. Images obtained by optical microscopy of the PAITC thin film (yellow color) deposited on a silicon wafer after removing the hexagonal grid (A) and image of the edge of the film (B); result obtained from analyzing the thickness of the same sample (156 nm) by AFM (C); images of the wrinkles (dotted black arrow) appeared in the PAITC thin film on a medical silicone substrate after removing the hexagonal grid, where the pink area corresponds to the polymer-free silicone and the bluish area to the deposited polymer (D); the white arrows indicate the lines on the surface of the silicone due to scratches on the surface of the mold (E); the black arrows indicate the straight line geometry of the deposited polymer following the lines of the silicone surface (D, E and F).

After measuring the PAITC thin film thickness with an atomic force microscope (AFM) it was decided to evaluate the potential of this film to bind proteins, bacteria, and cells. In this way we will obtain data on the reactivity of the isothiocyanate groups.

The first assay performed was to evaluate the ability of isothiocyanate groups to bind animal proteins. In this case fluorescein-labeled albumin was used. The results using fluorescence microscopy (Figure IV-19) showed a clear intensity of fluorescence in the area where there was the PAITC thin film in hexagonal form, showing practically no signal in the area where there was only silicon. This indicates a clear binding capacity of the amino groups of the albumin Lysines to the isothiocyanate groups.

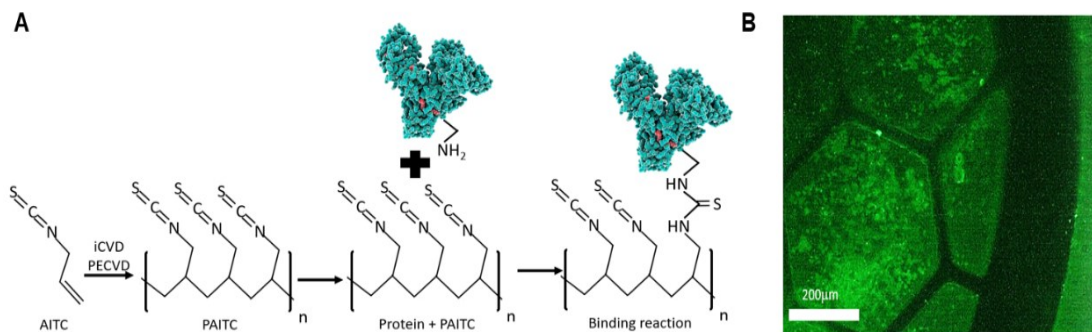


Figure IV-19. Process of deposition of the PAITC thin film and reaction of binding to the amino groups of lysins present in the external part of albumin (A); and image obtained with a fluorescence microscope of the PAITC surface with the hexagonal pattern where an intense green signal can be observed, indicating the presence of fluorescein-labeled albumin (B).

Once it was demonstrated that the proteins were able to bind to the polymeric surface, it was decided to test the adhesion of bacteria on the polymer. *Escherichia coli* was chosen because it is a bacterium widely known and used in research, and moreover, they are easily identified by their morphology. On the other hand, *Pseudomona aeruginosa* was also used because they are known to form biofilms quickly. To evaluate the presence of *E. coli* bacteria, a SEM was used, where the images obtained (Figure IV-20) showed not only the presence of *E. coli* on their surface but also the clear arrangement of these bacteria on the concave part of the wrinkles. This could be explained by the fact that the size of *E. coli* coincides with the depth of the wrinkle coming into contact with a greater number of isothiocyanate groups (Figure IV-20 C and D). Furthermore, it can be clearly seen that in the area where there is no polymer there are practically no bacteria, thus demonstrating that the PAITC film is able to bind bacteria. And in reference to the straight lines where the polymer has grown according to the geometry, it was observed that the bacteria were arranged in a row following the geometry of the concavity of the adjacent wrinkle, reinforcing the reasoning that it could have interesting applications.

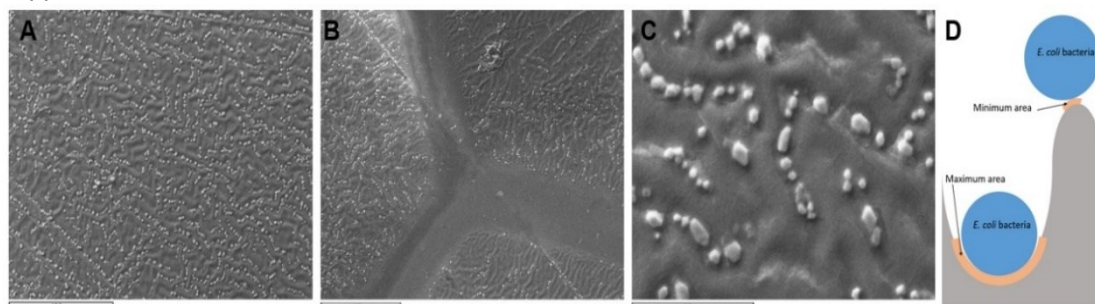


Figure IV-20. SEM images of PAITC surface where adhering *E. coli* bacteria can be seen (A, B and C); at non polymerized surface there are not bacteria adhered (B); the location of bacteria on the concave part of the wrinkles could be explained by the scheme (D).

In parallel, a silicone disc with half polymerized and half unpolymerized side was submerged in medium with *P. aeruginosa*, and after allowing it to grow for 48 hours, the biofilm was formed with violet crystal. Macroscopically it was possible to see that half of the disc was covered by biofilm, especially in the polymerized part (Figure IV-21 A). Macroscopically it is possible to see how the biofilm grows in an irregular way, and it is distributed covering part of the silicone zone without polymer, but it is not fixed there. The biofilm grows from the area with the PAITC thin film, where it is fixed. Observing in more detail the polymer limit zone with optical microscopy (Figure IV-21 B and C), it was clearly observed that the biofilm with violet glass was located in the PAITC zone and not in the clear part.

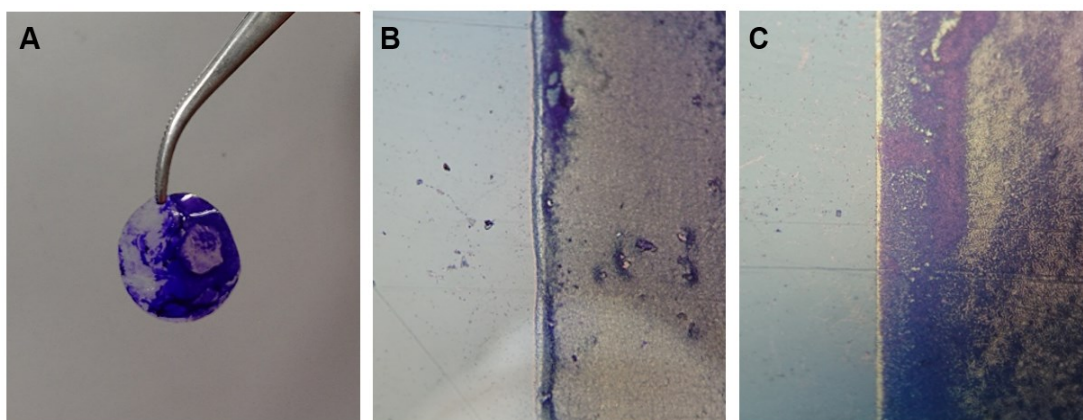


Figure IV-21. Macroscopic view of the disc with a half part with biofilm of *P. aeruginosa* (A). Microscopic images 4x (B), and 20x (C) of the edge of the polymerization zone (right side).

These two results, therefore, corroborate the ability of the thin film to bind, in this case to two types of bacteria through the isothiocyanate groups.

Finally, the last assay to evaluate PAITC binding was performed with human cells. The aim was to verify that the cells were able to bind to isothiocyanate groups through their membrane proteins. Therefore, human normal dermal fibroblasts (HNDF) and mammary gland cells derived from metastatic adenocarcinoma that express green fluorescein protein (MDA/GFP) were cultured on medical silicone discs with half side with PAITC and the other half without polymerization, this is with the fresh silicone. The reason for using these two cell lines was to obtain information on the differences between a culture with physiologically healthy cells and one with tumoral cells, and whether the binding affected them in the same or different ways. The results obtained (Figure IV-22) showed low cell viability in both cases. A greater confluence of cells was expected in the PAITC zone than was actually observed. Moreover, live cells can be observed, although some of them do not have the expected morphology for

the cell lineage. The change in morphology and the low number of cells could be due to several factors. On the one hand, the cells would not be comfortable in the PAITC substrate and would not divide, remaining "lethargic", although some cells maintain the morphology of the cell line. Another explanation could be that there is a cytotoxic effect in which some cells die remaining in an arrested and immobilized form due to attachment to isothiocyanate groups, while others survive. And another explanation could be that the cells are disposed on the substrate remaining immobilized and unable to migrate on the substrate. Some more than others. While generating these hypotheses to try to explain the images obtained, it was clear that the cells are at the limit of polymerization without migrating to the silicone zone, being alive, dormant or dead. It seems that the PAITC thin film binds in some more or less reversible way the membrane proteins of the cells allowing them to bind to the polymerized zone, as opposed to the non-polymerized zone.

From the results obtained in all these protein, bacterial and cell adhesion assays, it was concluded that the isothiocyanate groups on the PAITC surface were indeed able to react with amino groups. What happened, and could be related to other functional monomers such as GMA or PFM, is that the binding speed to amino groups is not fast enough to be used as an adhesive that acts in 5-10 minutes. Furthermore, in the absence of any cytotoxicity test, the results with cell immobilization showed a non-quantified but evident cytotoxicity. The cells were not comfortably positioned against the PAITC thin film.

All these data questioned the main strategy to make the silicone disc have adhesion capabilities thanks to the deposition of any thin film with adhesive properties. This made us reconsider the strategy and the need to find another type of adhesive that would react quickly enough to keep the patch attached to the amnios.

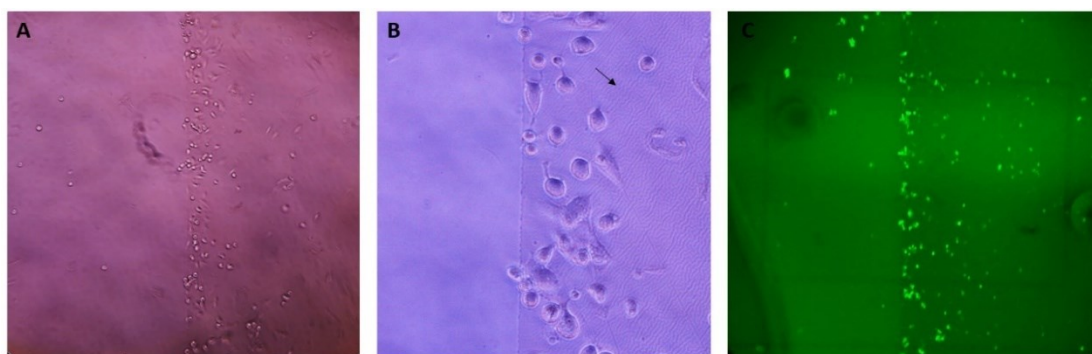


Figure IV-22. Images of culture of human normal dermal fibroblastes (HNDF) 4x (A) and 40x (B) where the wrinkles of the PAITC (black arrow) and the cells morfology can be identify; and mammary gland cells derived from metastatic adenocarcinoma that express green fluoresein protein (MDA/GFP) at 4X. At both cultures the cells are disposed in the polymeric part (right side), especially close to the limit..

4.3.2. Bioadhesive inspired on marine mussel glue: dopaminated Hyaluronic Acid (DHA)

After analyzing all the results obtained in the deposition of polymeric thin films with adhesive properties, a series of conclusions were reached that differed from the initial approach. Although the first strategy was to obtain a thin adhesive layer, it was found that, apart from not obtaining sufficient adhesion in the HAM tests due, among other things, to the lack of speed in forming covalent bonds, the thickness of this layer was insufficient for all the reactive groups present in the film to come into contact with the cell wall of the amnion. Moreover, the thin films did not prevent fluid penetration between the patch and the amnios. For this last reason, it was decided to develop an adhesive that would swell upon contact with the amniotic liquid. Thus, by capturing water and swelling, the reactive groups of the adhesive would be forced to come into contact with the proteins of the membrane due to the force exerted by the patch on the membranes wall thanks to the thread we use for traction. If there is sufficient reaction speed in forming molecular bonds with the amniotic surface proteins, it should support the movements and external forces that the patch may suffer. It should also have a low solubility in the amniotic fluid. In this direction we thought of hyaluronic acid, which is a polysaccharide present in tissues and organs of our body, with the interesting function of hydration and lubrication due to its great capacity to capture water and swell, as it has a large number of hydroxyl groups in its chain. Our group had previously worked with high molecular weight hyaluronic acid by adding quinone groups on the side of the chain with a substitution percentage of approximately 75%. In addition, the hyaluronic acid used was of pharmacological grade, so we already had one more step to avoid regulatory problems in case it had a strong adhesion capacity in the amnios and we finally used it as an adhesive for our medical device. In our case, the principal strategy to follow was to deposit the already dopaminated hyaluronic acid on the flat silicone discs with concave hemisphere micropatterns, so that the adhesive would have a larger contact surface with the patch and thus be able to covalently bind to it.

As already mentioned in the introduction concerning the functioning of adhesives, but which is necessary to remember, an adhesive must have an optimal bond between it and the substrate (medical silicone patch), an optimal cohesion between the chains that form it, and an optimal bond between the adhesive and the substrate where it wants to be fixed (amnios). Therefore, by means of oxygen plasma activation, radicals are created on the surface of the silicone which, together with the concavities of the micropattern, should increase the bonding with the partially activated adhesive. Partial activation of the adhesive would be done with oxidizing agents such as Na_2IO_4 , FeCl_3 , mushroom tyrosinase, ..., so that the catechol groups

hanging laterally from the hyaluronic acid chains would be converted into quinones. Some of these quinones would covalently bind to each other, cross-linking the hyaluronic acid chains. Others would react with the radicals created on the surface of the silicone, binding covalently. Others would have nowhere to bind as they could not find a place to react. And finally, as the AHD-based adhesive rapidly dehydrated, some quinone groups would not convert to catechol or find amino groups until the AHD film was rehydrated with the amniotic fluid. At this point oxidation would finish and the reaction with amniotic membrane proteins would occur. To achieve this, the first step was to increase the degree of dopamination of the hyaluronic acid to the maximum percentage of substitution that would allow synthesis. Using AHD with different degrees of substitution means that we cannot control oxidation in a clear way, in terms of finding a successful formulation with optimal reproducibility between the different batches synthesized.

Improvement of the degree of dopamination of hyaluronic acid.

In the first syntheses, substitution percentages between 70 and 85% were obtained, with undesirable variability. After doing some preliminary tests and observing variability in the results, it was decided to adjust the reaction to increase this degree of substitution by increasing the molar ratio from 1:3 to 1:5 of aldehyde versus amine. That is, by adding more dopamine hydrochloride. According to the ¹H-NMR described in the literature, the multiplet signal appears at $\delta=1.91$ ppm. In our case (Figure IV-23) the multiplet signal is at 2.03 ppm and is associated with the protons of the NH-COCH₃ groups.^{148,159} The triplet signals at $\delta=2.88$ ppm and $\delta=3.23$ ppm correspond to the ethylene protons of the -NHCH₂-CH₂- groups of the DOPA. And the signals between $\delta=6.75$ ppm and $\delta=6.92$ ppm are associated with the protons in ortho and meta position of the aromatic ring. The dopamination ratio or degree of substitution (DS) of DHA is obtained from the calculation of the integral of the area under the signal at $\delta=2.88$ ppm belonging to the DOPA group and $\delta=2.03$ ppm corresponding to hyaluronic acid, using the formula:

$$SD (\%) = I_{2.8 \text{ ppm}} / (I_{2.03 \text{ ppm}} / 2)$$

The calculations obtained for the first unmodified reactions showed a degree of substitution between 70 % and 85 % (Figure IV-23 A). Whereas, with the increase of the dopamine ratio a degree of substitution of approximately 98.5 % was obtained. (Figure IV-23 B).

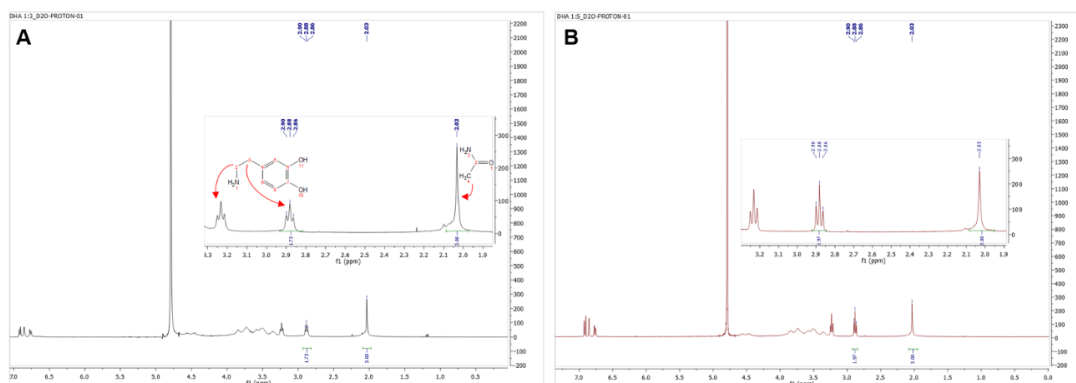


Figure IV-23. $^1\text{H-NMR}$ spectra of one of the first dopamine hyaluronic acid (DHA) (A) compared to the spectra of the final DHA (B), after modifying the synthesis (Annex 3).

Formulation and evaluation of oxidation in the formation of a DHA film.

The first step was to determine if a flexible DHA film could be formed, due to the fact that this film should be able to be deposited on the surface of the silicone disc and not crack when the patch was rolled up and introduced into the cannula. Therefore, we proceeded to perform a series of tests by depositing different volumes at different concentrations of DHA and FeCl_3 , IO_4Na_2 , on medical silicone discs with smooth surface and with the micropattern of concave hemispheres. Also, on oxygen plasma activated and not activated discs. It is important to emphasize that this process was done in parallel with the development of the disc as substrate for the adhesive and of the insertion system, so that sometimes, especially at the beginning, the substrate and the adhesive deposition techniques used and their formulations vary. Only some tests, results and some images obtained during these tests will be shown. The first part of the tests were aimed at obtaining quick feed-backs to delimit the concentrations and volumes on which we had to work. The main objective was to obtain information on the bonding of the films to the silicone disc. The flexibility of the dehydrated films, and if they were breakable. If they solubilized quickly when re-hydrated with water. If the plasma activation of the silicones allowed to deposit the entire volume homogeneously on the disc or if it was necessary to modify the substrate. In conclusion, to identify the best strategy to obtain a film ready to rehydrate with adhesive properties, and finally to obtain a specific volume and concentrations.

As tests were carried out, conclusions were reached to continue the search for the best formulation. It was concluded that the substrate had to be plasma activated so that the DHA formulation would extend over the entire surface of the disc due to the fact that the medical silicone was highly hydrophobic and once dehydrated the DHA film would separate from the substrate (Figure IV-24 A). That the substrate should have micro-roughness so that the adhesive would have a larger contact surface and adhere better. That the mixing of DHA and oxidant should be done before dehydration and not after, due to the fact that the dehydrated DHA film without oxidant was not flexible and was breakable. That at very high concentrations of DHA and FeCl_2 a clot was formed, and it was not possible to form a film (Figure IV-24 B and C). That at low concentrations of DHA and FeCl_3 a film was formed but solubilized in a few minutes upon rehydration with water, so it was critical to find the balance between the possibility of forming a compact and flexible film but not solubilizing quickly.

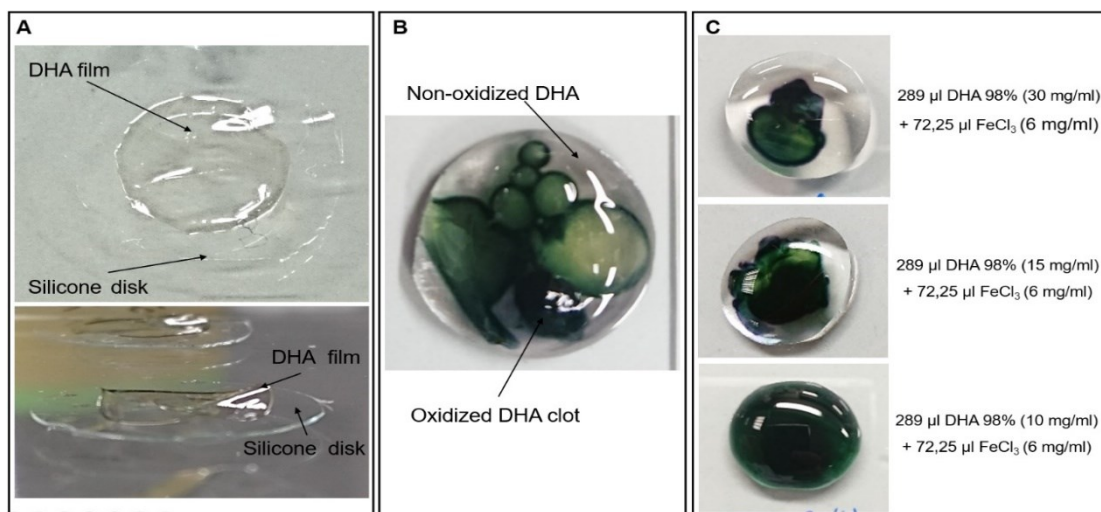


Figure IV-24. Images where the DHA film is separated from the medical silicone disc is shown, in addition to presenting high rigidity. It also does not occupy the entire surface of the disc due to insufficient plasma activation (A); formation of clots within the DHA mixture just when it comes into contact with drops of FeCl_3 (289 μl of DHA (30 mg/ml) + 172.5 μl of FeCl_3 (6 mg/mL)), showing the impossibility of making a homogeneous mixture (B); clot formation at DHA concentrations of 30 mg/mL and 15 mg/mL, until the optimal formulation is found to obtain a homogeneous mixture at 10 mg/mL (C).

In order for the DHA-based adhesive to have a larger contact surface area with the silicone, and to have more points to covalently bind to after activation with oxygen plasma, a micropattern of concave hemispheres was added to the silicone surface (see Chapter 2.2.3 and 2.3.3.). This micropattern was incorporated definitively in all the silicone discs used in the subsequent *ex vivo* and *in vivo* tests. (Figure IV-25).

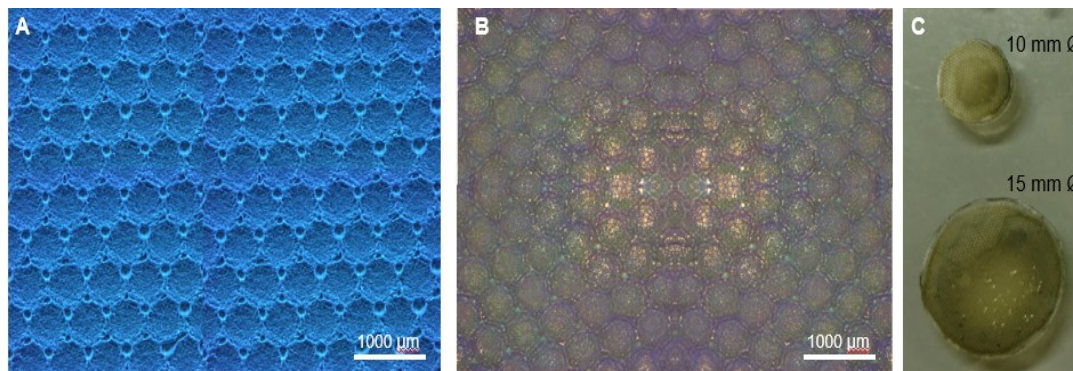


Figure IV-25. Optical microscopy images of the silicone surface with the micropattern (A); of the oxidized and dehydrated DHA formulation (B); and 10 mm and 15 mm diameter patches (C).

Once the optimal volumes and concentrations of DHA and FeCl_3 were obtained, formulation was also added to the discs with electrospun Silicone/PCU for *ex vivo* adhesion tests. Disc deposition was performed with the 85 % and 98 % dopaminated DHA batches. The most promising results were obtained with 98 % as a homogeneous mixture without aggregates was achieved. Higher aggregate or clot formation was expected with the formulation using 98% DHA due to the higher number of dopa groups, but the results showed the opposite. This could be explained because there is a higher amount of FeCl_3 for a lower number of dopa groups in the 85% DHA preparation, all available dopa would react. The results also showed that deposition on micropatterned silicone discs resulted in a more homogeneous patch with less deformation and stiffness than deposition on electrospun silicon/PCU discs. This could be due to the fact that the oxidized DHA chains, when covalently bonded to the PCU fibers and dehydrated, produce tensile forces that deform the patch (Figure IV-26).

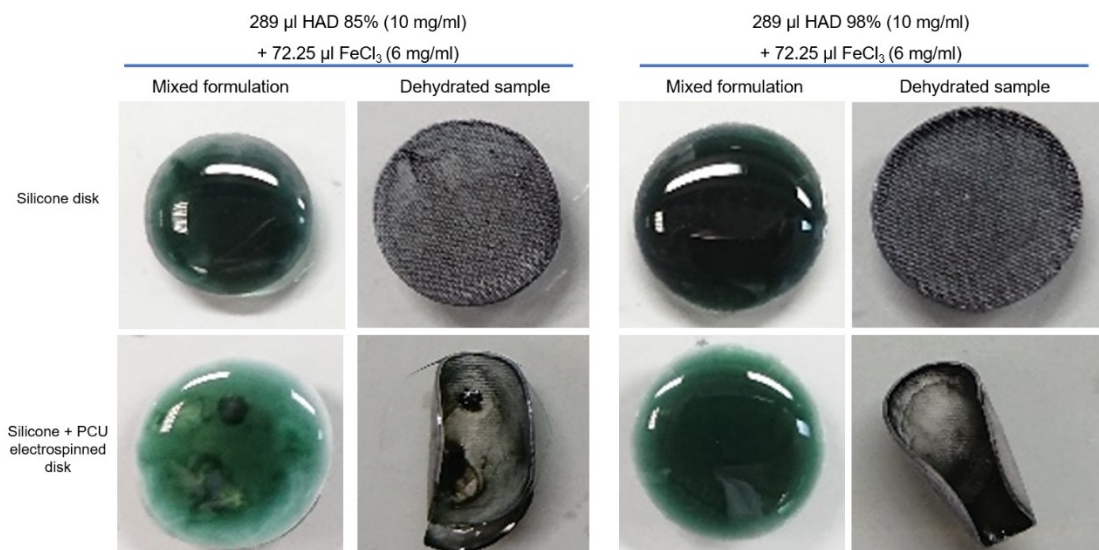


Figure IV-26. Images of the silicone (top) and silicone/PCU electrospun (bottom) discs with the final formulations before and after dehydration, but with the synthesized batches of DHA at 85% (left) and 98% (right).

Evaluation of adhesion on human amniotic membrane (HAM)

The evaluation of the adhesion of the patches with DHA and FeCl₃ was first performed with direct adhesion tests on AMH, then with the multiaxial and phantom test, and finally with *in vivo* assays on pregnant rabbits, as the first animal model used.

a. Adhesion test by lateral traction and elevation.

While formulations were being found with which to create a homogeneous film on the silicone disc, adhesion tests were carried out in HAM. The tests consisted of hydrating the area with physiological saline and depositing the patches on the amnion for 1-5 minutes, pressing lightly. After this time the patch was pulled laterally with tweezers to see if there was any resistance and tension in the amnion, indicating adhesion. Finally, if there was lateral adhesion, the patch was elevated with the tweezers from one extreme.

The FeCl₃ and NaIO₄ formulations formed flexible films, but the FeCl₃ formulations had better adhesion results in HAM than NaIO₄. Lateral adhesion was never obtained with the DHA and NaIO₄ formulations. This difference in adhesive properties could be explained by the formation of coordination bridges with iron, or because there are differences in the degree of oxidation. It is not exactly known whether or not to convert all the catechol groups to quinone, due to the fact that the remaining catechol groups can be covalently bonded by Michael addition, by the formation of Schiff bases, etc. In fact, a mixture of several of these reactions is likely to occur, which we have little control over, with the type of iron salt

used, pH, temperature, concentrations and ratios, etc. also coming into play.^{92,131,160,161} Hypothetically, this variability in the reaction mechanism could lead to poorly reproducible results in terms of adhesion values, a fact that could difficult the development itself. Even so, the adhesion results of the DHA formulations with FeCl_3 , although improvable, were promising. There was some resistance to lateral movement and vertical detachment by lifting but it appeared that the cohesion in the chains was not high enough due to the fact that fragments of DHA were observed on the amnion (Figure IV-27). That is, there was adhesion of DHA to the amnion and silicone but not enough cohesion between the DHA chains.

It was very important to test potential candidates on *ex vivo* models such as the multiaxial test due to the quantitative data that we did not have so far.

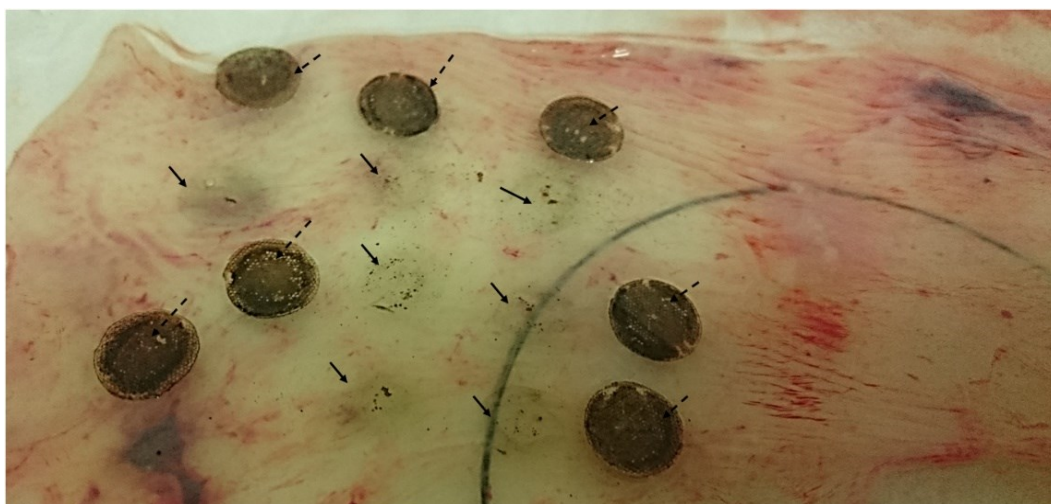


Figure IV-27. Image of the adhesion test by lateral traction and vertical detachment. The HDA + FeCl_3 patches (black dotted arrows) have risen from the HAM leaving traces of DHA on the HAM (black arrows.)

b. Multiaxial test

The multiaxial test provides data concerning the effect of the patch on the punctured chorioamniotic membrane. Quantitative data are obtained by recording the increase in pressure up to the maximum value supported by the chorioamniotic membrane with the patch attached as the volume of fluid in the system increases. It also provides information on the pressure at which leakage occurs and the pressure at which the membrane breaks. By the time the multiaxial test was completed, the first candidate and formulation had already been selected. Therefore, a formulation of 298 μL of DHA (10 mg/mL) + 72 μL of FeCl_2 (6 mg/mL) was tested on silicone discs with pattern and silicone discs with integrated electrospun PCU. In addition, a commercial ethylcyanoacrylate-based adhesive (SuperCeys® Unick®, from Ceys®), which is more flexible than commonly used ethylcyanoacrylate but also not suitable for use on human tissues, was also included. The flexible cyanoacrylate was deposited only on flat silicone disc with micropattern. An $n=8$ of the two adhesives was used for this test. Normal reference values of intrauterine pressure in common pregnancies is maximum 14 mm Hg in basal state and rises between 30 and 50 mmHg during labor contractions. Values above 14 mmHg for rupture or leakage are therefore considered acceptable. However, the higher the pressure values, the more promising the patch is as a candidate.

The results of the multiaxial test (Figure IV-28) (these results are part of the published article (annex)) with the cyanoacrylate patch showed little reproducibility, although the leakage pressure values appeared at higher pressures than in the two DHA patches. The leakage values of the DHA patches gave values below the marked limit of 14 mmHg. This could be due to the fact that DHA swells and allows water to penetrate between its chains, producing an initial leakage but supporting the increase in pressure up to 50-60 mmHg. Between the leakage values of the two DHA patches, better results were obtained in the silicone patch with electrospun PCU, even without reaching a pressure of 14 mmHg. This could be explained by the fact that the DHA penetrates between the electrospun fibers of the PCU, which serve as anchor points, thus improving the bond between the patch and the HAM. This result could indicate that the bonding of the DHA with the silicone surface is not enough strong to obtain an adhesion force between the two that exceeds 14 mmHg. In contrast, in both patches, the leakage produced at low pressures (≈ 5 mmHg) stabilized and disappeared as the pressure increased, obtaining promising results on the burst pressure of the HAM. In the silicone patch with PCU, HAM burst pressures were slightly higher than the patch without PCU. It is interesting to mention the acceptable results obtained with cyanoacrylate, both in leakage and HAM rupture, although stiffness of the

adhesive was observed once the adhesive had cured, in addition to the already known toxicity. In any case, the use of cyanoacrylates should not be discarded due to the fact that their formulation could be modified to obtain an adhesive that, once cured, is more flexible and elastic than the current ones, using longer chain cyanoacrylates.

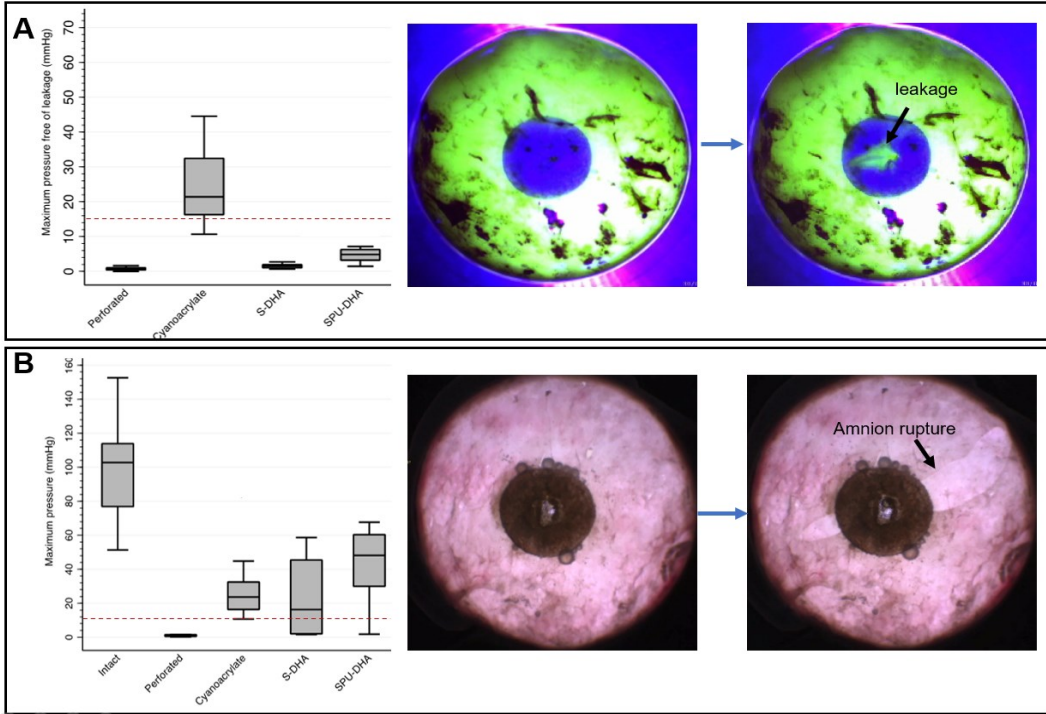


Figure IV-28. Results obtained with the multi-axial test. On the one hand the graph shows the maximum pressure free of leakage (A), and on the other the graph shows the maximum pressures that the corioamniotic membrane supports before appears the rupture (B) with membrane rupture pressures (B). The samples used are patches of silicone and silicone/PCU with cyanoacrylate and DHA. The images show the appearance of the first leakage (A) and the rupture of the amnion.

It is true that the multi-axial test pushes to the limit the behavior of the patch and the AMH individually, as well as together. In addition, the multi-axial test does not allow the chorion and amnion to slide over each other, and the curvature of the HAM suffered by increasing fluid pressure is not representative of reality. Therefore, the information obtained only tells us whether the candidate is promising. It is necessary, then, to perform complementary tests such as the phantom adhesion test, which will bring us closer to the *in vivo* model. Tests are also necessary to identify whether the adhesive we are using is toxic to the cells that are in contact with it.

c. Toxicity tests

In parallel to the *ex vivo* adhesion tests, the collaborating medical team performed pyknotic nucleotide and lactic acid dehydrogenase (LDH) tests (these results are part of the published article (annex)). Both tests are used to indicate cytotoxicity by contact. The first test indicates damage to the cells of the amnion monolayer with light microscopic visualization of abnormalities in the cell nuclei by hematoxylin-eosin staining. And the second indicates tissue damage by the presence of free LDH in the medium.

The results of the pyknotic nuclei test (Figure IV-29 A) indicated a pyknotic index below 2 % in the DHA patches at 24 and 48 hours, compared to the positive toxicity control used, which presented values between 30-40 % at 24h and 20-35 % after 48 hours.

The results obtained in the LDH test (Figure IV-29 B) indicated a cytotoxicity of the DHA patches between 3 and 8 U/L as low as in the untreated sample ($p = 0.154$), compared to the positive control showing values higher than 1754 U/L after 24 and 48 hours (IQR 998.5 - 2775.5, $p < 0.01$).

Therefore, the results obtained by these two tests indicate that the DHA-based adhesive is biocompatible with the cells and tissue forming the HAM.

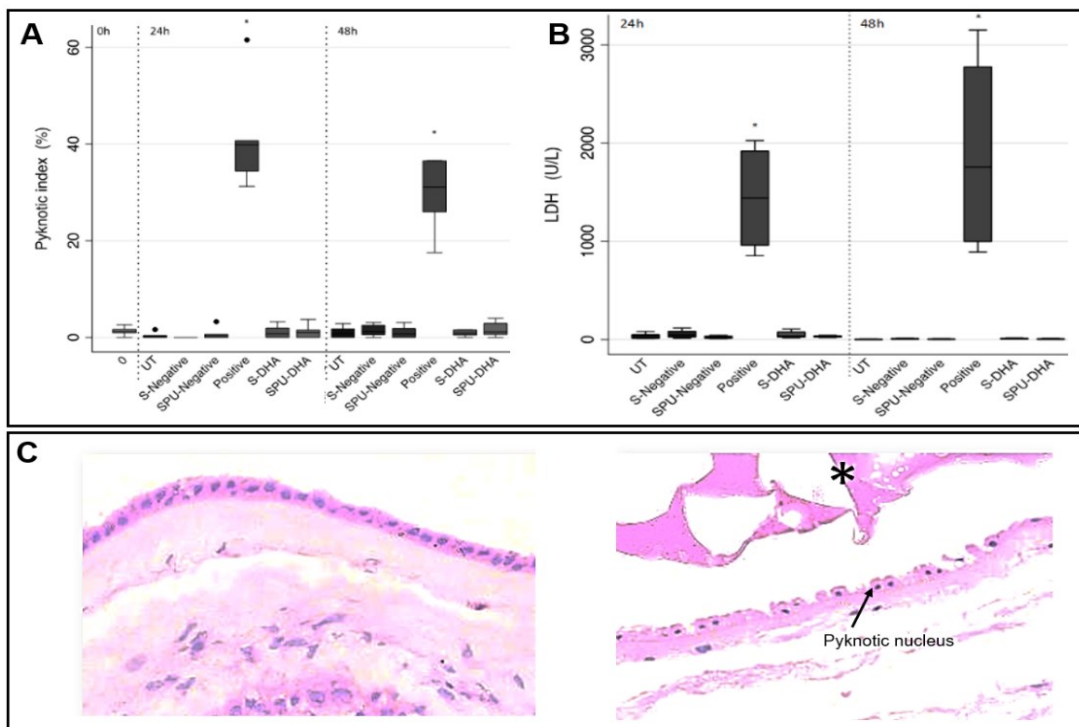


Figure IV-29. Results obtained in toxicity tests of pyknotic index (A) and LDH (B). The microscopic images (40X) show normal nucleus in the cells of untreated amniotic membrane (left), and some pyknotic nucleus (arrow) on the cells of the amniotic membrane treated with a positive toxicity control (right). The toxic adhesive layer (asterisk) can be observed.

d. Phantom test

After performing the multiaxial test and evaluating the toxicity of DHA, the phantom test was performed. The phantom simulates the tissues and layers that we must go through with the trocar to access to the fetus cavity. This test not only gives us information about the adhesion of the patch on the HAM, also, using the introducer or insertion system, we obtain information on the insertion process itself, and on the viability of the technique by being able to evaluate the unfolding of the patch and its mechanism of fixation to the amniotic membrane.

The phantom test showed an effectiveness of 100 % (N = 5) in the insertion, release, unfolding and fixation of the silicone patch with micropattern and DHA in the HAM with an inclination of 90° and 45°. Indicating that the insertion method and strategy works optimally.

In reference to the adhesion produced, the results (Table IV-4) were not encouraging due to the fact that with an introducer inclination of 90° 1/5 of the patches remained adhered to the HAM. On the other hand, with an introducer inclination of 45°, three of the five patches did not adhere correctly to the HAM, and even one of them is detached after a few seconds.

Table IV-4. Results of the *ex vivo* assay with phantom test.

		90° (N = 5)	45° (N = 5)
Insertion			
	Complete	5/5	5/5
Adhesion			
	Complete	4/5	2/5
	Partial	0/5	2/5
	Absent	1/5	1/5

These results showed that the introduction system was optimal, but the DHA-based adhesive did not have sufficient adhesive power to remain attached to the AMH in 100% of the cases. Nevertheless, it was decided to test the silicone and DHA patches in an animal model.

e. *In vivo* test

Before implanting the patches in the amniotic membrane of pregnant rabbits, two patches of silicone with micropattern and DHA were implanted in the peritoneum of a rabbit for 4 days (Figure IV-30). The results showed that the patches remained attached in the same area although one of them was slightly displaced. The presence of the adhesive was observed but when the patches were separated from the peritoneum the adhesive fragmented easily. This fact can be explained by a lack of cohesion of the adhesive chains.

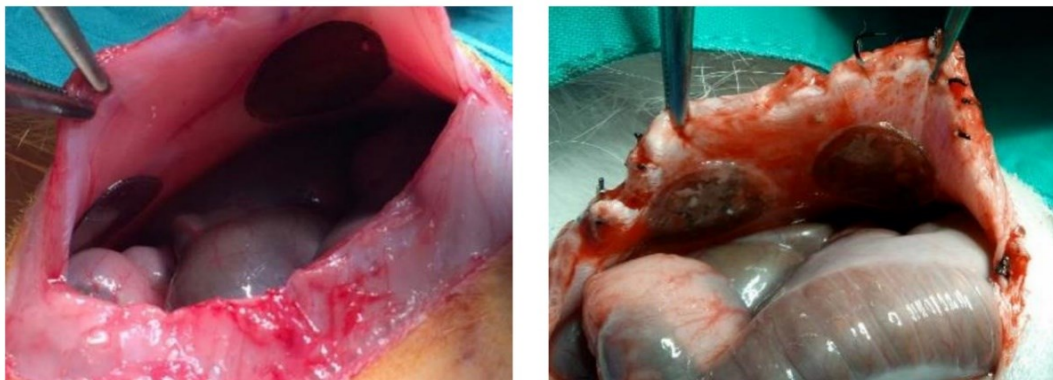


Figure IV-30. Images of peritoneal rabbit surgery, obtained during (left) and after 4 days (right) of the implantation of the silicone patches with HDA.

After evaluating the adhesion in peritoneum, 4 patches of the same candidate were implanted in 25-day-old pregnant rabbits. The insertion results showed that rabbit membranes are extremely thin and elastic, probably due to the fact that rabbits usually have about 5-8 baby rabbits per litter, so the chorioamniotic membranes need to be extremely adaptable to the number of fetuses. In addition, there is practically no space between the membranes and the offspring, making it difficult to insert and unfold the patch. It should be noted that the size of the trocar and patch was adapted to the rabbit model, finally using a 7 F trocar instead of 10 F, and a 10 mm diameter patch instead of 17 mm. The handling of the introduction system was acceptable although some improvements were applied.

Regarding the adhesion of the patches, 7 days after implantation it was observed that any of the patches were not in the site where they were initially implanted. In addition, no adhesive was observed on the surface of the silicone discs (Figure IV-31 right), verifying a lack of cohesion and adhesion of the adhesive. Considering that the fetuses have their own movements inside and that during surgery the fetal sac is repositioned and repositioned together with the fetuses, it is expected that the patch supports all these movements. Since this is not the case, it is concluded that the candidate patch consisting of a silicone disc with micropattern and DHA does not meet the expected adhesion criteria.

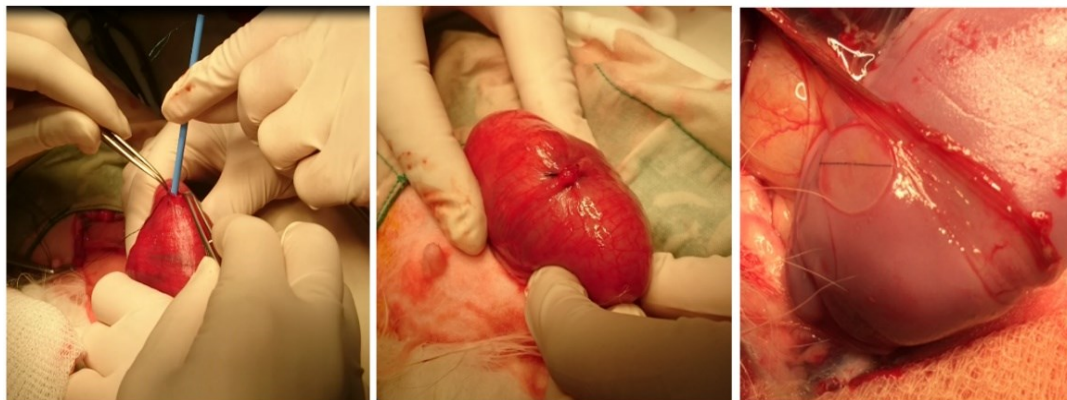


Figure IV-31. Images of pregnant rabbit surgery obtained during (left and center) and after 7 days (right) of the silicone and DHA patches implantation.

It is true that the strategy of binding the adhesive to the amnion by covalent bonds is interesting, and in fact it seems to happen with DHA, but covalent bonding may not be entirely controllable due to the need for prior oxidation of the DHA and subsequent dehydration so that the adhesive can be deposited on the surface of the silicone disc. In fact, we can make the adhesive deposition and the dehydrated film does not break when it is rolled on the cannula and subsequently unfolded, but the forces supported by the DHA chains are not enough to obtain a sufficiently cohesive adhesive. The presence of enzymes may also influence the degradation of DHA due to the presence of hyaluronidases in organisms, for example, which degrade hyaluronic acid. This factor, added to the forces that the patch must support, means that hyaluronic acid, even if it is long chain, is not a good option for producing adhesives that must support so many tensile movements. The possibility of substituting the hyaluronic acid chain for another type of chain that would not degrade so rapidly was considered. But it was concluded that using a strategy based on the oxidation of the dopa groups not only offered poorly reproducible results, but it was also very difficult to control the degree of oxidation. It was very difficult to control the mechanism necessary to stabilize such oxidation in an adhesive that needs to be dehydrated and rehydrated to get the maximum adhesion capacity.

Therefore, it is necessary to modify the strategy by looking for other polymers that are not influenced or are minimally influenced by enzymes of the organism, whose chains have a greater capacity to crosslink between them, between them and the silicone substrate, and between them and the proteins of the domain, without using a mechanism as dependent on different factors as is the dopamination of molecules.

4.3.3. Bioadhesive inspired in the formation of hydrogels with cellulose derivatives

Hydroxypropyl methylcellulose (HPMC)

Considering the results obtained previously with the bioadhesive based on dopaminated hyaluronic acid, it was decided to use other polymers that are widely known and used in the pharmaceutical industry. Celluloses, such as HA, also offer high water catchment, so that an adhesive based on cellulose biopolymers would have the capacity to swell when rehydrated with amniotic fluid, which together with the silicone substrate would block its exit through the wound produced in the chorioamniotic membrane.

Hypromellose or hydroxypropyl methylcellulose (HPMC) was chosen first because it binds easily to moist substrates such as mucous membranes. Furthermore, being of vegetable origin, they cannot be degraded by any human enzyme. The only way to lose adhesive would be by mechanical causes or by its degree of solubility in aqueous media, always depending on the length of its chains and the crosslinking between them.

HPMC has the peculiarity that as the water temperature increases, it becomes less soluble. This property is very interesting due to the fact that we will try to find out the degree of solubility at 37 °C, which is the temperature around which the adhesive would be found inside the fetal sac. Upon rehydration, as the cellulose chains are rich in hydroxyl groups, they would form hydrogen bonds with the other hydroxyl and amino groups of the amnion proteins. These bonds, although not as strong as ionic and covalent bonds, have the capacity to create interactions constantly over time. This would result in an adhesive that, when applied to the patch, would adapt to the different movements and tensions that occur in the chorioamniotic membrane during pregnancy.

The strategy to be followed represents a paradigm shift in that it is intended to obtain an adhesive that will adhere dynamically instead of covalently bonding and remaining immovable at a specific point. It should be remembered that the basic function of the patch is to prevent the leakage of amniotic fluid during the first minutes after removal of the trocar, and thus avoid the penetration of fluid between the amnion and the chorion, resulting in the rupture of these layers. Theoretically, therefore, it would not be necessary for the patch to be attached to the membrane until the moment of birth, as long as it significantly reduces the risk of membrane rupture. Ideally, however, the patch should remain attached to the amnion until birth, when it would be removed together with the placenta.

After some initial trials with different volumes and concentrations of HPMC, it was finally decided to use a formulation of 300 µL of HPMC (10 mg/mL). This volume was deposited on 17 mm silicone and silicone/PCU discs, previously activated with oxygen plasma according

to optimized conditions (Chapter 2.2.3 and 2.3.3). Once the required volume was deposited, it was dehydrated in an oven at 40 °C for 8 hours.

Multiaxial assay

The results obtained in the multiaxial test (Figure IV-32) (these results are part of the published article (annex)) showed that the patches with silicone and silicone/PCU with 300 μ L of HPMC (10 mg/mL) had a similar but slightly higher burst pressure than the results obtained with DHA, thus obtaining more than acceptable pressures, in addition to having results with lower variability. The most important result was observed in the leakage appearance pressures, in which there was a significant improvement. Leakage appearance pressures in the HPMC patches were higher than 25 mmHg with a maximum of 65 mmHg, compared to pressures lower than 10 mmHg in the DHA patches. The results were also better than those obtained with the flexible cyanoacrylate, both in the burst pressure and in the pressure with leakage appearance.

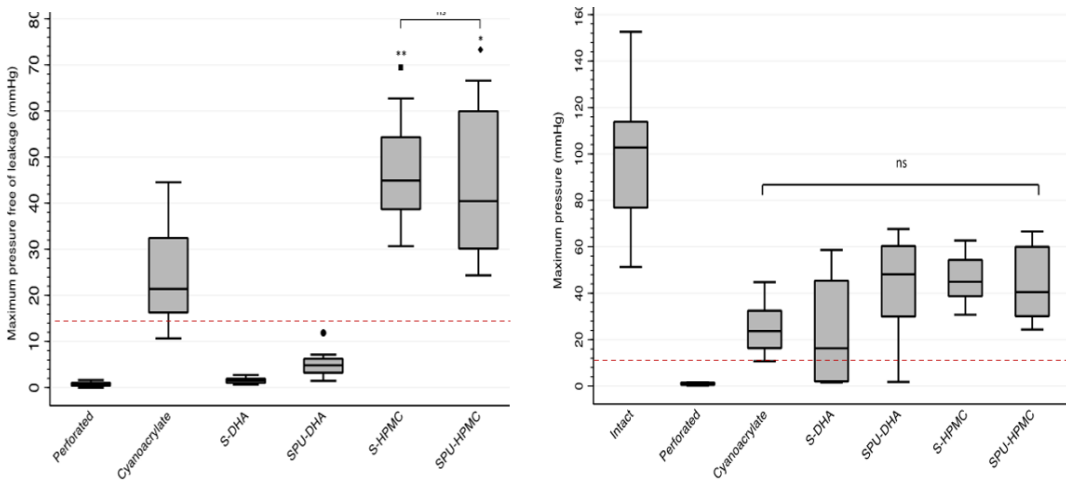


Figure IV-32. Results obtained with the multiaxial test. It can observe the results obtained between de patches with HPMC against HDA, related the maximum pressure free of leakage and the maximum pressure of rupture.

These first results showed that the HPMC-based adhesive could be a good candidate for *in vivo* assays in pregnant rabbits, but first it was necessary to test the patches in the phantom model.

Phantom assay

For the phantom test, the same samples were used as for the multiaxial test. That is, 10 silicone patches with the 300 μL formulation of HPMC (10 mg/mL) and 10 silicone and electrospun PCU patches with the same formulation were introduced using the developed insertion system allowing 60 seconds to rehydrate the HPMC.

The results obtained (Table IV-5) showed that all the patches could be correctly inserted and attached to the phantom. The patches with the silicone substrate remained attached to the amnion in their entirety during the 5 minutes of the test, whereas 50% of the patches with the silicone substrate and electrospun PCU detached before the end of these 5 minutes. This detachment could be due to the fact that when the 300 μL of HPMC is deposited on the electrospun PCU layer it penetrates between the fibers and upon dehydration it hides between the fibers. During the rehydration process, the HPMC does not have sufficient swelling to expose the polymeric chains of the HPMC in sufficient quantity for it to optimally achieve its adhesive properties on the amnion.

Table IV-5. Results obtained in the phantom test.

	n	Silicone + HPMC	Silicone/PCU + HPMC
Patch insertion	10	10	10
Patch placement	10	10	10
Patch adhesion after 5 mins	10	10	5

Therefore, it is concluded that although the PCU fibers can protect the adhesive from mechanical degradation at the time of rolling it into the cannula, this quantity is not sufficient for optimal adhesion. It would be necessary to adjust the thickness of the electrospun layer and the porosity of the fibers to adjust the final volume and concentration of the adhesive. For this reason and due to the optimal adhesion results obtained in the phantom test of the silicone patches with HPMC, it was decided to test these patches in the *in vivo* test in pregnant rabbits.

In vivo assay with rabbits

Due to the small size of the rabbit model, 14 mm diameter patches were prepared with the formulation adapted to the new patch surface. Therefore, patches with a deposited volume of 203 μL of HPMC (10 mg/mL) were prepared, introduced into the insertion systems. Finally, two of them were implanted. It was important to obtain information on the ability to adhere to the amnion, in addition to obtaining quantitative data on the amount of adhesive that remained adhered to the patch after 4 days of implantation.

Concerning implantation, the two patches were optimally positioned on the chorioamniotic membrane and could even be seen by ultrasound once the abdominal suture was closed (Figure IV-33). After 4 days the position of the patches was evaluated. The two patches were slightly displaced from the original implantation site, but no amniotic fluid leakage was observed. The patches were removed to assess the presence or loss of HPMC.

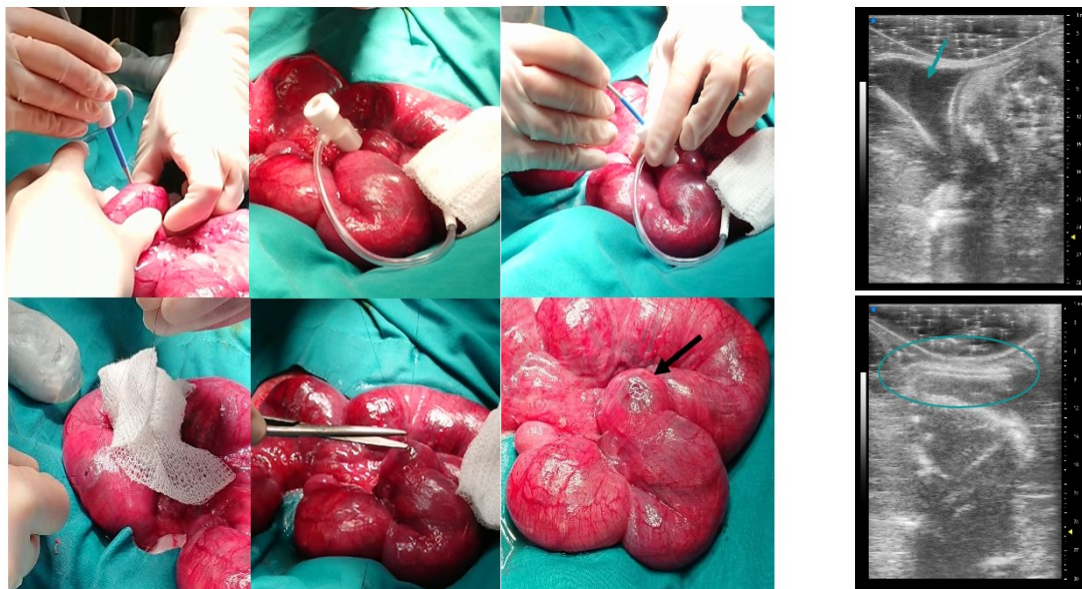


Figure IV-33. Images of the pregnant rabbit surgery with the implantation of the patches (black arrow) with HPMC in pregnant rabbit model (left). The echography images (right) shown an adhered patch to the amniotic membrane (blue arrow and circle).

The amount of adhesive present in the patch was quantified by thermogravimetric assay (TGA). The results obtained showed a loss of HPMC of 29 % in the first disc and 21 % in the second disc. This weight loss can be attributed to two factors. The first could be explained by the fact that part of the adhesive remained stuck to the surface of the amnion, indicating good interaction of the HPMC chains with the amnion but insufficient cohesion between the chains, due to the fact that the patches were not in the expected place. Secondly, some solubilization of the adhesive would occur when in contact with the amniotic fluid, although the adhesive, being between the membrane and the silicone disc, would be partially protected.

To establish the degree of solubilization of the HPMC formulation in the disc, a solubility test of the same silicone patches with HPMC was performed. In triplicate, the patches were left under gentle agitation and 37 °C, in miliQ water and simulated body fluid (SBF) for 1, 7 and 14 days. Subsequently, the presence of HPMC was quantified by TGA.

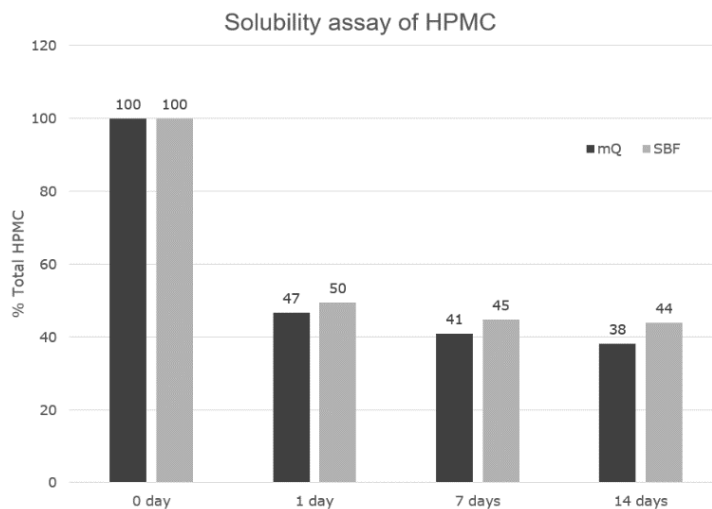


Figure IV-34. Results obtained in the solubility test of the samples with HPMC after 1,7 and 14 days.

The results obtained (Figure IV-34) showed that there was a quick initial solubilization of the HPMC after 24 hours. Remaining 45 % of adhesive in the patches in miliQ water, and 50 % in the patches with SBF. The loss of HPMC increases slightly at 7 and 14 days, and to a greater degree in the miliQ water medium due to the lack of salts in its composition, which increases the solubility of the HPMC. In fact, this type of test and these aqueous media are used as accelerated solubilization media, giving an indicative information of the solubility of the adhesive. Therefore, although initially useful, they are far from the real solubilization produced inside the fetal sac.

The large difference in HPMC percentage between the patches quantified in the *in vivo* pregnant rabbit test and the solubility test can be explained by the fact that in the solubility test the adhesive is not protected because is entirely in contact with the aqueous medium. In addition, the constant agitation movement accentuates this difference in solubility. On the other hand, the patch inside the fetal sac suffers some movement produced by the fetuses, but this movement does not occur constantly and does not seem to have an excessive influence.

After evaluating the surgeries performed on rabbits, together with the medical team, it was concluded that the pregnant rabbit model was not a valid model for implantation due to the fact that rabbits have a very high number of fetus and they are arranged in a sequential manner in a fetal sac, that is far from being similar to the human model. In addition, the patch must be reduced in size due to the fact that it must be adapted to the size of the rabbit fetal sac. For these reasons and to get closer to the human model, it was decided to use sheep for the following *in vivo* tests and no longer use the rabbit model.

Cytotoxicity test

In parallel to the *in vivo* tests, cytotoxicity tests were performed with the silicone and silicone/PCU patches with the selected formulation of 300 µL of HPMC (10 mg/mL). The results obtained (these results are part of the published article (annex)) in both the pyknotic nuclei index assay and the LDH assay (Figure IV-35) showed relatively low rates of toxicity and very similar to those obtained with the patches with DHA and the negative cytotoxicity control (silicone and silicone/PCU disc without adhesive). Although an increase in LDH values is observed in the 24-hour sample of silicone with HPMC, it does not reach 500 U/L of LDH nor the lower limit of the positive toxicity controls. Therefore, we can conclude that the patch with the HPMC formulation does not present toxicity on the cells of the amnion monolayer.

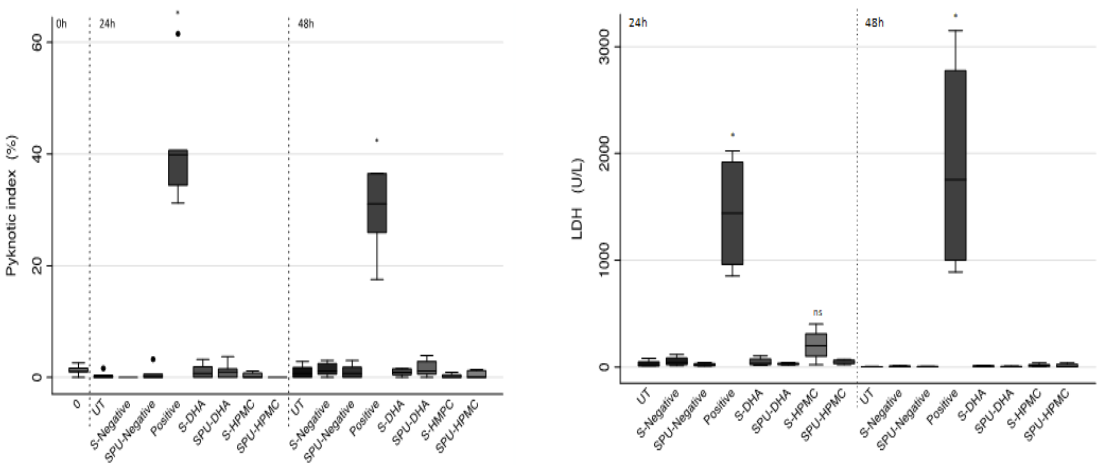


Figure IV-35. Graphs with the results obtained from the pyknotic nucleus and LDH assay.

In vivo assay with sheep

With excellent toxicity results, it was decided to realize a test on pregnant sheep by implanting 16 silicone patches with HPMC. But before testing the patches it was important to establish a method to sterilize the entire sealing system. That is, it was necessary to use a sterilization method that would sterilize the patch with the adhesive already assembled in the insertion system, without altering the properties of the adhesive. After evaluating the different sterilization methods such as dry or wet pressure sterilization, gamma rays, etc. It was decided to use ethylene oxide (EtO) sterilization at 37 °C as the method that theoretically least altered the different materials, and because of the relative simplicity of sterilizing with this method. Once the sterilization method was selected, a quick test was performed in the multiaxial test with three silicone patches with the chosen formulation of HPMC. In this way we would know that the adhesion capacity would be altered if the amnion rupture pressure

decreased in relation to the results obtained previously (Figure IV-32). The results showed a mean rupture pressure of 69.6 mmHg, with a minimum value of 53.9 mmHg and a maximum of 97.6 mmHg. These values were slightly higher than those already obtained, so EtO sterilization did not decrease the patch adhesion and sealing capacity. Therefore, it was concluded that the EtO sterilization method was optimal in terms of patch sealing properties, thus allowing the initiation of the test in pregnant sheep.

The *in vivo* test in a large animal model (in this case sheep) allows us to evaluate different aspects of the sealing system: on the one hand, the viability of the insertion technique in real conditions more similar to surgery in humans, the visualization of the patch placement by fetoscopy, the adhesion of the patch during implantation, at the end of the intervention and after 7 days. It also allows us to identify signs of injury in the area corresponding to the orifice created, rupture of the amnion, and whether the chorioamniotic membranes separate from each other.

Four pregnant sheep were used where 4 silicone patches with the dehydrated HPCM formulation of 300 μ L (10 mg/mL) were implanted in each one. After removing the uterine horns and filling them with serum to increase intrauterine pressure and better navigate with the fetoscope, they were punctured and the patches were placed one at a time, tracking their position with the fetoscope until all 4 patches were placed in each sheep (Figure IV-36).

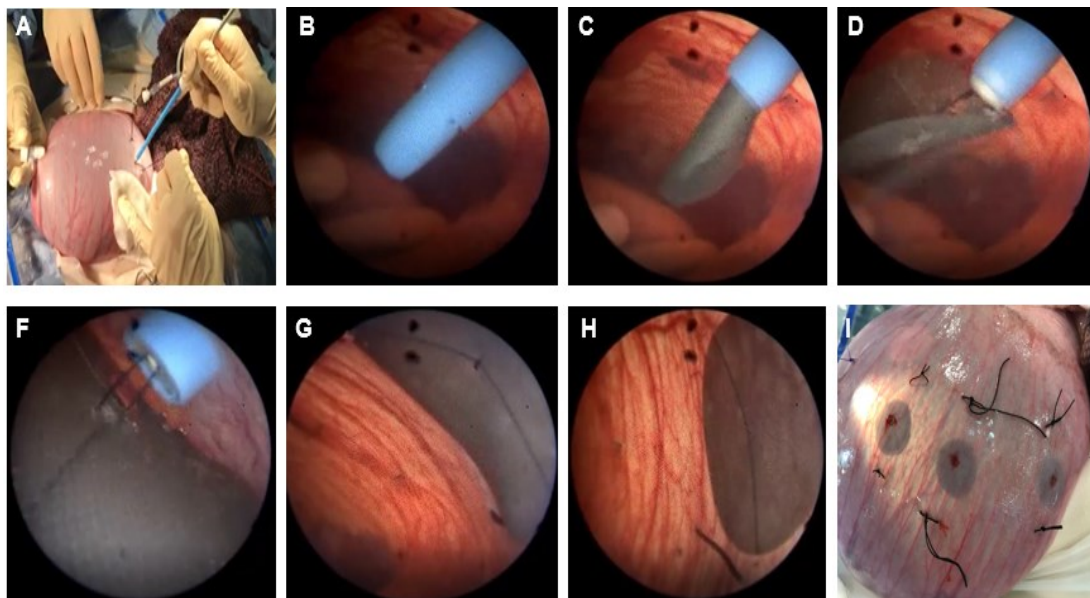


Figure IV-36. Image of implantation process in pregnant sheep. First of all, the trocar is introduced with Salinger technique (A). The introducer is introduced through the 12 F trocar (B) and the patch is deployed (C and D). After the rehydration process the patch is fixed to the amnios with the traction threat (F and G). After 5 minutes the patch is observed (H). The presence of 3 patches adhered to the amnion can be observed moments before reintroducing the fetal sac (I).

The results obtained (Table IV-6) showed that of the 16 patches implanted, 9 of them (56.2 %) were attached at the end of the intervention, and 7 of them detached during the manipulation of the uterine horns or during the implantation of the remaining patches. In some cases it could be observed how the fetal membrane was naturally retracted due to stimulation in the area, making it difficult to fix the patch. And in other cases, spontaneously, the patches were detached from membrane. It could be that this lack of adhesion was also influenced by the concave shape that the patch adopts when unfolded, due to the fact that for several days the patch is rolled up in the cannula of the insertion system, causing that when unfolded it does not adopt the original flat disc shape. After 7 days of implantation, the presence of the discs in the implanted position was evaluated. None of the remaining 9 patches were adhered to the implantation site. In fact, all the patches were found to be glued on top of each other. This could be due to the adhesive not having enough time to rehydrate and reach its maximum adhesion capacity, and/or the adhesive not having sufficient cohesive power and its chains not supporting the movements produced during the emptying and reintroduction of the uterine horn into the uterine cavity.

Table IV-6. Summary table of the results obtained in the *in vivo* assay with sheep.

	Cases
Adhesion at the end of 1st surgery	9/16 (56 %)
Adhesion at 2nd look surgery	0/16
Macroscopic lesions SS sites	0/16
Macroscopic lesions fetuses	0/4

In all sheep, the fetuses of the uterine horns where the 4 patches were implanted were healthy, there were no lesions beyond the orifice itself, and no leakage of amniotic fluid was observed through any of them

The adhesive quantification on the surface of the implanted patches was performed by TGA. The results (Figure IV-37) showed a loss of HPMC on the patch surface between 18 % and 40 %, with an average HPMC presence of 70 %, a median of 67 % and a SD of 6.6 %. Always bearing in mind that we do not know the time at which each patch was detached, nor the degree to which the movements that occur within the amniotic sac up to the time of recovery at 7 days may affect the integrity of the adhesive.

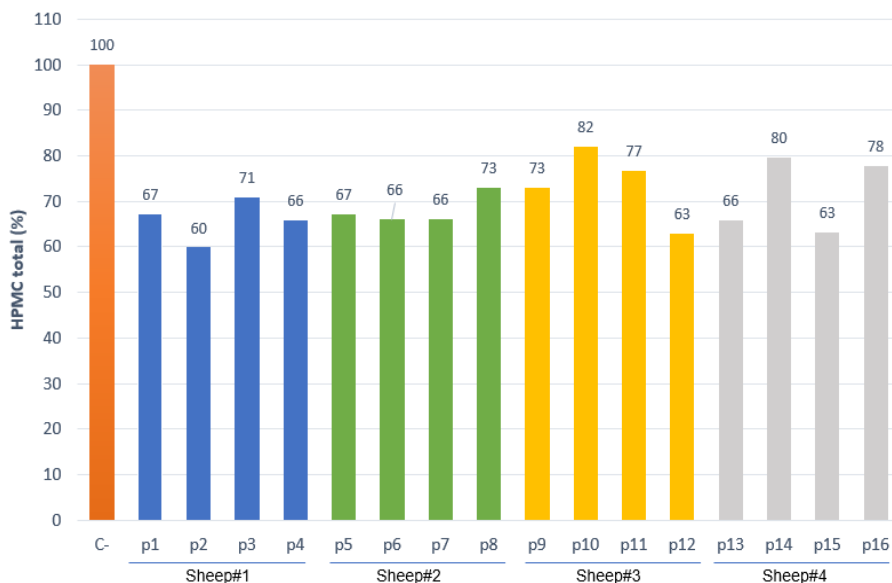


Figure IV-37. Comparative graph of the remaining total HPMC in the 16 patches implanted in 4 sheep, after 7 days.

From the results of the *in vivo* test in sheep it was concluded that the insertion system allowed the optimal implantation of the patch, with an easy to use mechanism for the medical team. That the use of the patches and the insertion technique did not adversely affect the health status of the fetuses. As for the adhesion of the patch, it was concluded that the adhesive and cohesive capacity of the HPMC formulation should be improved in order to support longer adherence to the amnion, although no leakage of amniotic fluid was observed at any time.

Formulations with pharma grade HPMC and HEC

The reduction of adhesive on the surface of the patches led us to consider four improvements: on the one hand, the need to test the following patches with a pharma grade HPMC; the need to increase the chain length due to a decrease in solubility; the need to increase the hydroxyl groups to increase the hydrostatic forces between the amnion and the adhesive; and the need to cross-link the polymer chains to improve the cohesion of the adhesive. For this reason, pharma grade HPMC was used for the new formulations and tests. Metolose 90SH 15M HPMC and Metolose 90SH 100M HPMC (ShinEtsu) were chosen. Some of these formulations included hydroxyethyl cellulose (HEC) (Natrosol M and HHX, from Ashland), which is a cellulose that is very similar to HPMC but with a higher number of hydroxyl groups. Finally, citric acid (CA) was also added in some of these formulations as a crosslinker to increase the cohesion of the adhesive.^{146,162,163} From this point on, the tests were carried out exclusively with silicone discs with the selected micropattern.

Phantom test

The first phantom test trial was performed with the pharma grade HPMC. It was intended to find out whether the new HPMC also allowed the patch to remain attached to the HAM, although an enhancement using amniotic fluid at 37 °C was added to obtain an *ex vivo* model even closer to reality. The three EtO-sterilized patches, with the 300 µL deposited formulation of 15M HPMC (10 mg/mL) and dehydrated, were optimally attached with the introduction system. All the patches are detached before the first 15 min. Concluding that while the patch could adhere during the first few minutes, this time was not sufficient to bring this formulation to *in vivo* tests in sheep. Further tests showed that the 15M HPMC, although easily rehydrated, solubilized too quickly (data not shown).

At this point it was decided to test some formulations with HPMC, HEC and citric acid as crosslinker. After selecting the most promising formulations, another *ex vivo* test was performed with phantom, HAM and amniotic fluid at 37 °C. The patches used contained a total deposited and dehydrated volume of 300 µL of the following formulations:

- A) HEC 250M (10 mg/mL)
- B) HEC 250M (10 mg/mL) + CA 1.25 %
- C) HPMC 15M (10 mg/mL)/ HEC 250M (10 mg/mL) 1:3 + CA 1.25 %

The results showed that all patches lasted at least 1 hour adhered to the HAM. At which time each test was interrupted. As an interesting and merely informative note, the test performed with the HPMC/HEC+CA formulation patch was left for a whole weekend, so that the patch remained adhered to the HAM for between 3 and 68 hours.

At this point, a solubility test of the three formulations was performed in order to choose the most promising one. The data obtained (Figure IV-38) showed that the solubility values of the HPMC/HEC+CA formulations were better than the other two formulations. Above all, a lower initial adhesive loss was observed for HPMC/HEC+CA in the order of 23 %, compared to 40 and 54 % for HEC and HEC+CA, respectively. In addition, a more real trend in adhesive loss can be observed as time progressed. This can be explained by the fact that in the first two formulations the saturation point of the medium is reached faster. That is, the extraction media (miliQ water and SBF) do not allow more adhesive to solubilize due to the saturation of the medium itself due to the fact that HEC and HEC+CA solubilize rapidly during the first 12 hours. This can be seen especially in the data obtained in the medium with miliQ water where the lack of salts produces a higher degree of solubilization compared to the data obtained with the medium with SBF. It must be said that this method has its limitations but it gives us important information, especially on the degree of solubility during the first 12 hours.



Figure IV-38. Comparative graph of the remaining total cellulose based formulations in the solubility test with miliQ water and SBF.

Patches with the HEC and HEC+CA formulations were discarded and an *ex vivo* phantom test was initiated for patches with the HPMC/HEC+CA formulation. Eight patches were implanted with the criterion that if 80% of these attached for at least 72 hours this formulation would be used for *in vivo* trials in sheep. The results obtained showed that of the 8 patches tested, one remained attached for 96 hours but only partially (Figure IV-39); one held for 2 hours until membrane rupture, perhaps due to excess tension when placing the chorioamniotic membrane in the phantom; another stayed for 30 mins and the remaining 5 detached before the first 5 minutes. Therefore, with a success rate of 12.5 %, the criterion of 80 % of patches adhered for at least 72 hours was not achieved.

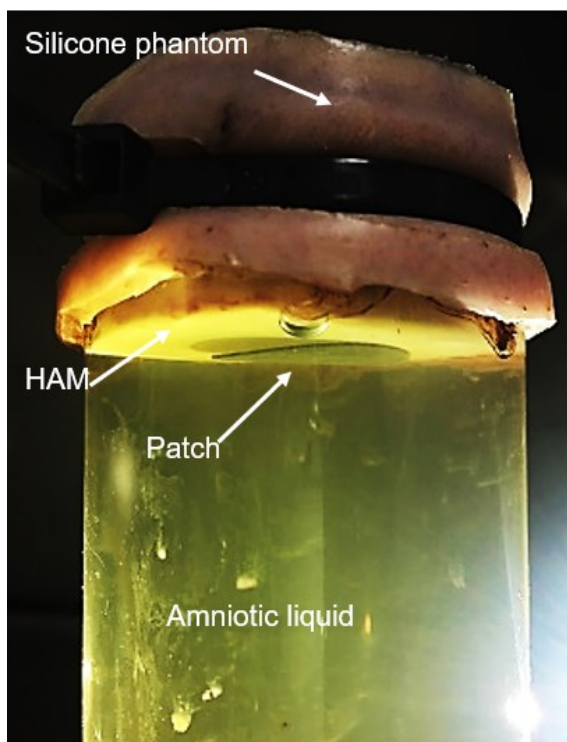


Figure IV-39. Picture of the first patch tested at 96 h. Partial detachment can be observed.

These data led us to consider improvements in the *in vitro* and *ex vivo* assays previous to the multi-axial and phantom tests, due to the fact that obtaining HAM and amniotic fluid limits large-scale assays. Therefore, it was of vital importance to obtain a method in our laboratory that would allow us to have adhesion values prior to the assays where a larger amount of HAM is used. In this direction, a dynamometric adhesion test was customized and developed.

Dynamometric assay

In order to obtain quantitative adhesion data before testing with the *ex vivo* phantom model, a dynamometric adhesion test was set up by customizing the equipment. A foam was applied on the flat metal head about 6 mm thick where a piece of HAM is placed (Figure IV-12). This foam allows us to apply a force between 1 and 1.5 N more precisely, simulating the force exerted when the patch is pulled against the amnion with the fastening thread. Tests in the laboratory indicated that tensile forces greater than 2 N caused the deformation of the patch, even breaking the silk thread. Therefore, dynamometer tests are performed by applying a maximum compressive force of 1.5 N for 1 minute, after rehydrating the patch with PBS for 2 minutes. The force value obtained when trying to separate the head with the chorioamniotic membrane from the patch is the value we take as a reference to compare the adhesion of the patches with the different formulations.

The adhesion values obtained by dynamometry of the patches that had already been tested previously in *ex vivo* phantom tests were used as a reference value, and compared with the new formulations. The results obtained in the dynamometry tests showed that the highest adhesion value was shown by the patch with HPMC 15M with 2.25 N, but we knew that it showed a very high solubility. Also as a reference we obtained the adhesion values of the patch with HPMC 15M/HEC 250M (1:3) + 1.25 % CA which, although we had obtained the best results in the *ex vivo* test with phantom, in the dynamometry test it obtained a low adhesion values of 0.15 N. Taking into account these two values and the adhesion results in the *ex vivo* phantom test, we were able to select the patch with the formulation that had the highest adhesion value. The highest adhesion value was the patch formulated exclusively with HPMC 100M, with an adhesion value of 1.4 N, followed by the same with CA, with a value of 1.03 N. This could be explained due to the fact that HPMC 100M having longer chains than HPMC 15M would produce a greater number of crosslinks between them, obtaining greater cohesion of the adhesive but maintaining the capacity to form hydrogen bonds. This ability to form bonds was reduced by adding CA, at the expense of further increasing the cohesion of the adhesive by forming covalent bonds between the chains. Therefore, it was decided to use the 100M HPMC formulation to perform the following *ex vivo* phantom tests.

Table IV-7. Summary table with the tension forces supported by the patches in the dynamometric assay.

Formulations	Disc material	Flexibility of the film	Force max. (N)	SD (%)
HPMC 15M	Silicone	Ok	2.25	0.13
HPMC 15M/HEC M (1:3) + 1.25 % CA	Silicone	Ok	0.15	0.00
HPMC 100M	Silicone	Ok	1.40	0.19
HPMC 100M/HEC HHX (1:1)	Silicone	Ok	0.27	0.10
HPMC 100M/HEC HHX (3:1)	Silicone	Ok	0.33	0.07
HPMC 100M + 0.5 % CA	Silicone	Ok	1.03	0.02
HPMC 100M + HEC HHX (1:1) + 0.5 % CA	Silicone	Ok	0.07	0.00
HPMC 100M + HEC HHX (3:1) + 0.5 % CA	Silicone	Ok	0.73	0.06

At this point, before proceeding with *ex vivo* tests with the new formulation, improvements to the patch were considered. It was concluded that the rehydration of the adhesive was critical but at the same time we could not establish a point of equilibrium between rehydration, adhesion and cohesion. That is, we could not establish a time when these properties would be at their maximum values. From the moment it was decided to modify the sealing strategy we understood and accepted that developing a "dynamic" adhesive represented a challenge due to the fact that its adhesive behavior is difficult to predict and evaluate. For this reason, one thing that could facilitate the increase in adhesion and cohesion while the adhesive rehydrates, was to add a physical bond in addition to that already produced by the traction thread that keeps the patch in contact with the amnion for 1-2 minutes while the chains interact between them, between them and the disc, and between them and the amnion. So finally the physical bonding, in addition to the chemical bonding produced by the adhesive, would allow the equilibrium of rehydration, adhesion and cohesion to be established while the patch is physically bonded. This physical adhesion was proposed as the incorporation of small microhooks or microarpoons attached to the surface of the patch, which we will see in the following chapter, together with the remaining tests until the last *in vivo* test in sheep.

4.4. Concluding Remarks

During the development of the different adhesives, it has been necessary to understand and analyze the true meaning of the results in the same time that they were obtained. The initial strategy of developing a patch with a thin polymeric film with adhesive properties by means of covalent bonds has evolved to obtain a patch with an adhesive that has a dynamic adhesion capacity. In other words, it would adapt and adhere as needed. This strategy was opposed to the initial strategy. A fact that was widely discussed and debated among us. The development of an adhesive that could be deposited on the surface of the disc in the form of a thin film, that was flexible, that could be rolled on a cannula without self-adhering, and that once rehydrated would swell and acquire adhesive and sealing properties together with the patch, although ambitious, could be possible. The results obtained especially from the use of HA made us understand the importance of an adhesive with the ability to swell to seal the flow of amniotic fluid between the disc and the membrane, as well as to penetrate partially through the orifice of the chorioamniotic membrane allowing the natural movement of the membranes. It could be affirmed that the importance of adhesion was reduced in favor of increasing the sealing capacity, for the maximum possible time. Obtaining a dynamic adhesive with sealing ability was only possible if the adhesive chains interact constantly with each other, with each other and the disc, and with each other and the amnion. And developing a bioadhesive that formed covalent bonds did not allow this. Therefore, efforts were directed to use molecules that form a large number of bonds by hydrostatic forces, such as HPMC.

This chapter concluded that with the high viscosity HPMC-based adhesive/sealant it was of utmost importance to ensure that the adhesive could rehydrate and partially swell in a short time, and that once sufficiently rehydrated a tensile force not exceeding 1.5-2 N could be applied. A tensile force higher than these values would deform the patch through the hole in the membranes and would not allow a constant force of pressure to be applied from the entire surface of the patch to the amnion.

This series of conclusions point the way to the incorporation of some modifications in the patch, in order to improve the sealing capacity of the patch.

Chapter V. Latest advances and next steps

Latest advances and next steps

This last chapter shows the latest modifications introduced in the patch to add a physical anchorage in the form of microarpoons, in addition to the chemical adhesion provided by the adhesive. As well as the results obtained in *ex vivo* and *in vivo* studies derived from these modifications. It also includes a description of the possibility of incorporating a hexagonal mesh-shaped skeleton inside the silicone disc, in order to increase the stiffness of the patch and avoid deformations. Finally, the next steps to follow are briefly discussed with the clear objective of creating a startup where the sealing system can progress as quickly as possible and reach the first assays in pregnant women.

5.1. Introduction

During the implantation of the patch, in order to save time in the rehydration and swelling of the adhesive, and so that its adhesion power would not depend on the time we are pulling with the traction thread, it was decided to incorporate a physical bond in the form of microarpoons in the patch.

In nature, there is a wide range of strategies (Figure V-1) for achieving physical bonding. It is therefore natural for research to look to those anchoring methods that nature has perfected over millennia. Bio-inspired engineering tries to draw inspiration from these designs already existing in nature to adapt and incorporate them, as in the case that brings us here, to the medical device sector. Plants such as the burdock have hooks so that their seeds can get caught in the hair of animals and thus be transported much farther than if they were to simply fall to the ground. Geckos have a kind of microbrush on their toes that allows them to climb vertical walls. Lampreys and squids have teeth that, thanks to contraction, anchor themselves by means of a suction effect. In the same way, octopuses attach themselves by means of suction cups, but without the need to have teeth on them. Mosquitoes introduce their sting into the skin by means of a system inspired by medical needles. And a long etcetera.^{164,165}



Figure V-1. Some strategies that exist in nature and that serve as examples for bio-inspired engineering.

We were inspired by a harpoon design that also exists in nature. For example, the teeth of some snakes are oriented in such a way that when the snake is swallowed it is impossible to get out. In the same way the skin of sharks or scales of fish and reptiles are oriented so that there is practically no resistance in one direction but yes in the opposite direction. That is why we clearly look at the design of harpoons and fishhooks used in fishing, which consist of a needle-shaped end and a "death" so that once the harpoon penetrates, it is anchored and does not come out easily. Thus, by incorporating multiple microarpoons in the external part of the surface of the patch, it is intended to physically attach the patch to the amnion so that the microarpoons penetrate the membrane and cannot go backwards, the patch remaining attached while the adhesive acquires its maximum adhesive properties on the membrane.

5.2. Materials and Methods

5.2.1. Incorporation of a microarpoons corona

Design and fabrication

The microarpoons design was carried out using Solid Works design software. The microarpoons strips were fabricated using S304 stainless steel sheets 0.01 mm x 100 mm x 1000 mm. Laser cutting was carried out using the Laser P400U machine from GF Machining Solutions, with the Amplitude Satsuma 20 W femtosecond laser source (Microrrelleus S.A.).

Once the microarpoons strips were obtained, they were immersed in acetone and ethanol and sonicated for 5 minutes. They were dried at room temperature and the ends were glued with ethylcyanoacrylate.

The Nusil® medical silicone discs with the concave hemisphere micropattern were manufactured as explained in chapter 2.2.3, but with a diameter of 15 mm and a thickness of 0.25 mm. This disc was placed on a 0.5 mm uncured silicone film and pressed to a thickness of 0.5 mm. The excess silicone has been leveled to the height of the cured patch and with micro-tweezers the micro-harpoon crown is inserted into the uncured silicone just outside the cured silicone disc. Once we make sure that the crown is integrated in the silicone with the help of a binocular magnifying glass (Leica M165C), the discs are introduced in the oven at 50 °C for 8 hours and it is left to rest at room temperature. Finally, it is cut with a 17 mm diameter metal punch.

Preparation of the patches

The patches are cleaned with 5% Hellmanex II solution, miliQ water and ethanol. It is dried with filtered compressed air and activated with oxygen plasma (chapter 2.2.3) and 300 mcl of HPMC Metolose® 90SH 100k (ShinEtsu) 10 mg/ml in miliQ water is added. It is placed in oven at 45°C for 2 hours and allowed to stand o.n.

5.2.2. Validation assays for the patch

Multiaxial *ex vivo* test

Two patches with the microarpoons strip with square fenestrations are used for the multiaxial test with HAM (Figure V-1A). And the test is performed in the same way as in chapter 4.2.2. evaluating the leakage pressure and the amnion rupture pressure.

Stability tests

To realize the stability test, a disc with the "S" design of the microarpoons strip was used (Figure V-1 B and Figure V-5). One of the discs was placed in a 12 F cannula for 24 hours. When deployed, the condition of the microarpoons and the crown were evaluated.

In vivo test with pregnant sheep

For the *in vivo* assay, 2 pregnant sheep were used. Five patches were implanted in each sheep with the second micro-harpoon design (Figure V-1 B and Figure V-5). The same procedure was followed as in the *in vivo* test performed with DHA in Chapter 4.2.2. After implanting each patch, we waited 5 minutes and observed their behavior with a fetoscope. After implanting the last patch of each sheep, we evaluated the presence and state of the 5 patches that had adhered to the amnion. After 7 days we observe the position of the patches by reopening and removing the placenta with the fetus. The presence of adhesive on the patch is evaluated by direct observation. We also evaluate the state of the orifices, presence of leakage, state of the fetuses by means of their cardiac pulse, etc.

5.3. Results and Discussion

5.3.1. Incorporation of a microarpoons crown.

Design and fabrication

The main design was proposed in such a way that the microarpoons would be manufactured in the form of a zipper tape. That is, each micro-harpoon would be represented by each of the teeth that form each of the strips of a zipper, with each microarpoon unit repeating until it forms a strip, which when joined at both ends forms a crown.

Before creating the design of this microarpoons tape, it was important to consider several factors. On the one hand, the functionality of the microarpoon was important, so the length, thickness, shape, total number of microarpoons and the distance between them had to be established. The microarpoons should completely cross the amnion, but not penetrate too far into the chorion. If the microarpoons were to penetrate deeply into the chorion, they would not allow free movement of one membrane over the other. And, on the other hand, it was also important to establish how this crown was anchored inside the silicone disc, allowing it to roll up inside the cannula and unfold completely.

Another important thing to consider before making the designs was to identify the way in which we would manufacture this microarpoons crown, due to the fact that the manufacturing technique can limit the measurements when working on a microscopic scale. Several methods were evaluated that would allow us to fabricate these microarpoons, including 3D printing, injection molding, and laser cutting.

Having evaluated various methods of obtaining this harpoon tape, it was finally decided to use the laser cutting technique, due to the fact that, without being economical, it is the method that offered the possibility of manufacturing components on the scale we needed. We contacted several microtexturing and laser cutting companies and asked them about the limits of their lasers. The limit was set by the diameter of the laser beam. Meaning that, the smaller the diameter of the laser beam, the more details we can add in the design and the more accurate the final cut will be to this design. Identifying this limit was very important due to the fact that the material chosen to manufacture this crown was stainless steel film of a 0.01 mm thick. Although biocompatible metals such as Nitinol and titanium are used for implantology, stainless steel was useful for the prototype validation tests due to the fact that it does not oxidize in aqueous media and is not easily altered at the silicone curing temperature. In addition to being flexible with the thickness of the selected film and not having a very high cost, compared to the other options.

The first reference measurements for the design were obtained from the thickness of the stainless-steel film, which was 0.01 mm. The only way to have microarpoon as close as possible to a cylinder shape was by means of an orthohedron with a depth of 0.01 mm and a base of 0.01 mm. Another reference measurement was obtained according to the thickness of the amnion, which ranges from 0.010 mm to 0.050 mm depending on the tension exerted and the stage of pregnancy. As the microarpoons crown is integrated into the silicone disc, the total length of the microarpoons to be optimally anchored in the amnion should be between 0.05 mm and 0.250 mm, varying according to the depth that we introduce the crown into the silicone disc to anchor it sufficiently so that it does not separate. The other reference measure is the thickness of the silicone disc, which ranges between 0.475 and 0.525 mm, so the part from where the microarpoons grows and which has the function of anchoring to the silicone should be between 0.05 mm and 0.2 mm.

With the Solid Works design program, we designed several types of microarpoons strips (Figure V-2) taking into account the measurements we had as reference. Three parts distinguish these microarpoons strips: the microarpoons; the tabs and holes at the ends of the strip; and the fenestrations at the base, which have the purpose of allowing the silicone to penetrate between them, anchoring the strip inside the disc.

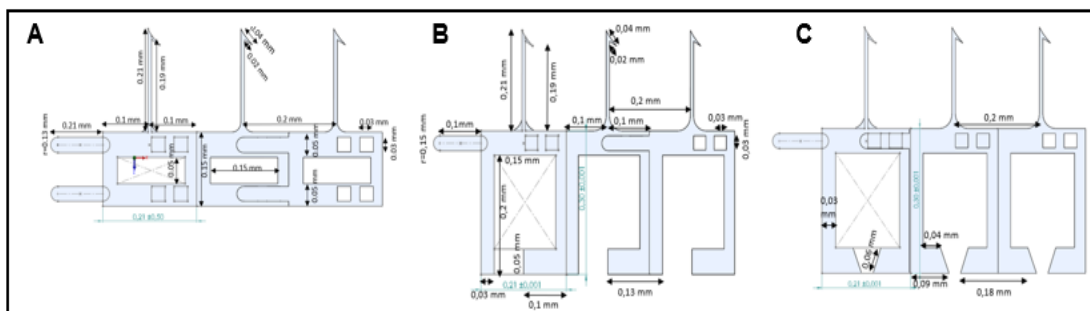


Figure V-2. Three possible designs (A-C) with three repeating subunits of the microarpoons are shown. Designs B and C are intended to allow the crown to be more mobile during the folding and unfolding of the patch. In addition to having greater penetrability in the silicone substrate due to a larger size of the base.

Finally, after several meetings and discussions, we found a company (Microrelleus SA. Sabadell) capable of manufacturing the microarpoons strips with a femtosecond laser. This laser is ultra-short pulsed and offers high precision and low temperature cutting, so there is an absence of burrs in the cut material. The smaller head of this equipment allows projecting a laser with a beam diameter of 0.005 mm. Enough to cut the micro-harpoon with the details of our design. Especially with regard to the most critical part of the design, which is the "death" of the micro harpoon.

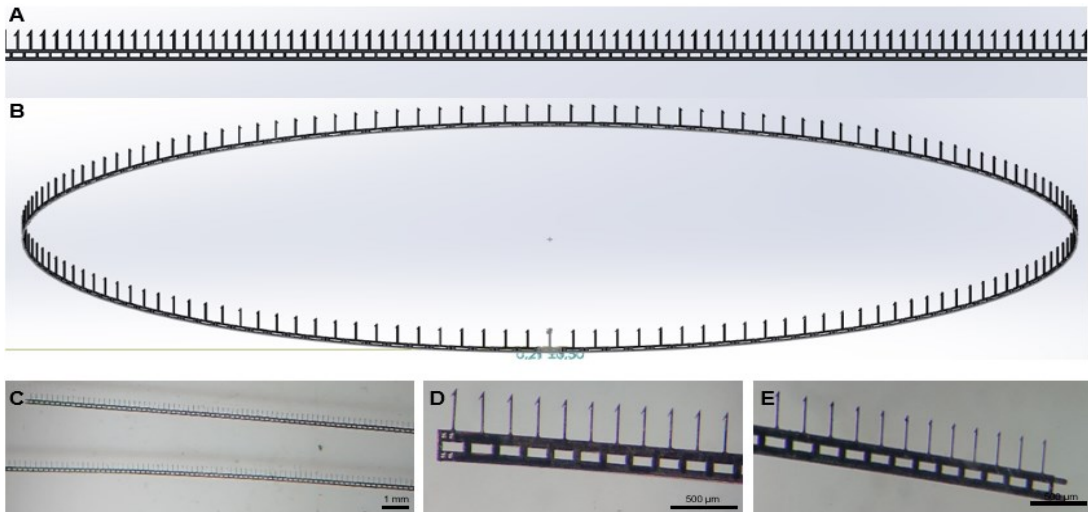


Figure V-3. Microarpoons tape from the repetition of a microarpoon unit in .stl format (A) and a real image with a binocular magnifying (C-E); same ribbon but joined at its ends forming the crown in .stl format (B); real images with binocular magnifying glass of the details of the microarpoons, fenestrations of the base and tabs and holes at the ends (D and E).

Once the microarpoons strips were obtained (Figure V-3 C), the objective was to join them at their ends in such a way as to form a crown with the microarpoons oriented upwards (Figure V-3 B). In order to join it, tabs were designed at one end to fit through the holes at the other end (Figure V-3 D and E). Although this was attempted, the size we were working with was too small, so it was solved by joining the ends with an extra fast curing adhesive (Figure V-4 A). Once we had the crowns prepared, we thought about the best way to incorporate them into the silicone disc. After some trials, it was decided to use a dual cure system for the silicone. First, a micropatterned disc of 0.25 mm thick cured silicone was placed on a 0.5 mm base of uncured silicone. It is pressed to a total thickness of 0.5 mm and the excess is flattened to the same level as the cured disc. The crown is placed on the outside of the cured disc. Carefully and without bending the micro-hoops, insert enough so that only the micro-hoops remain on the outside. It is introduced in the oven at 50 °C for 8 hours. Once the silicone is cured, it is left to rest at room temperature for about 8 hours and with a 17 mm diameter punch the silicone disc with the integrated microarpoons crown is cut (Figure V-4 B).

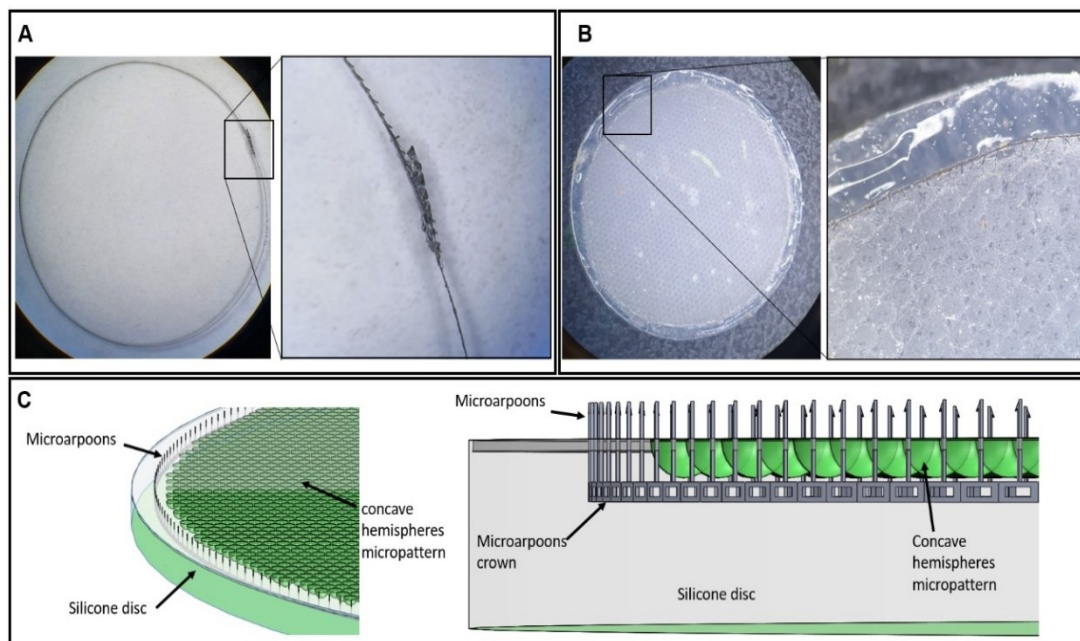


Figure V-4. Real image of the crown of microarpoons approximately 15 mm in diameter, attached with adhesive at its ends (A) and of the crown integrated in the silicone disc (B), and schematic images of the crown embedded in the silicone disc (C).

It should be noted that the first discs with the microarpoons crown were made with the microarpoon design with the base fenestrated in the shape of a square window (Figure V-2 A and Figure V-3 C-E) Finally, it was decided to use the design with the S-shaped base (Figure V-2 B and Figure V-5 A and B) due to the fact that it allowed more dynamism of the crown when rolling and unfolding the patch.

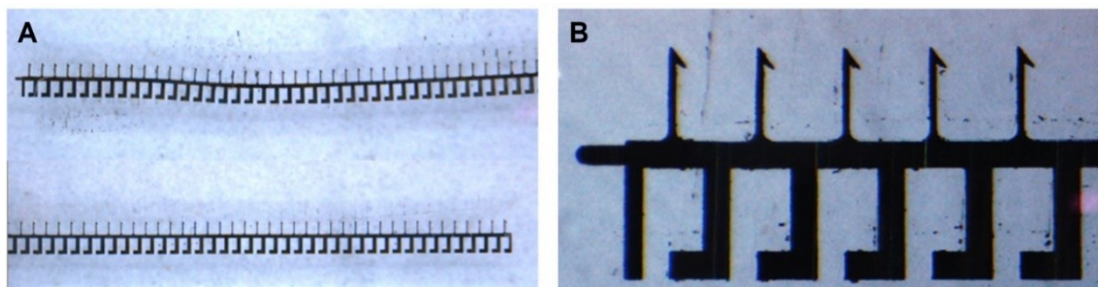


Figure V-5. Real image of the microarpoons tape with the final design selected, with the base defenestrated in the S shape (A and B).

5.3.2. Validation assays for the patch

Multiaxial *ex vivo* test

The cost of manufacturing the microarpoons crowns is very high, so fewer tests were performed than desired. A first test was performed to evaluate the sealing of the HAM orifice using the multiaxial test with the first microarpoons design (Figure V-2 A and Figure V-3 C-E). Two silicone patches with the integrated microarpoons crown were used. One without adhesive to see if the patch with adhesive remained anchored to the chorioamniotic membrane only through the microarpoons, and the second with the 300 μ L formulation of dehydrated HPMC 100M. The results obtained showed appearance of leakage at a pressure of 24.2 mmHg in the patch with the HPMC formulation. This pressure did not increase further as more liquid was lost than entered the system. This value is above the 15 mmHg reference intrauterine pressure, so this patch modification was still sealing the membrane above physiological pressure. It was not possible to identify whether the patch attachment was due to physical binding because the patch without adhesive did not hold attached to the chorioamniotic membrane during the first few seconds of the test. This was probably due to the fact that the patch was not completely flat, and that some sectors of the microarpoons were hidden under the silicone. It was this result that led to the modification of the design to a larger strip base up to 0.3 mm in height. Precisely to make it easier and simpler to place the crown inside the silicone so that once cured it would be better integrated.

Another aspect to be evaluated was whether the crown and arpoons would have undergone any damage after being subjected to a pressure of 24.2 mmHg. For this reason, the patch and all its microarpoons were photographed before and after the test. The results of the microscopy image analysis showed that in some sectors the crown had separated from the silicone disc and that some microarpoons had undergone some deformation. This result reinforced the idea of modifying the design and verified that the stainless steel microarpoons

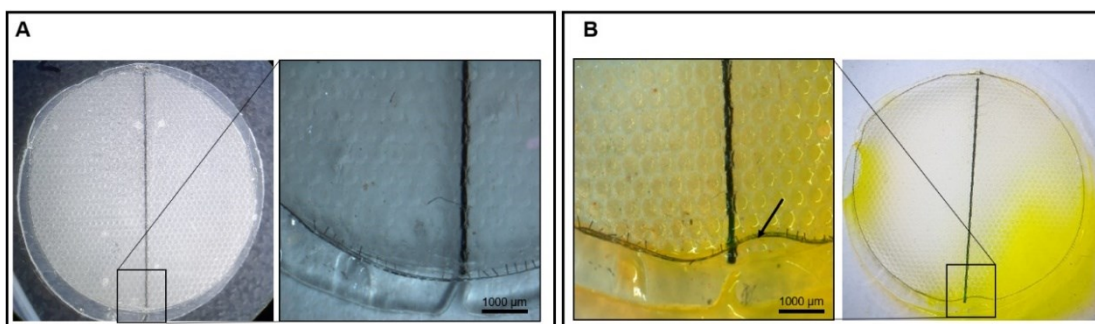


Figure V-6. Image obtained with a binocular loupe of the silicone patch with micropattern and microarpoons crown incorporated, before (A) and after (B) the multiaxial test. An example of one of the analyzed sectors is shown, where a deformation and disengagement of the microarpoons crown (black arrow) is observed.

deformed when they penetrated the chorioamniotic membrane and exerted tension up to 24.2 mmHg.

Stability tests for the microarpoons and deployment of the patch

One of the things we were worried about when incorporating this microarpoons crown into the silicone disc was the stiffness it could acquire. Until now, the disc without the microarpoons crown could roll up inside the cannula and unfold without deforming. This incorporation could alter the properties of the memory effect that silicone has. One of the reasons why this viscoelastic material was selected. Another factor to be taken into account was the stability of these microarpoons. We had already observed that some of the microarpoons could lose their vertical orientation due to tensile forces on the microarpoons. However, at this point we wanted to know if the microarpoons would bend or break after the patch was deployed. If this happened, we would not be able to implant the patch in sheep using the insertion system we had developed.

Previously, and together with the medical team, the decision to increase the diameter of the introducer from 10 F to 12 F was taken. It was not worth the risk of losing any patch due to the small diameter of the cannula. y It was not worth the risk of losing any patch due to the small diameter of the cannula. The patch when rolled into the cannula of the introducer could be too tight and forced into the cannula, deforming the microarpoons. So we could not use it for posterior implantation in sheep. Again, 10 microarpoons strips were fabricated with the "S" shaped base design (Figure V-1 B), the crowns were formed and integrated into the silicone discs. Only one of them was used to perform the stability study. By rolling the patch in the cannula and then unfolding it after 24 hours, its deformation, the anchorage of the crown within the silicone disc, and the integrity of the microarpoons were evaluated.

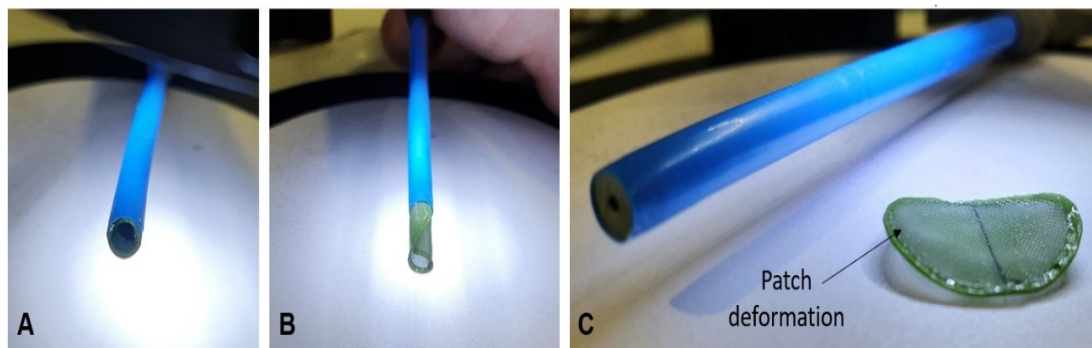


Figure V-7. Images where the folded patch can be seen inside the cannula of the introducer (A); moment at which it is pushed outside after 14 hours of folding (B); and the unfolded patch with a slight "U"-shaped deformation (C).

The results showed that the microarpoons crown was well integrated into the silicone and the patch could be deployed correctly. But a slight deformation of the disc was also observed, it did not completely recover its flat shape. This deformation was attributed to the choice of stainless steel as material, so it could easily be avoided by using another material such as Nitinol or some thermopolymer that was more elastic and could be laser cut. Previously, this type of deformation had already been observed in some silicone discs of lower thickness and after being rolled inside the cannula for several days.

As for the integrity of the microarpoons, the entire perimeter of the microarpoons was analyzed with a binocular magnifying glass to evaluate any deformation, comparing the images before rolling the patch and inserting it into the introducer cannula and after being deployed after 14 hours. The results of the images analyzed of the microarpoons before folding showed that in most of the perimeter the microarpoons were in good condition, and in some sector there was silicone between them. Analyzing the images of the unfolded disc, it was possible to observe slight deformations in some microarpoons, but the most remarkable result was the rupture of the crown in the place where the ends meet. This result verifies that there is a need for improvement in our crown design and assembly. Subsequently, an analysis of the integrity of the crown and microarpoons of the remaining 9 patches was made, and even knowing their limitations, it was decided to use them with the introducer or insertion system in the *in vivo* test in sheep.

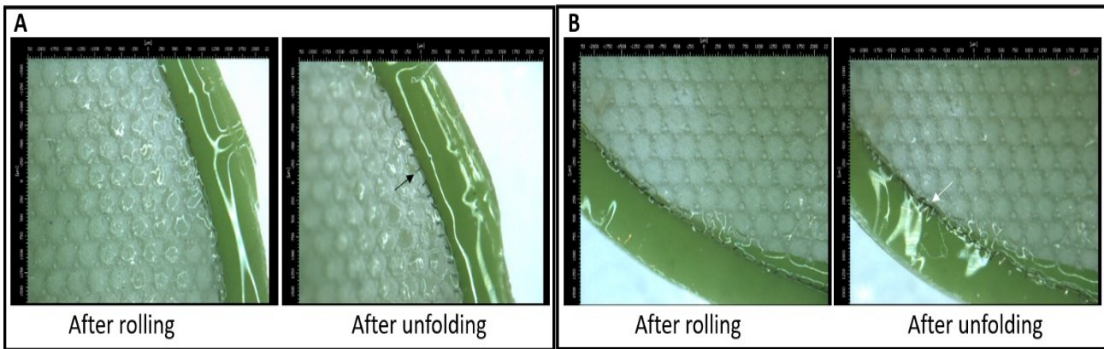


Figure V-8. Two examples of the binocular microscope analysis of the integrity of the microarpoons and the crown before and after unfolding. A slight deformation of the microarpoons can be seen (black arrow) but that should allow an optimal anchoring in the HAM (A), and a deformation of the crown (white arrow) due to the stress that the crown supports when being rolled (B).

In vivo test with sheep

In two pregnant sheep, the ten patches that had been manufactured were implanted (five in each fetal sac), including the one we had used in the stability test for the crown and the microarpon (Figure V-9). The same procedure was followed as in the *in vivo* test performed with the DHA. In the same way we implanted each patch, waiting 5 minutes observing its behavior, and when implanting the last patch of each sheep we evaluated the presence and attachment of the 5 adhered patches.

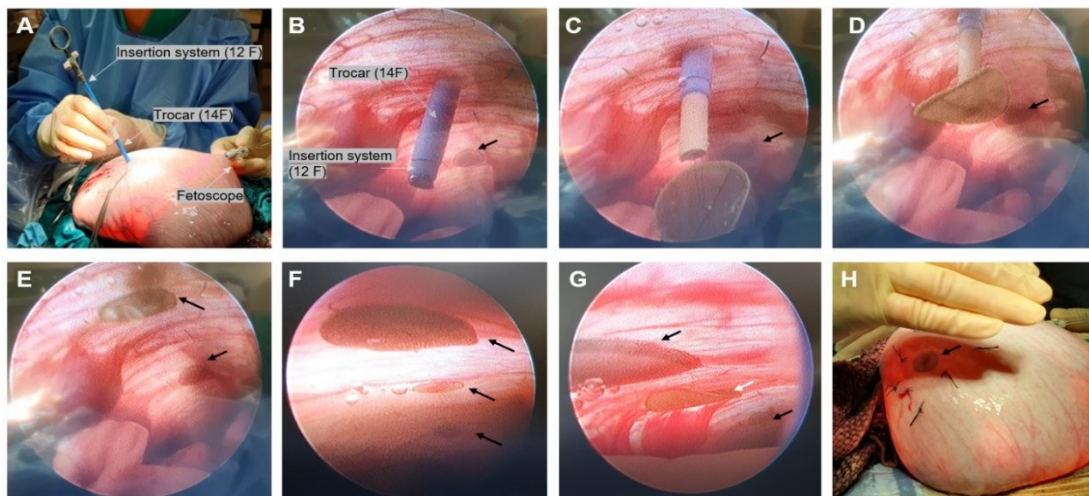


Figure V-9. Images of the implantation of the patches from outside the fetal sac in pregnant sheep model (A); from the inside with the fetoscope camera where unfolding (B), rehydration (C) and fixation of the patch in the amnion (E) can be seen; image with 3 adhered patches on the amnion of sheep # 1 (F) and sheep # 2 (G); once implanted the patches can be seen from the outside thanks to the dark color of the patch (H). The black arrows indicate the adhered patches and the white arrow the deformation of some of the patches in a "U" shape.

The results obtained (Table V-1) showed a correct insertion of all the patches with the introducer/insertion system adapted to 12 F cannula. The substitution of the braided silk traction thread by a Nylon monofilament also gave optimal results. This substitution was made due to the real danger that the silk thread could be damaged or entangled in the microarpoons. As for patch adhesion, fetoscopic camera monitoring showed that 7/10 patches remained attached to the amnion for a minimum of 12 minutes. Of which 4 of them detached before reintroducing the fetal sac into the abdominal cavity with a maximum of 45 minutes. 3/10 of the patches detached from the amnion during the first 5 minutes of observation. It was possible to identify, just at the moment of detachment, that the shape of the patch acquired the "U" shape that we had already observed previously in the stability test. This could explain why the patch detaches by exerting an opposing force on the membrane when we pulled with the fastening thread to anchor the microneedles and activate the adhesive. Finally, 3/10 patches remained attached to the implantation site until the end of each intervention (one

patch in the first sheep and two in the second). No amniotic liquid leakage was observed in any case, so the orifices were successfully sealed. It could be that the HPMC penetrates through the orifice and helps to seal the two membranes while allowing the membranes to slide between them.

Table V-1. Summary table with the implantation times in sheep of the 10 silicone patches with microarpoon crown and formulation of HPMC 100M.

NºSS	SS1	SS2	SS3	SS4	SS5	SS6	SS7	SS8	SS9	SS10
Nº sheep	#1	#1	#1	#1	#1	#2	#2	#2	#2	#2
Adhesive	HPMC	HPMC	HPMC	HPMC	HPMC	HPMC	HPMC	HPMC	HPMC	HPMC
After 5 min	Ok	Detached	Ok	Ok	Ok	Detached	Ok	Detached	Ok	Ok
End of surgery	Ok		Detached	Detached	Detached		Detached		Ok	Ok
After 7 days	Detached								Detached	Detached
Detachment	<7 days	<5 mins	14 mins	26 mins	12 mins	<5 mins	45 mins	<5 mins	<7 days	<7 days

After 7 days, the presence and position of the three patches that had remained attached at the end of the first intervention were evaluated, and it was observed that none of the three patches were in the initial implanted position. No loss of amniotic fluid or inflammatory alterations of the membrane in the zone of the orifice were observed. Both fetuses were healthy.

Once recovered (Figure V-10), 9 of the 10 patches were analyzed (SS2 was not found). In all patches, practically no separation of the microarpoons crown with the silicone disc, nor zig-zag crown bending was observed. Most of the microarpoons remained unchanged from before rolling into the cannula, although some had slight deformation. Organic debris was present on the adhesive face. This was not the case on the external flat side. This means that part of the adhesive remains adhered to the face of the micropattern, although macroscopically it is difficult to appreciate. Most likely, part of the adhesive has remained adhered to the wall of the amnion, has solubilized, degraded, or mechanically separate.

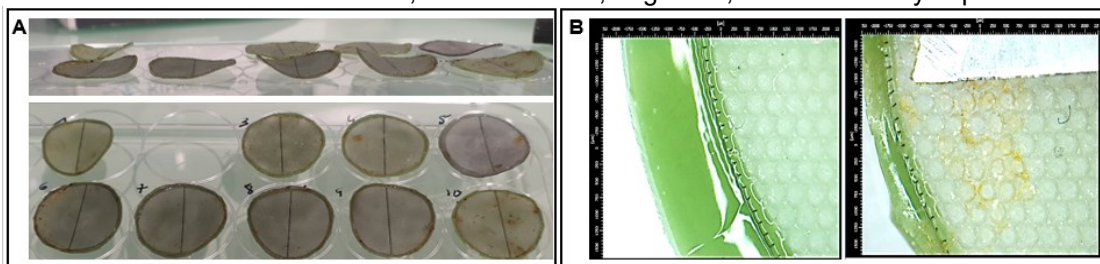


Figure V-10. Patches recovered after evaluation surgery at 7 days (one disc not found). In the image above you can see the "U"-shape deformation that some patches have. It can also see the remains of organic matter adhering to part of the adhesive present on the surface of the patch (A); Unaltered microarpoons in a sector of the SS1 patch before (left) and after 7 days of implantation (right) (B).

Evaluating the final results, it is important to note that the U-shaped deformation observed in the unfolded patches is due to the stiffness of the material used in the microarpoons crown, which seems to have influenced the detachment of the patches, especially in the first minutes. So, a simple and necessary solution would be to change the material they are manufactured from, and/or add an internal Nitinol mesh attached to or separate from the microarpoons. This mesh would also preserve the flat shape of the disc and could exert a greater and more homogeneous traction force.

Although there has been an optimal sealing of the holes avoiding leakage, the bonding capacity of the adhesive should be improved. Functional groups could be incorporated into the HPMC chain such as succinimidyl groups, dopamine, isothiocyanates, etc. due to the fact that this would improve not only adhesion to the amnion but also cohesion between the polymeric chains. And one thing to keep in mind, according to the fact that all the holes made have been optimally sealed, is that the adhesive has not allowed the leakage of amniotic liquid. Precisely this could lead to the possibility of substituting a non-biodegradable material such as silicone for one that can biodegrade in a few hours or days, because the sealing system would have done its purpose, which is precisely to seal the orifice, prevent the leakage of amniotic liquid and avoid rupture of the amnion. Therefore, if it could be demonstrated to be an advantage over using nothing, it could be perfectly viable.

In reference to the use of the sheep model, although it gives us a large idea of the mechanism and the capacity of adhesion in amniotic membrane, it does not allow an optimal simulation of the conditions that we would find in a surgery in humans. To implant the patches, the entire fetal sac must be removed, the intrauterine volume increased with saline, and stitches made so that the amnion does not separate from the chorion when the trocar is introduced. After implant the patches, we reduce the volume of fluid and reintroduce the sac into the abdominal cavity. These movements of tension and distension of the chorioamniotic membrane, together with the low resistance of the membranes at the moment of traction of the patch on the amnion, make it difficult for the patches to remain stable on the amniotic membrane. Performing an approach inside the fetal sac only with minimally invasive surgery and placing the patch as if it were fetal surgery in humans could give us valuable information. It would also be interesting to use a non-invasive method to be able to track the position of the patches day-to-day. Returning to the idea of the internal mesh of Nitinol, its incorporation, in addition to the advantages already mentioned, could provide sufficient signal to be able to observe the patch by ultrasound. In this way we could optimally and truthfully assess the time the patch remains adhered.

5.4. Next steps

5.4.1. Internal hexagonal mesh for the patch

We have found it interesting to add one more point to this thesis, in order to show a future improvement, already mentioned at the end of the previous point. Incorporating an internal mesh in the form of a hexagonal pattern, for example, inside the silicone would not only allow the patch to unfold completely flat, but also a greater force could be applied with the traction thread and this shape would be more homogeneous throughout the patch, making the microarpoons better anchored. In addition, the thickness of the patch could be reduced, so that it could be of larger diameter or could be used in introducers/insertion system with cannulas smaller than 10 F. This internal mesh could be manufactured in Nitinol by laser cutting at a high economic cost, using some biocompatible polymeric material with laser cutting or injection in micromolds.

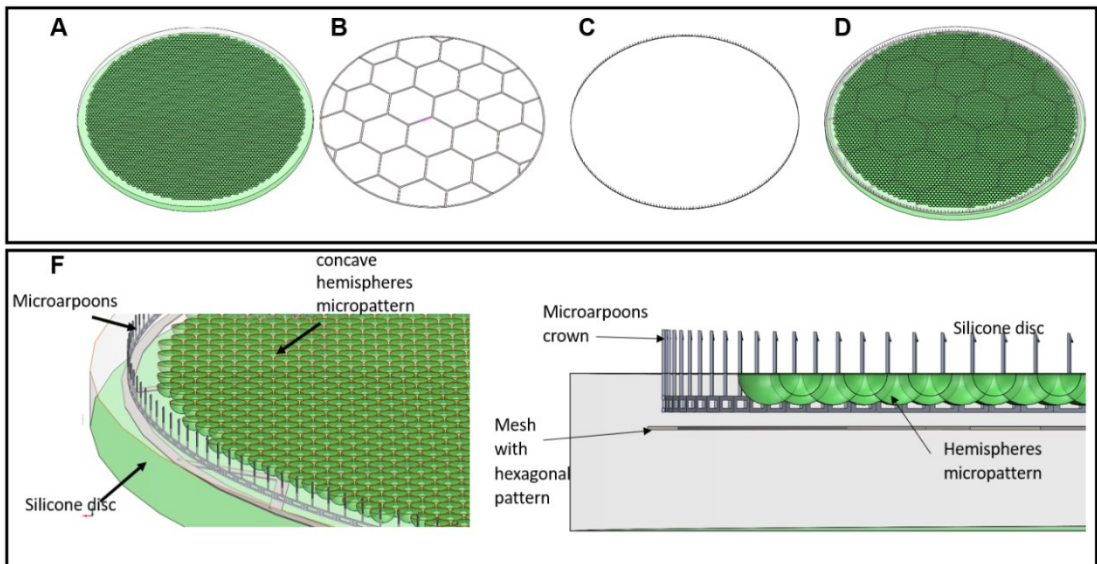


Figure V-11. Design of the internal hexagonal mesh. Design created in Solid Works of the silicone patch with the hemisphere micropattern (A), the mesh with hexagonal pattern (B), the microarpoon crown (C) and the three previous elements together (D) in the patch model final without adhesive, and its details (F).

There are other possibilities, although technical feasibility and cost studies are pending. One of these options would consist of manufacturing the mesh and the microarpoons in a single piece, with the advantages that it would not be necessary to manufacture a crown avoiding the effect of the base of this, and in addition it could be integrated into the silicone disc in just one step.

One of the next steps, in addition to the importance of improving the adhesive, would be to repeat the chain of tests that has been developed with patches with half-lentil shape. A

promising design, especially because the empty space in the dome of the patch could be used to integrate sensors for monitoring pregnancy by the physician. A pressure sensor could be added, for example, in order to correlate intrauterine pressure with the volume of amniotic fluid present and that through a Bluetooth system would send the information on a daily, weekly, monthly, ..., to be evaluated remotely by the physician without the need to visit the patient personally. Although discussing, assessing, and developing this and other possibilities would already be part of a future project that would continue with the development of the sealing system that has been discussed in this thesis.

5.5. Concluding Remarks

In this last chapter, the silicone disc has been modified by incorporating microarpoons that have the function of physically attaching the patch to the amnion while the adhesive rehydrates and acquires its higher adhesion and sealing properties. A first prototype has been successfully fabricated by attaching these microarpoons inside the silicone, and *ex vivo* and *in vivo* tests have been performed to prove the efficacy of the entire sealing system.

The *ex vivo* and *in vivo* stability tests of these microarpoons and the crown they form have laid the basis of the methodology for their evaluation. Their development and fabrication has meant entry into microscale manufacturing of components for medical devices. Both the techniques that can be used and the materials that can be used. Assessing their advantages and disadvantages, as well as working with them has made us understand to a great detail how and when they should be used.

The results in the *in vivo* test in pregnant sheep, although improvable, are also promising. We know that there is margin for improvement in terms of patch adhesion, but it should be remembered that the main objective is to seal the orifices, prevent amniotic fluid leakage and chorioamniotic membrane rupture. And this objective has been achieved in the 10 orifices made in the fetal sacs of the two sheep. We also validated the introduction system, which was improved as the present thesis progressed.

Finally, at this point and globally, as we were developing the sealing system and obtaining results, we were learning and understanding the importance of the membranes that protect the integrity of the fetus throughout its development. Membranes prepared so that nothing penetrates, nothing comes out and nothing adheres to them, while being extremely elastic and at the same time highly resistant. Confronting this type of tissue and developing a sealing system that "repairs" the hole created by ourselves has made us understand why, for so many years, the strategies used to solve this problem have not prospered. It is also true, and thanks are always due to all those researchers and physicians who tried it first and published their results. Without their results and conclusions, we might never have come up with the strategy and strategies that have been developed in this thesis. When one faces challenges of this magnitude in applied research one really understands the significance and applicability in the field of medicine and health. Debating, discussing, designing, developing, and modifying a sealing system of this caliber and in collaboration with a medical team has brought us closer than ever to a possible solution for iatrogenic fetal membrane rupture.

Conclusions

- A first prototype of a medical device for use in fetal surgery has been developed. This medical device consists of a sealing system that aims to prevent the loss of amniotic fluid and rupture of fetal membranes, after performing minimally invasive surgery on the fetus, in a pregnant woman.
- The parts that compose the sealing system have been developed and evaluated: the patch, the adhesive that is activated in wet environment; and the insertion system or introducer, used to implant the patch with the selected adhesive.
- A disc-shaped patch and a semi-lentil shaped patch have been developed. These patches have been manufactured in medical grade silicone.
- The surface of the patch has been modified using laboratory techniques in order to deposit various types of adhesive. a) a physical and permanent modification, by the incorporation of a micropattern of concave hemispheres and/or integrating an electrospun layer of PCU, to increase the contact surface with the adhesive; and b) a temporal modification with oxygen plasma to form covalent bonds with the adhesives.
- The electrospun layer integrated into the silicone allows the thickness of the patch to be reduced while maintaining its elastic properties.
- Several strategies have been tested and developed to achieve an adhesive surface on the patch. The first strategy consisted of binding proteins and cells but lacking a higher adhesive power. It was concluded that an adhesive with swelling behavior was needed.
- The next adhesive development strategies were based on the use of biomolecules with high water absorption capacity and covalent bonding inspired by mussel glue. The results have shown the need to use a polymer with higher cohesion and lower degradation.
- The development of the latest formulations with cellulose derivatives such as hydroxypropyl methylcellulose have shown promising results but with improved adhesion time of the patch to the amnion.
- Formulations with HPMC have shown no cytotoxicity and are therefore perfectly biocompatible.
- *Ex vivo* adhesion tests with HPMC formulations have shown promising sealing properties that prevent amniotic fluid leakage at higher than physiological intrauterine pressures.
- A final prototype introducer or introducer system has been developed, It allows the patch with the adhesive to be implanted in *in vivo* models of pregnant rabbits and sheep. The introducer also allows the surgeon to implant the patch in an efficient, simple, fast and safe way.

Conclusions

- *In vivo* results in pregnant sheep have shown that, after 7 days, the implanted patches were not attached to the amnion but the orifices were sealed. In addition, the fetuses and pregnant sheep were in good health. It is hypothesized that the adhesive penetrates the orifice, blocks the leakage of amniotic fluid, but does not avoid the natural movement of the chorioamniotic membranes.
- The sealing system, consisting of the introducer, the patch with adhesive, and the thread, can be packaged and sterilized with ethylene oxide.
- Microarpoons have been added to the surface of the patch in order to physically anchor it to the amnion while the adhesive rehydrates and acquires its maximum sealing properties.
- Possible advances for future patch modifications have been shown in the form of the integration of a hexagonal patterned mesh to achieve a more homogeneous traction force on the patch.
- A series of characterization and *ex vivo* tests have been created and developed, which would allow a much faster evaluation of any new adhesive formulation to be incorporated into the developed patches.

References

- (1) Mex, G. O. Cirugía Fetal Endoscópica. **2014**, 325–336.
- (2) Winer, N.; Ville, Y.; Deprest, J.; Senat, M.-V.; Paupe, A.; Boulvain, M. Endoscopic Laser Surgery versus Serial Amnioreduction for Severe Twin-to-Twin Transfusion Syndrome. *N. Engl. J. Med.* **2004**, *351* (2), 136–144.
- (3) Deprest, J.; Gratacos, E.; Nicolaidis, K. H. Fetoscopic Tracheal Occlusion (FETO) for Severe Congenital Diaphragmatic Hernia: Evolution of a Technique and Preliminary Results. *Ultrasound Obstet. Gynecol.* **2004**, *24* (2), 121–126.
- (4) Copeland, Michael L.; Bruner, Joseph P.; Richards, William O.; Sundell, Hakan W.; Tulipan, N. B. A Model for In Utero Endoscopic Treatment of Myelomeningocele. *Neurosurgery* **1993**, *33* (3), 542–545.
- (5) Bruner, J.P.; Tulipan N.E.; Richards, W. O. Endoscopic Coverage of Fetal Open Myelomeningocele in Utero. *Am. J. Obstet. Gynecol.* **1999**, *180* (1 I), 153–158.
- (6) Devlieger, R.; Gratacós, E.; Wu, J.; Verbist, L.; Pijnenborg, R.; Deprest, J. A. M. An Organ-Culture for in Vitro Evaluation of Fetal Membrane Healing Capacity. *Eur. J. Obstet. Gynecol. Reprod. Biol.* **2000**, *92* (1), 145–150.
- (7) Gratacós, E.; Sanin-Blair, J.; Lewi, L.; Toran, N.; Verbist, G.; Cabero, G.; Deprest, J. A Histological Study of Fetoscopic Membrane Defects to Document Membrane Healing. *Placenta* **2006**, *27* (4–5), 452–456.
- (8) Tabor, A.; Mette, M.; Obel, E. B.; Philip, J.; Jens, B.; Norgaard-Pedersen, B. Randomised Controlled Trial of Genetic Amniocentesis in 4606 Low-Risk Women. *Lancet* **1986**, No. 7569, 1287–1293.
- (9) Reece, E. A. Early and Midtrimester Genetic Amniocentesis. *Obstet. Gynecol. clinics north Am.* **1997**, *24* (1), 71–81.
- (10) Ville, Y.; Hecher, K.; Gagnon, A.; Sebire, N.; Hyett, J.; Nicolaidis, K. Endoscopic Laser Coagulation in the Management of Severe Twin-to-Twin Transfusion Syndrome. *British J. Obstet. Gynaecol.* **1998**, *105* (4), 446–453.
- (11) Deprest, J. A.; Van Ballaer, Paul Evrard, Veerle, A.; Peers, K.; Spitz, B.; Steegers, E. A.; Vandenberghe, K. Experience with Fetoscopic Cord Ligation. *Eur. J. Obstet. Gynecol. Reprod. Biol.* **1998**, *81* (2), 157–164.
- (12) Harrison MR, GB Mychaliska, CT Albanese, RW Jennings, JA Farrell, S Hawgood, P Sandberg, AH Levine, E Lobo, R. F. Correction of Congenital Diaphragmatic Hernia in Utero IX: Fetuses with Poor Prognosis (Liver Herniation and Low Lung-to-Head Ratio) Can Be Saved by Fetoscopic Temporary Tracheal Occlusion. *J. Pediatr. Surg.*

- 1998, 33, 1017–1023.
- (13) Papadopoulos, Nikolaos A. Van Ballaer, P. P.; Ordoñez, J. L.; Laermans, I. J.; Vandenberghe, K.; Lerut, T. E.; Deprest, J. A. Fetal Membrane Closure Techniques after Hysteroamniotomy in the Midgestational Rabbit Model. *Am. J. Obstet. Gynecol.* **1998**, 178 (5), 938–942.
- (14) Deprest, J. A.; Papadopoulos, N. A.; Lerut, T. E.; Gratacós, E.; Yamamoto, H.; Decaluwé, H. Closure Techniques for Fetoscopic Access Sites in the Rabbit at Mid-Gestation. *Hum. Reprod.* **1999**, 14 (7), 1730–1734.
- (15) Quintero, R.; Morales, W. J.; Allen, M.; Bornick, W.; Arroyo, J.; LeParc, G. Treatment of Iatrogenic Previa Premature Rupture of Membranes with Int Cryoprecipitate (Amniopatch): Preliminary Experience. *Am J Obs. Gynecol* **1999**, 181 (September), 744–749.
- (16) Luks, F. I.; Deprest, J. A.; Peers, K. H. E.; Steegers, E. A. P.; van der Wildt, B. Gelatin Sponge Plug to Seal Fetoscopy Port Sites: Technique in Ovine and Primate Models. *Am. J. Obstet. Gynecol.* **1999**, 181 (4), 995–996.
- (17) Gratacós, E.; Wu, J.; Yesildaglar, N.; Devlieger, R.; Pijnenborg, R.; Deprest, J. a. Successful Sealing of Fetoscopic Access Sites with Collagen Plugs in the Rabbit Model. *Am. J. Obstet. Gynecol.* **2000**, 182 (1 Pt 1), 142–146.
- (18) Devlieger, R.; Ardon, H.; Verbist, L.; Gratacós, E.; Pijnenborg, R.; Deprest, J. A. Increased Polymorphonuclear Infiltration and Iatrogenic Amniotic Band after Closure of Fetoscopic Access Sites with a Bioactive Membrane in the Rabbit at Midgestation. *Am. J. Obstet. Gynecol.* **2003**, 188 (3), 844–848.
- (19) Ochsenein-Kölbl, N.; Bilic, G.; Hall, H.; Huch, R.; Zimmermann, R. Inducing Proliferation of Human Amnion Epithelial and Mesenchymal Cells for Prospective Engineering of Membrane Repair. *J. Perinat. Med.* **2003**, 31 (4), 287–294.
- (20) Papadopoulos, N. A.; Klotz, S.; Raith, A.; Foehn, M.; Schillinger, U.; Henke, J.; Kovacs, L.; Horch, R. E.; Biemer, E. Amnion Cells Engineering: A New Perspective in Fetal Membrane Healing after Intrauterine Surgery? *Fetal Diagn. Ther.* **2006**, 21 (6), 494–500.
- (21) Mallik, A. S.; Fichter, M. A.; Rieder, S.; Bilic, G.; Stergioula, S.; Biemer, E.; Kurmanavicius, J.; Henke, J.; Zimmermann, R.; Schneider, K.-T. M.; et al. Fetoscopic Closure of Punctured Fetal Membranes With Acellular Human Amnion Plugs in a Rabbit Model. *Obstet. Gynecol.* **2007**, 110 (5), 1121–1129.
- (22) Ochsenein-Kölbl, N.; Jani, J.; Lewi, L.; Verbist, G.; Vercruyssen, L.; Portmann-Lanz, B.; Marquardt, K.; Zimmermann, R.; Deprest, J. Enhancing Sealing of Fetal Membrane

- Defects Using Tissue Engineered Native Amniotic Scaffolds in the Rabbit Model. *Am. J. Obstet. Gynecol.* **2007**, *196* (3), 263.e1-263.e7.
- (23) Bilic, G.; Brubaker, C.; Messersmith, P. B.; Mallik, A. S.; Quinn, T. M.; Haller, C.; Done, E.; Gucciardo, L.; Zeisberger, S. M.; Zimmermann, R.; et al. Injectable Candidate Sealants for Fetal Membrane Repair: Bonding and Toxicity in Vitro. *Am. J. Obstet. Gynecol.* **2010**, *202* (1), 85.e1-85.e9.
- (24) Haller, C.; Buerzle, W.; Brubaker, C.; Messersmith, P.; Mazza, E.; Ochsenbein-Koelble, N.; Zimmermann, R.; Ehrbar, M. Mussel-Mimetic Tissue Adhesive for Fetal Membrane Repair: A Standardized Ex Vivo Evaluation Using Elastomeric Membranes. *Prenat. Diagn.* **2011**, *31* (10), 645–660.
- (25) Haller, C. M.; Buerzle, W.; Kivelio, A.; Perrini, M.; Brubaker, C. E.; Gubeli, R. J.; Mallik, A. S.; Weber, W.; Messersmith, P. B.; Mazza, E.; et al. Mussel-Mimetic Tissue Adhesive for Fetal Membrane Repair: An Ex Vivo Evaluation. *Acta Biomater.* **2012**, *8* (12), 4365–4370.
- (26) Perrini, M.; Barrett, D.; Ochsenbein-Koelble, N.; Zimmermann, R.; Messersmith, P.; Ehrbar, M. A Comparative Investigation of Mussel-Mimetic Sealants for Fetal Membrane Repair. *J. Mech. Behav. Biomed. Mater.* **2016**, *58*, 57–64.
- (27) Pensabene, V.; Patel, P. P.; Williams, P.; Cooper, T. L.; Kirkbride, K. C.; Giorgio, T. D.; Tulipan, N. B. Repairing Fetal Membranes with a Self-Adhesive Ultrathin Polymeric Film: Evaluation in Mid-Gestational Rabbit Model. *Ann. Biomed. Eng.* **2015**, *43* (8), 1978–1988.
- (28) Devaud, Y. R.; Züger, S.; Zimmermann, R.; Ehrbar, M.; Ochsenbein-Kölble, N. Minimally Invasive Surgical Device for Precise Application of Bioadhesives to Prevent IPPROM. *Fetal Diagn. Ther.* **2018**, 1–9.
- (29) Murphy, C. M.; O'Brien, F. J.; Little, D. G.; Schindeler, A. Cell-Scaffold Interactions in the Bone Tissue Engineering Triad. *Eur. Cells Mater.* **2013**, *26*, 120–132.
- (30) Parry, S.; Strauss III, J. Premature Rupture of the Fetal Membranes. *N. Engl. J. Med.* **1998**, *338*, 663–670.
- (31) Jabareen, M.; Sankar, A.; Bilic, G.; Hugo, A.; Mazza, E. Relation between Mechanical Properties and Microstructure of Human Fetal Membranes : An Attempt towards a Quantitative Analysis. *Eur. J. Obstet. Gynecol. Reprod. Biol.* **2009**, 134–141.
- (32) Harirah, HM. Borahay, MA. Zaman, W. Ahmed, M. H. G. Increased Apoptosis in Chorionic Trophoblasts of Human Fetal Membranes with Labor at Term. *Int. J. Clin. Med.* **2012**, *3*, 136–142.
- (33) Subramaniam, A.; Sethuraman, S. Biomedical Applications of Nondegradable

- Polymers. *Nat. Synth. Biomed. Polym.* **2014**, 301–308.
- (34) Shastri, V. Non-Degradable Biocompatible Polymers in Medicine: Past, Present and Future. *Curr. Pharm. Biotechnol.* **2003**, 4 (5), 331–337.
- (35) Willerth, S. *Synthetic Biomaterials for Engineering Neural Tissue from Stem Cells*; 2017.
- (36) Fujii, T. PDMS-Based Microfluidic Devices for Biomedical Applications. *Microelectron. Eng.* **2002**, 61–62, 907–914.
- (37) Bhagat, A. A. S.; Jothimuthu, P.; Papautsky, I. Photodefinable Polydimethylsiloxane (PDMS) for Rapid Lab-on-a-Chip Prototyping. *Lab Chip* **2007**, 7 (9), 1192–1197.
- (38) Sosa-Hernández, J. E.; Villalba-Rodríguez, A. M.; Romero-Castillo, K. D.; Aguilar-Aguila-Isaías, M. A.; García-Reyes, I. E.; Hernández-Antonio, A.; Ahmed, I.; Sharma, A.; Parra-Saldivar, R.; Iqbal, H. M. N. Organs-on-a-Chip Module: A Review from the Development and Applications Perspective. *Micromachines* **2018**, 9 (10), 536.
- (39) Wu, M. H. Simple Poly(Dimethylsiloxane) Surface Modification to Control Cell Adhesion. *Surf. Interface Anal.* **2009**, 41 (1), 11–16.
- (40) Daebritz, S. H.; Fausten, B.; Hermanns, B.; Schroeder, J.; Groetzner, J.; Autschbach, R.; Messmer, B. J.; Sachweh, J. S. Introduction of a Flexible Polymeric Heart Valve Prosthesis with Special Design for Aortic Position. *Eur. J. Cardio-thoracic Surg.* **2004**, 25 (6), 946–952.
- (41) Handel, N.; Gutierrez, J. Long-Term Safety and Efficacy of Polyurethane Foam-Covered Breast Implants. *Aesthetic Surg. J.* **2006**, 26 (3), 265–274.
- (42) Davis, F. J.; Mitchell, G. R. Polyurethane Based Materials with Applications in Medical Devices. *Bio-Materials Prototyp. Appl. Med.* **2008**, 27–48.
- (43) Ratner, B.; Hoffman, A.; FJ, S.; Lemons, J. *Biomaterials Science. An Introduction to Materials in Medicine*, 3rd ed.; Elsevier Inc.: Kidlington, Oxford. UK, 2013.
- (44) Akduman, C.; Kumbasar, E. P. A. Electrospun Polyurethane Nanofibers. *Asp. Polyurethanes* **2017**.
- (45) Bellan, L. M.; Craighead, H. G. Applications of Controlled Electrospinning Systems. *Polym. Adv. Technol.* **2011**, 22 (3), 304–309.
- (46) Honarasa, H. E. A. and G. Fabrication of Polyurethane and Thermoplastic Polyurethane Nanofiber by Controlling the Electrospinning Parameters. *Mater. Res. Express* **2017**, 0–17.
- (47) Corey, J. M.; Gertz, C. C.; Wang, B. S.; Birrell, L. K.; Johnson, S. L.; Martin, D. C.; Feldman, E. L. The Design of Electrospun PLLA Nanofiber Scaffolds Compatible with Serum-Free Growth of Primary Motor and Sensory Neurons. *Acta Biomater.* **2008**, 4

- (4), 863–875.
- (48) Yoshimoto, H.; Shin, Y. M.; Terai, H.; Vacanti, J. P. A Biodegradable Nanofiber Scaffold by Electrospinning and Its Potential for Bone Tissue Engineering. *Biomaterials* **2003**, *24* (12), 2077–2082.
- (49) Sun, T.; Mai, S.; Norton, D.; Haycock, J. W.; Ryan, A. J.; MacNeil, S. Self-Organization of Skin Cells in Three-Dimensional Electrospun Polystyrene Scaffolds. *Tissue Eng.* **2005**, *11* (7–8), 1023–1033.
- (50) Matthews JA, Wnek GE, Simpson DG, B. G. Electrospinning of Collagen Nanofibers. **2002**, *1* (August), 232–238.
- (51) Law, J. X.; Liao, L. L.; Saim, A.; Yang, Y.; Idrus, R. Electrospun Collagen Nanofibers and Their Applications in Skin Tissue Engineering. *Tissue Eng. Regen. Med.* **2017**, *14* (6), 699–718.
- (52) Hall Barrientos, I. J.; Paladino, E.; Szabó, P.; Brozio, S.; Hall, P. J.; Oseghale, C. I.; Passarelli, M. K.; Moug, S. J.; Black, R. A.; Wilson, C. G.; et al. Electrospun Collagen-Based Nanofibres: A Sustainable Material for Improved Antibiotic Utilisation in Tissue Engineering Applications. *Int. J. Pharm.* **2017**, *531* (1), 67–79.
- (53) Wnek, G. E.; Carr, M. E.; Simpson, D. G.; Bowlin, G. L. Electrospinning of Nanofiber Fibrinogen Structures. *Nano Lett.* **2003**, *3* (2), 213–216.
- (54) Min, B. M.; Lee, G.; Kim, S. H.; Nam, Y. S.; Lee, T. S.; Park, W. H. Electrospinning of Silk Fibroin Nanofibers and Its Effect on the Adhesion and Spreading of Normal Human Keratinocytes and Fibroblasts in Vitro. *Biomaterials* **2004**, *25* (7–8), 1289–1297.
- (55) Sedghi, R.; Shaabani, A.; Mohammadi, Z.; Samadi, F. Y.; Isaei, E. Biocompatible Electrospinning Chitosan Nanofibers: A Novel Delivery System with Superior Local Cancer Therapy. *Carbohydr. Polym.* **2017**, *159*, 1–10.
- (56) Brenner, E. K.; Schiffman, J. D.; Thompson, E. A.; Toth, L. J.; Schauer, C. L. Electrospinning of Hyaluronic Acid Nanofibers from Aqueous Ammonium Solutions. *Carbohydr. Polym.* **2012**, *87* (1), 926–929.
- (57) Bhardwaj, N.; Kundu, S. C. Electrospinning: A Fascinating Fiber Fabrication Technique. *Biotechnol. Adv.* **2010**, *28* (3), 325–347.
- (58) Li, D.; Wang, Y.; Xia, Y. Electrospinning of Polymeric and Ceramic Nanofibers as Uniaxially Aligned Arrays. *Nano Lett.* **2003**, *3* (8), 1167–1171.
- (59) Coles, S. R.; Jacobs, D. K.; Meredith, J. O.; Barker, G.; Clark, A. J.; Kirwan, K.; Stanger, J.; Tucker, N. A Design of Experiments (DoE) Approach to Material Properties Optimization of Electrospun Nanofibers. *J. Appl. Polym. Sci.* **2010**, *117*,

- 2251–2257.
- (60) Chu, P. K.; Chen, J. Y.; Wang, L. P.; Huang, N. Plasma-Surface Modification of Biomaterials. **2002**, *36*, 143–206.
- (61) Wasy, A.; Balakrishnan, G.; Lee, S. H.; Kim, J. K.; Kim, D. G.; Kim, T. G.; Song, J. I. Argon Plasma Treatment on Metal Substrates and Effects on Diamond-like Carbon (DLC) Coating Properties. *Cryst. Res. Technol.* **2014**, *49* (1), 55–62.
- (62) Galvin, E.; Morshed, M. M.; Cummins, C.; Daniels, S.; Lally, C.; MacDonald, B. Surface Modification of Absorbable Magnesium Stents by Reactive Ion Etching. *Plasma Chem. Plasma Process.* **2013**, *33* (6), 1137–1152.
- (63) Pablo, C.; Gustavo, A. *Biomateriales Aplicados Al Diseño de Sistemas Terapéuticos Avanzados*; Sousa HC, Braga MEM, S. A., Ed.; Coimbra, 2015.
- (64) Khan, I.; Smith, N.; Jones, E.; Finch, D. S.; Elizabeth, R. Analysis and Evaluation of a Biomedical Polycarbonate Urethane Tested in an in Vitro Study and an Ovine Arthroplasty Model . Part I : Materials Selection and Evaluation. **2005**, *26*, 621–631.
- (65) Jacobs, E.; Roth, A. K.; Arts, J. J.; Rhijn, L. W. Van; Willems, P. C.; Roth, A. K. Reduction of Intradiscal Pressure by the Use of Polycarbonate- Urethane Rods as Compared to Titanium Rods in Posterior Thoracolumbar Spinal Fixation. *J. Mater. Sci. Mater. Med.* **2017**, 1–8.
- (66) Cooper, S. L.; Guan, J. *Advances in Polyurethane Biomaterials*; Cooper, S. L., Guan, J., Eds.; Elsevier Ltd: Cambridge, 2016.
- (67) Karaka, H.; Saraç, A. S.; Polat, T.; Budak, E. G.; Bayram, S.; Da, N.; Jahangiri, S. Polyurethane Nanofibers Obtained By Electrospinning Process. **2013**, *7* (3), 177–180.
- (68) Fong, H.; Chun, I.; Reneker, D. H. Beaded Nanofibers Formed during Electrospinning. *Polymer (Guildf).* **1999**, *40*, 4585–4592.
- (69) Shawon, J.; Sung, C. Electrospinning of Polycarbonate Nanofibers with Solvent Mixtures THF and DMF. **2004**, *9*, 4605–4613.
- (70) FDA. Product classification. <https://www.accessdata.fda.gov/scripts/cdrh/cfdocs/cfPCD/classification.cfm?ID=NWV> (accessed Jun 21, 2020).
- (71) Sastri, V. R. *Plastics in Medical Devices*; Ebnesajjad, S., Ed.; Matthew Deans: Chadds Ford, PA, USA, 2010.
- (72) Madrid, M. Tecnología de La Adhesión. **1990**, 59.
- (73) Vallejo Díaz, B. M.; Perilla, J. E. Elementos Conceptuales Para Estudiar El Comportamiento Bioadhesivo En Polímeros. *Rev. Colomb. Cienc. Quim. Farm.* **2008**, *37* (1), 33–61.

References

- (74) Khanlari, S.; Dubé, M. A. Bioadhesives: A Review. *Macromol. React. Eng.* **2013**, *7* (11), 573–587.
- (75) Misra, R. D. K. *Biomaterials and Bio-Medical Engineering*; 2010; Vol. 25.
- (76) Zhu, W.; Chuah, Y. J.; Wang, D. A. Bioadhesives for Internal Medical Applications: A Review. *Acta Biomater.* **2018**, *74* (April), 1–16.
- (77) Spotnitz, W. D.; Burks, S. Hemostats, Sealants, and Adhesives III: A New Update as Well as Cost and Regulatory Considerations for Components of the Surgical Toolbox. *Transfusion* **2012**, *52* (10), 2243–2255.
- (78) Meyers, M. A.; Chen, P.-Y. *Biological Materials Science. Biological Materials, Bioinspired Materials, and Biomaterials.*; 2014.
- (79) Wheat, J. C.; Wolf, J. S. Advances in Bioadhesives , Tissue Sealants, and Hemostatic Agents. *Urol. Clin. NA* **2009**, *36* (2), 265–275.
- (80) Pursifull, NF. Allen, F. Tissue Glues and Nonsuturing Techniques. *Curr Opin Urol* **2007**, *17*, 396–401.
- (81) Dural, D.; System, S. Integra®. DuraSeal® Dural Sealant System [Package Insert].
- (82) Esposito, C.; Damiano, R.; Settimi, A.; Marco, M. De; Maglio, P.; Centonze, A. Experience with the Use of Tissue Adhesives in Pediatric Endoscopic Surgery. *Surg. Endosc.* **2004**, *18*, 290–292.
- (83) Donkerwolcke, M.; Burny, F.; Muster, D. Tissues and Bone Adhesives Historical Aspects. *Biomaterials* **1998**, *19* (16), 1461–1466.
- (84) Marshall, S. J.; Bayne, S. C.; Baier, R.; Tomsia, A. P.; Marshall, G. W. A Review of Adhesion Science. *Dent. Mater.* **2010**, *26* (2), 11–16.
- (85) Liu, X.; Zhang, Q.; Gao, G. Bioinspired Adhesive Hydrogels Tackified by Nucleobases. *Adv. Funct. Mater.* **2017**, *27* (44), 2–7.
- (86) Wang, Z.; Tai, L. R.; McLean, D.; Wright, E. J.; Florence, G. J.; Brown, S. I.; Andre, P.; Cuschieri, A. Mucoadhesive Polymer Films for Tissue Retraction in Laparoscopic Surgery: Ex-Vivo Study on Their Mechanical Properties. *Biomed. Mater. Eng.* **2014**, *24* (1), 445–451.
- (87) Le Thi, P.; Lee, Y.; Nguyen, D. H.; Park, K. D. In Situ Forming Gelatin Hydrogels by Dual-Enzymatic Cross-Linking for Enhanced Tissue Adhesiveness. *J. Mater. Chem. B* **2017**, *5* (4), 757–764.
- (88) Kretlow, J. D.; Klouda, L.; Mikos, A. G. Injectable Matrices and Scaffolds for Drug Delivery in Tissue Engineering. *Adv. Drug Deliv. Rev.* **2007**, *59* (4–5), 263–273.
- (89) Spotnitz, W. D. Tissue Adhesives: Science, Products, and Clinical Use. In *Musculoskeletal Tissue Regeneration*; 2008; pp 531–546.

References

- (90) Meraney, A. M.; Gill, I. S. Financial Analysis of Open versus Laparoscopic Radical Nephrectomy and Nephroureterectomy. *J. Urol.* **2002**, *167* (4 I), 1757–1762.
- (91) Assmann, A.; Vegh, A.; Ghasemi-rad, M.; Bagherifard, S.; Cheng, G.; Sani, E. S.; Ruiz-esparza, G. U.; Noshadi, I.; Lassaletta, A.; Gangadharan, S.; et al. A Highly Adhesive and Naturally Derived Sealant. *Biomaterials* **2017**.
- (92) Ryu, J. H.; Hong, S.; Lee, H. Bio-Inspired Adhesive Catechol-Conjugated Chitosan for Biomedical Applications: A Mini Review. *Acta Biomater.* **2015**, *27*, 101–115.
- (93) Bruschi, M. L.; Borghi-Pangoni, F. B.; Junqueira, M. V.; de Souza Ferreira, S. B. *Nanostructured Therapeutic Systems with Bioadhesive and Thermoresponsive Properties*; Elsevier Inc., 2017.
- (94) Yuan, L.; Wu, Y.; Fang, J.; Wei, X.; Gu, Q.; El-hamshary, H.; Al-deyab, S. S.; Morsi, Y.; Mo, X. Modified Alginate and Gelatin Cross-Linked Hydrogels for Soft Tissue Adhesive. *Artif. cells, Nanomedicine, Biotechnol.* **2017**, *45*, 76–83.
- (95) Taguchi, T.; Saito, H.; Uchida, Y.; Sakane, M. Bonding of Soft Tissues Using a Novel Tissue Adhesive Consisting of a Citric Acid Derivative and Collagen. **2004**, *24*, 775–780.
- (96) Fan, C.; Fu, J.; Zhu, W.; Wang, D. A Mussel-Inspired Double-Crosslinked Tissue Adhesive Intended for Internal Medical Use. *Acta Biomater.* **2016**, *33*, 51–63.
- (97) Shazly, T. M.; Baker, A. B.; Naber, J. R.; Bon, A.; Van Vliet, K. J.; Edelman, E. R. Augmentation of Postswelling Surgical Sealant Potential of Adhesive Hydrogels. *J. Biomed. Mater. Res. Part A* **2010**, *95A* (4), 1159–1169.
- (98) Cohen, B.; Pinkas, O.; Fook, M.; Zilberman, M. Gelatin – Alginate Novel Tissue Adhesives and Their Formulation – Strength Effects. *Acta Biomater.* **2013**, *9* (11), 9004–9011.
- (99) Wang, T.; Nie, J.; Yang, D. Dextran and Gelatin Based Photocrosslinkable Tissue Adhesive. *Carbohydr. Polym.* **2012**, *90* (4), 1428–1436.
- (100) Lih, E.; Lee, J. S.; Park, K. M.; Park, K. D. Rapidly Curable Chitosan – PEG Hydrogels as Tissue Adhesives for Hemostasis and Wound Healing. *Acta Biomater.* **2012**, *8* (9), 3261–3269.
- (101) Strehin, I.; Nahas, Z.; Arora, K.; Nguyen, T.; Elisseeff, J. A Versatile PH Sensitive Chondroitin Sulfate – PEG Tissue Adhesive and Hydrogel. *Biomaterials* **2010**, *31* (10), 2788–2797.
- (102) Ju, Y.; Sung, H.; Bok, G.; Hye, J.; Choi, S.; Lee, G.; Park, H. Enhanced Biocompatibility and Wound Healing Properties of Biodegradable Polymer-Modified Allyl 2-Cyanoacrylate Tissue Adhesive. *Mater. Sci. Eng. C* **2015**, *51*, 43–50.

References

- (103) Ryu, J. H.; Lee, Y.; Kong, W. H.; Kim, T. G.; Park, T. G.; Lee, H. Catechol-Functionalized Chitosan/Pluronic Hydrogels for Tissue Adhesives and Hemostatic Materials. **2011**, 2653–2659.
- (104) Cencer, M.; Liu, Y.; Winter, A.; Murley, M.; Meng, H.; Lee, B. P. Effect of PH on the Rate of Curing and Bioadhesive Properties of Dopamine Functionalized Poly(Ethylene Glycol) Hydrogels. *Biomacromolecules* **2014**, *11* (15), 2861–2869.
- (105) Brubaker, C. E.; Kissler, H.; Wang, L.; Kaufman, D. B.; Messersmith, P. B. Biological Performance of Mussel-Inspired Adhesive in Extrahepatic Islet Transplantation. *Biomaterials* **2010**, *31* (3), 420–427.
- (106) Mehdizadeh, M.; Weng, H.; Gyawali, D.; Tang, L.; Yang, J. Injectable Citrate-Based Mussel-Inspired Tissue Bioadhesives with High Wet Strength for Sutureless Wound Closure. *Biomaterials* **2012**, *33* (32), 7972–7983.
- (107) Shin, J.; Lee, J. S.; Lee, C.; Park, H.; Yang, K.; Jin, Y.; Ryu, J. H.; Hong, K. S.; Moon, S.; Chung, H.; et al. Tissue Adhesive Catechol-Modified Hyaluronic Acid Hydrogel for Effective, Minimally Invasive Cell Therapy. **2015**, 3814–3824.
- (108) Wang W, Xu Y, li A, Liu M, Klitzing R, Ober CK, Kayitmazer AB, Li L, G. X. Zinc Induced Polyelectrolyte Coacervate Bioadhesive and Its Transition to Self-Healing Hydrogel. *RSC Adv.* **2015**, *5*, 66871–66878.
- (109) Westwood, G.; Horton, T. N.; Wilker, J. J.; V, P. U.; Dri, O. V. V; Lafayette, W.; February, R. V; Re, V.; Recei, M.; March, V. Simplified Polymer Mimics of Cross-Linking Adhesive Proteins. **2007**, 3960–3964.
- (110) Xue, J.; Wang, T.; Nie, J.; Yang, D. Preparation and Characterization of a Bioadhesive with Poly (Vinyl Alcohol) Crosslinking Agent. *J. Appl. Polym. Sci.* **2013**, *127* (6), 5051–5058.
- (111) Gleason, K. K. *CVD Polymers. Fabrication of Organic Surfaces and Devices*; Gleason, K. K., Ed.; Wiley-VCH, 2015.
- (112) Vohrer, U. *Interfacial Engineering of Functional Textiles for Biomedical Applications*; Woodhead Publishing Limited, 2007.
- (113) Li, P. H.; Chu, P. K. Thin Film Deposition Technologies and Processing of Biomaterials. In *Thin Film Coatings for Biomaterials and Biomedical Applications*; 2016; pp 3–28.
- (114) Sreenivasan, B. R.; Gleason, K. K. Overview of Strategies for the CVD of Organic Films and Functional Polymer Layers **. **2009**, 77–90.
- (115) Baxamusa, S. H.; Im, S. G.; Gleason, K. K. Initiated and Oxidative Chemical Vapor Deposition: A Scalable Method for Conformal and Functional Polymer Films on Real

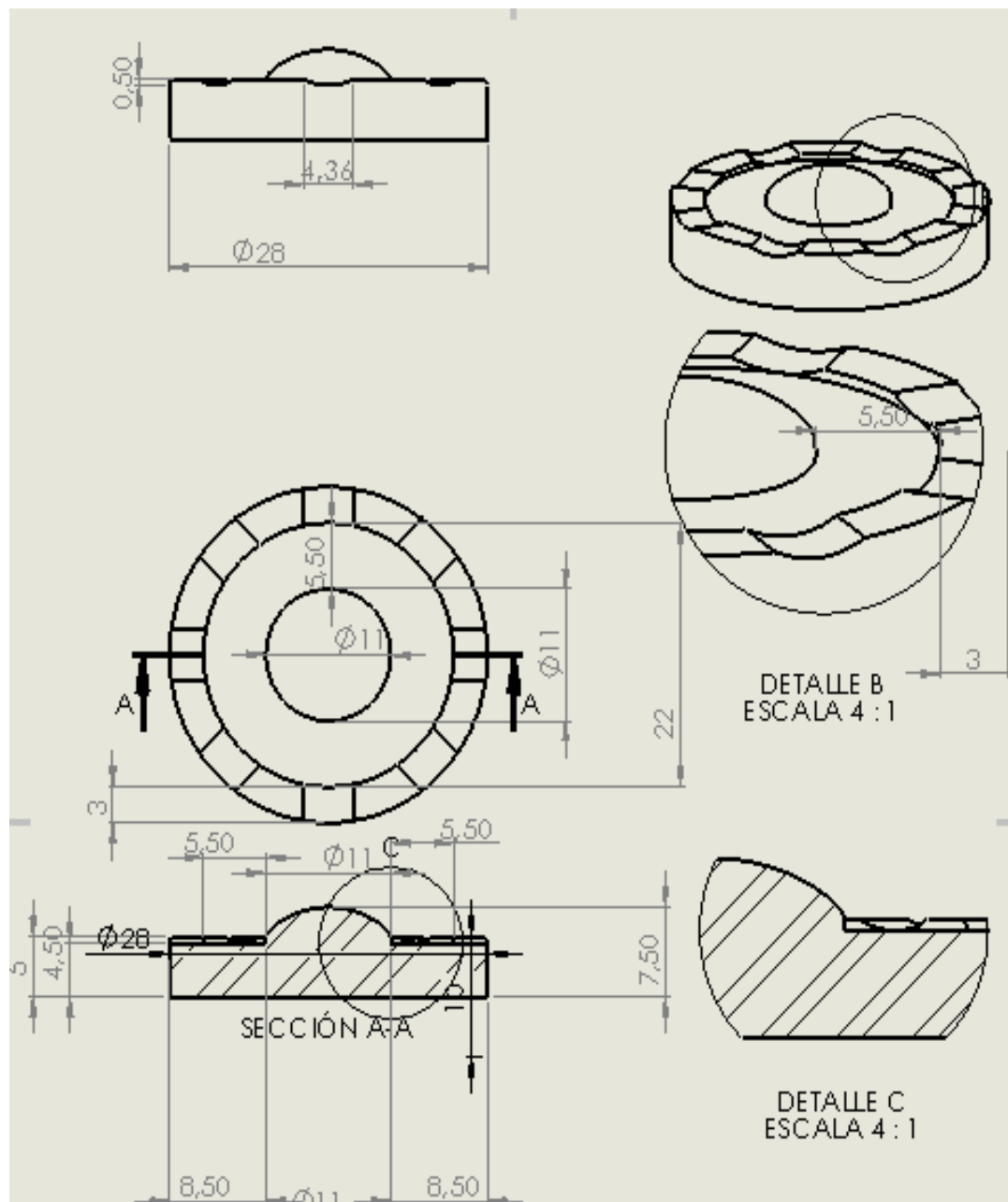
- Substrates. *Phys. Chem. Chem. Phys.* **2009**, *11* (26), 5227–5240.
- (116) Gleason Group <http://web.mit.edu/gleason-lab/iCVD.html> (accessed Apr 6, 2021).
- (117) Choy, K. L. Chemical Vapour Deposition of Coatings. *Prog. Mater. Sci.* **2003**, *48*, 57–170.
- (118) H, Y. *Luminous Chemical Vapor Deposition and Interface Engineering*; Dekker, M., Ed.; New York, 2005.
- (119) Hamedani, Y.; Macha, P.; Bunning, T. J.; Naik, R. R.; Vasudev, M. C. Plasma-Enhanced Chemical Vapor Deposition: Where We Are and the Outlook for the Future. *Chem. Vap. Depos. - Recent Adv. Appl. Opt. Sol. Cells Solid State Devices* **2016**.
- (120) Dion, C. A. D.; Tavares, J. R. Photo-Initiated Chemical Vapor Deposition as a Scalable Particle Functionalization Technology (a Practical Review). *Powder Technol.* **2013**, *239*, 484–491.
- (121) Vasudev, M. C.; Anderson, K. D.; Bunning, T. J.; Tsukruk, V. V.; Naik, R. R. Exploration of Plasma-Enhanced Chemical Vapor Deposition as a Method for Thin-Film Fabrication with Biological Applications. *ACS Appl. Mater. Interfaces* **2013**, *5* (10), 3983–3994.
- (122) Xu, J.; Gleason, K. K. Conformal, Amine-Functionalized Thin Films by Initiated Chemical Vapor Deposition (ICVD) for Hydrolytically Stable Microfluidic Devices. *Chem. Mater.* **2010**, *22* (3), 1732–1738.
- (123) Im, S. G.; Bong, K. W.; Lee, C.-H.; Doyle, P. S.; Gleason, K. K. A Conformal Nano-Adhesive via Initiated Chemical Vapor Deposition for Microfluidic Devices. *Lab Chip* **2009**, *9* (3), 411–416.
- (124) Friedrich, J. Mechanisms of Plasma Polymerization - Reviewed from a Chemical Point of View. *Plasma Process. Polym.* **2011**, *8* (9), 783–802.
- (125) Cross, V. L.; Zheng, Y.; Choi, N. W.; Verbridge, S. S.; Bryan, A.; Bonassar, L. J.; Fischbach, C.; Stroock, A. D. Dense Type I Collagen Matrices That Support Cellular Remodeling and Microfabrication for Studies of Tumor Angiogenesis and Vasculogenesis in Vitro Valerie. **2011**, *31* (33), 8596–8607.
- (126) De Geyter, N.; Morent, R. *Cold Plasma Surface Modification of Biodegradable Polymer Biomaterials*; Woodhead Publishing Limited, 2014.
- (127) Förch, R.; Zhang, Z.; Knoll, W. Soft Plasma Treated Surfaces: Tailoring of Structure and Properties for Biomaterial Applications. *Plasma Process. Polym.* **2005**, *2* (5), 351–372.
- (128) Thejass, P.; Kuttan, G. Allyl Isothiocyanate (AITC) and Phenyl Isothiocyanate (PITC) Inhibit Tumour-Specific Angiogenesis by Downregulating Nitric Oxide (NO) and

- Tumour Necrosis Factor- α (TNF- α) Production. *Nitric Oxide - Biol. Chem.* **2007**, *16* (2), 247–257.
- (129) Cifuentes, A.; Borrós, S. Comparison of Two Different Plasma Surface-Modification Techniques for the Covalent Immobilization of Protein Monolayers. *Langmuir* **2013**, *29* (22), 6645–6651.
- (130) Marí-Buyé, N.; O'Shaughnessy, S.; Colominas, C.; Semino, C. E.; Gleason, K. K.; Borrós, S. Functionalized, Swellable Hydrogel Layers as a Platform for Cell Studies. *Adv. Funct. Mater.* **2009**, *19* (8), 1276–1286.
- (131) Kaushik, N. K.; Kaushik, N.; Pardeshi, S.; Sharma, J. G.; Lee, S. H.; Choi, E. H. Biomedical and Clinical Importance of Mussel-Inspired Polymers and Materials. *Mar. Drugs* **2015**, *13* (11), 6792–6817.
- (132) Stewart, R. J.; Ransom, T. C.; Hlady, V. Natural Underwater Adhesives. **2011**, *49* (11), 757–771.
- (133) Kord Forooshani, P.; Lee, B. P. Recent Approaches in Designing Bioadhesive Materials Inspired by Mussel Adhesive Protein. *J. Polym. Sci. Part A Polym. Chem.* **2017**, *55* (1), 9–33.
- (134) Liu, B.; Burdine, L.; Kodadek, T. Chemistry of Periodate-Mediated Cross-Linking of 3,4-Dihydroxyphenylalanine-Containing Molecules to Proteins. *J. Am. Chem. Soc.* **2006**, *128* (47), 15228–15235.
- (135) Yang, J.; Saggiomo, V.; Velders, A. H.; Stuart, M. A. C.; Kamperman, M. Reaction Pathways in Catechol/Primary Amine Mixtures: A Window on Crosslinking Chemistry. *PLoS One* **2016**, *11* (12), 1–17.
- (136) Lee, B. P.; Dalsin, J. L.; Messersmith, P. B. Synthesis and Gelation of DOPA-Modified Poly(Ethylene Glycol) Hydrogels. *Biomacromolecules* **2002**, *3* (5), 1038–1047.
- (137) Ninan, L.; Stroshine, R. L.; Wilker, J. J.; Shi, R. Adhesive Strength and Curing Rate of Marine Mussel Protein Extracts on Porcine Small Intestinal Submucosa. *Acta Biomater.* **2007**, *3* (5), 687–694.
- (138) Lyngé, M. E.; van der Westen, R.; Postma, A.; Städler, B. PDA39-Polydopamine—a Nature-Inspired Polymer Coating for Biomedical Science. *Nanoscale* **2011**, *3* (12), 4916.
- (139) Dreyer, D. R.; Miller, D. J.; Freeman, B. D.; Paul, D. R.; Bielawski, C. W. Perspectives on Poly(Dopamine). *Chem. Sci.* **2013**, *4* (10), 3796–3802.
- (140) Ahmed, E. M. Hydrogel : Preparation , Characterization , and Applications : A Review. *J. Adv. Res.* **2015**, *6* (2), 105–121.
- (141) Kadajji, V. G.; Betageri, G. V. Water Soluble Polymers for Pharmaceutical

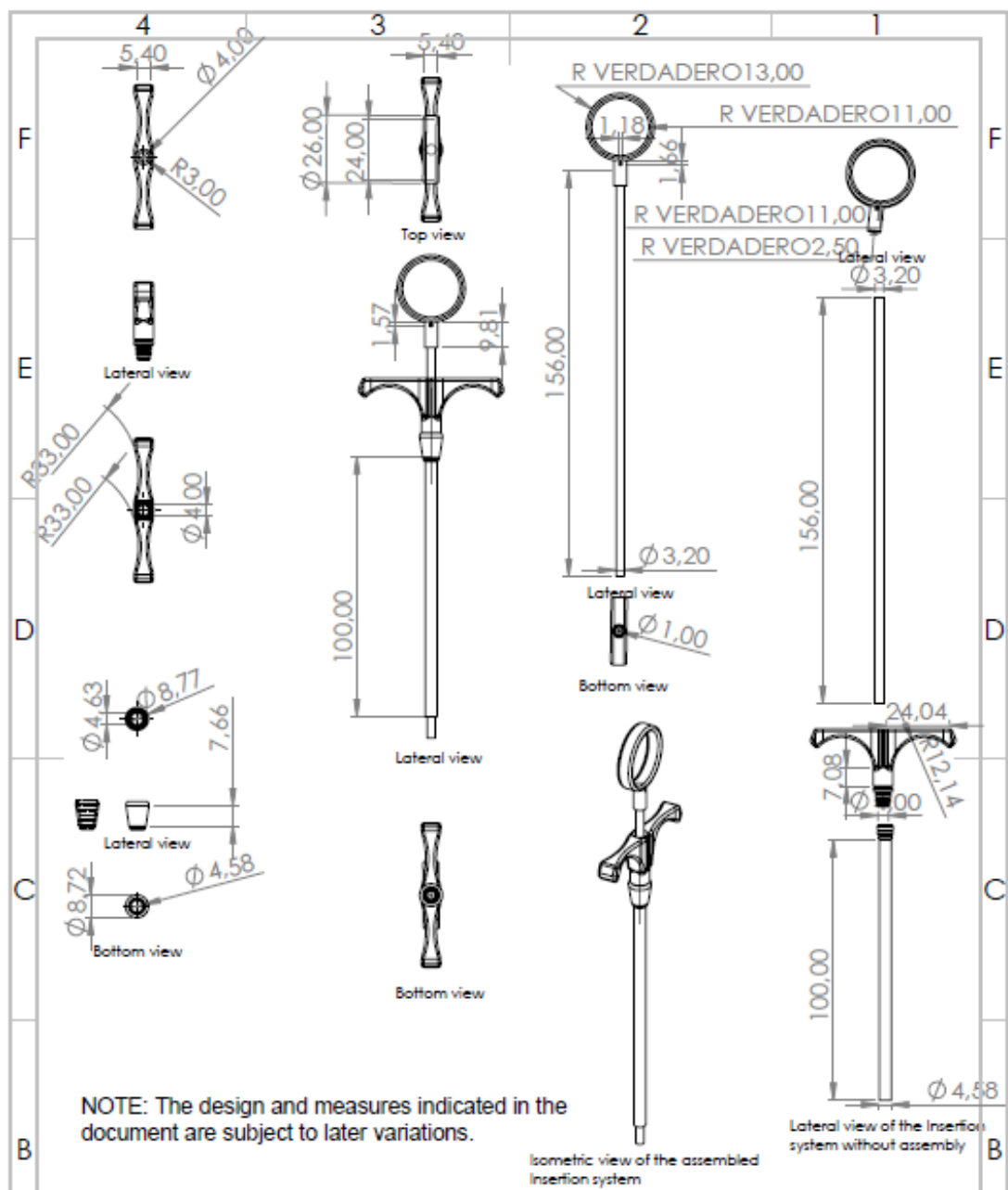
- Applications. *Polymers (Basel)*. **2011**, 3 (4), 1972–2009.
- (142) Song, X.; Li, J. *Functional Hydrogels as Biomaterials*; 2018.
- (143) Sannino, A.; Maffezzoli, A.; Nicolais, L. Introduction of Molecular Spacers between the Crosslinks of a Cellulose-Based Superabsorbent Hydrogel: Effects on the Equilibrium Sorption Properties. *J. Appl. Polym. Sci.* **2003**, 90 (1), 168–174.
- (144) Sannino, A.; Nicolais, L. Concurrent Effect of Microporosity and Chemical Structure on the Equilibrium Sorption Properties of Cellulose-Based Hydrogels. *Polymer (Guildf)*. **2005**, 46 (13), 4676–4685.
- (145) Delivery, C. D. *Science and Principles of Biodegradable and Bioresorbable Medical Polymers*; 2016.
- (146) Liu, Y.; Li, L.; Dong, G.; Yang, Y.; Zheng, C.; Yang, R. Preparation of Cellulose-Based Hydrogels and Their Characteristics for Cell Culture. *Cellul. Chem. Technol.* **2016**, 50, 897–903.
- (147) Kabir, S. M. F.; Sikdar, P. P.; Haque, B.; Bhuiyan, M. A. R.; Ali, A.; Islam, M. N. Cellulose-Based Hydrogel Materials: Chemistry, Properties and Their Prospective Applications. *Prog. Biomater.* **2018**, 7 (3), 153–174.
- (148) Texidó, R.; Orgaz, A.; Ramos-Pérez, V.; Borrós, S. Stretchable Conductive Polypyrrole Films Modified with Dopaminated Hyaluronic Acid. *Mater. Sci. Eng. C* **2017**, 76, 295–300.
- (149) Walters, B. D.; Stegemann, J. P. Strategies for Directing the Structure and Function of Three-Dimensional Collagen Biomaterials across Length Scales. *Acta Biomater.* **2014**, 10 (4), 1488–1501.
- (150) Acocella, M. R.; Corcione, C. E.; Giuri, A.; Maggio, M.; Maffezzoli, A.; Guerra, G. Graphene Oxide as a Catalyst for Ring Opening Reactions in Amine Crosslinking of Epoxy Resins. *RSC Adv.* **2016**, 6 (28), 23858–23865.
- (151) Francesch, L.; Borros, S.; Knoll, W.; Förch, R. Surface Reactivity of Pulsed-Plasma Polymerized Pentafluorophenyl Methacrylate (PFM) toward Amines and Proteins in Solution. *Langmuir* **2007**, 23 (7), 3927–3931.
- (152) Mart, G.; Llin, M. C.; Borr, S. Isothiocyanate-Functionalized Mesoporous Silica Nanoparticles as Building Blocks for the Design of Nanovehicles with Optimized Drug Release Profile. *Nanomaterials* **2019**, 9.
- (153) Rumens, C. V.; Ziai, M. A.; Belsey, K. E.; Batchelor, J. C.; Holder, S. J. Swelling of PDMS Networks in Solvent Vapours; Applications for Passive RFID Wireless Sensors. *J. Mater. Chem. C* **2015**, 3 (39), 10091–10098.
- (154) González-Henríquez, C. M.; Sarabia Vallejos, M. A.; Rodríguez-Hernández, J.

- Wrinkles Obtained by Frontal Polymerization/Vitrification. *Wrinkled Polym. Surfaces Strateg. Methods Appl.* **2019**, 63–84.
- (155) Palacios-Cuesta, M.; Cortajarena, A. L.; García, O.; Rodríguez-Hernández, J. Fabrication of Functional Wrinkled Interfaces from Polymer Blends: Role of the Surface Functionality on the Bacterial Adhesion. *Polymers (Basel)*. **2014**, 6 (11), 2845–2861.
- (156) Rodríguez-Hernández, J. Wrinkled Interfaces: Taking Advantage of Surface Instabilities to Pattern Polymer Surfaces. *Prog. Polym. Sci.* **2015**, 42, 1–41.
- (157) E., G.; J., D. Current Experience with Fetoscopy and the Eurofoetus Registry for Fetoscopic Procedures. *Eur. J. Obstet. Gynecol. Reprod. Biol.* **2000**, 92 (1), 151–159.
- (158) Yagüe, J. L.; Yin, J.; Boyce, M. C.; Gleason, K. K. Design of Ordered Wrinkled Patterns with Dynamically Tuned Properties. *Phys. Procedia* **2013**, 46 (Eurocvd 19), 40–45.
- (159) Neto, A. I.; Cibrão, A. C.; Correia, C. R.; Carvalho, R. R.; Luz, G. M.; Ferrer, G. G.; Botelho, G.; Picart, C.; Alves, N. M.; Mano, J. F. Nanostructured Polymeric Coatings Based on Chitosan and Dopamine-Modified Hyaluronic Acid for Biomedical Applications. *Polym. Coatings* **2014**, 10 (12), 2459–2469.
- (160) Andersen, A.; Chen, Y.; Birkedal, H. Bioinspired Metal-Polyphenol Materials: Self-Healing and Beyond. *Biomimetics* **2019**, 4 (2), 1–20.
- (161) Bijlsma, J.; de Bruijn, W. J. C.; Hageman, J. A.; Goos, P.; Velikov, K. P.; Vincken, J. P. Revealing the Main Factors and Two-Way Interactions Contributing to Food Discolouration Caused by Iron-Catechol Complexation. *Sci. Rep.* **2020**, 10 (1), 1–11.
- (162) Raucci, M. G.; Alvarez-Perez, M. A.; Demitri, C.; Giugliano, D.; De Benedictis, V.; Sannino, A.; Ambrosio, L. Effect of Citric Acid Crosslinking Cellulose-Based Hydrogels on Osteogenic Differentiation. *J. Biomed. Mater. Res. - Part A* **2015**, 103 (6), 2045–2056.
- (163) Coma, V.; Sebti, I.; Pardon, P.; Pichavant, F. H.; Deschamps, A. Film Properties from Crosslinking of Cellulosic Derivatives with a Polyfunctional Carboxylic Acid. *Carbohydr. Polym.* **2002**, 51 (3), 265–271.
- (164) Favi, P. M.; Yi, S.; Lenaghan, S. C.; Xia, L.; Zhang, M. Inspiration from the Natural World: From Bio-Adhesives to Bio-Inspired Adhesives. *J. Adhes. Sci. Technol.* **2014**, 28 (3–4), 290–319.
- (165) Liu, Z.; Zhang, Z.; Ritchie, R. O. On the Materials Science of Nature's Arms Race. *Adv. Mater.* **2018**, 30 (32), 1–16.

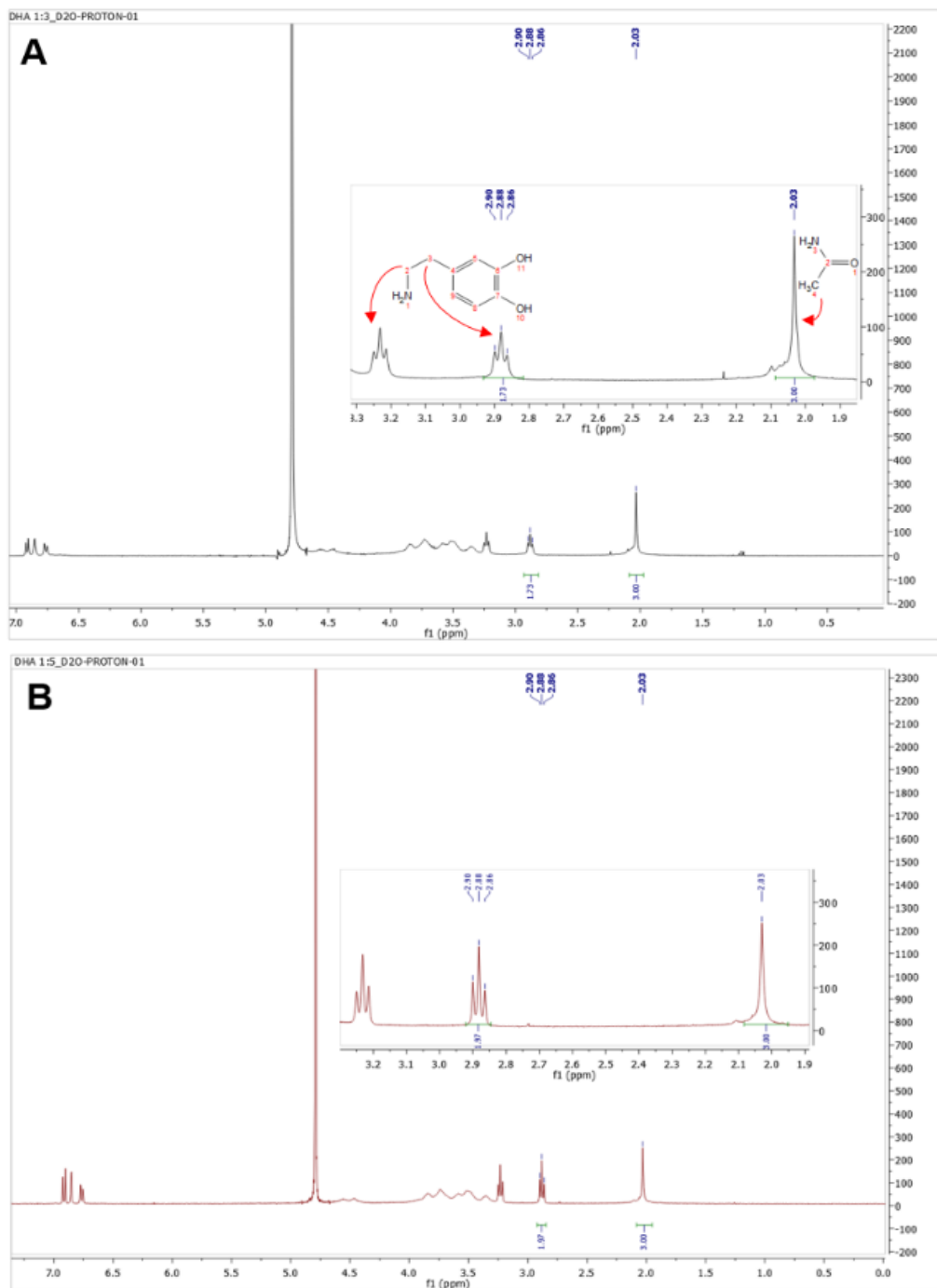
Annex



Annex 1. Solid works plan of final semi-lentil shape mold.



Annex 2. Solid work plan of final design of introducer.



Annex 3. ¹H-NMR spectra of one of the first dopamine hyaluronic acid (DHA) compared to the spectra of the final DHA, after modifying the synthesis (see annex for more details).



OPEN

Ex-vivo mechanical sealing properties and toxicity of a bioadhesive patch as sealing system for fetal membrane iatrogenic defects

Talita Micheletti^{1,2}, Elisenda Eixarch^{1,2,3,✉}, Sergio Berdun¹, Germán Febas⁴, Edoardo Mazza^{5,6}, Salvador Borrós⁴ & Eduard Gratacos^{1,2,3,7}

Preterm prelabor rupture of membranes (PPROM) is the most frequent complication of fetal surgery. Strategies to seal the membrane defect created by fetoscopy aiming to reduce the occurrence of PPRM have been attempted with little success. The objective of this study was to evaluate the ex-vivo mechanical sealing properties and toxicity of four different bioadhesives integrated in semi-rigid patches for fetal membranes. We performed an ex-vivo study using term human fetal membranes to compare the four integrated patches composed of silicone or silicone-polyurethane combined with dopaminated-hyaluronic acid or hydroxypropyl methylcellulose (HPMC). For mechanical sealing properties, membranes were mounted in a multiaxial inflation device with saline, perforated and sealed with the 4 combinations. We measured bursting pressure and maximum pressure free of leakage (n = 8). For toxicity, an organ culture of membranes sealed with the patches was used to measure pyknotic index (PI) and lactate dehydrogenase (LDH) concentration (n = 5). All bioadhesives achieved appropriate bursting pressures, but only HPMC forms achieved high maximum pressures free of leakage. Concerning toxicity, bioadhesives showed low PI and LDH levels, suggesting no cell toxicity. We conclude that a semi-rigid patch coated with HPMC achieved ex-vivo sealing of iatrogenic defects in fetal membranes with no signs of cell toxicity. These results warrant further research addressing long-term adhesiveness and feasibility as a sealing system for fetoscopy.

Fetoscopic surgery is used in thousands of pregnancies worldwide yearly for a variety of fetal indications¹. One of the main unsolved drawbacks of fetoscopy is the damage created to fetal membranes, which is thought to explain that iatrogenic preterm prelabor rupture of membranes (PPROM) occurs in up to 30% of cases^{1,1}. PPRM is the main complication after fetoscopy and its occurrence substantially increases the risk of preterm birth and perinatal morbidity^{1,1}.

In most instances, PPRM occurs weeks after fetoscopy⁴. Previous studies have shown that human fetal membranes do not heal after the creation of an iatrogenic defect⁵⁻⁹. However, it has also been shown how the natural sliding of the amnion over the chorion might provide a natural protective mechanism against PPRM⁶, which may explain why only a very small fraction of patients have PPRM within days of the procedure. On the other hand, mechanical factors such as chorioamniotic membrane separation after fetoscopy^{10,10} or septostomy¹² increase the risk of PPRM weeks later. This suggests that mechanical factors interfering with the adhesion between chorion and decidua may be an important trigger eventually leading to PPRM.

¹BCNatal | Fetal Medicine Research Center (Hospital Clínic and Hospital Sant Joan de Déu), University of Barcelona, Building Helios 2, Sabino Arana Street, 1, 08028 Barcelona, Spain. ²Institut d'Investigacions Biomèdiques August Pi i Sunyer (IDIBAPS), Barcelona, Spain. ³Centre for Biomedical Research on Rare Diseases (CIBER-ER), Madrid, Spain. ⁴Grup d'Enginyeria de Materials (GEMAT), Institut Químic de Sarrià, Universitat Ramon Llull, Barcelona, Spain. ⁵Swiss Federal Institute of Technology, Zurich, Switzerland. ⁶Empa, Materials Science and Technology, Dübendorf, Switzerland. ⁷Institut de Recerca Sant Joan de Déu, Esplugues de Llobregat, Spain. ✉email: eixarch@clinic.cat

Type of patch	Abbreviation	Semi-rigid patch	Bioadhesive component
Silicone-DHA	S-DHA	Medical silicone disc (450 µm-thick and 17 mm-diameter)	DHA 70–80% of dopamination, 10 mg/mL
Silicone-polyurethane-DHA	SPU-DHA	Medical silicone with electrospun polyurethane disc (480 µm-thick and 17 mm-diameter)	
Silicone-HPMC	S-HPMC	Medical silicone disc (450 µm-thick and 17 mm-diameter)	HPMC 300 µL, 10 mg/ml
Silicone-polyurethane-HPMC	SPU-HPMC	Medical silicone with electrospun polyurethane disc (480 µm-thick and 17 mm-diameter)	

Table 1. Types of sealing systems and composition. DHA, dopaminated hyaluronic acid; HPMC, hydroxypropyl methylcellulose; S, silicone; SPU, silicone-polyurethane.

Several systems have been attempted to seal fetal membranes, mainly in ex-vivo studies, so far without success. The injection of fluid adhesives, such as mussel-glues^{13,13} and medical sealants^{15–17} needs to overcome the problem of applying a fluid adhesive in the amniotic fluid wet environment. The use of collagen plugs across the membrane defect has shown poor results when tested in clinical conditions^{18,18}. We hypothesized that a semi-rigid disc patch coated with bioadhesives could seal the amniotic defect, preventing exposure of the chorion to amniotic fluid and reducing the risks of chorion-decidua separation. To this end, we designed a semi-rigid patch made up of silicone, which can be coated with different combinations of bioadhesives.

In this study we tested the proof of concept that this integrated semi-rigid disc bioadhesive patch could achieve effective adhesion properties in human fetal membranes similar to well known adhesives, such as cyanoacrylate glue, but without their limitations to intrauterine use.

Results

Patients. Fetal membranes from a total of 27 donors were collected, 22 for mechanical tests and 5 for toxicity tests. Gestational age at delivery was 39.1 weeks (range 39–39.4) and mean birth weight was 3213.6 g ± 457.9. Indications for cesarean section were previous C-section (59.3%), breech presentation (29.6%) and more uncommonly placenta previa, pelvic tumors and previous pelvic floor surgery.

Bioadhesives. Four different bioadhesive-coated patches were developed, by combining a semi-rigid patch and a bioadhesive component. The candidates were composed of silicone-dopaminated hyaluronic acid (S-DHA), silicone with polyurethane-dopaminated hyaluronic acid (SPU-DHA), silicone-hydroxypropyl methylcellulose (S-HPMC) or silicone with polyurethane-hydroxypropyl methylcellulose (SPU-HPMC), as indicated in Table 1 and shown in Fig. 1.

Mechanical properties. As expected, bursting pressures after perforation and sealing were much lower than those observed in intact membranes (intact vs. any adhesive, $p < 0.05$).

Membranes sealed with either cyanoacrylate or integrated systems S-DHA, SPU-DHA, S-HPMC or SPU-HPMC showed median values of bursting pressures in the range of 16–48 mmHg, with no significant differences among groups (Fig. 2).

In terms of maximum pressure free of leakage (Figs. 3, 4), S- and SPU-DHA patches presented leakage at low pressures (medians ranging from 1.6 to 4.8 mmHg). On the contrary, S- and SPU-HPMC candidates showed leakage at higher pressures [S-HPMC 44.9 mmHg (IQR 38.7–54.3) and SPU-HPMC 40.5 mmHg (IQR 30.1–59.9)], which were significantly higher than those observed with cyanoacrylate [21.4 mmHg (IQR 16.3–32.4)], $p = 0.005$ and 0.02 respectively.

Toxicity. Pyknotic index at 48 h of culture (Fig. 5) was on average below 2% in all bioadhesives tested and in non-exposed membranes ($p = 0.483$), while in positive controls with commercial adhesive it was 31.1% (IQR 26.0–36.5), $p < 0.05$ (Fig. 6).

Likewise, median LDH concentration at 48 h of culture ranged from 3 to 8 U/L and was similar to non-exposed membranes ($p = 0.154$). The levels of LDH were significantly higher in the positive control 1754 U/L (IQR 998.5–2775.5), $p < 0.01$ (Fig. 7).

Discussion

In this study we tested an innovative integration of a semi-rigid biocompatible patch coated with bioadhesive. The results demonstrated that such system can achieve effective sealing of a defect created in human membranes ex vivo, with similar adhesiveness to that achieved by cyanoacrylate, but without cell toxicity. These results open new possibilities for the development of membrane sealing systems aiming at reducing the prevalence of PPROM after fetoscopy.

Our sealing system is based on the concept of sealing fetal membranes from the amniotic side. This may offer advantages to previously tested solutions. Collagen-based plugs have shown negative results when used clinically^{18,18}. Among other reasons, plugs can migrate, increase the size of the defect and they dissolve quickly in most instances^{18,18}. In addition, a physical plug across membranes might interfere with the natural protection against PPROM provided by the sliding of the amniotic over the chorionic membrane layers⁶. Among fluid adhesives available for medical use, cyanoacrylate glues are extremely adhesive to tissues even in wet conditions. However, when applied as a glue, they show non-elastic adhesion with risk of damage due to traction²⁰ and its

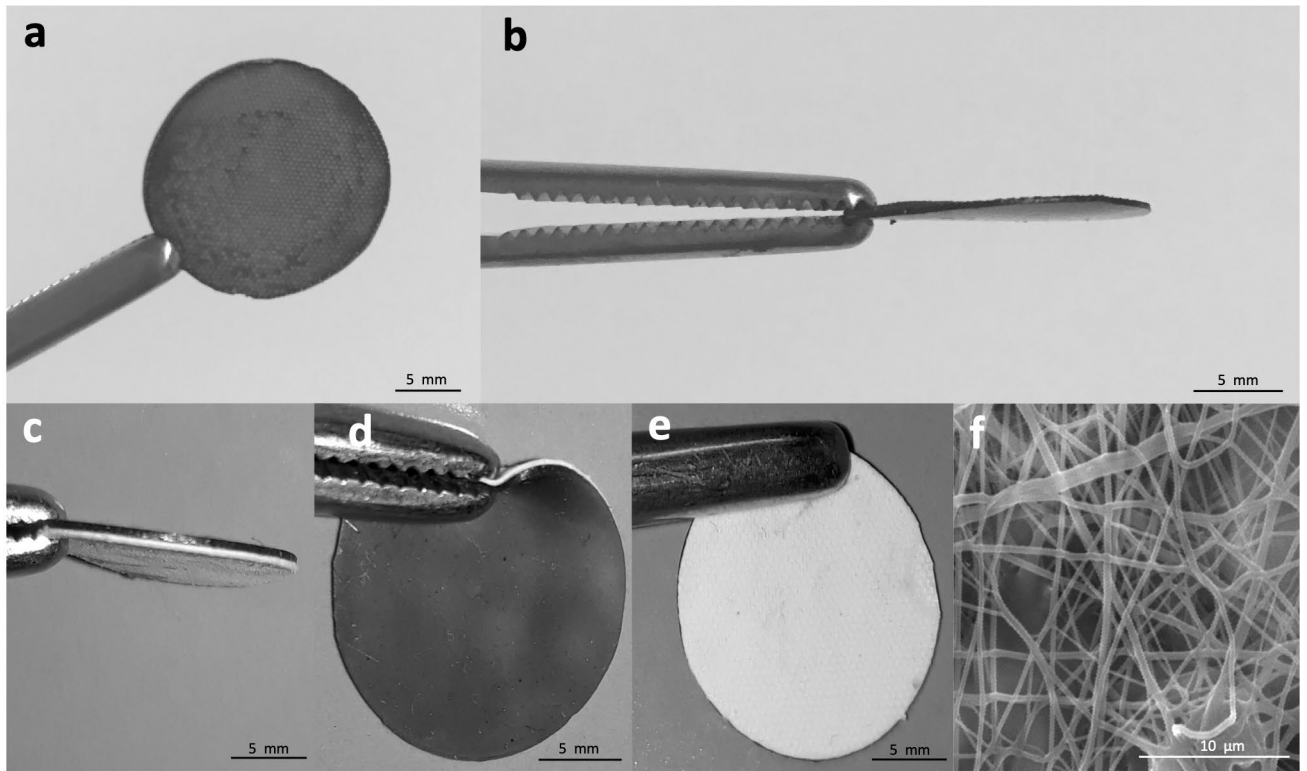


Figure 1. Semi-rigid patches composed of silicone only or silicone combined with electrospun polyurethane. (a,b) Silicone patch coated with dopaminated hyaluronic acid (DHA) in anterior and lateral views. (c–e) Silicone with electrospun polyurethane patch in lateral, posterior and anterior views. (f) Detail: electrospun polyurethane.

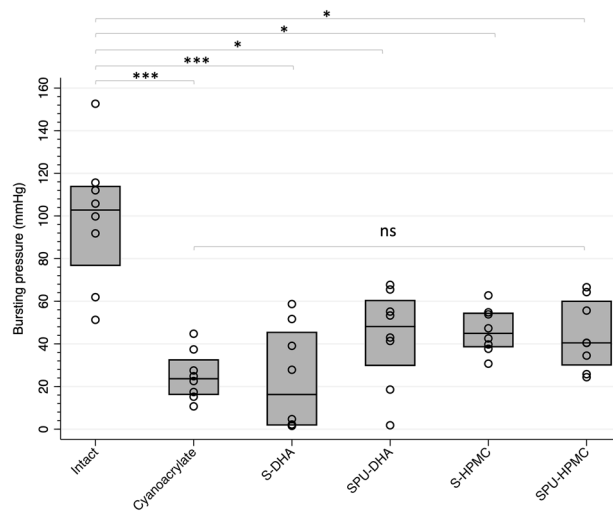


Figure 2. Bursting pressure (mmHg) of fetal membranes in the study groups. Distributional plots express median and interquartile range, n = 8. Intact: intact membrane; Cyanoacrylate: positive control; S-DHA: silicone with dopaminated hyaluronic acid; SPU-DHA: silicone-polyurethane with dopaminated hyaluronic acid; S-HPMC: silicone with hydroxypropyl methylcellulose; SPU-HPMC: silicone-polyurethane with hydroxypropyl methylcellulose; ns: non-significant. Figure created using Stata 14.2.

application in intrauterine environment is complex due to its non-solid condition. Previous studies have investigated the use of mussel-like glues as an alternative to cyanoacrylate¹⁵, since they are based on a catechol side chain of 3,4-dihydroxyphenylalanine (DOPA) amino acid that theoretically secures strong adhesion to almost any surface even underwater^{15,15}. Indeed, dopaminated-poly(ethylene glycol) (PEG), a mussel-like bioadhesive, was able to achieve leak-proof closure of 3.5-mm-trocar defects while stretched in vitro¹⁵ and has shown to

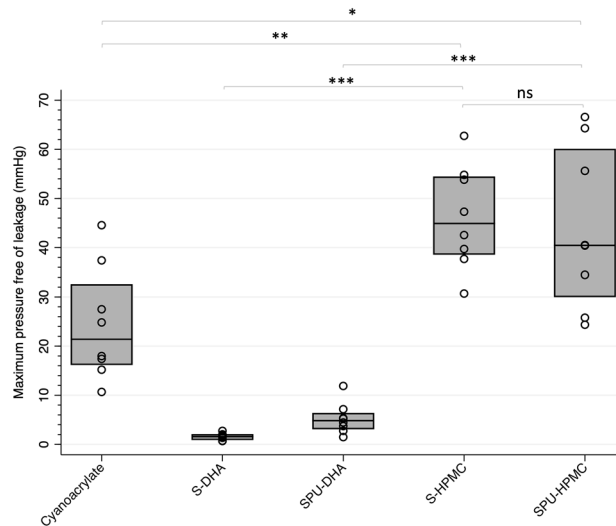


Figure 3. Maximum pressure free of leakage (mmHg) supported by fetal membranes according to treatment. Distributional plots express median and interquartile range, $n = 8$. * $p < 0.05$, ** $p < 0.01$, *** $p < 0.001$. Intact: intact membrane; Cyanoacrylate: positive control; S-DHA: silicone with dopaminated hyaluronic acid; SPU-DHA: silicone-polyurethane with dopaminated hyaluronic acid; S-HPMC: silicone with hydroxypropyl methylcellulose; SPU-HPMC: silicone-polyurethane with hydroxypropyl methylcellulose; ns: non-significant. Figure created using Stata 14.2.

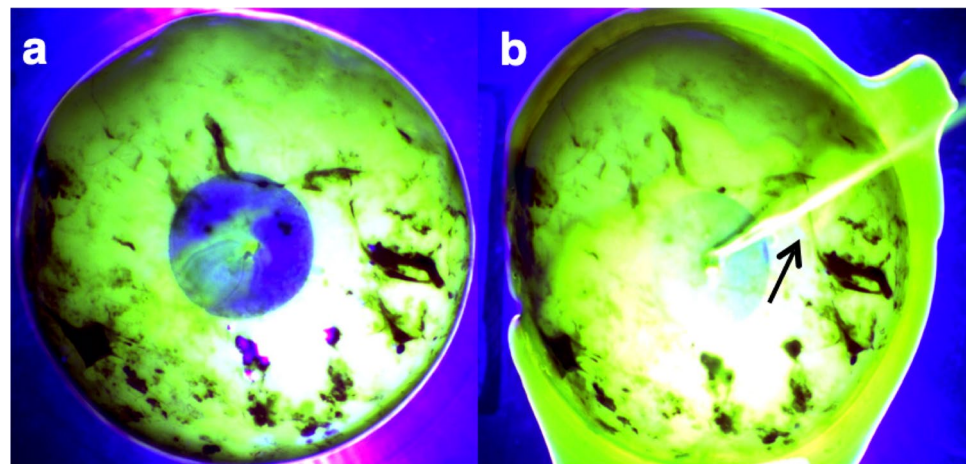


Figure 4. Representative images of leakage, rupture and completely sealed membrane. (a) Fluorescent light: leakage is observed as fluorescent flow through the lesion. (b) Fluorescent light: rupture of membrane characterized by a sudden decrease of internal pressure associated or not with an important fluorescein flow through the lesion (long arrow).

withstand bursting pressures around 35–40 mmHg^{13,13}. In general, the application of glues on amniotic side of fetal membranes in clinical conditions is challenging^{13,14,22}. One study reported the development and ex vivo testing of an umbrella-like device supported by a purpose-designed mesh as a potential solution to apply a liquid mussel-glue to the amnion defect¹⁷.

In this study we tested different adhesive polymers. To achieve a system similar to the dopamination of mussel-glues, we produced DHA from the polysaccharide hyaluronic acid. DHA adhered initially to membranes in the multiaxial device and achieved bursting pressures of 16–48 mmHg, similar to those reported using other bioadhesives mainly based on mussel-glue-like systems^{13,15,22}. However, DHA showed leakage from pressures as low as 1.6 mmHg. We decided to evaluate HPMC polysaccharide in the study due to its natural adhesive properties²³. Contrary to DHA, HPMC supported high bursting pressures preventing leakage up to 40–45 mmHg. Regarding the composition of the semi-rigid patch, S and SPU are largely used in medical devices^{24,24}. Since S is extremely hydrophobic and poorly adherent, polyurethane was added to tune the hydrophobicity. Moreover, such coating reduces the stiffness of the surface in contact with the tissue, making the materials mechanically friendly with the amniotic membrane. We demonstrated that both materials (S and SPU), coated with HPMC,

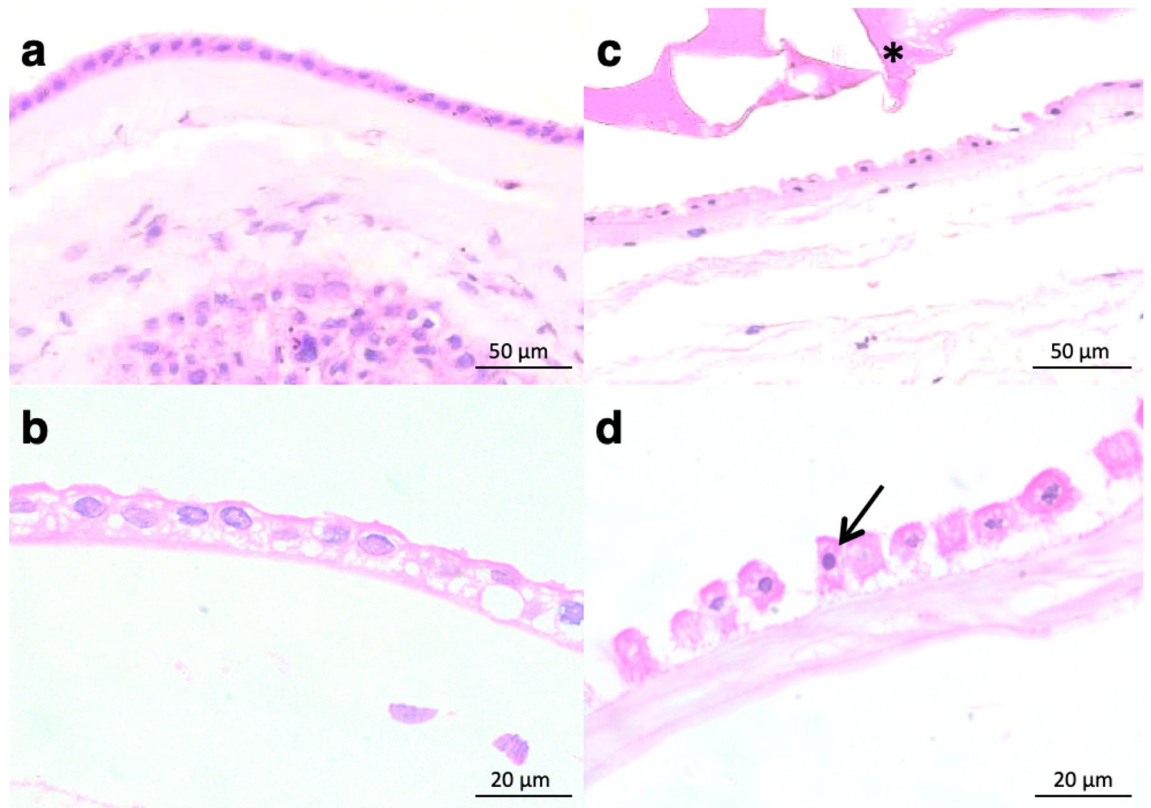


Figure 5. Histological assessment of toxic effects on fetal membrane amniotic layer (hematoxylin eosin) after 48 h of culture. **(a,b)** Non-exposed (NE) membrane at $\times 400$ and $\times 1000$ magnification, respectively. **(c,d)** Membrane exposed to positive control at $\times 400$ and $\times 1000$ magnification, respectively. In this group, pyknotic nucleus is identified (arrow). *Eosinophilic material corresponding to positive control.

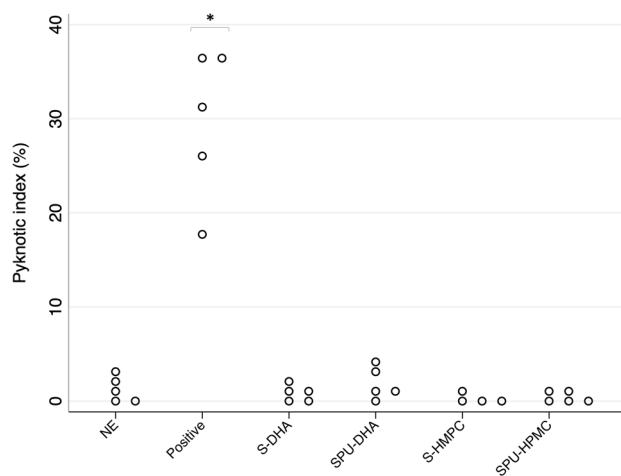


Figure 6. Pyknotic index of amniotic cells nuclei (in percentage) according to bioadhesive groups at 48 h of culture. Distributional dotplots, $n = 5$. * $p < 0.05$ (comparison between positive control and the other groups). NE: non-exposed cultured membrane. Positive: positive control (component B of DrSails glue); S-DHA: silicone with dopaminated hyaluronic acid; SPU-DHA: silicone-polyurethane with dopaminated hyaluronic acid; S-HPMC: silicone with hydroxypropyl methylcellulose; SPU-HPMC: silicone-polyurethane with hydroxypropyl methylcellulose. Figure created using Stata 14.2

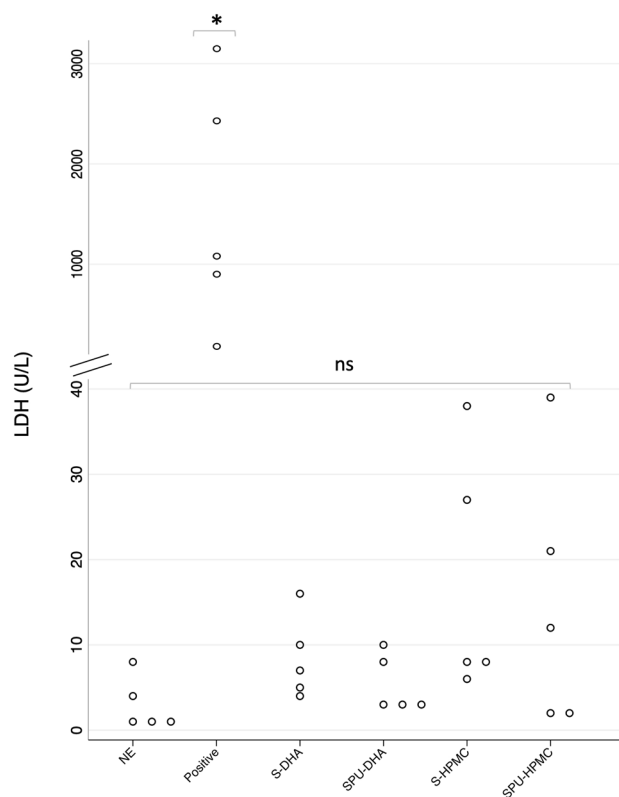


Figure 7. Concentration of lactate dehydrogenase (LDH) in U/L in supernatants according to bioadhesive group at 48 h of culture. Distributional dotplots, $n = 5$. $*p < 0.01$ (comparison between positive control and the other groups). NE: non-exposed cultured membrane. Positive: positive control (component B of DrSails glue); S-DHA: silicone with dopaminated hyaluronic acid; SPU-DHA: silicone-polyurethane with dopaminated hyaluronic acid; S-HPMC: silicone with hydroxypropyl methylcellulose; SPU-HPMC: silicone-polyurethane with hydroxypropyl methylcellulose; ns: non-significant. Figure created using Stata 14.2.

had a good performance ex vivo. It is important to highlight that both S and SPU patches were produced with a micropatterning in order to increase the contact surface and to generate friction force. These features would contribute to improve attachment of the bioadhesive to a slippery surface such as the fetal membrane.

This study has clinical and research implications. Preventing iatrogenic PPRM is one of the major challenges in fetoscopic surgery. The system here presented has some potential advantages that would make it a suitable candidate for clinical testing. The use of a semi-rigid patch allows insertion through a fetoscopic trocar and eliminates the challenges of applying in an efficient and safe fashion a liquid glue on human membranes¹⁷. The biocompatible, non-absorbable nature of the materials used allows long-term use and prevents degradation in a biological environment, as observed with the use of other candidate systems for membrane sealing^{15,15}. Research on the feasibility of application and efficacy of the bioadhesive patches in an experimental model of fetoscopic surgery is now under way.

Among the strengths of the study, we used an ex vivo model with real human membranes. The adaptation of a previously validated approach^{13,26,27} with the addition of fluorescein, allowed detection of subtle leakage more objectively. Contrary to previous studies in which glues were tested over chorion or myometrium^{13,13,13}, we applied the sealing system over the amnion, upside down and under a fluid environment, reproducing the conditions of a clinical application. Finally, we challenged substantially the system using pressures far above the range of 15–30 mmHg of human pregnancy^{29,30}. Among the limitations, these ex vivo results require further validation in other systems evaluating long-term adhesion and feasibility in experiments simulating real clinical conditions. We used term membranes and although there are no remarkable histological differences with preterm membranes³¹, it could be argued that adhesiveness could be lower on the latter, especially due to differences in stiffness³².

In conclusion, an integrated semi-rigid patch using HPMC as bioadhesive achieved levels of adhesion similar to a well-known adhesive as cyanoacrylate glue, but with the advantage of composing a non-toxic and ready-to-use system. The results warrant further research to test long-term adhesiveness and feasibility as a sealing system for fetoscopic procedures.

Methods

Ethical aspects. All methods were carried out in accordance with relevant guidelines and regulations of the ethics committee. The experimental protocols were approved by the Ethical Committee of Hospital Clinic (HCB/2016/0236) and of Hospital Sant Joan de Déu (PIC-40-16). Informed consent was obtained from all patients, none of them under 18. Confidentiality and anonymity were ensured, and data was used only for scientific purposes.

Fetal membrane collection. Fetal membranes were collected after written consent from elective cesarean sections of singletons at term (gestational age from 37 to 41 weeks). Exclusion criteria were: clinical chorioamnionitis, infections (HIV, hepatitis, syphilis), disturbances of amniotic fluid (oligo or polyhydramnios at the last scan), maternal conditions such as hypertension, diabetes, anemia, connective tissue disorders, under nutrition, use of tobacco, fetal growth anomalies, major fetal malformations or chromosomal abnormalities. Patients with history of contractions, preterm cervical dilatation or premature rupture of membranes were also excluded.

Production of the patches and bioadhesive systems. The semi-rigid patches were produced using either medical silicone (S—NuSil, NuSil Technology LLC, United States) or medical silicone combined with electrospun polyurethane (SPU—NuSil and Bionate Thermoplastic Polycarbonate-Urethane, DSM Biomedical Headquarters, United States). Both patches were produced in a 17-mm diameter disc shape, from 450 to 480 μm -thick. The surface was prepared for receiving the bioadhesive component by producing a 150 μm deep micropatterning on it, to enhance contact surface and adhesion. All sealing systems were used up to 35 days after their production.

Both silicone (S) and silicone-polyurethane (SPU) disc patches were coated with bioadhesive components composed either by dopaminated hyaluronic acid (DHA) or hydroxypropyl methylcellulose (HPMC). DHA was used at 10 mg/mL and oxidized with ferric chloride, with 70–80% dopamination. HPMC was used at 10 mg/mL after plasma activation of S or SPU.

Membrane processing. After collection, fetal membranes were separated from the placenta. Areas with visible clots or decidual contamination were removed. Specimens were transported to the laboratory for further handling in saline solution at room temperature within 30 min. Explants were cut at 2 cm from placental edge to avoid heterogeneity of the tissue³³ and used within 6 h. In case the membranes were not used immediately, samples were kept at 4 °C until use.

A total of 27 fetal membranes were needed. For mechanical experiments, each sealing system and control was tested 8 times with membranes from different donors, to reduce the possible effects of membrane variability between donors. Each fetal membrane was used, in average, for 2–5 tests, depending on the conditions of the membrane. For toxicity, each experiment with sealing system and control was done 5 times with membranes from different donors, to reduce the possible effects of membrane variability between donors.

For mechanical properties, fetal membranes were prepared as follows. Explants were cut in 7 cm diameter circles with scalpel. Sand papers rings (waterproof paper, no 180, ADSEng, Germany) with 50 mm inner and 70 mm outer diameter were glued on both sides of the membrane with superglue (Super Glue-3 Original, Loctite, Barcelona, Spain). Samples were kept moist with phosphate buffered saline (PBS) during the whole process. Before mounting the fetal membranes over the inflation device, explants were perforated with a 10Fr-metallic punch (3.33 mm—Karl Storz SE and Co, Germany), from chorion to amnion (simulating clinical condition) in the center of the circumferential membranous explant. Perforated membranes were then sealed with the different sealing systems or a positive control (Cyanoacrylate). Sealing systems or positive controls were placed with tweezers over the amnion to cover the defect and adjusted with gentle pressure for 60 s. After 2.5 min, fetal membranes were then mounted over the cylinder with the amnion facing a fluorescein saline solution, as followed explained.

For toxicity experiments, samples were handled in sterile fashion and used immediately after collection. Membranes were cut in 6 fragments of 2 × 2 cm and applied in contact with the different experimental groups.

Mechanical properties. A multiaxial inflation device was used to evaluate the mechanical properties of the sealed membranes. It consists of a custom-built device that was previously characterized by Haller et al.^{13,13} and provided to us by the Department of Mechanical Engineering of Swiss Federal Institute of Technology (Zurich, Switzerland). Briefly, the device consists of an aluminum cylinder with a 50 mm-inner diameter that was mounted by clamping membrane samples between the cylinder and a cover ring. The cylinder was connected to inlet and outlet tubes. A peristaltic pump (Reglo Digital ISM834C, four channels, max 35 ml/min per channel, Ismatec Laboratory Pumps, Wertheim, Germany) connected to the inlet tube was used to gradually fill the cylinder with fluorescein 0.1% prepared in PBS (Fluorescein oculos 10%, SERB Specialty Pharmaceuticals, Belgium). Fluorescein was used for detection of leakage out of the iatrogenic defect.

The cylinder was inflated by increasing the solution volume with a constant pumped rate flow of 2 ml/min. The difference of pressure generated was measured throughout the experiment with a hydrostatic pressure sensor (digital manometer, LEX 1, – 1 to 2 bar, accuracy within 0.05%, Keller, Switzerland) positioned at the outlet tube and connected to a computer with a converter (K-114 A USB to RS485 Converter, Keller, Switzerland). An UV flashlight (UV light 400 nm 51-LED flashlight) was used to improve detection of fluorescein leakage. The deformation of the membrane was monitored with a video camera (CMOS Camera 1280 × 1024, Color, USB2.0, 18–108 mm EFL Zoom Lens w/Focus Control 2/3" format, Thorlabs, Munich, Germany) mounted on the top of the cylinder.

Intact membranes (without perforation) and membranes sealed with an industrial cyanoacrylate glue (2-ethyl cyanoacrylate 75%, 1,4-dihydroxybenzene, hydroquinone, quinol—Superceys Unick, Ceys S.A., Barcelona, Spain) were used as controls. Cyanoacrylate glue was added manually to 17-mm diameter disc-shaped silicone patches a few moments before the test and therefore did not compose an integrated system.

Mounted membranes were inflated by continuously increasing the pressure in the cylinder until rupture of the membrane. Rupture was characterized by a sudden decrease of internal pressure being associated or not with an important fluorescein flow through the lesion. Bursting pressure was registered. The occurrence of leakage before bursting pressure was defined as detection of fluorescein flow through lesion while the pressure was still increasing and the membrane still inflating. Maximum pressure free of leakage was also registered.

Toxicity. The toxicity test was performed as previously reported⁸. Under a laminar airflow hood, the membrane explants were washed in sterile PBS (PBS pH7.4-1x—Gibco by Life Technologies, USA) at 37 °C. Areas with visible blood clots or decidual contaminations were removed. The explants were mounted over an acellular collagen support (Lyostyp—B. Braun, Germany) in 12-well plates, with the chorion facing the collagen support.

Different sealing systems and controls were placed on the amnion surface of fetal membrane fragments and incubated with a complete culture medium for amniocytes (Amniomax—Complete Medium—Gibco by Life Technologies, USA) at 37 °C and 5% CO₂ air up to 48 h. Initial experiments with cyanoacrylate showed remarkable tissue destruction. To achieve tissue integrity allowing histological evaluation it was decided to replace cyanoacrylate by another commercial adhesive that also works in underwater conditions (DrSails—Sailing Technologies, S.L., Spain—component B, composed of modified polyamine). Tissue and supernatants of each group were harvested at 48 h. The groups studied for toxicity were: non-exposed membranes (cultured membranes without treatment), positive control (cultured membranes with 1 ml of component B of DrSails glue—Sailing Technologies, S.L., Spain) and sealing systems S-DHA, SPU-DHA, S-HPMC and SPU-HPMC (cultured membranes with sealing systems).

Tissue samples were fixed in 4% formalin for 24 h and embedded in paraffin. Transversal sections were obtained (4 µm) and stained with hematoxylin–eosin (HE). Overall morphological condition of the membranes was examined and pyknotic index, which is a characteristic feature of apoptosis^{35,35}, was determined in the amnion layer to evaluate toxicity. Pyknotic and non-pyknotic nuclei were counted under light microscopy at 40-power magnification level (total magnification × 400) in 5 non-overlapping fields. Pyknotic nuclei were identified as small-sized nuclei and with highly condensed chromatin³⁷. The pyknotic index was calculated by determining the percentage of pyknotic nuclei over the total number of amniotic nuclei.

Supernatants were stored at –20° and used for quantitative determination of cytotoxicity based on quantification of lactate dehydrogenase (LDH) enzyme released into culture medium (ADVIA Chemistry Systems Lactate Dehydrogenase L-P (LDLP) assay, Siemens Healthcare S.L.U, Spain). Absorbance was read at 340/410 nm.

Statistical analysis. Categorical variables were expressed as number of cases out of total and proportion (%). Normal distribution was verified using standardized normal probability plots, box plot graphs and Shapiro–Wilk normality test. Parametric data was expressed as mean ± standard deviation and non-parametric data was expressed as median (interquartile range). Homogeneity of variances was verified with Levene's test. Inferential analysis for numeric non-parametric variables was performed using Kruskal–Wallis test with Bonferroni error correction or Wilcoxon rank test (Mann–Whitney). Statistical significance was defined as *p* value < 0.05 for all analysis. Data was processed using Stata 14.2 (StataCorp. 2015. Stata Statistical Software: Release 14. College Station, TX: StataCorp LP).

Data availability

The datasets generated during and/or analyzed during the current study are available from the corresponding author on reasonable request.

Received: 2 June 2020; Accepted: 28 September 2020

Published online: 29 October 2020

References

- Beck, V., Lewi, P., Gucciardo, L. & Devlieger, R. Preterm prelabor rupture of membranes and fetal survival after minimally invasive fetal surgery: a systematic review of the literature. *Fetal Diagn. Ther.* **31**, 1–9 (2012).
- Maggio, L. *et al.* Iatrogenic preterm premature rupture of membranes after fetoscopic laser ablative surgery. *Fetal Diagn. Ther.* **38**, 29–34 (2015).
- Papanna, R. *et al.* Risk factors associated with preterm delivery after fetoscopic laser ablation for twin–twin transfusion syndrome. *Ultrasound Obstet. Gynecol.* **43**, 48–53 (2014).
- Snowise, S. *et al.* Preterm prelabor rupture of membranes after fetoscopic laser surgery for twin–twin transfusion syndrome. *Ultrasound Obstet. Gynecol.* **49**, 607–611 (2017).
- Devlieger, R., Millar, L. K., Bryant-Greenwood, G., Lewi, L. & Deprest, J. A. Fetal membrane healing after spontaneous and iatrogenic membrane rupture: a review of current evidence. *Am. J. Obstet. Gynecol.* **195**, 1512–1520 (2006).
- Gratacós, E. *et al.* A histological study of fetoscopic membrane defects to document membrane healing. *Placenta* **27**, 452–456 (2006).
- Papanna, R. *et al.* Histologic changes of the fetal membranes after fetoscopic laser surgery for twin–twin transfusion syndrome. *Pediatr. Res.* **78**, 247–255 (2015).
- Devlieger, R. *et al.* An organ-culture for in vitro evaluation of fetal membrane healing capacity. *Eur. J. Obstet. Gynecol. Reprod. Biol.* **92**, 145–150 (2000).
- Papanna, R., Bebbington, M. W. & Moise, K. Novel findings of iatrogenic fetal membrane defect after previous fetoscopy for twin–twin transfusion syndrome. *Ultrasound Obstet. Gynecol.* **42**, 118–119 (2013).

10. Papanna, R., Mann, L. K., Johnson, A., Sangi-Haghpeykar, H. & Moise, K. J. Chorioamniotic separation as a risk for preterm premature rupture of membranes after laser therapy for twin–twin transfusion syndrome. *Obstet. Gynecol.* **115**, 771–776 (2010).
11. Ortiz, J. U. *et al.* Chorioamniotic membrane separation after fetoscopy in monochorionic twin pregnancy: incidence and impact on perinatal outcome. *Ultrasound Obstet. Gynecol.* **47**, 345–349 (2016).
12. Cruz-Martinez, R. *et al.* Incidence and clinical implications of early inadvertent septostomy after laser therapy for twin–twin transfusion syndrome. *Ultrasound Obstet. Gynecol.* **37**, 458–462 (2011).
13. Haller, C. M. *et al.* Mussel-mimetic tissue adhesive for fetal membrane repair: an ex vivo evaluation. *Acta Biomater.* **8**, 4365–4370 (2012).
14. Kivelio, A. *et al.* Mussel mimetic tissue adhesive for fetal membrane repair: initial in vivo investigation in rabbits. *Eur. J. Obstet. Gynecol. Reprod. Biol.* **171**, 240–245 (2013).
15. Bilic, G. *et al.* Injectable candidate sealants for fetal membrane repair: bonding and toxicity in vitro. *Am. J. Obstet. Gynecol.* **202**(85), e1–e9 (2010).
16. Engels, A. C. *et al.* Tissuepatch is biocompatible and seals iatrogenic membrane defects in a rabbit model. *Prenat. Diagn.* **38**, 99–105 (2018).
17. Devaud, Y. R., Züger, S., Zimmermann, R., Ehrbar, M. & Ochslein-Köblle, N. Minimally invasive surgical device for precise application of bioadhesives to prevent iPPROM. *Fetal Diagn. Ther.* **45**, 102–110 (2019).
18. Papanna, R., Mann, L. K., Moise, K. Y., Johnson, A. & Moise, K. J. Absorbable gelatin plug does not prevent iatrogenic preterm premature rupture of membranes after fetoscopic laser surgery for twin–twin transfusion syndrome. *Ultrasound Obstet. Gynecol.* **42**, 456–460 (2013).
19. Engels, A. C. *et al.* Collagen plug sealing of iatrogenic fetal membrane defects after fetoscopic surgery for congenital diaphragmatic hernia. *Ultrasound Obstet. Gynecol.* **43**, 54–59 (2014).
20. Petrie, E. M. Cyanoacrylate adhesives in surgical applications. *Rev. Adhes. Adhes.* **2**, 253–310 (2014).
21. Lee, H., Lee, B. P. & Messersmith, P. B. A reversible wet/dry adhesive inspired by mussels and geckos. *Nature* **448**, 338–341 (2007).
22. Perrini, M. *et al.* A comparative investigation of mussel-mimetic sealants for fetal membrane repair. *J. Mech. Behav. Biomed. Mater.* **58**, 57–64 (2016).
23. Tedesco, M. P., Monaco-Lourenço, C. A. & Carvalho, R. A. Gelatin/hydroxypropyl methylcellulose matrices: polymer interactions approach for oral disintegrating films. *Mater. Sci. Eng. C* **69**, 668–674 (2016).
24. Shin, B. H. *et al.* Silicone breast implant modification review: overcoming capsular contracture. *Biomater. Res.* **22**, 37 (2018).
25. Stoddard, R. J., Steger, A. L., Blakney, A. K. & Woodrow, K. A. In pursuit of functional electrospun materials for clinical applications in humans. *Ther. Deliv.* **7**, 387–409 (2016).
26. Haller, C. M. *et al.* Mussel-mimetic tissue adhesive for fetal membrane repair: a standardized ex vivo evaluation using elastomeric membranes. *Prenat. Diagn.* **31**, 654–660 (2011).
27. Perrini, M. *et al.* Contractions, a risk for premature rupture of fetal membranes: a new protocol with cyclic biaxial tension. *Med. Eng. Phys.* **35**, 846–851 (2013).
28. Pensabene, V. *et al.* Repairing fetal membranes with a self-adhesive ultrathin polymeric film: evaluation in mid-gestational rabbit model. *Ann. Biomed. Eng.* **43**, 1978–1988 (2015).
29. Katsura, D. *et al.* Intra-amniotic pressure of twin-to-twin transfusion syndrome. *Fetal Diagn. Ther.* **44**, 160–160 (2018).
30. Bergh, E. P. *et al.* Effect of intra-amniotic fluid pressure from polyhydramnios on cervical length in patients with twin–twin transfusion syndrome undergoing fetoscopic laser surgery. *Ultrasound Obstet. Gynecol.* **54**, 774–779 (2019).
31. Benson-Martin, J. *et al.* The Young's modulus of fetal preterm and term amniotic membranes. *Eur. J. Obstet. Gynecol. Reprod. Biol.* **128**, 103–107 (2006).
32. Millar, L. K., Stollberg, J., DeBuque, L. & Bryant-Greenwood, G. Fetal membrane distention: determination of the intrauterine surface area and distention of the fetal membranes preterm and at term. *Am. J. Obstet. Gynecol.* **182**, 128–134 (2000).
33. McLaren, J., Malak, T. M. & Bell, S. C. Structural characteristics of term human fetal membranes prior to labour: identification of an area of altered morphology overlying the cervix. *Hum. Reprod.* **14**, 237–241 (1999).
34. Buerzle, W. *et al.* Multiaxial mechanical behavior of human fetal membranes and its relationship to microstructure. *Biomech. Model. Mechanobiol.* **12**, 747–762 (2013).
35. Kim, C. J., Romero, R., Chaemsithong, P. & Kim, J.-S. Chronic inflammation of the placenta: definition, classification, pathogenesis, and clinical significance. *Am. J. Obstet. Gynecol.* **213**, S53–69 (2015).
36. Elmore, S. Apoptosis: a review of programmed cell death. *Toxicol. Pathol.* **35**, 495–516 (2007).
37. Lowe, S. W. & Lin, A. W. Apoptosis in cancer. *Carcinogenesis* **21**, 485–495 (2000).

Acknowledgements

This work was supported by Cellex Foundation and Erasmus + Programme of the European Union (Framework Agreement Number: 2013-0040). T.M. was supported by predoctoral grant from Erasmus Mundus FetalMedPhD. E.E. has received funding from the Departament de Salut under Grant SLT008/18/00156. We thank Prof. Edoardo Mazza's team (Marina Vita and Kevin Bircher) from Department of Mechanical and Process Engineering/Institute of Mechanical Systems – Swiss Federal Institute of Technology Zurich (ETH Zurich) for providing us with the multiaxial inflation device and training. We also thank: Carlota Rovira from Department of Pathology and Johanna Parra from Department of Obstetrics and Gynecology of Hospital Sant Joan de Déu, Barcelona, Spain; Joan Junyent for engineering support; Sabrina Gea for the technical support; and the medical and nursing staff of Hospital Clinic – Maternitat who contributed immensely with collection of fetal membranes.

Author contributions

E.G., E.E. and T.M. conceived the study project. G.F. and S.B. produced the materials to be tested. T.M. and S.B. performed and E.E. supervised the experiments. E.M. provided material and training for the ex-vivo mechanical properties tests. T.M., S.B., E.E. and E.G. wrote the manuscript final version. G.F. prepared Fig. 1. T.M., S.B. and E.E. prepared Figs. 2, 3, 4, 5, 6 and 7. All authors reviewed de manuscript, approved the submitted version, and have agreed both to be personal accountable for the author's own contributions and to ensure that questions related to the accuracy or integrity of any part of the work, even ones in which the author was not personally involved are appropriately investigated, resolved and the resolution documented in the literature.

Funding

This project has been partially funded with support of the Erasmus + Programme of the European Union (Framework Agreement number: 2013-0040). This publication reflects the views only of the author, and the Commission cannot be held responsible for any use, which may be made of the information contained therein.

Additionally, this research has been partially funded with support from Cellex Foundation. The sealing system developed was patented under number PCT/EP2020/064523.

Competing interests

The authors declare no competing interests.

Additional information

Correspondence and requests for materials should be addressed to E.E.

Reprints and permissions information is available at www.nature.com/reprints.

Publisher's note Springer Nature remains neutral with regard to jurisdictional claims in published maps and institutional affiliations.



Open Access This article is licensed under a Creative Commons Attribution 4.0 International License, which permits use, sharing, adaptation, distribution and reproduction in any medium or format, as long as you give appropriate credit to the original author(s) and the source, provide a link to the Creative Commons licence, and indicate if changes were made. The images or other third party material in this article are included in the article's Creative Commons licence, unless indicated otherwise in a credit line to the material. If material is not included in the article's Creative Commons licence and your intended use is not permitted by statutory regulation or exceeds the permitted use, you will need to obtain permission directly from the copyright holder. To view a copy of this licence, visit <http://creativecommons.org/licenses/by/4.0/>.

© The Author(s) 2020